INTERACTIONS BETWEEN ANIONIC RADIONUCLIDES (^{129}I, ^{79}Se AND ^{99}Tc) AND SOIL GEOCOLLOIDS

HEATHER K. SANDERS

(BSc. Environmental Biology 2014**)**

Thesis submitted to the University of Nottingham

for the degree of Doctor of Philosophy

2018

I dedicate this work to my parents,

without whose love, support and encouragement

this wouldn't have been possible.

ABSTRACT

The aim of this work was to investigate the interactions of anionic radionuclides ^{129}I, ^{77}Se (as a proxy for ^{79}Se) and ^{99}Tc with soil geocolloids under a range of conditions. These anionic fission products are of specific concern to policy makers regarding human and environmental risk assessments. Previous research has demonstrated strong links between soil organic matter (SOM) content and reduced mobility of these radionuclides. Negatively charged humic substances (HS), such as humic acid (HA) and fulvic acid (FA), may constitute 80% of organic matter and the mechanisms that allow anionic radionuclide to interaction with these HSs are not well understood. In the case of all three radionuclides, speciation plays a significant role in controlling their environmental mobility, therefore HPLC and SEC coupled to ICP-MS was used to monitor the speciation changes as the isotopes were progressively incorporated into HA. X-ray absorption spectroscopy was also employed in order to establish the solid phase speciation of Se after reaction with soil geocolloids.

Surface charge development of the HA significantly affected reaction with iodate ($^{129}IO_3^-$) and iodide ($^{129}I^-$). Iodide added to HA systems demonstrated slow oxidation and formation of organically bound iodine (Org-^{129}I) predominantly at higher pH (pH 6). Conversely IO_3^-, was rapidly transformed to form both I^- and Org-I. As pH decreased, the rate of this reduction reaction increased. Increasing HA concentration also increased the rate of IO_3^- reduction and formation of Org-I. Previous research has suggested that the most likely mechanism is IO_3^- reduction to I_2 or HOI which then binds with phenolic groups on OM forming Org-I species. However, IO_3^- was observed to rapidly bind to HA forming Org-I species with no initial evidence of I^- formation; I^- concentration then increased over time as Org-I decreased. Where Fe^{2+}/Fe^{3+} was present increased reduction

of IO_3^- to I^- was observed, mediated by association with HA, resulting in less Org-I formation overall. Instantaneous reaction of I^- with HA was observed in the presence of Fe^{2+}/Fe^{3+}, with bonding via cation bridging. Some I^- was subsequently re-released as I^- likely due to ongoing Fe hydrolysis. Modelling of the systems alone was successful and will assist the improvement of whole soil assemblage models.

Selenite ($Se^{(IV)}$) reaction with HA was most rapid at low pH, with minimal/no reduction occurring at > pH 6. Reduction of selenate ($Se^{(VI)}$) also occurred but this was less than for $Se^{(IV)}$, at low pH. No formation of $Se^{(VI)}$ from $Se^{(IV)}$ was observed, suggesting no oxidation took place, however some formation of $Se^{(IV)}$ from $Se^{(VI)}$ was observed, also the formation of an unknown Se species suspected to be organic in nature. Humic acid concentration had no significant effect on the rate of $Se^{(IV)}$ or $Se^{(VI)}$ reduction, suggesting that HA itself was not responsible for the reduction. X-ray absorption spectroscopy (XAS) demonstrated the potential for significant reduction to $Se^{(0)}$ at pH 4 and bonding through a Se-O-C chain. The role of microbial communities on $Se^{(IV)}$ and $Se^{(VI)}$ reduction in the HA systems was demonstrated through the use of soil inoculum and glucose additions in sterile and non-sterile systems. No reduction of $Se^{(IV)}$ or $Se^{(VI)}$ and bonding to HA was observed in filter and γ-irradiation systems. Additions of inoculum and glucose increased the rate of reduction. Additions of Fe^{2+} did not increase reduction of $Se^{(IV)}$ or $Se^{(VI)}$ when compared to non-sterile HA systems, however XAS analysis demonstrated formation of HA-Fe cation bridges.

No reaction of pertechnetate ($^{99}Tc^{(VII)}$) with HA was observed in these aerobic systems. An unknown Tc species was occasionally observed (<0.005 μ L^{-1}) and it is possible that this is an organic-Tc species. Significant incorporation of Tc into the solid phase was

observed in aerobic soils, with most Tc$^{(VII)}$ being retained in soils with high OM contents and low pH.

The mechanisms considered here build upon the basic processes considered in current biosphere models for I and Se. Assemblage models must be used in order to reliably model the interactions of elements within soils due to the complexity of the systems. In order to understand the long-term radiological risks associated with geological repositories, the fine-scale mechanisms must be understood geochemically across a range of different soil types and conditions. The effect of I and Se speciation on bioavailability in soils determines both the potential transfer of radioactive isotopes to the food chain from GDF's and from aerial sources of contamination. Alongside this, the work also has significant implications for advising on cost-effect fertiliser application methods for both I and Se, in order to tackle nutrient deficiencies worldwide.

ACKNOWLEDGEMENTS

I would also like to thank the following people on a personal note who have helped me achieve this PhD and so much more;

- The wonderful people I have met during my time at the University of Nottingham at both Undergraduate and Postgraduate who have supported me tirelessly over the past 6 years, in particular; Maisie Lord, Beth May, Leanne O'Brien, Georgina Feilding-Martin, Saskia Trewavas, Lara Gibson, Josie du Preez, Stuart Bagley, Alex Fletcher, Rosie Brian, Hannah Cooper, Steven Grundy, Dorien Vanhees, Nick Girkin, and many many more,
- My family and Alex Tremlett for believing in me, encouraging me to aim high, and for being proud even when it wasn't clear exactly what I was doing,
- Last but not least my science teachers; Mrs. Grunwald, Mrs. Williams, Mr Anderson, Mrs. Annable and Mr. Knight, for sparking my interest and encouraging me to pursue a career in Science.

CONTENTS PAGE

TABLE OF FIGURES

TABLE OF TABLES

GLOSSARY OF TERMS

B_T	blank titre volume (mL)
C	Concentration
Co	concentration of Se ($\mu g\ L^{-1}$)
$COOH_c$	concentration of carboxyl groups in solution (mol L^{-1})
$COOH_t$	total carboxyl content of HA or FA (mol kg^{-1})
C_V	crystal violet
ESS	error sum of squares
EXAFS	extended x-ray absorption fine structure
FA	fulvic acid
Fe_{MW}	molar weight of iron (g mol^{-1})
Fe_W	amount of iron (mg)
GDF	geological disposal facility
HA	humic acid
HA_s	concentration of HA in solution (g L^{-1})
HA_{WT}	weight of HA (g)
HF	hydrofluoric acid
HOI	Hypoiodous acid
HPLC	high throughput liquid chromatography
HS	humic substances
IDD	iodine deficient disorders
IR	infrared spectroscopy
K_1, K_2, K_3, K_4	rate constants (day^{-1})
K_a	acid dissociation constant
K_{int}	intrinsic dissociation constant
LCV	leucocrystal violet
M	molar concentration
n	number of wash steps
NMR	nuclear magnetic resonance
Occ	required carboxyl occupancy (%)
OM	organic matter
Org-I	Organic iodine species
pK_a	negative logarithmic of the acid dissociation constant
S_{em}	mass of Se (μg)
SF	sample factor

SOM	soil organic matter
S_T	sample titre volume (mL)
T_{acid}	total acidity (mol kg^{-1})
V	volume (mL)
V_{init}	initial sample volume (mL)
V_o	initial solution volume (mL)
V_p	volume of entrained liquid following centrifugation (mL)
V_{titre}	volume titrated (mL)
V_w	volume of wash solution (mL)
w	electrostatic interaction factor
XANES	x-ray absorption near-edge structure
XAS	x-ray absorption spectroscopy
γ	activity coefficient
γ-irradiated	Gamma-irradiated
Z	surface charge of HA or FA (mol kg^{-1})
Z_{Meas}	measured surface charge (mol kg^{-1})
Z_{Model}	modelled surface charge (mol kg^{-1})

BACKGROUND

The research presented here forms part of the Transfer Exposure and Effects (TREE) project as funded by the Natural Environment Research Council (NERC), the Environment Agency (EA) and Radioactive Waste Management Limited (RWM) under the Radioactivity and the Environment (RATE) program. The aim of the TREE project is to reduce the uncertainty surrounding radioactive risk assessments for humans and wildlife through understanding the underlying processes and mechanisms that lead to exposure. Research within the programme has focused on: the biogeochemical behaviour of radionuclides in soils, radionuclide transfer from soils-plants, exposure mechanisms for humans and wildlife, and prediction of the long-term environmental fate of key radionuclides. The research presented here forms a significant part of the investigations into the biogeochemical behaviour of radionuclides in soils, the aim of which is to be able to predict the behaviour of ^{129}I, ^{79}Se, ^{99}Tc and U isotopes in soils. From this the hope is that short term measurements, over 2.5 years, could be used to validate models to predict the long-term behaviour. A soils incubation experiment included 20 soils from the UK, and 10 soils from the Chernobyl Exclusion Zone (CEZ), with a range of characteristics (pH, OM content, Fe/Mn oxide content) from various land uses (woodland, grassland, arable). The field-moist soils were spiked with ^{129}I, ^{79}Se, ^{99}Tc and ^{238}U, incubated under aerobic conditions at 10°C, and sampled 15 times over the course of 2.5 years. At each time point the four analytes were fractionated and speciated. The data presented in this thesis report on the interactions between ^{129}I, ^{79}Se and ^{99}Tc and selected soil geocolloids (Humic and fulvic acid; Fe oxide) to complement the soils experiment. Working with single isolated geocolloids provided greater certainty in elucidating the interactions involved and enabled comparison of biotic and abiotic reaction mechanisms. Understanding the underlying reactions between radionuclides and

26

soils will enable further development of comprehensive soil assemblage kinetic models and thereby improve the validity of long-term predictions of radionuclide fate.

1. INTRODUCTION

1.1 RADIATION HAZARD

Radioactive waste has accumulated in the UK from a number of sources, the most predominant being the operation of nuclear power stations to generate electricity. In 2008 the UK government began a process to find a suitable underground location to store legacy waste in a Geological Disposal Facility (GDF) based on the initial 2008 White Paper titled *"Managing radioactive waste safely – A framework for implementing geological disposal"* (DEFRA and BERR, 2008). Many radiotoxic elements found in nuclear waste repositories invoke relatively little concern, due to their low mobility. However there are a number of radionuclides that are highly mobile and able to reach the biosphere, thus contributing to long-term exposure risks (Grambow, 2008). Release from GDF's is one way in which high risk radionuclides can enter the environment, other pathways include release from historic weapons testing and with the widespread development of nuclear power comes the inevitable, yet rare, nuclear accident. The world's most serious nuclear accident occurred in the Ukraine at the Chernobyl Nuclear Power Plant on 26 April 1986.The subsequent discharge resulted in the contamination of large areas of the northern hemisphere including Belarus, Russia, Poland, Norway, Sweden and parts of the UK (Collier & Davies, 1986). Across these countries soil types and properties vary, resulting in different environmental mobilities and therefore bioavailabilites of deposited radionuclides (Bell and Shaw, 2005). The fission and activation products that are of primary concern tend to be anionic radionuclides as migration times and distances can be large, these include; ^{129}I, ^{79}Se and ^{99}Tc (Grambow, 2008; Marivoet and Weetjens, 2012). Each of these radionuclides have long half-lives; 1.57 x 10^7, 3.27 x 10^5 and 2.13 x 10^5 respectively, and this combined with their high inventory in radioactive waste make them of specific

concern due to their environmental persistence and contribution to human and animal dose rates. Upon release from GDF's mobile anionic radionuclides can migrate to the surface where soil conditions pH, redox status, clay content, organic matter (OM) content and metal oxide content will play an important role in determining their mobility in the terrestrial environment.

1.2 HUMIC SUBSTANCES

Carbon stored in soil organic matter (SOM) is thought to exceed the amount stored in living vegetation by a factor of 2-3 (Schlesinger, 1990). Soil organic matter is predominantly composed of humus, 80% of which can be accounted for by macromolecular and colloidal humic substances (HS). The rate of formation of HS (humification) is determined by factors including climate, vegetation, parent material, topography and cropping (Tipping, 2002; Zech *et al.,* 1997). Humification results in dark-coloured, biologically refractory, heterogeneous organic compounds produced as by-products of microbial metabolism of plant and animal remains in soils (Sposito, 2008). Therefore HS structural composition varies significantly depending upon the nature of the organic inputs to the humification process. Humic substances can be divided into three operationally defined fractions: humin, humic acid and fulvic acid (Goure-Doubi *et al.*, 2014). Humin is insoluble in both acid and alkaline conditions and contains fibrous plant material and mineral-occluded hydrophobic constituents. Humic acid (HA) is the alkali-soluble fraction that is insoluble under acidic conditions and bridges the molecular-to-colloidal divide with an apparent molecular weight range of 100-700 kDa (Perminova *et al.,* 2003). The fulvic acid (FA) fraction has a lower molecular weight range (1-5 kDa) and is highly substituted with oxy-acid functional groups (more hydrophilic than HA) and so is soluble in both acidic and alkaline

conditions (Güngör & Bekbölet, 2010; Kamei-Ishikawa *et al.*, 2008). Humic and fulvic acids differ in quantity and chemical composition; consequently this heterogeneity makes chemically defining their structure and reactivity challenging (Traversa *et al.*, 2014). Infrared spectroscopy (IR) and nuclear magnetic resonance (NMR) can be used to investigate the functional groups present and the three-dimensional properties of HA and FA, which aids understanding of their behaviour in terrestrial and aquatic environments. In the same context the acid-base equilibrium of HA and FA is also important, as it provides useful information on the complexing abilities of HA. The proton equilibria of HA can be investigated by interpretation of potentiometric titration data, which provides information on the dissociation of functional groups with pH and can be extremely useful in modelling HS environmental behaviour. Humic substances participate in a variety of electron transfer reactions. Lovley *et al.* (1996) established that humic substances can act as electron acceptors for anaerobic microbial oxidation of organic compounds and, by also acting as an electron shuttle, can enable microbial humic-mediated reduction of metals. This functionality is due to the high proportion of oxygen-containing functional groups; i.e. phenol, hydroxyl, ketone and hydroquinone groups, which are capable of interacting with metal ions, metal oxides/hydroxides and minerals (Kerndorff and Schnitzer, 1980). By measuring the formal electrode potential of 3 standard humic acids, during titration with I_2, Struyk & Sposito (2001) were able to demonstrate that the oxidation capacity of a HA was positively correlated with the stable free radical (semiquinone) content. The structure of HS plays an important role in the functionality of the soil ecosystems as a whole, and is considered instrumental in determining the bioavailability of organic and inorganic substances therein (Piccolo, 2002).

1.3 IODINE IN THE ENVIRONMENT

Iodine is an essential nutrient for humans and animals, and severe deficiency can lead to iodine deficiency disorders (IDD) the most common of which is goitre; the hypertrophy of the thyroid gland (Fordyce, 2013; Fuge, 2005; Johnson, 2003b). The average stable iodine content of surface soils (top 15 cm) worldwide is quoted as c. 5 mg kg^{-1} (Fuge and Johnson, 1986; Johnson, 2003). Whitehead (1984) suggests UK soils have a mean concentration of 9.2 mg kg^{-1} due to proximity to the coast, high amounts of rainfall and relatively high SOM contents. However due to the skewed nature of the data Johnson (2003) suggests the geometric mean is probably closer to 3.0 mg kg^{-1} for the UK. Atmospheric iodine inputs are considered to be the most important factor that determines soil iodine concentrations (Whitehead, 1984). Most environmental iodine originates from the oceans, and following volatilisation, rainfall can then wash it out of the atmosphere (Fuge, 1996; Leblanc *et al.*, 2006). Due to the high inventory of oceanic iodine, coastal areas tend to have higher soil iodine concentrations than inland areas due to sea inundation of land, sea spray and rainfall (Bowley, 2013; Q. Hu *et al.*, 2009). The importance of rainfall can be demonstrated by the presence of 'rain shadows' where each side of a mountain receives different rainfall patterns that correlate directly with soil iodine concentrations (Fuge & Johnson, 2015; Slavin, 2005).

1.3.1 Anthropogenic [129]Iodine

Iodine-129 has been released through anthropogenic actions such as weapons testing (50-150 kg between 1945-1964), nuclear fuel reprocessing or nuclear accidents such as the Chernobyl accident that released a further 6 kg (Gómez-Guzmán *et al.,* 2014; Xu *et al.,* 2012). The naturally occurring inventory of [129]I has been estimated to be 230 kg,

from cosmic-ray spallation of Xe and fission of U in the geosphere (Fabryka-Martin *et al.*, 1985; Rao and Fehn, 1999). The largest sustained anthropogenic release of ^{129}I has been suggested to arise from nuclear fuel reprocessing plants such as Sellafield, England (Gómez-Guzmán *et al.,* 2014). Modelling of historic discharge data from Sellafield estimates that 1371 kg of ^{129}I was discharged between 1952 and 2004 into the NE Irish Sea, with a further 182 kg released to the atmosphere (Gómez-Guzmán *et al.*, 2014, 2013; López-Gutiérrez *et al.,* 2004). It is difficult to know the exact amount released as it wasn't monitored closely in the first few years. Worldwide it is estimated that 68,000 kg of anthropogenic ^{129}I has been produced in nuclear power reactors up until the year 2005, the majority of which is contained in spent fuel (Hou *et al.,* 2009). This substantial inventory and the long half-life of ^{129}I make it an important radionuclide in the safety case for nuclear waste disposal (Bostock *et al.*, 2003). Also as a constituent of thyroid hormones ^{129}I can accumulate in the thyroid gland and has been linked to increased occurrences of thyroid cancer (Amachi, 2008), for this reason is recognised as an important radionuclide when considering long-term health effects (Hu *et al.*, 2012).

1.3.2 Iodine species

Iodine is multivalent, and depending on the pH and redox status of the environment can be found in a range of inorganic and organic forms. The chemical form of iodine has a significant effect on its environmental behaviour and consequently its bioavailability (Dai *et al*., 2009; Hu *et al*., 2012). The primary inorganic species include iodide (I^-), iodate (IO_3^-) and elemental iodine (I_2), and when in contact with OM can also be found as organic-iodine species (Liu & Von Gunten, 1988; Yamada *et al.*, 2002; Yamada *et al*., 1999). Although both IO_3^- and I^- are monovalent anions they show significantly

different sorption mechanisms within environmental compartments, which has been verified by many laboratory studies and will be discussed further throughout this thesis.

1.3.3 Iodine in soil

The role soils and sediment fractions play in the environmental cycling and fate of iodine has been widely recognised (Amachi, 2008; Shetaya *et al.*, 2012; Yamada *et al.*, 1999; Yamaguchi *et al.*, 2010). Iodine can be significantly sorbed and accumulated within soils, however the interaction is strongly affected by various physiochemical parameters such as soil type, pH, redox potential (Eh), salinity, metal oxide content, and OM content. A number of studies have also discussed the interactions of microbial communities on the speciation and interaction of iodine with soils (Amachi, 2008; Seki *et al.,* 2013; Sheppard and Hawkins, 1995; Yamaguchi *et al.,* 2010).

1.3.3.1 Effect of soil redox status

Ashworth *et al.* (2003) found that the redox potential of a soil has a significant effect on iodine mobility. Through investigating the migration of ^{125}I through soil columns, it was observed that ^{125}I is mobile throughout the anoxic, saturated, low redox zone of the soil (bottom of column), but accumulates in the zone between anoxic and oxic soil where the Eh increases. This demonstrates that a decrease in Eh leads to an increase in iodine solubility and therefore greater plant availability. Release of iodine from soil to soil solution under anoxic conditions has been consistently reported with Hansen *et al.* (2011) demonstrating greater iodine mobility and availability in anoxic marine sediments in comparison to oxic sediments.

1.3.3.2 Iodine interaction with OM

It has long been recognised that soils with a high OM content, such as peat soils, often alongside a low pH, have a strong ability to retain iodine leading to the theory that iodine can interact significantly with OM, often binding as organic-iodine species therefore reducing its environmental mobility (Francois, 1987; Seki *et al.,* 2013; Whitehead, 1984, 1973; Xu *et al.,* 2013; Yamada *et al.,* 2002; Yamaguchi *et al.,* 2010). Francois (1987) discussed the potential redox reactions that could take place with IO_3^- and I^- in soils, whereby reduction of IO_3^- and oxidation of I^- leads to the formation of reactive intermediates such as I_2 and HOI that are then capable of binding with OM. This was elucidated through the use of a benzenediol, resorcinol, with its two electron-donor groups it is capable of undergoing electrophilic substitution with I_2 or HOI competitively instead of humics. Reduced iodine content in the humics demonstrated the presence of these electropositive iodine species as reactive intermediates. In addition to this the formation of I_2 and HOI during IO_3^- reduction by OM can be quantified by the oxidation of leucocrystal violet (LCV), by I_2 or HOI, to crystal violet (CV) measured by visible spectroscopy as demonstrated by Steinberg *et al*. (2008). Shetaya *et al*. (2012) also demonstrated the instantaneous conversion of added [129]I from inorganic into the organic phase when incubated with a range of soils under differing pH and temperature conditions. The most significant removal of [129]I from solution was observed in soils at high temperatures, low pH levels and high OM content. Yamaguchi *et al*. (2010) used a different approach involving x-ray absorption spectroscopy (XAS), namely K-edge X-ray absorption near-edge structure (XANES), to investigate the transformations of inorganic iodine in soils with varying OM contents and found that after 60 days incubation both I^- and IO_3^- were converted to Org-I species when the soils

contained a substantial amount of OM, compared to those with limited OM where added IO_3^- remained unchanged.

The iodination of humic substances is now widely accepted as the mechanism by which iodine interacts with SOM, yet there is still much to learn about the mechanisms involved. Schlegel *et al.* (2006) compared XANES data for naturally iodinated humic substances to organic iodine reference standards, and found structural features consistent with electrophilic substitution into organic molecules. The corresponding extended X-ray absorption fine structure (EXAFS) data indicated that iodine incorporated into humic substances is surrounded by carbon shells at distances corresponding to those for aromatic-bound iodine references. Reiller *et al.* (2006) and Xu *et al.* (2011) were both able to demonstrate that an increase in H/C ratio leads to a corresponding increase in iodination kinetics and organo-iodine i.e. increasing aromaticity of the OM, again highlighting the probability of a covalent aromatic C-I bond accounting for organo-iodine species in the field. The mechanisms associated with these interactions, especially the pH dependent kinetics, are poorly understood and there is little quantitative data from which to assess reaction rates and the inherent stability of the resulting organic complexes.

1.3.3.3 Iodine interaction with metal oxides

Metal oxides are also considered important in determining the environmental mobility of iodine species. Iron oxide and manganese oxide are two of the most important oxidants in the earth crust, and are highly abundant in natural environments. Not only are they capable of readily oxidising I^- to reactive intermediates for association with OM (Allard *et al.*, 2009; Gallard *et al.*, 2009), but they also have positively charged

surfaces available for association with anionic species (Whitehead, 1984). Kodama *et al.* (2006) used K-edge XANES to demonstrate the significant ability of ferromanganese oxides to selectively incorporate IO_3^- even when systems received additions of I^-, once again highlighting the strong capacity for oxidising I^- and I_2. Aluminium, iron and manganese oxides have all been recognised, to differing degrees, to play an important role in iodine dynamics within soils; for example there is much evidence describing the role of MnO_2 in increasing I reaction with OM through driving required redox reactions (Anschutz *et al.,* 2000). This association of I with metal oxides/hydroxides is highly pH dependent and sorption with Fe, Al and Mn hydroxides/oxides generally decreases with increasing pH. Organic matter in the presence of MnO_2 demonstrated increased iodination at pH 3-4 than without MnO_2, and showed a decrease as pH increased beyond pH 7 (Xu *et al*., 2011). Hematite demonstrated significant reaction with IO_3^- at pH levels below 9, by substitution for hydroxide ions on the surface, whilst above this showed a decrease (Couture and Seitz, 1983). This is due to the increased net positive charge of metal oxide surfaces at low pH, and decrease at high pH (Fuhrmann *et al*., 1998).

1.3.3.4 Role of soil microorganisms in iodine mobility

Microorganisms play a vital role in natural iodine cycling and therefore under certain conditions can determine the mobility and fate of iodine. Often, determining the role of microorganisms on interactions within soils involves autoclaving to remove all biological activity to see if this changes the mobility and fate of a specific element. Muramatsu *et al.* (2004) discussed the observed effects of autoclaving on both iodate and iodide sorption in soils, and found that iodide sorption was reduced by more than 80% in autoclaved soils. This is attributed to the destruction of microorganisms and the

products of microorganisms such as enzymes. This has also been documented by Seki *et al*., (2013) whereby autoclaving, heating and γ-irradiation were employed to destroy microorganisms. Both autoclaving and γ-irradiation (autoclaving to a greater degree than irradiation) have been shown to significantly alter the characteristics of OM by decreasing aromaticity and polycondensation and causing changes to the carbohydrate and N-alkyl regions of OM (Berns *et al.*, 2008). This can make it hard to determine whether the effects are solely biological. Alongside an inhibition in iodide sorption on soils it was acknowledged that there was a reduction in soil laccase activity. Upon addition of bacterial laccase back into the system after autoclaving, partial return of iodide sorption was observed. This highlights the importance of enzymes in the oxidation of iodide to reactive intermediates which can go on to associate with SOM. The effect of autoclaving on iodate sorption in soils differs from iodide; Yamaguchi *et al.* (2008) demonstrated that soils spiked with iodate showed no retardation of iodate transformation to Org-I when microbial activity was reduced by γ-irradiation. The summation of this evidence suggests that microbial activity has a significant effect on iodide sorption on soils through oxidation, yet little/no effect on iodate sorption and reduction.

1.4 SELENIUM IN THE ENVIRONMENT

Selenium is an essential dietary trace element; as a constituent of selenoproteins, Se has structural and enzymatic roles (Rayman, 2000; Vinceti *et al.*, 2014). Selenium is well known to be both toxic at high concentrations (> 400 µg day^{-1}) and to cause dietary deficiency at low concentrations (< 40 µg day^{-1}), with the range between these being the narrowest of all essential elements (Rayman, 2000). Environmental Se concentrations are determined predominantly by geological conditions, therefore Se

status varies widely worldwide (Fordyce, 2013). Selenium in rocks comprises 40% of Se in the Earth's crust, making biogeochemical processes such as the weathering of rocks and rock-water interactions the primary determinant of environmental Se concentrations (Rosenfield and Beath, 1964; Wang and Gao, 2001). World average Se soil concentrations are 0.01-2 mg kg^{-1}, with seleniferous soils containing 1-1,200 mg kg^{-1} and Se deficient soils 0.004-0.48 mg kg^{-1} (Fordyce, 2013). Given that the majority of environmental Se comes from rocks, Se deficiencies and toxicities are often determined by local biogeochemical characteristics. Organo-mineral associations are subject to environmental changes, therefore it is expected that climate change will inevitably have an effect on Se environmental behaviour (Tolu *et al*., 2014). Using moderate climate change scenarios for 2080-2099 Jones *et al*. (2017) predicts that as climate change continues, a decrease in soil Se concentrations will be seen with a corresponding increase in Se deficiency particularly in agricultural areas (66% of croplands predicted to lose 8.7% selenium), highlighting the increasing importance of understanding Se environmental mobility.

1.4.1 Se isotopes

Stable (non-radioactive) isotopes of Se dominate the environment with 73% of Se being found as ^{80}Se and ^{78}Se. Similarly to iodine, most other radioactive (unstable) Se isotopes are short-lived with half-lives ranging from 21 seconds to 121 days. Selenium-79 is the only radioactive isotope of serious environmental concern due to its long half-life and its β-emitting nature (Shaw and Ashworth, 2011).

1.4.2 Anthropogenic Se

Selenium has been released by a number of anthropogenic processes such as Se-rich coal combustion, wastewater discharge from oil refineries and release from radioactive waste repositories (Shaw and Ashworth, 2011). The latter is the primary source of ^{79}Se as a fission product of ^{235}U and is present in spent fuel and wastes in relatively large amounts. The yield of ^{79}Se from fission is relatively low at about 0.04% meaning that ^{79}Se is only found in significant quantities in spent fuel and wastes created by spent fuel reprocessing (Bienvenu *et al*., 2007; Shaw and Ashworth, 2011).

1.4.3 Selenium species

Like iodine the species that selenium is present as strongly determines the environmental mobility and consequently bioavailability. Selenium can exist in 5 chemical forms; selenide (Se^{2-}), elemental Se (Se^0), selenite (Se^{4+} or Se^{IV}), selenate (Se^{6+} or Se^{VI}) and organic Se. Most soluble selenium is considered to be in the form of Se^{VI}, whereas the less mobile Se^{IV} is normally bound within soils to OM, metal oxides and hydroxides, or mineral surfaces (Kamei-Ishikawa *et al.*, 2007; Zawislanski *et al*., 2003). Elemental Se (Se^0) is the least soluble Se species and considered the most stable.

1.4.4 Selenium in soil

1.4.4.1 Selenium interaction with OM

It is well documented that Se concentrations in soils and sediments correlates strongly with organic carbon content, highlighting the importance of OM in Se fixation (Dhillon and Dhillon, 1999; Li *et al*., 2017; Tolu *et al*., 2014; Wiramanaden *et al.*, 2010a, 2010b). Dutch soils containing low Se concentrations demonstrated a strong correlation between extractable organic carbon and Se concentrations, showing that Se present in

these soils is predominantly associated with OM (Supriatin *et al*., 2015). Tolu *et al.* (2014) in a similar study compared Se adsorption within a range of soils including agricultural, meadow and forest soils using HPLC-ICP-MS and demonstrated that Se in soils containing less than 20% OM was associated with crystalline oxy-hydroxides, whereas association with OM is important in soils with higher OM contents thus reducing Se leaching in podzol and peat soils. Selenium association with OM has been attributed to reactions with humic substances specifically, due to the functional groups present here being highly reactive. Selenium chemistry is analogous with sulphur chemistry, which makes it likely that when interacting with humic substances, Se could replace sulphur where sulphur is bonded to carbon on the surface. Kang *et al.* (1991) found that Se bound to the humic acid fraction was closely associated with the amino acids in the acid hydrolysate, and concluded that the Se most likely displaces sulphur in amino acids and forms seleno-amino acids. Gustafsson and Johnsson (1994) added labelled and unlabelled selenite to two forest floors and through sequential extraction were able to demonstrate significant incorporation into the humic fraction. Both the contribution of microbial reduction of selenite prior to association, and incorporation of inorganic selenite to metal-humic complexes were highlighted. Alongside this Coppin *et al.* (2009) concluded that Se interaction is mainly by indirect association through surface Fe oxides on OM; however, they did not completely rule out direct association. Meanwhile Martin *et al*. (2017) demonstrated the contribution of cation bridging in the association of Se with OM, highlighting the significant reaction of $Se^{(IV)}$ and the lack of $Se^{(VI)}$ association. The interactions of $Se^{(VI)}$ with OM is a topic of great uncertainty with much contradicting literature surrounding whether or not $Se^{(VI)}$ is capable of directly reacting with OM.

1.4.4.2 Selenium interaction with metal oxides

Metal oxides are ubiquitous in soil environments and have been shown to play a significant role in determining selenium bioavailability. There is much evidence surrounding the sorption of $Se^{(IV)}$ and $Se^{(VI)}$ on Al, Fe and Mn oxides under a range of conditions (Chan *et al.*, 2009; Peak, 2006; Rovira *et al.,* 2008; Scott and Morgan, 1996). Both $Se^{(IV)}$ and $Se^{(VI)}$ have demonstrated interactions with metal oxides, however it has been shown that $Se^{(IV)}$ is more strongly sorbed than $Se^{(VI)}$, which is thought to be due to $Se^{(IV)}$ being more polar than $Se^{(VI)}$ (Wiramanaden *et al.*, 2010b), with $Se^{(IV)}$ predominantly forming stronger inner-sphere complexes (Fernández-Martínez and Charlet, 2009). Unlike the reactions of $Se^{(VI)}$ with OM, there is much literature describing the reactions of $Se^{(VI)}$ with iron oxides. Selenate has been shown to be sorbed weakly by Fe-oxides such as goethite, however there has been much discussion as to whether this is by inner- or outer-surface complexes, with Peak and Sparks (2002) concluding that $Se^{(VI)}$ is capable of forming a mixture of both depending on the pH or ionic strength of the system. In the case of $Se^{(VI)}$ it has been shown that at pH levels above 6 outer-sphere complexes are likely to form, whereas below pH 6 inner-sphere complexes will form (Peak and Sparks, 2002). Selenite complexation with hematite and goethite is also significant, again predominantly at acidic pH, and tends to form $FeOSe(O)O^-$ complexes on hematite, and a combination of $FeOSe(O)O^-$ and $FeOSe(O)OH$ on goethite (Rovira *et al*., 2008).

1.4.4.3 Role of soil microorganisms in selenium mobility

The biotic processes determining Se environmental mobility are significant and have been widely documented, with microbial reduction of $Se^{(IV)}$ and $Se^{(VI)}$ to $Se^{(0)}$ being considered the most important process (Doran and Alexander, 1977; Li *et al*., 2017;

Lusa, 2015; Oremland *et al.*, 1989). During this reduction process there are a number of different bacteria and archaea that can use Se as a terminal electron acceptor thus driving this reaction (Oremland *et al.*, 1989). Alongside the microbial reduction to insoluble $Se^{(0)}$ it has been shown that due to the chemical similarities between selenium and sulphur, Se has been found to replace S where S is incorporated into amino acids forming selenoamino acids such as selenomethionine and selenocystein (Doran and Alexander, 1977; Turner *et al.*, 1998). Gustafsson and Johnsson (1994) demonstrated the role of microbial reductive incorporation of selenium into OM, specifically the low molecular weight fraction of humic substances. It was thought here that the main reductive mechanisms were biotically driven but that the underlying sorption to the humic substances was abiotic, demonstrating the biotic and abiotic connections and the complexity of this in terms of selenium mobility. Alongside microbial incorporation of Se into OM, it has been shown that biological volatilisation by microbes can also occur in soils and sediments whereby up to 30% of Se added has been transformed into volatile species and lost to the atmosphere (Cooke and Bruland, 1987; Hansen *et al.*, 1998). As previously discussed in the case of iodine, sterilisation is often used to determine the contribution of microbes to selenium reduction in soils. Soils that are sterilised show less reduction and retention of Se in soils; Lusa (2015) demonstrated that sterilised soils only sorbed 1% of the $Se^{(IV)}$ that was incorporated in the non-sterilised soils. However, once again these soils were autoclaved which provides problems with regards to OM structural changes. Darcheville *et al.* (2008) used irradiation to sterilise, which is considered to affect OM structure less (McNamara *et al.*, 2003), and found that soils lacking microbial activity retained less Se, and those that weren't sterilised retained more and the strength of retention was also greater, i.e. less exchangeable selenium.

1.5 TECHNETIUM IN THE ENVIRONMENT

Unlike iodine and selenium, technetium is an entirely artificial element the main sources of which are from nuclear power, nuclear weapons and medical applications. Therefore Tc found in the environment is always from anthropogenic sources (Garcia-León, 2005). Technetium is also known to only have radioactive isotopes, there are no stable Tc isotopes, with half-lives ranging from milliseconds to millions of years. The most environmentally relevant Tc isotope is ^{99}Tc due to its long half-life (2.13 x 10^5 years) and its inventory in nuclear waste. This long half-life ensures that once ^{99}Tc is released into the environment it remains over long time scales potentially providing a significant dose to humans and wildlife. A value of 9 kg of ^{99}Tc per 1 GW of energy per year has been estimated from PWR fuels, which was up scaled to a value of 15000 TBq of ^{99}Tc worldwide by 1983 (Luykx, 1986). Thirty-four years on this value has only continued to increase due to the rising concerns associated with using fossil fuels, resulting in a significant pool of ^{99}Tc within the environment.

1.5.1 Technetium species

Technetium can exist in valence states from +7 to -1, with the +4 and 0 states being the most stable. The most commonly released species of Tc into the environment is the highly mobile pertechnetate ion (^{99}Tc$^{(VII)}$O$_4^-$) which is produced during the processing of nuclear waste (Darab and Smith, 1996). The oxidation state of Tc is particularly important in determining the environmental behaviour of Tc chemical species (Begg *et al.*, 2007; Szecsody *et al.*, 2014).

1.5.2 Technetium in soil

1.5.2.1 Technetium interaction with OM

Technetium interaction with soils has received much attention over recent years, following discussions regarding the safe confinement of radioactive waste. Interactions between Tc and humic substances have been demonstrated (Geraedts *et al.*, 2002; Maes *et al.*, 2004), however before this can occur it has been shown that reduction from $Tc^{(VII)}$ to $Tc^{(IV)}$ must occur. The understanding is that under aerobic conditions Tc is present as the highly mobile $Tc^{(VII)}$, whereas under anaerobic or reducing conditions it is found as the less soluble reduced $Tc^{(IV)}$ (Bennett and Willey, 2003; Sheppard *et al.*, 1990). Stalmans *et al.* (1986) demonstrated that the OM fraction within soils plays an important role in immobilising Tc through association with HA. However experiments were run over a limited neutral to high pH range, and although the soil investigated was aerobic initially, the soils were flooded and kept under a N_2 atmosphere after $Tc^{(VII)}$ addition, therefore encouraging reduction. A study by Sheppard *et al.* (1990) however found no correlation between Tc immobilisation in anaerobic soils and OM content, with only a slight correlation in the aerobic soils. More recently Abdelouas *et al.* (2005) demonstrated through sequential extraction on a range of OM-rich soils that the majority of Tc was extracted alongside the OM fraction (60-66%) followed by 23-31% that was released with Fe-oxyhydroxides. Technetium interaction with humic acid specifically has been demonstrated; in the case of Sekine *et al.* (1993) association with HA was demonstrated at pH 4 in the presence of Sn^{2+} as a reducing agent, showing increasing Tc complexation with increasing concentrations of Sn^{2+}. However it appears as though when increasing the concentration of HA in solution alongside a range of Sn^{2+} concentrations, the residual Tc in solution (%) was greater at higher HA concentrations suggesting that HA concentration was not the determining factor, but

that the reduction step was most limiting. This is once again confirmed by Geraedts *et al.* (2002) who showed how in the presence of Gorleben groundwater (high natural HS content) $Tc^{(VII)}$ could be reduced with or without humic substances by the addition of a reducing surface, but in the presence of HS Tc-organic colloids associated with HS were precipitated. However, once again this was at neutral to high pH levels. EXAFS analysis of Tc in combination with humic substances demonstrated no direct connection between Tc and HS via a Tc-C bond as would be expected during complexation (Maes *et al.*, 2004), which has led to the theory that $Tc^{(IV)}$ oxidic polymers may interact with humic substances by colloid sorption. Although Tc interaction with humic substances specifically has been demonstrated in a number of studies, in all cases the Tc has undergone reduction prior to association.

1.5.2.2 Technetium interaction with metal oxides and ions

Alongside Tc interactions with OM, it is expected that Tc associations with metal oxides could be significant in soils containing high concentrations of metal oxides. Most evidence surrounding Tc interactions with metal ions involves $Fe^{(II)}$ acting as an electron donor and reducing $Tc^{(VII)}$ to $Tc^{(IV)}$ thus immobilising it under anaerobic conditions (Jaisi and Plymale, 2009; Li and Kaplan, 2012; Peretyazhko *et al.*, 2008; Thorpe *et al.*, 2014; Zachara *et al.*, 2007). The abiotic reduction of $Tc^{(VII)}$ by aqueous $Fe^{(II)}$ showed strong pH dependency, resulting in a precipitated $Fe/Tc^{(IV)}$ product (Zachara *et al.*, 2007). Using scanning transmission electron microscopy, Tc was shown to be associated with nanometre size $Fe^{(II)}$-rich particles when present at a high concentration in sediments, providing evidence for Tc reduction and association with metal ions (Druteikiene *et al.*, 2014). It was also demonstrated that when precipitated in this form rather than as $Tc^{(IV)}O_2 \cdot nH_2O$ it was much less likely to remobilise when

conditions were oxidising (Jaisi and Plymale, 2009; Zachara *et al*., 2007), thus keeping the Tc immobilised. Iron oxides, hydroxides and (oxy)hydroxides have all been shown to significantly reduce $Tc^{(VII)}$ to $Tc^{(IV)}$ in solution, and reduce re-oxidation, thus have been considered as a potential component of barrier systems for geological disposal of nuclear waste because of this (Jaisi and Plymale, 2009; Um *et al.,* 2011).

1.5.2.3 Role of soil microorganisms in technetium mobility

Whilst there is much evidence for Tc reduction by metal oxides, there is also significant evidence surrounding microbial reduction, whether that is directly (i.e. during respiration or enzyme-mediated) (De Luca *et al.*, 2001; Lloyd *et al.*, 1999), or indirectly (i.e. through microbial alteration of the redox potential) (Tagami and Uchida, 1996; Thorpe *et al.*, 2014). Abdelouas *et al*. (2005) demonstrated that the presence of metal- and sulphate-reducing bacteria has a significant effect on the reduction and immobilisation of Tc in soils with a high OM content. In systems without these microorganisms (0.22µm sterilisation) $Tc^{(VII)}$ was not reduced and therefore remained mobile in solution. The role of hydrogenase in the reduction of $Tc^{(VII)}$ is well documented. The enzyme hydrogenase uses hydrogen as an electron donor in the reduction of $Tc^{(VII)}$, and in experiments with microbial communities with and without functioning hydrogenase production, $Tc^{(VII)}$ reduction is present in communities capable of production, and absent in communities that are not (De Luca *et al.*, 2001; Lloyd *et al.*, 1999). Istok *et al.* (2004) demonstrated a lack of $Tc^{(VII)}$ reduction in the absence of a electron donor, however in the presence of a suitable donor and NO_3^-, denitrification occurred and concomitantly $Tc^{(VII)}$ reduction. This suggests that microbial reduction of Tc is predominant in environmental systems, whereas chemical reduction plays a less significant role. Reduction of $Tc^{(VII)}$ in microbially $Fe^{(III)}$-

reducing sediments was shown to be the most significant reduction mechanism by Burke *et al.* (2010) where both microbially-active reducing sediments and pre-reduced sediments showed significant removal of Tc within 10 mins to 36 days. The ability of microorganisms to directly or indirectly drive reduction of $Tc^{(VII)}$ within soils and sediments is so reliable at immobilising Tc that it is being investigated as a means of bioremediation for Tc contaminated environments (De Luca *et al.*, 2001; Marshall *et al.*, 2008; Wildung *et al.*, 2000). Newsome *et al.* (2017) investigated the potential of microbially-mediated reducing conditions in the *in situ* bioremediation of $Tc^{(VII)}$ through using alternative slow release electron donor and chemical reduction based substrates. They were able to demonstrate not only the precipitation and consequent immobilisation of $Tc^{(VII)}$ as $Tc^{(IV)}$ but also the resilience of these formed hydrous $Tc^{(IV)}$-oxides and $Tc^{(IV)}$-sulfides to reoxidation, providing evidence for how the microbially induced reduction of $Tc^{(VII)}$ could be used as a viable bioremediation technique.

1.6 AIMS

Iodine, selenium and technetium are all key radionuclides of concern with regards to nuclear waste disposal due to their environmental persistence. Soil properties affect the speciation of these 3 elements and therefore their mobility and bioavailability. The OM content, metal oxide content and pH of a soil have been recognised as some of the most important factors governing their transformations within the soil ecosystem. There is limited data regarding the interactions of these 3 radionuclides with OM specifically, in its purest forms of humic acid and fulvic acid, alone and in combination with metal oxides at different pH levels. Through investigation of the abiotic interactions between these radionuclides and OM, it will allow a better understanding of the interactions within soil environments as a whole. Currently the TREE project is developing

predictive models for these radionuclides based on data collected from 30 different soils with varying properties including OM content, metal oxide content, pH and texture. The interactions with HA and FA investigated here under varying pH conditions will allow a better understanding of the short- and long-term fate of these elements when released from underground sources and aerially deposited loads.

In this work, four main questions are explored:

1. How do environmental factors such as pH and temperature influence the interactions of I, Se and Tc with soil humic and fulvic acids?

2. How does the presence of metal ions affect the interactions of I, Se and Tc with humic and fulvic acids?

3. How do the interactions with HA and FA compare to interactions within whole soils?

4. Can the interactions observed be reliably modelled, alone and in combination with whole soil data, to allow prediction of the fate of these elements?

2. MATERIALS AND METHODS

2.1 INTRODUCTION

Humic and fulvic acids used in this work were extracted from an Irish moss peat purchased from Sycamore Trading, County Derry, Ireland. Irish moss peat has a high OM content allowing maximum HA and FA extraction yield. Sample extraction and processing are detailed below. Purifying HA and FA of inorganic impurities is vital in order to avoid complications and errors associated with the analyses of HA (Malcom, 1976). This chapter describes methods used throughout the work to extract and purify the HA and FA. The analytical methods used to assay I, Se and Tc are also described.

2.2 HUMIC ACID EXTRACTION

Humic acid (HA) was extracted from Irish moss peat soil according to the procedures recommended by the International Humic Substances Society (IHSS). Approximately 300 g of <2 mm sieved peat was saturated with 1 L of 1 M NaOH and then made to 10 L with 0.1 M NaOH under an N_2 blanket, giving an extractant-to-peat ratio of 10:1. Intermittent shaking for 4 h ensured complete mixing prior to leaving overnight under N_2. The supernatant was then siphoned off from the humin before acidification with constant stirring to pH 1 with 6 M HCl to precipitate the HA. This was then left for 12-16 h to allow the HA to settle. The supernatant (which contains the fulvic acid fraction) was decanted and retained for further processing while the HA floc was centrifuged (Model Z 400, Hermle) at 25,000 rpm for 15 minutes in order to completely remove all supernatant, which was added to the FA stock. The precipitated HA fraction was then re-dissolved in the minimum amount of 0.1 M KOH, under an N_2 blanket, to pH 13, before solid KCl was added to give a concentration of 0.3 M $[K^+]$. The solution was then

centrifuged to remove suspended inorganic solids and acidified to pH 1 by adding 6 M HCl, to re-precipitate the HA. The suspension was left to stand for another 12-16 hours before the supernatant was discarded. The HA was then mixed with Milli-Q water (18.2 MΩ cm) to generate a slurry before it was transferred to 10,000 Dalton visking dialysis tubing against Milli-Q water. Dialysis was continued, with frequent replacement of Milli-Q water, until a negative Cl-test with silver nitrate ($AgNO_3^-$) was achieved. The HA was then transferred into universal tubes and frozen at -84°C prior to freeze drying (Model Alpha 2.4, Christ).

2.3 FULVIC ACID EXTRACTION

2.3.1 Column Preparation

The supernatant collected following the initial acid-precipitation of HA contains the FA fraction. To separate the FA from salts present following HA flocculation the supernatant must be passed through a Superlite DAX-8 resin (Sigma-Aldrich, U.K.) column (50 mL) before acidification of the FA functional groups by passing through an Amberlite IR-120 (Sigma-Aldrich, U.K.) column (50 mL). The FA must be passed through both columns in quick succession in order to reduce organic oxidation by oxygen uptake under alkaline conditions (Malcom, 1976), therefore both must be prepared at the same time.

To prepare the columns, a small amount of quartz wool was placed in the bottom of two 60 mL polypropylene syringes before the resins were added with a 2-3 cm head of Milli-Q water to ensure that they remained wet. The Superlite DAX-8 resin was soaked in methanol for 15 min in a fume hood before the methanol was decanted and replaced with Milli-Q water for 10 min to ensure that it was sufficiently wet. The Amberlite IR-120 resin initially in the Na^+ form was washed with 5-10 column volumes of 0.1 M HCl to

convert the strong acid sulphonate groups to the H^+ form. It was then washed through with Milli-Q water to remove extraneous Cl^- ions, before being ready to use. It was wetted with Milli-Q water for 15 minutes prior to use. Approximately 0.15 mL of Superlite DAX-8 resin is required per gram of initial sample dry weight; for the peat FA 50 mL was enough to process 1 L of FA solution.

2.3.2 DAX-8 Resin Column Procedure

Acidification with HCl was used to separate FA from HA resulting in an excess of NaCl is the FA fraction. The FA solution was passed through the Superlite DAX-8 column at a flow rate of 15 bed volumes per hour, whilst collecting the effluent which was discarded. The column was then washed with Milli-Q water in order to wash out the excess NaCl. Desorption of FA from the Superlite DAX-8 resin with 1 column volume of 0.1 M NaOH and 2-3 column volumes of Milli-Q water was performed in order to increase recovery of the hydrophobic FA by concentrating the FA into a smaller volume (Thurman and Malcolm, 1981).

2.3.3 Amberlite IR-120 Column Procedure

The eluate from the Superlite DAX-8 column was passed through the H^+-Amberlite IR-120 column in order to convert the sodium salt of the FA to its free-acid form (hydrogen saturated) (Thurman and Malcolm, 1981). It was then divided into polypropylene tubes and frozen before being freeze dried (Model Alpha 2.4, Christ) until constant weight was achieved (typically 4 – 5 days).

2.4 HUMIC AND FULVIC ACID CHARACTERISATION

2.4.1 Carbon and Nitrogen Content

To determine the carbon, nitrogen and sulphur content of the HA and FA, 8.22 mg of HA was weighed directly into a tin capsule and combusted at 900-1000°C using an Organic Elemental Analyser (Model Flash 2000, CE Instruments).

2.4.2 Ash Content

Samples were dried at 105°C for 24 hours to removal all moisture. Ash content by was determined by combustion at 550°C for 4 hours in a muffle furnace (AAF 1100, Carbolite) (Stevenson, 1982).

2.4.3 Total elemental composition

Total elemental composition of the HA and FA was determined by ICP-MS following nitric acid digestion of the purified fractions. Approximately 50 mg ($\pm$1.8 mg) was weighed directly into Teflon microwave digestion tubes with 2 mL of HNO_3 (70% Trace Analysis grade), 1 mL H_2O_2 and 1 mL Milli-Q water. The samples were then digested with microwave heating (Anton Paar, Multiwave-3000 fitted with a 48-place rotor) at 1400 W for 90 minutes. Digested samples, once opened in a fume hood, were diluted with 15 mL Milli-Q water and transferred into polypropylene tubes. A 1:10 dilution of the samples with Milli-Q water was undertaken immediately prior to ICP-MS analysis (Section 2.6.2).

2.4.4 Multi-elemental analysis

Multi-element analysis of diluted solutions was undertaken by ICP-MS (Thermo-Fisher Scientific iCAP-Q; Thermo Fisher Scientific, Bremen, Germany). Samples were

introduced from an autosampler (Cetac ASX-520) incorporating an ASXpress™ rapid uptake module through a PEEK nebulizer (Burgener Mira Mist). Internal standards were introduced to the sample stream on a separate line via the ASXpress unit and included Sc (20 µg L^{-1}), Rh (10 µg L^{-1}), Ge (10 µg L^{-1}) and Ir (5 µg L^{-1}) in 2% trace analysis grade (Fisher Scientific, UK) HNO$_3$. External multi-element calibration standards (Claritas-PPT grade CLMS-2 from SPEX Certiprep Inc., Metuchen, NJ, USA) included Ag, Al, As, B, Ba, Cd, Ca, Co, Cr, Cs, Cu, Fe, K, Mg, Mn, Mo, Na, Ni, P, Pb, Rb, S, Se, Sr, Ti (semi-quant), U, V and Zn, in the range 0 – 100 µg L^{-1} (0, 20, 40, 100 µg L^{-1}). A bespoke external multi-element calibration solution (PlasmaCAL, SCP Science, France) was used to prepare Ca, Mg, Na and K standards in the range 0-30 mg L^{-1}. Phosphorus, B and S calibration utilized in-house standard solutions (KH$_2$PO$_4$, K$_2$SO$_4$ and H$_3$BO$_3$). In-sample switching was used to measure B and P in STD mode, Se in H$_2$-cell mode and all other elements in He-cell mode. Sample processing was undertaken using Qtegra™ software (Thermo-Fisher Scientific) utilizing external cross-calibration between pulse-counting and analogue detector modes when required.

2.4.5 Iodine and Selenium Content

TMAH-extractable I and Se were determined after dissolving 50 mg (±1.30 mg) of HA in 2 mL 5% TMAH in polypropylene tubes before being left for 20 minutes with occasional agitation. An aliquot of 8 mL Milli-Q water was added to make a final solution of 1% TMAH which was then analysed by ICP-MS without further dilution (Section 2.5.1).

2.5 ICP-MS for quantification

ICP-MS is commonly used for the determination of I, Se and Tc in environmental samples typically with typical detection limits of 0.0051-0.3 µg L^{-1} for ^{129}I (Brown, Geiszler and Lindberg, 2007; Shetaya et $al.$, 2012), 0.016-0.086 µg L^{-1} for ^{77}Se (Peng et $al.$, 2015; Paul, 2016) and 0.2-47 ppt for ^{99}Tc (Rameback et $al.$, 1998; Más et $al.$, 2002). There are a number of factors to consider when measuring I, Se and Tc in environmental samples including matrix matching, interferences from isotopes of other elements and polyatomics formed in or after the plasma. The major interferences include ^{129}Xe^{+}, ^{127}IH$_2$+ and ^{127}ID^{+} ions for ^{129}I (Izmer et $al.$, 2004; Reid et $al.$, 2008; Ohno et $al.$, 2013), ^{40}Ar^{36}ArH^{+}, ^{38}Ar$_2$H^{+} and ^{40}Ar^{37}Cl^{+} for ^{77}Se (Hinojosa Reyes et $al.,$ 2003), and ^{99}Ru, ^{98}MoH, ^{59}Co^{40}Ar, ^{87}Sr^{12}C, ^{87}Rb^{12}C, ^{43}Ca^{16}O^{40}Ar, ^{40}Ar^{18}OH and ^{40}Ca^{18}OH^{40}Ar for ^{99}Tc (Keith-Roach et $al.$, 2002; Más et $al.$, 2002).

2.5.1 Totals analysis

All ICP-MS analysis was carried out at the University of Nottingham on a Thermo-Scientific iCAPQ. The instrument was run employing three operational modes, including (i) a collision-cell using He with kinetic energy discrimination (He-cell) to remove polyatomic interferences when determining ^{99}Tc, (ii) standard mode (STD) in which the collision cell is evacuated for total ^{129}I and (iii) hydrogen mode (H$_2$-cell) in which H$_2$ gas is used as the cell gas for total ^{77}Se and speciation analysis of ^{129}I and ^{77}Se. Internal standards included ^{103}Rh, ^{185}Re and ^{115}In, in a matrix of 2% TMAH and 4% methanol for ^{129}I analysis. Sample and wash matrices were 1% TMAH to ensure full wash-out of I between samples. Internal standards for ^{77}Se and Tc analysis were ^{103}Rh and ^{185}Re prepared in a 2% HNO$_3$ matrix. Selenium and Tc analysis was performed with sample matrices of 2% HNO$_3$ to ensure full wash-out between samples.

2.5.1 Isotopic Spikes ^{129}I, ^{77}Se and ^{99}Tc

An ^{129}I stock standard was obtained from High Technology Sources Ltd, UK, provided as a 5 mL ampoule in the I$^-$ form and was made up to 100 mL with 0.01 M NaOH for storage in a lead safe in a radiation laboratory. Working standards for ^{129}I were prepared from this stock. Oxidation of the ^{129}I$^-$ stock to form ^{129}IO$_3^-$ was performed by first neutralising 100 mL of the ^{129}I$^-$ stock with 0.1 M HCl, then immediately adding 10 mL 0.2 M chlorite for oxidation.

Selenium-77 standards were purchased from Isoflex, USA, and were prepared from an elemental stock of enriched ^{77}Se^0 (50 mg: 99.2 % isotopic enrichment) as per Collins *et al.*, (2006). The ^{77}Se$^{(IV)}$ was prepared by dissolving ^{77}Se^0 in 70% HNO$_3$ in a conical flask and heating at 60°C on a Teflon-coated block digester until all liquid was evaporated. The remaining material was dissolved in 2% HNO$_3$ and stored in the dark at room temperature. To prepare the ^{77}Se$^{(VI)}$ stock, ^{77}Se^0 was dissolved in 30% H$_2$O$_2$ and 2.0 M KOH in a conical flask and heated at 90°C on a Teflon-coated graphite block digester until all the liquid was evaporated. The remaining material was dissolved in 30% H$_2$O$_2$ and heated at 90°C, this was repeated thrice. The remaining material was then dissolved in 2% HNO$_3$ and also stored in the dark at room temperature. The concentrations of the final stock solutions were 231 mg L^{-1} for ^{77}Se$^{(IV)}$ and 259 mg L^{-1} for ^{77}Se$^{(VI)}$.

Technetium-99 standards were purchased from the American National Institute of Standards (NIST), U.S.A, and provided as a 5 mL ampoule of ^{99}Tc in 0.001 M KOH. This was transferred into a 100 mL volumetric flask and diluted with Milli-Q water. Stored in a lead safe in a radiation laboratory at room temperature.

2.5.2 Solution phase speciation

Chromatography to separate *inorganic* I and Se species was undertaken using HPLC (Dionex, ICS-3000) coupled to the ICP-MS with a Hamilton PRP *x*-100 column (5 μm, 4.1 x 100 mm). Samples (100 μl) were injected into an eluent (50 mM ammonium nitrate, 2% methanol, 1 x 10^{-5} EDTA, adjusted to pH 9 using TRIS buffer) at a flow rate of 1.6 mL min^{-1} eluent. Good separation was achieved within 320 seconds. Inorganic Tc species were separated independently of I and Se in the same way using a Hamilton PRP x-50 column (5μm, 4.1 x 50 mm) with an eluent (50 mM ammonium perchlorate) flow rate of 1 mL min^{-1}. Species-specific standards of $^{129}IO_3^-$ and $^{129}I^-$ at 1-10 μg L^{-1}, $^{77}Se^{(IV)}$ and $^{77}Se^{(VI)}$ at 1-5 μg L^{-1}, and $^{99}TcO_4^-$ at 1 μg L^{-1}, freshly prepared in Milli-Q water were used for calibration. Data processing was carried out for all species using Plasmalab software (Version 2.5.1.276). Organic species formation was calculated from a mass balance as shown here for I (Eqn. 1.1).

$$Org\text{-}^{129}I = {}^{129}I_A - {}^{129}I_F \tag{1.1}$$

Org-^{129}I is the estimated concentration of organic I formed (μg L^{-1}), $^{129}I_A$ is the total inorganic I spike added either as $^{129}IO_3^-$ or $^{129}I^-$ (μg L^{-1}), and $^{129}I_F$ is the total inorganic I species formed ($^{129}IO_3^-$ plus $^{129}I^-$, μg L^{-1}). Drift correction was applied using standards repeated regularly throughout the analysis.

2.5.3 Organic iodine and selenium speciation

Further chromatographic investigation to verify the presence of high MW *organic* iodine species employed size exclusion chromatography (SEC-ICP-MS) with a Superose 12 10/300 column (GE Healthcare) with a 100 μl injection into the same eluent used for separation of the inorganic species (Section 2.5.2) flowing at 1 mL min^{-1} over 2000 s.

3. CHARACTERISATION OF HUMIC AND FULVIC ACID

3.1 INTRODUCTION

Humic substances (HS) have a significant effect on the mobility of cationic and anion species, due to their ubiquitous occurrence in the environment (Baidoo *et al*., 2014; Benedetti *et al*., 1996; Tipping, 1994). The acid-base characteristics of HS, can be determined by potentiometric titration against a standard acid to quantify surface chemistry and predict their environmental behaviour (Avena *et al.*, 1999; Baidoo *et al.*, 2014; Gamble, 1972). Characterisation of surface charge is also the logical first step in the application of surface complexation models as the degree of negative charge on HS will affect the kinetics of anion reduction and binding (Lützenkirchen, 1999).

Humic moieties are weak acid polyelectrolytes that deprotonate less readily than strong acids and will therefore be only partially dissociated at intermediate pHs (Fukushima *et al*., 1995). Carboxyl and phenolic hydroxyl groups on HA and FA, dissociate at different pHs (Baidoo *et al.,* 2014). It can be difficult to quantify the separate contributions of carboxyl and phenolic groups to the total acidity of HA and FA. It is often assumed that all carboxyl groups are dissociated by pH 8.0 (Santos *et al*., 1999) with phenolic groups dissociating between pH 8.0 and pH 10.0 (Bowles *et al*., 1994) with some overlap around pH 8.0. Baidoo *et al.* (2014) successfully employed potentiometric titration methods, similar to those employed in this study, for quantification of acidic groups present on tropical humic acids. He estimated the phenolic content as half the measured carboxyl content due to uncertainties in calculations above pH 8. Numerical models that optimise the proportions of carboxyl and phenolic groups as model parameters in fitting the charge curves can also be used to determine the relative contributions of phenolic and carboxyl groups to HS surface charge development (Ritchie and Perdue, 2003; Weber *et al.*, 2006).

The monitoring of HS charge development with pH allows consideration of surface charge in terms of ion bonding to HA and FA. Dissolved I, Se and Tc are anionic and therefore most likely to interact with HA and FA when the negative surface charge is at a minimum. To understand the interaction of I, Se and Tc with natural humic substances rapid forward titrations of extracted HA and FA were performed, and an empirical pH-based method used to obtain estimates of total acidity (charge density at pH 8) and descriptive titration curves.

3.2 AIMS AND OBJECTIVES

The aim of this work was to characterise how the HA and FA surface charge changes as a function of pH and ionic strength.

The specific objectives were to:

1. Reliably estimate HA and FA total acidity;

2. Establish changes in HA and FA surface charge as a function of pH and ionic strength;

3.3 MATERIALS AND METHODS

3.3.1 Total Acidity

The total acidity of the extracted HA and FA was determined using a modified version of the barium hydroxide method proposed by Schnitzer and Khan, (1972). Freeze dried HA (0.05 g) and FA (0.03 g) was dissolved in 5 mL of 0.1 M NaOH, and shaken for 1 hour. Barium chloride (2.5 mL, 0.2 M) was then added before the tubes were flushed with N_2 and shaken overnight. The suspension was then centrifuged at 1500 rpm for 15

minutes, and 5 mL of the supernatant collected for titration. For titration, 55 mL of 1 M NaCl was added to the 5 mL of HA/FA supernatant in a beaker titrated under N_2 whilst stirring down to pH 2.64-2.44 with 0.2 mL additions of 0.1 M HNO_3. Blank titrations were also conducted and the volume of acid required to titrate to the pH in the equivalent HA/FA titration was recorded. The difference between sample and blank titrations was used to obtain total acidity (mol kg^{-1}) (Eqn. 3.1):

$$T_{acid} = \frac{B_T - S_T \text{ x } S_F}{HA_{wt} \text{ x } 1000} \tag{3.1}$$

Where B_T is the blank titre (mL), S_T is the sample titre (mL), HA_{wt} is the weight of humic acid used (g), and S_F is the sample factor (Eqn. 3.2):

$$S_F = \frac{V_{init}}{V_{titre}} \tag{3.2}$$

Where V_{init} is the initial sample volume (mL), and V_{titre} is the volume titrated (mL).

3.3.3 Surface Charge Model Development

Information to parameterise a surface charge model was collected by titrating 0.05 g of HA dissolved in 5 mL of 0.1 M NaOH from pH 11.0 to pH 2.0 at three ionic strengths (65 mL of 0.1, 0.05 and 0.01 M NaCl), pH was recorded after each 0.1 mL addition of 0.1 M HNO_3.

Ionic strength (I) was calculated using the sum of the concentration of all ions in solution (C, mol L^{-1}) multiplied by their valence squared (z^2) according to Eqn. 3.3:

$$I = \frac{1}{2}\Sigma C_i z_i^2 \qquad (3.3)$$

Which was approximated for a monovalent electrolyte as Eqn. 3.4:

$$I = \Sigma C_{Cation} \qquad (3.4)$$

From the ionic strength the activity coefficient (γ) of the HA was calculated according to Eqn. 3.5:

$$\gamma = 10^{-0.509 \times \frac{\sqrt{I}}{1+\sqrt{I}} - 0.3I} \qquad (3.5)$$

The humic surface charge (Z) was calculated from Equation 3.6, after conversion of H^+ and OH^- activity, to concentrations (Eqn. 3.6):

$$Z = \frac{[OH^-] + [NO_3^-] - [H^+] - [Na^+]}{[HA]} \qquad (3.6)$$

The negative logarithm of the acid dissociation constant (pK_a) was defined as (Eqn. 3.7):

$$pK_a = -\log_{10} K_a \qquad (3.7)$$

Where:

$$K_a = \frac{[A_i^-][H^+]}{[HA]} \qquad (3.8)$$

and Ka is the acid dissociation constant and A_i^- represents deprotonated groups on the humic acid.

A second method to calculate change in surface charge as a function of pH is to determine the difference in acid addition required for a sample and blank titration to achieve a desired pH. (Eqn. 3.9):

$$Z = \frac{(B_T - S_T)[Acid]}{Mass}$$

(3.9)

Where Z is the HA/FA surface charge, B_T is the acid volume used for the blank titration (mL), S_T is the acid volume used in the sample titration (mL) multiplied by the acid concentration (M) and divided by the mass (g) of HA/FA used.

3.3.4 Calculation of Model Optimised Parameter Values

The proton binding groups of humic substances are heterogeneous, and therefore have a range of intrinsic pK values. Two types of acid groups are distinguished, carboxyl (Type A) and phenolic hydroxyl (Type B), which are each then subdivided into four different sub-groups assumed to be present in equal amounts. The proportion of Type A and B groups (mol kg^{-1}) assumes that Type B groups contribute one third of the total acidity, and Type A the remaining two thirds. Each of the 4 sub-groups will have a median pK_A or pK_B value and a spreading factor (ΔpKA and ΔpKB) that define a range of 4 pK_a values around the mean intrinsic pK value. These pK values are calculated from Eqn. 3.10:

$$pK = pK_{int} + wZ$$

(3.10)

Where K_{int} is the intrinsic dissociation constant, w is the electrostatic interaction factor (Equ 3.11), and Z is the surface charge (mol kg^{-1}).

$$w = P log_{10} I \exp(Q|Z|) \tag{3.11}$$

where I is the ionic strength (M), and P and Q are fitted parameters.

The surface charge contribution of each of the sub-groups is calculated at each pH (Eqn. 3.12 and 3.13):

$$Z = [A_1^-] + [A_2^-] + [A_3^-] + [A_4^-] + [B_1^-] + [B_2^-] + [B_3^-] + [B_4^-] \tag{3.12}$$

$$[A_1^-] = \frac{T_{A1}}{1+\left(\frac{K_{int}10^{-wZ}}{(H^+)}\right)} \tag{3.13}$$

Where [A$_1^-$] is the surface charge of the type A sub-group 1, [B$_1^-$] is the surface charge of type B sub-group 1 etc., T$_{A1}$ is the total concentration of Type A sub-group 1 (mol kg^{-1}), K$_{int}$ is the intrinsic dissociation constant, w is the electrostatic interaction factor (see Equ 3.11), and Z is the charge (mol kg^{-1}).

The surface charge across all 8 acid groups was summed to give a Model Charge value (mol kg^{-1}) at each pH. The error sum of squares (ESS) for each pH was also calculated (Eqn. 3. 14):

$$ESS = (Z_{Meas} - Z_{Model})^2 \tag{3.14}$$

Where both the surface charge (Z_{Meas}) and model charge (Z_{Model}) are in mol kg^{-1}. The electrostatic factor (P) (Eqn. 3.11), which accounts for non-uniform charge distribution around humic molecules, average intrinsic pK values, and the spreading factors were optimised based on the ESS in order to establish the best model fit to the measured data at each ionic strength.

By including the proportion of Type A (and B) groups as an optimised value (T_{Prop}), it is possible to further refine the model fit (Eqn. 3. 15 and 3.16):

$$T_A = T_{acid} \times T_{Prop} \tag{3.15}$$

$$T_B = T_{acid} \times (1 - T_{Prop}) \tag{3.16}$$

4.5 Surface Charge Prediction Model

Fixing the Type A and Type B groups, means that optimising the ESS enables reliable prediction of the surface charge of the HA or FA based on the pH and the ionic strength.

$$[A_1^-] = \frac{T_{A1}}{1 + \left(\frac{K_{int}10^{-wz_{in}}}{(H^+)} \right)}$$

$$Z_{out} = \sum_{n=1}^{4}[A_n^-] + \sum_{n=1}^{4}[B_n^-]$$

Is $Z_{in} = Z_{out}$?

Yes   No
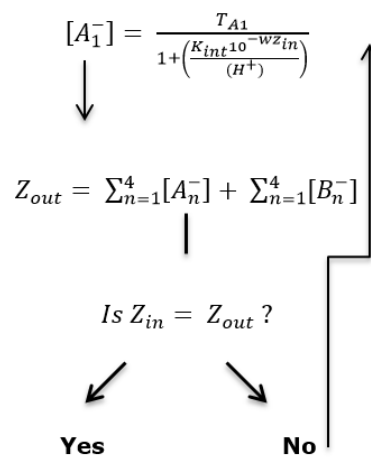
Figure 3.1. Schematic of the model structure used to optimise the ESS for model optimisation.

The measured surface charge (Z_{in}) was therefore optimised against the modelled surface charge (Z_{out}) output by minimising the ESS (Figure 3.1).

3.4 RESULTS AND DISCUSSION

3.4.1 Humic acid composition

The nature of the parent material and the purification steps undertaken during extraction and preparation (Section 2.4) have resulted in a relatively pure HA sample (**Table. 3.1**).

Table 3.1. Measured characteristics of humic acid (HA) collected from Irish moss peat.

Characteristic	Value	Units
Ash Content	0.056	%
C	48.71	%
N	2.12	%
H	4.91	%
Fe content	95.79	mg kg^{-1}
Al content	100.30	mg kg^{-1}
^{127}I	20.36	µg g^{-1}
^{78}Se	1.57	µg g^{-1}

3.4.2 Acidic group abundance

3.4.2.1 FTIR

The FTIR spectra of the HA is similar to others in the literature and confirms the HA is typical (**Figure 3.2**). The band around 1700 cm^{-1} indicates carboxylic groups, and the band around 1590 cm^{-1} is typical of C=O stretching associated with aromatic rings (Doskocil *et al.*, 2018; Manzak *et al.*, 2017). The broad band around 3200-3600 cm^{-1} is associated with aliphatic chains, and that at 2915 cm^{-1} describes symmetric stretching of methylene (C-H) groups (Doskocil *et al.*, 2018; Traversa *et al.*, 2014).
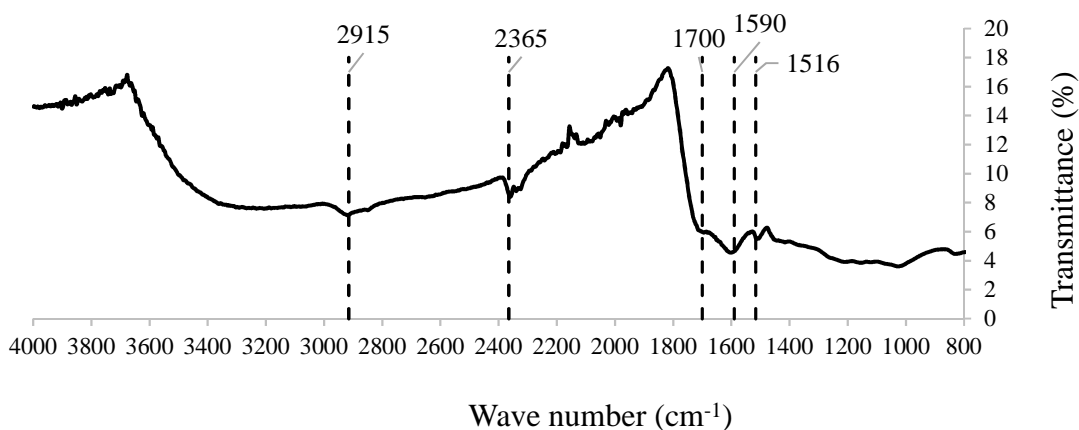
Figure 3.2. FTIR spectra for HA.

3.4.2.2 NMR

Quantitative analysis of HA by NMR demonstrated a large number of different carbon environments. The ^{13}C magnetic angle spinning (MAS) spectrum shows a broad spectrum with overlapping peaks (**Figure 3.3**), highlighting the polymeric nature of HA. The MAS rate of 12.5 kHz is fast enough to allow separation between the spinning sidebands and central intensity. Cross polarisation (CP) relaxation analysis was also acquired and is shown in **Figure 3.4**. This enabled correction of the ^{13}C MAS spectrum
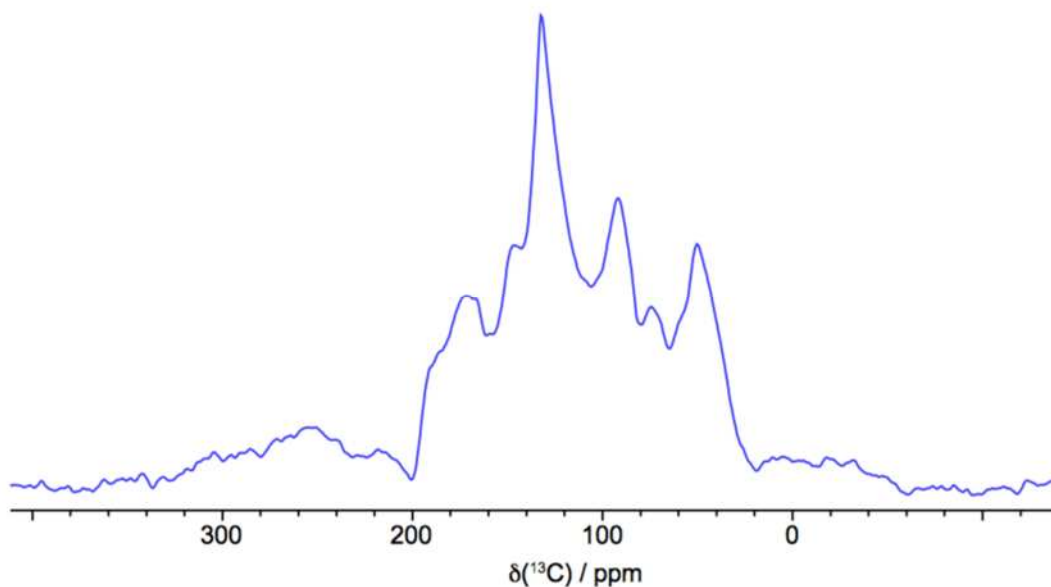
Figure 3.3. ^{13}C MAS spectrum of HA at a MAS rate 12.5 kHz.

(**Figure 3.3**) by accounting for relaxation effects by calculation of the ratio of peak area missing in the spectrum. Given the broad nature of this spectrum it was not possible to identify individual sites so the quantitative analysis was determined for aliphatic, carbohydrate, aromatic and carboxylic sites (**Table 3.2**).
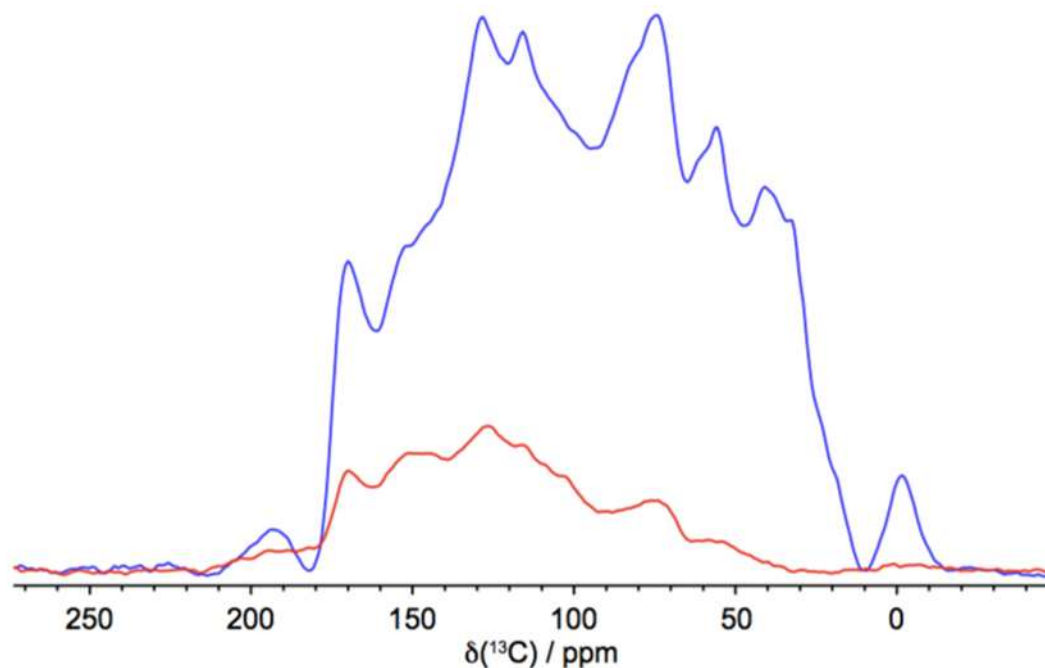
Figure 3.4. ^{13}C CPMAS spectrum of HA with a MAS rate of 6 kHz and a relaxation delay of 0.0001 seconds (blue) and 25 seconds (red) with a relaxation delay of 2 seconds.

Table 3.2. Percentage composition of the HA used in this work.

	Composition (%)
Aliphatic (0 – 50 ppm)	11 ± 1.5
Carbohydrate (50 – 108 ppm)	30 ± 1.1
Aromatic (108 – 162 ppm)	43 ± 1.3
Carboxylic (162 – 220 ppm)	15 ± 0.7
Sp^2/Sp^3 (108 – 162 ppm)/(0 – 108 ppm)	1.4 ± 0.05

The parent material and environment in which HA forms, determines the composition and structure of the HA; it can therefore vary greatly between soils (**Table 3.3**). For example, González Pérez *et al.* (2004) demonstrated that a non-cultivated oxisol in Brazil had a lower aromaticity (%) and a higher aliphatic content than the same oxisol under conventional tillage practice and maize-fallow cultivation. The no-till system resulted in continuous accumulation of plant residues at the surface, providing fresh crop residues for microbial metabolism, resulting in OM with a higher aliphatic content. This perfectly demonstrates how systems under different stresses result in differing degrees of humification of HA. The HA extracted from the Irish moss peat that is under investigation here has a higher aromatic C content (%) than many other HAs (**Table 3.3**). Aromaticity of HA typically increases with humification, demonstrated by an increase in C/H ratio (Stevenson, 1982), and since this peat soil has a high OM content the degree of humification is likely to be high. The aliphatic content of the HA is correspondingly lower than many other HAs (**Table 3.3**).

Table 3.3. Distribution of ^{13}C in humic acids from a range of different soil types by CP/MAS ^{13}C NMR.

Soil	Region	Composition(%)	Reference
Mangrove lake	Aromatic C	33	(Hatcher, 1980)
Ombotrophic peat bog	Aromatic C	21/23[a]	(Gondar et al., 2005)
	Carboxylic C	8/12[a]	
Forest podzol	Aliphatic C	34.3	(Cook and Langford, 1998)
	Aromatic C	18.7	
	Carboxylic C	15.7	
	Carbohydrate C	21	
Calcaric cambisol	Aromatic C	14.7	(Adani et al., 2006)
	Carboxylic C	16.2	
	Aliphatic C	30.9	
Oxisol (NC)	Aromatic C	24	(González Pérez et al., 2004)

	Carboxylic C	16	
	Aliphatic C (0-65 ppm)	42	
Oxisol (CT1)	Aromatic C	30	(González Pérez et al., 2004)
	Carboxylic C	17	
	Aliphatic C (0 – 65 ppm)	37	

[a] surface horizon/deeper horizon, NC = Not Cultivated,
CT1 = Conventionally tilled, maize-bare fallow

3.4.2.3 Total acidity

The abundance of acidic groups differed between the HA (6.523 mol kg^{-1}) and the FA (8.225 mol kg^{-1}) fractions, with the FA fraction having a higher total acidity. This is consistent with the results of previous workers (Gondar *et al.*, 2005; Ritchie and Michael Perdue, 2003; Weber and Wilson, 1975) and is thought to be due to the lower average molecular weight of FA as a result of HA hydrolysis. Humic acids undergo hydrolysis, where non-acidic ester groups are broken into aromatic acid and alcohol containing groups thus resulting in increased carboxyl content in the resulting FAs (Weber and Wilson, 1975).

3.4.2 Surface charge development

Surface charge data was plotted against pH. As pH increased, the negative surface charge also increased, with a 'dip' around pH 8.0 (**Figure 3.5**). This 'dip' is thought to be the point in the titration where all the carboxyl groups have dissociated, leaving the phenol hydroxyl groups to dissociate at higher pH (Marshall *et al.*, 1995). From comparison of the acid-base properties of HA and FA it is clear that the FA has a greater negative charge at any given pH than HA, an observation consistent with findings of previous studies (Gondar *et al.*, 2005; Milne *et al.*, 2001; Ritchie and Michael Perdue, 2003). The second method (described in Section 3.3.3, Eqn. 3.9) was used to calculate the FA surface

charge. Both methods were used to calculate HA surface charge. Both proved to be a reliable way to calculate the surface charge development (**Figure 3.6**), therefore comparisons between FA and HA data can be reliably made.
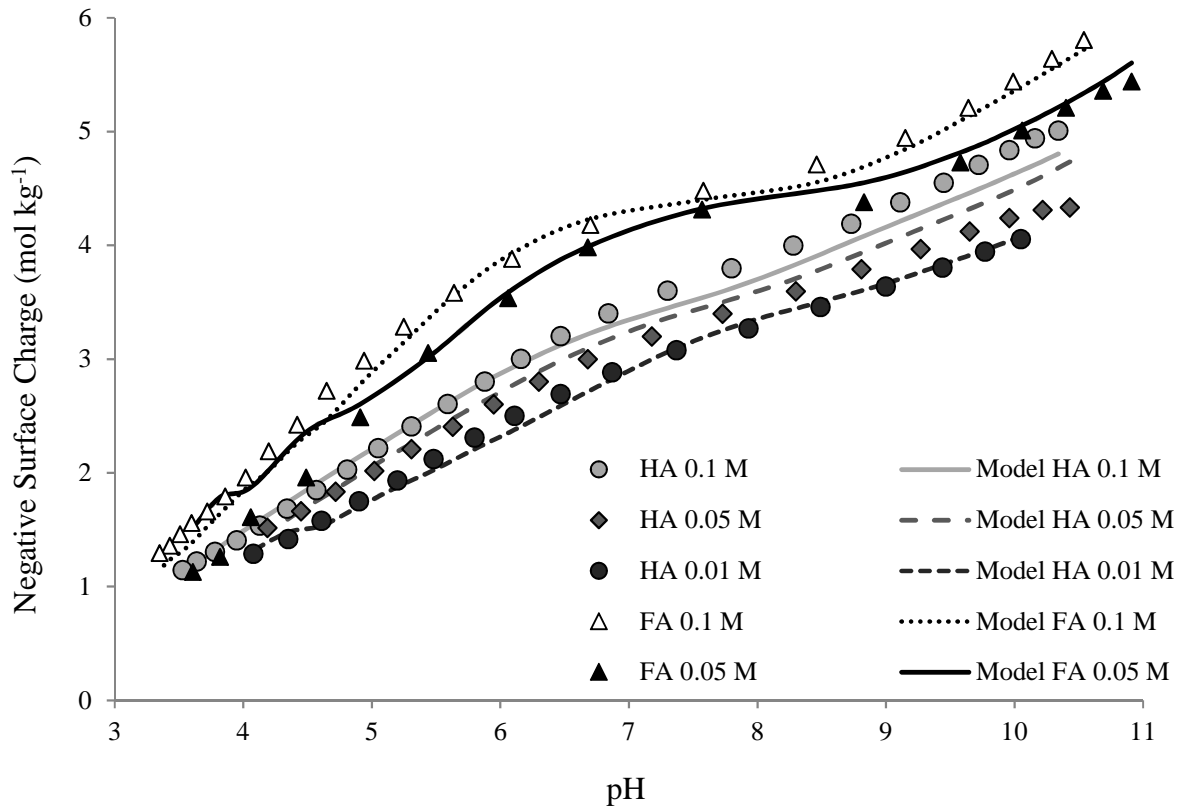
Figure 3.5. Charge development of HA and FA as a function of pH at different ionic strengths; 0.1 M, 0.05 M, and 0.01 M including model fits.

The binding of ions to HA and FA is influenced by charge variation. Cations form stronger bonds to HA and FA functional groups at higher pH (Catrouillet *et al.*, 2014; Tipping and Hurley, 1992; Xiong *et al.*, 2013). Anions are more likely to bind at low pH due to reduced electrostatic repulsion. Although there is a net negative charge on HA and FA, even at very low environmental pH values, there are amphiprotic groups such as $R-NH_2^+$ which could act as sites for anion adsorption.
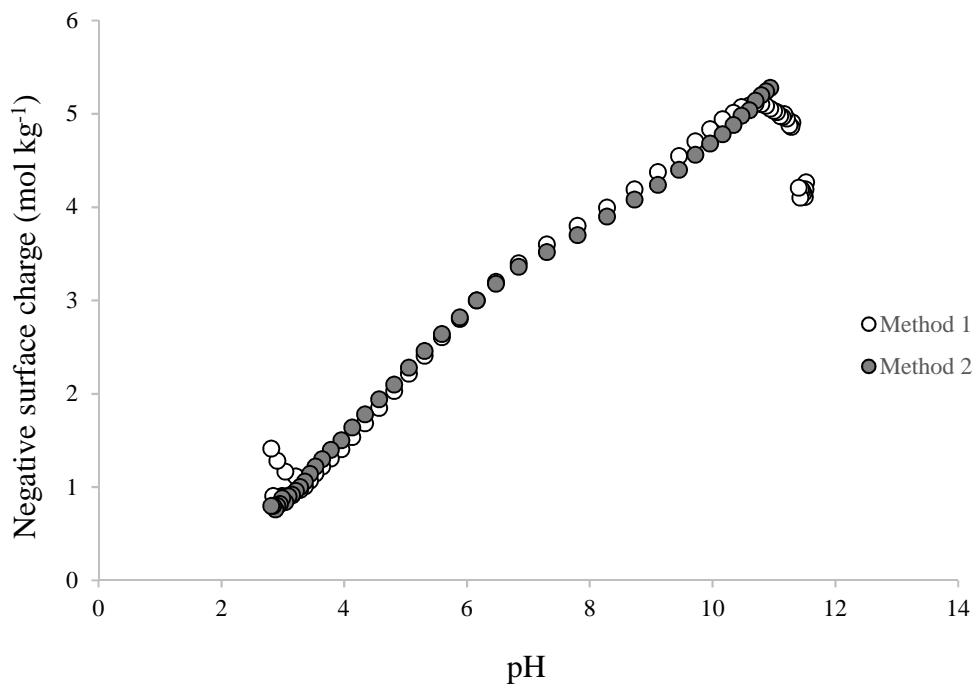
Figure 3.6. A comparison of the two methods for calculation of surface charge development as a function of pH.

Ionic strength had a significant effect on the charge development of HA and FA (**Figure 3.5**). At a given pH, both HA and FA carry a greater negative charge at higher ionic strengths. The dissociation of the acid groups was therefore enhanced with increasing salt concentrations (Fukushima *et al.*, 1995; Nederlof *et al.*, 1993). A higher counter ion availability (or concentration) in the bulk solution enables the generation of a higher surface charge because the de-stabilising effect of thermal diffusion on the counter-ion cloud is lowered (Baidoo *et al.*, 2014). The effect of ionic strength was less at low pH, but greater for HA at high pH. Baidoo *et al.* (2014) suggests that at low pH, the humic moiety will possess a smaller charge and therefore the fewer counter ions are needed to sustain the charge and therefore increasing ionic strength had less of an effect. At high pH where the humic molecules have a greater charge, availability of counter ions is more critical to the maintenance of surface charge, and so ionic strength has a greater effect. The effect of ionic strength on FA was different to that of HA with the least effect at neutral pHs. In the case of FA, the difference at varying ionic strengths did not converge

at low pH as it did in the HA, but instead appeared to converge between pH 7-8 and then diverge at higher pH values, as expected. The lack of convergence at lower pH values may reflect the stronger acidity of the FA. The apparent convergence at neutral pH values may simply be the product of less reliable data in the region of minimal buffer capacity close to the end of the carboxyl buffer region and before phenolic-OH groups had started to dissociate. It is noticeable that the asymptote associated with the carboxyl endpoint was much more pronounced for FA and especially for the lower ionic strength. Further and repeated experiments would be necessary to resolve these questions.

Charge development curves for HA at each ionic strength show a tendency to 'splay out' at the extremes of the pH range titrated (**Figure 3.7**). Marshall *et al.* (1995) suggested that this arises from unreliability in the humic charge calculation, that becomes increasingly sensitive to error at both high and low pHs. This results from the increasingly important role of $[H^+]$ in the charge balance calculation at low pH, and $[OH^-$
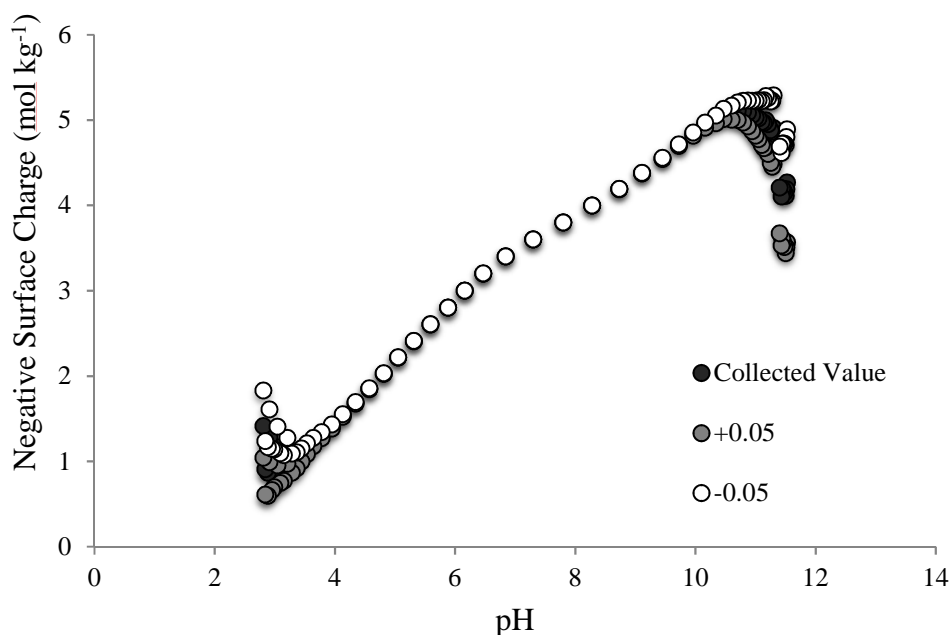
Figure 3.7. Charge development curves showing the effects of high and low pH on humic acid surface charge. Surface charge data plotted for the measured ionic strength of 0.1, and calculated for +0.05 and -0.05 pH values.

] at high pH, which increases the sensitivity to errors associated with the measured value of pH. This is demonstrated in **Figure 3.7** where the measured pH has been changed by ±0.05 and the surface charge re-calculated. It demonstrates how a slight error in pH measurement can result in significantly different values of surface charge being calculated at both low and high pH. For this reason when discussing surface charge development as a function of pH only the range pH 4 to 10 will be considered.
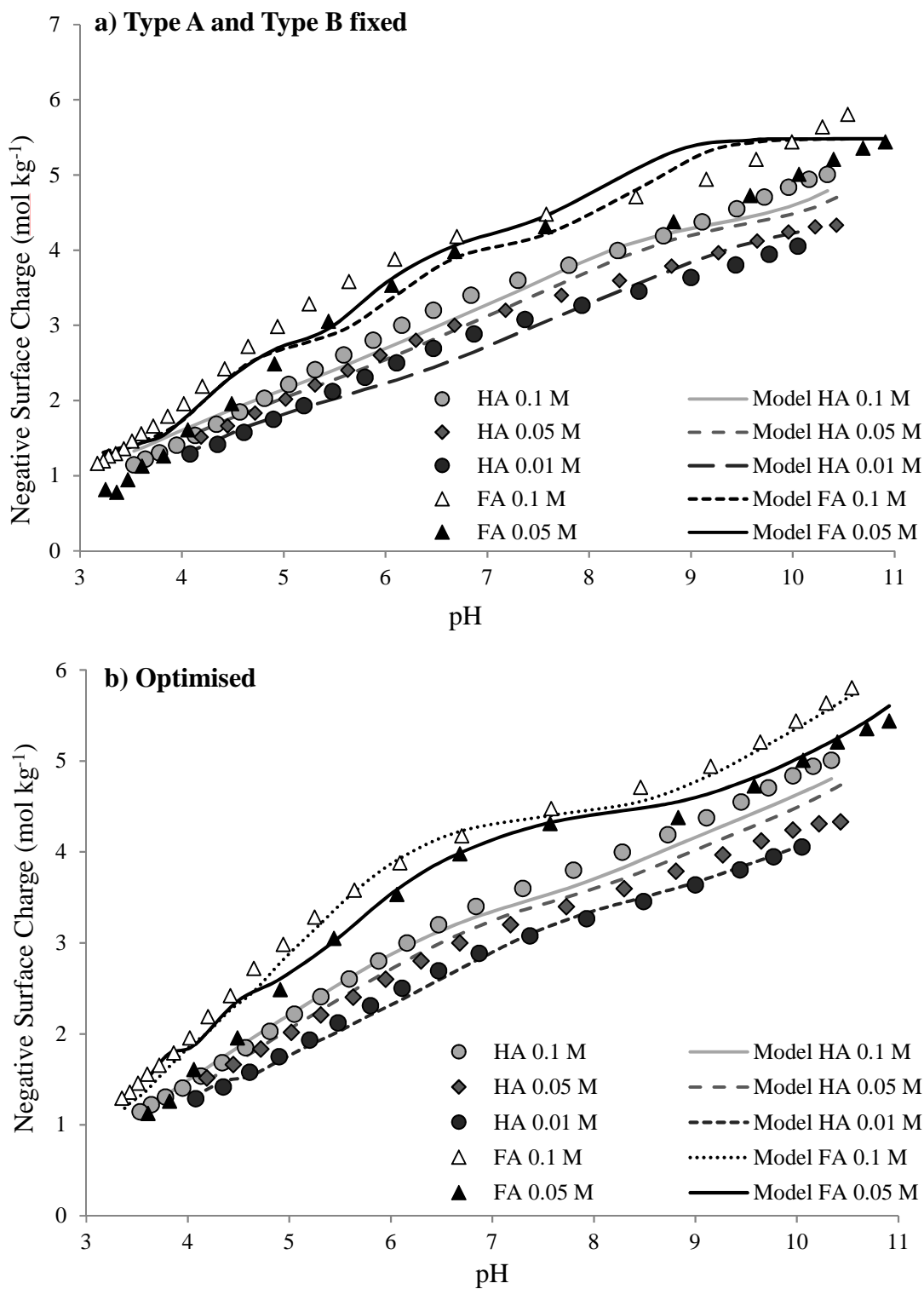
Figure 3.8. Charge development as a function of pH for HA and FA at different ionic strengths; 0.1 M, 0.05 M, 0.01 M. Model fits are also shown. (a) Type A and B parameters are set to ⅔ and ⅓, (b) Type A and B sites are optimised.

3.4.3 Modelling surface charge

Initially a constant capacitance type model was fitted using a fixed proportion of Type A and Type B groups (**Figure 3.8**); Type A was set to be ⅔ of the total acidity, and Type B as ⅓. This is a strict arrangement and although useful in simplifying the description of the binding of other ions (Tipping, 1994), it does not allow for the best possible fit as the proportions of Type A and Type B are unlikely to be that exact. To address this issue a 'Proportion Factor' was introduced, which improved the fit of the model (**Figure 3.8b**). Type A and Type B proportions were optimised to 0.529 and 0.471 respectively.

3.6 CONCLUSIONS

NMR and FTIR data demonstrate a significant contribution of aromatic groups and carboxyl groups to HA surface structure. The contribution of these groups will be instrumental in the interactions of HA with I, Se and Tc in the coming experiments.

A clear relationship between HA and FA surface charge and pH was observed. The surface charge of both HA and FA became increasingly negative with increasing pH as more acidic groups dissociated. Higher ionic strengths increased the negative charge on both HA and FA due to the stabilising effect of counter ions in solution. Surface charge was successfully modelled when the proportions of Type A and Type B groups were allowed to vary.

The effect of surface charge on the kinetics of I, Se and Tc reactions with HA and FA will be addressed in subsequent chapters to assist in understanding the reaction mechanisms.

4. IODINE INTERACTION WITH SOIL GEOCOLLOIDS

4.1 INTRODUCTION

Soils and sediments play an essential role in the environmental cycling and fate of I. Soil pH, OM content, oxide content, salinity and redox potential (Eh) all effect I sorption. The pH of the soil determines the net positive charge on metal oxides (Fuhrmann *et al.*, 1998); low pH results in a greater positive charge and consequently increased associations with anionic I species. Iron and manganese oxides provide positively charged surfaces to which both IO_3^- and I^- can adsorb. Ferromanganese oxides selectively incorporate IO_3^-, and oxidise added I^- prior to adsorption (Kodama *et al.*, 2006). Although metal oxides can adsorb I, it is thought that they play only a minor, transient role in influencing I behaviour in soils, and that OM is the predominant factor (Shetaya *et al.*, 2012).

There is an increasing body of evidence demonstrating significant I interactions with SOM (Section 1.3.3.2). Under acidic pH conditions, OM can reduce/oxidise inorganic I species (IO_3^- and I^-), to form reactive intermediates (e.g. HOI and I_2) (Francois, 1987), allowing them to sorb as organic-iodine species (Shetaya *et al.*, 2012; Whitehead, 1984; Yamaguchi *et al.*, 2010). A major constituent of OM is highly reactive HS, iodination of which is now widely accepted as the mechanism of I association with SOM. Understanding the dynamics of I interaction with HS is therefore important for cycling of I. Bowley *et al.* (2016), demonstrated rapid reduction of added IO_3^- in the presence of HA, and slow oxidation of added I^-, forming Org-I species. The mechanism of this association with HA is likely electrophilic substitution of I into aromatic structures (Reiller *et al.*, 2006; Schlegel *et al.*, 2006; Xu *et al.*, 2011). There is however a gap in the understanding of the effect of pH, HA concentration and temperature on these

interactions. It is suspected that as pH decreases, the negative surface charge of HS will reduce and therefore interactions with anionic I species are likely to increase. Alongside this as HA concentration increases the rate of reaction should also increase.

Speciation of I is important in determining its fate within the soil environment. The different sorption behaviour of I^- and IO_3^- in soils is evident in the literature, however it is difficult to identify the factors involved due to the complexity of soil environments. For example I^- was shown to be converted into organic species much more quickly than IO_3^- (Shetaya *et al*., 2012) in a wide range of soil types, which is in contrast to the findings of Hu *et al*., (2009) where IO_3^- interaction was most rapid. Monitoring the speciation of I is therefore vital in order to elucidate reaction mechanisms.

4.2 AIMS AND OBJECTIVES

The aim of the work in this chapter was to investigate the interactions of IO_3^- and I^- with soil geocolloids; specifically HA, HA in combination with metal ions and oxides, and FA, in order to improve understanding of I reactions with soils. Techniques including ICP-MS linked to SEC and HPLC were employed to monitor changes in speciation and incorporation into the organic phase under a range of conditions.

Specific objectives included:

- Investigation of the dynamics of IO_3^- and I^- reaction with HA alone and in combination with metal ions;
- Investigation of the effect of temperature, pH and metal oxides on the formation of organic-I species;

- Modelling of the interactions of IO_3^- and I^- with HA, alone and in the presence of metal ions.

4.3 MATERIALS AND METHODS

An overview of the experiments undertaken and their scope is given in **Table 4.1**.

4.3.1 Humic acid stock solutions

Freeze dried HA (0.5 g) was initially dissolved in 1 mL of 1 M NaOH, 9 mL of 1 M NaCl to adjust the ionic strength and 50 mL Milli-Q water (18.2 MΩ cm) before being made up to 1 L with Milli-Q water to give a stock solution of 0.5 g L^{-1} HA. A second stock solution of 1.5 g L^{-1} HA was also prepared by dissolving 0.3 g of HA in 0.2 mL of 1 M NaOH and 1.8 mL of 1M NaCl before being made to 200 mL. The pH of the stock solutions were adjusted from ~pH 7 to the desired pH using 0.1M HNO_3.

4.3.2 Isotope spike solutions

Isotope spike solutions (1000 µg L^{-1}) were prepared for each species ($^{129}IO_3^-$ and $^{129}I^-$) by dilution of concentrated stocks described in Section 2.5.1. Solutions were diluted in Milli-Q water to neutralise the basic pH of the concentrated stocks.

Table 4.1. Experiment overview.

Experiment	Treatments	Isotope spike	Purpose	Section
Range finding	• 0.05 g L^{-1} and 0.2 g L^{-1} HA • Fe^{2+} and Mn^{2+} (30% occupancy) • Goethite (20% by weight) • pH 4 and pH 6 • 4°C and 20°C • Spiked separately (ox. and red.)	pH 4 (Ox.) = 10 µg L^{-1} $^{129}IO_3^-$ pH 4 (Red.) = 5 µg L^{-1} $^{129}I^-$ pH 6 (Ox.) = 540 µg L^{-1} $^{129}IO_3^-$ pH 6 (Red.) = 5 µg L^{-1} $^{129}I^-$	To explore the system and narrow the focus of future experiments.	4.3.3 4.4.1.1
Effect of pH	• pH range 4-7 (0.5 increments) • 0.2 g L^{-1} HA • 4°C, 10°C and 20°C • Spiked separately (ox. and red.)	10 µg L^{-1} $^{129}IO_3^-$	Investigation of the effect of pH on IO_3^- reduction in HA systems.	4.3.4 4.4.1.2
Effect of HA concentration	• 0.01-1 g L^{-1} HA (5 concentrations) • pH 4 • 4°C, 10°C and 20°C	10 µg L^{-1} $^{129}IO_3^-$	Investigation of the effect of HA concentration on IO_3^- reduction in HA systems.	4.3.5 4.4.1.3
FA	• 0.2 g L^{-1} FA • pH 4 and pH 6 • 4°C and 20°C	10 µg L^{-1} $^{129}IO_3^-$	Investigation of the effect of FA on IO_3^- reduction for comparison with HA.	4.3.6 4.4.2
Effect of redox coupling	• 0.2 g L^{-1} HA • pH 4 • 4°C and 20°C • Mixed spike	Mixed spike of 10 µg L^{-1} $^{129}IO_3^-$ and $^{127}I^-$	Investigation of potential of redox coupling between IO_3^- and I^- in HA systems.	4.3.7 4.4.3.1

Effect of Microbes	• 0.2 g L^{-1} HA • Filtered (0.22 µm) and non-filtered • Glucose (10 mM) • Filtered and non-filtered soil inoculum • γ-irradiated and non-irradiated • pH 4 • 20°C	Mix spike of 10 µg L^{-1} $^{129}IO_3^-$ and $^{127}I^-$	Investigation of the effect of microbes on IO_3^- and I^- interactions with HA to establish if the reactions are abiotic or biotic.	4.3.8 4.4.4
Effect of Fe (Non-Sterile)	• 0.2 g L^{-1} HA • Fe^{2+} and Fe^{3+} (30% occupancy) • pH 4 and pH 6 • 4°C and 20°C	10 µg L^{-1} $^{129}IO_3^-$	Investigation of the effects of $Fe^{2+/3+}$ on the interactions of IO_3^- in HA systems.	4.3.9.1 4.4.5
Effect of Fe (Sterile)	• 0.2 g L^{-1} HA • Fe^{2+} and Fe^{3+} (10, 20 and 50% occupancy) • pH 6 • 4°C and 20°C	Mixed spike of 10 µg L^{-1} $^{129}IO_3^-$ and $^{127}I^-$	Investigation of both the effect of Fe concentration and filter sterilization on IO_3^- and I^- interactions with HA.	4.3.9.2 4.4.5

4.3.3 Range finding experiment

A range finding experiment was undertaken to investigate a range of factors in a single experiment, thereby allowing a more well-informed approach to designing subsequent experiments. The experimental set-up is shown in **Figure 4.1**.

Stock HA suspensions, calculated to contain either 0.05 g L^{-1} or 0.2 g L^{-1} HA after all subsequent additions, were prepared by dilution of a concentrated HA stock. Stock solutions of Fe^{2+} and Mn^{2+} (500 mg L^{-1}) were prepared from ferrous chloride and manganese (II) chloride. A suspension of goethite was prepared by dissolving ferric nitrate in 600 mL deionised water, 1 M NaOH was then added at a rate of 10 mL min^{-1} until pH 10.6 was obtained (~400 mL). The stock was aged at 60°C for 24 hours prior to dialysis against deionised water. This was diluted further by taking ~5.4 mL of solid goethite and diluting to 1 L with Milli-Q water, resulting in a concentration of ~14 g L^{-1} goethite in the stock used here.

Additions of Fe^{2+}, Mn^{2+} or goethite or Milli-Q water were added to portions of the HA solutions. Goethite was added at 20% of the weight of HA in the sample. Additions of Mn^{2+} and Fe^{2+} were at concentrations equivalent to 30% of the HA carboxyl group concentration (Eqn. 4.1.). Additions of Fe^{2+} (or Mn^{2+}) were calculated from the total carboxyl content (COOH$_t$) of the HA (mol kg^{-1} of HA) as follows:

$$COOH_t = \frac{T_{acid}}{2} \tag{4.1}$$

Where T$_{acid}$ is the total acidity of the HA (mol kg^{-1}). The concentration of carboxyl groups in solution (COOH$_c$, mol L^{-1}) is governed by the concentration of HA in solution and therefore:

$$COOH_c = COOH_t \times HA_s \times 0.001 \qquad\qquad (4.2)$$

Where HA_s is the concentration of HA in solution (g L^{-1}). The amount of Fe (Fe_w, mg) required to occupy a given percentage of the carboxyl groups present was:

$$Fe_w = COOH_c \times \left(\frac{Occ}{100}\right) \times 0.5 \times Fe_{MW} \times 1000 \times \left(\frac{V}{1000}\right) \qquad\qquad (4.3)$$

Where Occ is the required carboxyl occupancy, Fe_{MW} (g mol^{-1}) is the molecular weight of iron and V (mL) is the volume of stock solution required.

Solutions were pH adjusted using 0.1 M HNO_3 or 0.1 M NaOH to pH 4 or 6 and were left overnight as pH drift was anticipated before a second pH adjustment was made. Solutions were then divided into 8 x 14 mL aliquots based on treatment, pH, temperature and whether they were to receive an oxidised (IO_3^-) or reduced (I^-) isotope spike. All samples were prepared in duplicate. Oxidised samples at pH 4 samples were spiked with 10 µg L^{-1} $^{129}IO_3^-$ and reduced samples with 10 µg L^{-1} $^{129}I^-$. Oxidised pH 6 samples were spiked with 540 µg L^{-1} $^{129}IO_3^-$ and reduced samples were spiked with 5 µg L^{-1} $^{129}I^-$. Samples were stored in the dark at either 4°C or 20°C and shaken intermittently. Aliquots were removed for analysis at 12, 45, 80, 142, and 163 days for samples at pH 6, and 6, 12, 41, 88, and 122 days for samples at pH 4.
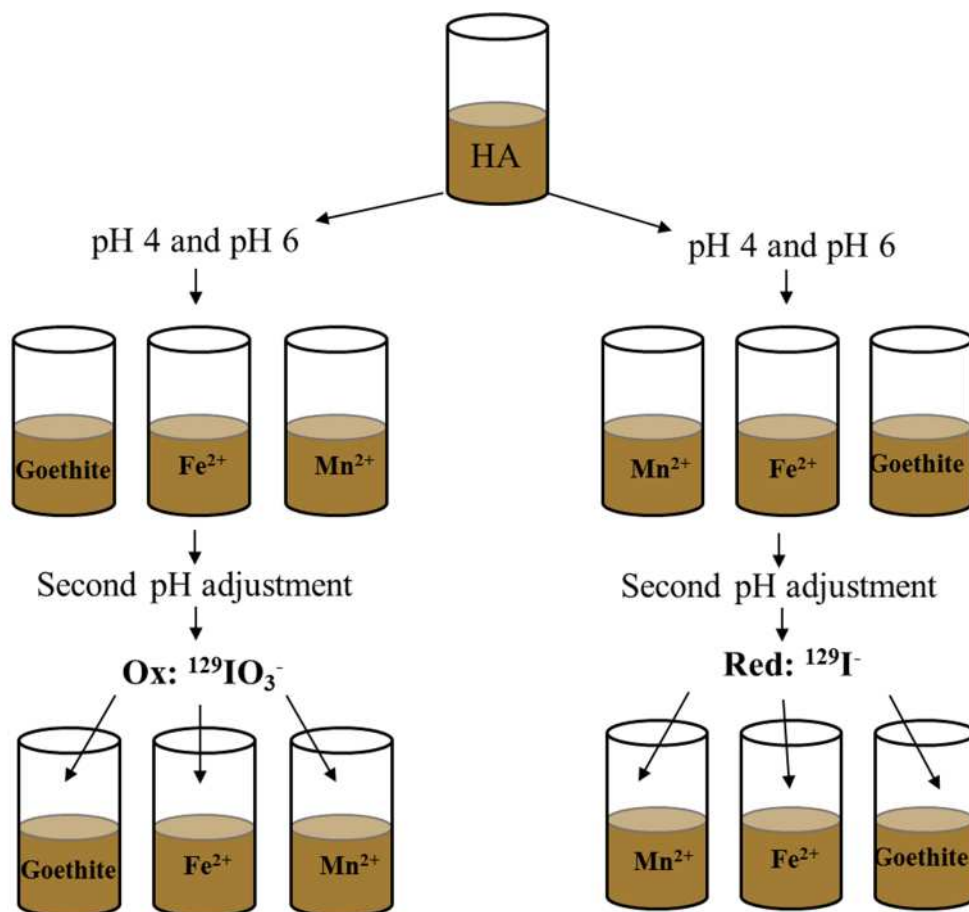
Figure 4.1. Graphical representation of the range finding experiment set up. After spiking samples were divided and stored at 4°C and 20°C.

4.3.4 Effect of pH on IO_3^- reaction with HA

Aliquots of a 0.5 g L^{-1} HA solution were diluted and pH adjusted using 0.1 M HNO_3 in order to achieve solutions of 0.2 g L^{-1} HA at pH 4, 4.4, 5, 5.5, 6, 6.5 and 7. After pH adjustment duplicate solutions were spiked with 10 μg L^{-1} IO_3^- and 10 μg L^{-1} selenate (see Chapter 5), stored in the dark at 4°C, 10°C and 20°C and shaken intermittently. Aliquots were removed for analysis after 3, 16, 30, 44, 65, and 86 days.

4.3.5 Effect of HA concentration on reaction with IO_3^-

Humic acid samples containing 1, 0.5, 0.1, 0.05, and 0.01 g L^{-1} HA were prepared as described in Section 4.3.3 by dilution of a 1.5 g L^{-1} HA stock before adjustment to pH 4

or pH 6 using 0.1 M HNO$_3$. A spike of ^{129}IO$_3^-$ was then added to give a final concentration of 10 µg L^{-1}. Samples were stored in the dark at 4°C, 10°C and 20°C. Aliquots were sampled for analysis after 2, 16, 37, 57, 71, 112 and 141 days.

4.3.6 Reaction of IO$_3^-$ with Fulvic Acid

Freeze dried FA was initially dissolved in 0.1 mL of 1 M NaOH and 0.9 mL of 1 M NaCl, to adjust the ionic strength, before dilution to give a stock solution of 0.2 g L^{-1} FA. Adjustment to pH 4 and pH 6 was achieved with 0.1 M HNO$_3$. Samples were filter sterilised using 0.22 µm filter units before a spike of ^{129}IO$_3^-$ was added to give a final concentration of 10 µg L^{-1} ^{129}IO$_3^-$. Samples were stored in the dark at 4°C and 20°C. Aliquots were sampled for analysis after 4, 18, 25 and 39 days.

4.3.7 Redox coupling between IO$_3^-$ and I$^-$ and reaction with HA

Humic acid samples (0.2 g L^{-1} at pH 6) were prepared according to Section 4.3.3. with a mixed spike of ^{129}IO$_3^-$ and ^{127}I$^-$ to achieve a final concentration of 10 µg L^{-1} of each isotope. Samples were stored in the dark at 4°C and 20°C and aliquots removed for analysis after 3, 15, 31, 50 and 92 days.

4.3.8 Effect of microbes on I interactions with HA

Humic acid samples (0.2 g L^{-1}) were prepared and adjusted to pH 4 according to the method described in Section 4.3.3. A soil inoculum from an acidic woodland soil (Sutton Bonington, U.K.) was prepared by shaking 10 g of freshly collected soil with 95 mL Milli-Q water and allowing particulate matter to settle. A 0.1 M D-glucose solution was prepared by gently heating and stirring until complete dissolution was achieved. Samples of HA were either filtered (0.22 µm) or non-filtered, with additions of filtered or non-

filtered soil inoculum and glucose (0.01 M). Samples were spiked with 10 µg L^{-1} ^{129}IO$_3^-$ and 10 µg L^{-1} ^{127}I$^-$, Se, (Chapter 5) and Tc (Chapter 6). Half of the samples were γ-irradiated (^{137}Cs) for 24 hours to achieve sterilisation, whilst the other half were kept in the dark nearby. Samples were then stored in the dark at 20°C. Aliquots were subsampled in a laminar flow hood using autoclaved pipette tips to maintain sterile environment, at 4, 18, 25 and 39 days.

4.3.9 Effect of Iron

4.3.9.1 Effect of Fe^{2+} and Fe^{3+} on IO$_3^-$ reaction with HA

Suspensions of HA were prepared as described in Section 4.3.3, but pH adjustment was only to pH 4 and 6. Aliquots of Fe^{2+} as ferrous chloride, and Fe^{3+} as ferric chloride were added with the aim of creating 30% occupancy of the HA carboxyl groups, prior to the addition of an ^{129}IO$_3^-$ spike to give a final concentration of 10 µg L^{-1} ^{129}IO$_3^-$ in solution in 0.2 g L^{-1} HA. Duplicate samples were stored in the dark at 4°C, 10°C and 20°C with intermittent shaking. Aliquots were removed for analysis after 3, 16, 30, 44, 65, and 86 days.

4.3.9.2 Effect of Fe^{2+}/Fe^{3+} concentration and sterilisation on I interactions with HA

Humic acid samples containing 0.2 g L^{-1} HA were prepared as described in Section 4.3.3 by dilution of a 1.6 g L^{-1} HA stock solution before adjustment to pH 6 using 0.01 M HNO$_3$ and additions of Fe^{2+} and Fe^{3+} sufficient to occupy 0%, 10%, 30%, and 50%, of the carboxyl groups. Samples were then left to stand overnight to allow for any pH drift before further adjustment using 0.01 M NaOH. A mixed IO$_3^-$/I$^-$ spike was then added to give 10 µg L^{-1} ^{129}IO$_3^-$ and 10 µg L^{-1} ^{127}I$^-$. Samples were stored in the dark at 4°C and 20°C

and shaken intermittently. Aliquots were sampled for analysis after 3, 15, 31, 50 and 92 days.

4.3.10 ICP-MS Analysis

Measurement of iodine total concentration was undertaken using ICP-MS as described in Section 2.5.1. Chromatography was used to analyse iodine species using a Dionex ICS-3000 HPLC (with Chromeleon 6.2 software plugin) coupled to ICP-MS as described in Section 2.5.2. Separation of organic iodine species from inorganic species was undertaken using SEC-ICP-MS as described in Section 2.5.3.

4.3.11 Modelling

Results were modelled using Open Model (http://openmodel.info/, Version 2.4.2). Observed [129]I transformations were represented as simultaneous ordinary differential equations (**Figure. 4.2**):

$$\frac{dIO_3^-}{dt} = -k_1 \times IO_3^- - k_2 \times IO_3^- \tag{4.4}$$

$$\frac{dI^-}{dt} = +k_2 \times IO_3^- + k_3 \times OrgI - k_4 \times I^- \tag{4.5}$$

$$\frac{dOrgI}{dt} = +k_1 \times IO_3^- + k_4 \times I^- - k_3 \times OrgI \tag{4.6}$$

where k_1, k_2, k_3 and k_4 are unknown rate coefficients (day^{-1}) estimated by fitting the model to the observed concentrations of $^{129}IO_3^-$, $^{129}I^-$ and Org-^{129}I.

The differential equations were solved using 4th order Runge-Kutta (Press *et al*., 2007) and fitting was performed using a Metropolis-Hastings search (Van Oijen *et al.*, 2005) supplemented with a Marquardt (Tarsitano *et al*., 2011) 'polishing'procedure. The observations were weighted using the estimated standard errors. The fitting procedure minimised residual sum of squares (RSS) between the modelled and measured values over all time points, pH levels, temperatures and HA concentrations. Alternative model structures were considered and will be discussed briefly in Section 4.5. The arrangement described in **Figure 4.2** (based on that presented in Bowley *et al.* (2016)) provided the best fit to the data.
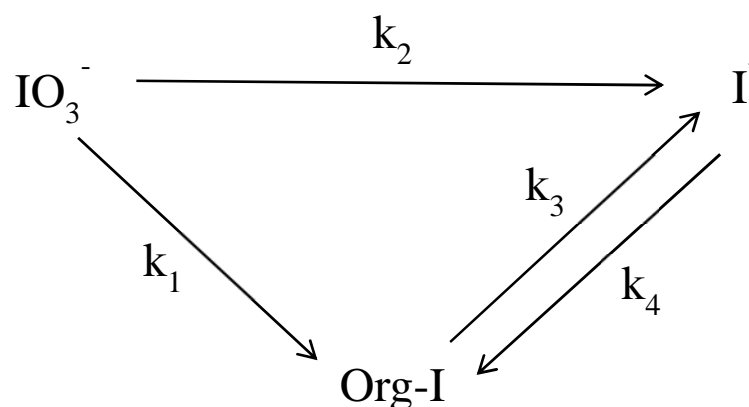
Figure 4.2. Conceptual model of the transformations of added $^{129}IO_3^-$ in the presence of HA. Rate constants k_1-k_4 describe first order reactions.

4.4 RESULTS AND DISCUSSION

4.4.1 Iodate interactions with humic acid

4.4.1.1 Range finding experiment

The aim of this experiment was to investigate the factors that had the most significant effect on $^{129}IO_3^-$ reactions with HA. **Figure 4.3** shows the changes observed in speciation over c. 3 months when HA suspensions at two concentrations at pH 4 were spiked with 10 µg L^{-1} $^{129}IO_3^-$ with additions of Fe^{2+} or Mn^{2+}. Concentrations of IO_3^- decreased and a corresponding increase in $^{129}I^-$ concentration and Org-^{129}I (not shown) was observed. Loss of $^{129}IO_3^-$ was initially very rapid and followed by a slower-time dependent sorption. Greatest initial loss was observed in samples at a higher temperature and higher HA concentration. On average ~84% of the added $^{129}IO_3^-$ was reduced within the first 6 days in 0.2 g L^{-1} samples at 20°C, compared to ~54% at 4°C, demonstrating a clear temperature dependency. The amount of $^{129}IO_3^-$ rapidly reduced at 20°C in 0.05 g L^{-1} HA systems was ~31% on average, significantly less than that in the 0.2 g L^{-1} system.
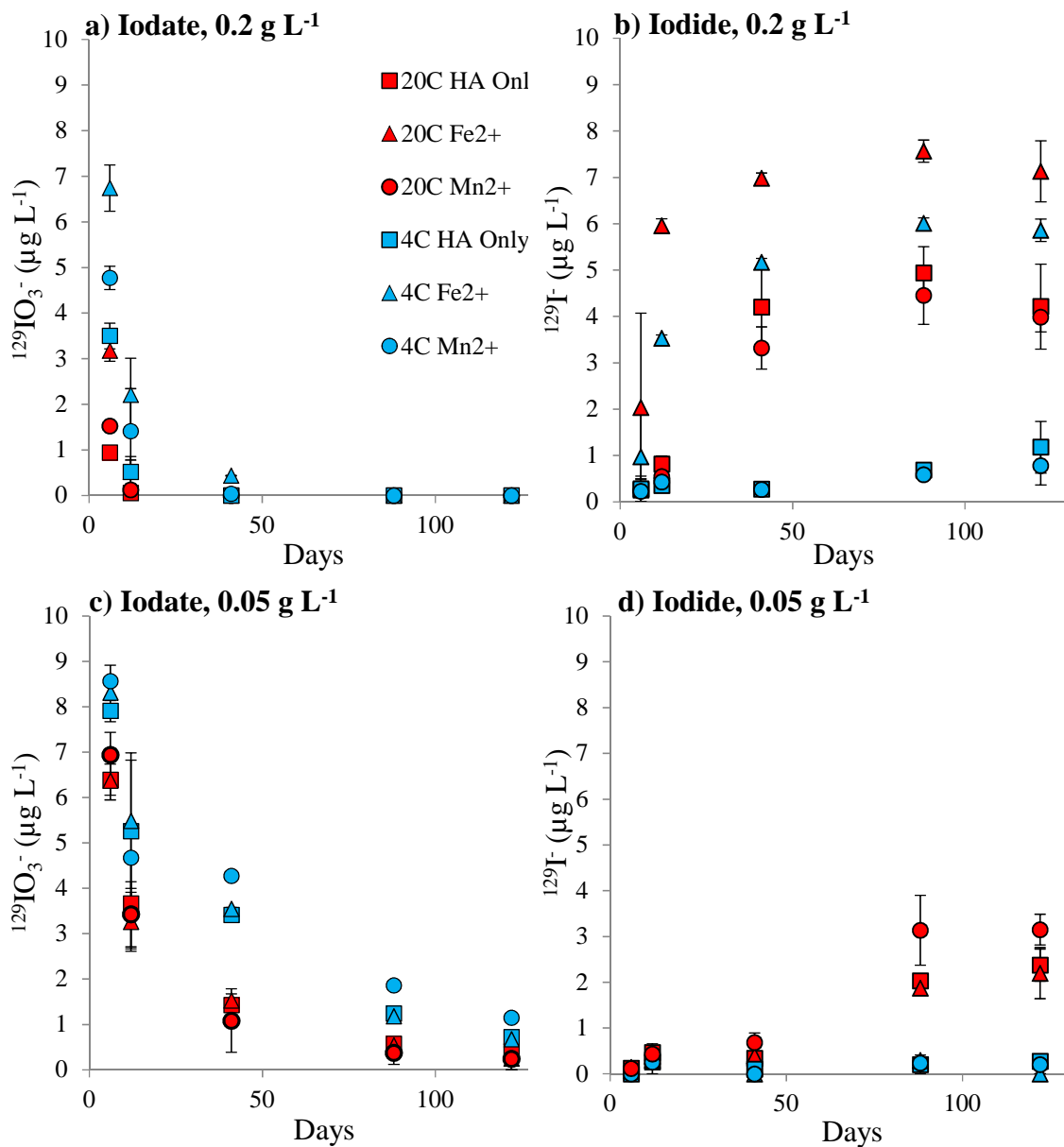
Figure 4.3. Transformations of added $^{129}IO_3^-$ (a, c) to $^{129}I^-$ (b, d) with time after an addition of 10 µg L^{-1} $^{129}IO_3^-$ to HA suspensions at pH 4 containing 0.2 g L^{-1} and 0.05 g L^{-1} with or without additions of Fe^{2+} (▲) and Mn^{2+} (●) at 4°C (blue) and 20°C (red). Error bars based on two replicates.

The differences observed between pH 4 and pH 6 seen in this experiment are hard to compare due to discrepancies in $^{129}IO_3^-$ spike concentrations; pH 4 samples were spiked with 10 µg L^{-1}, and pH 6 samples were unintentionally spiked with 540 µg L^{-1} (**Figure 4.4**). Nonetheless reduction of $^{129}IO_3^-$ was still apparent at pH 6, where ~30% reduction was observed at 20°C and ~23% at 4°C (0.2 g L^{-1}) over the entire 163 day experiment.

This demonstrates a significantly slower rate of reduction than seen at pH 4. Due to the differences in spiking concentration, it is hard to say whether or not the reduced rate of $^{129}IO_3^-$ removal and transformation is due to a pH effect, or an effect of the I:HA ratio. At such a high I:HA ratio as seen here, it is possible that the rate of $^{129}IO_3^-$ reduction was slower as the HA was over-saturated, therefore its capacity to reduce and transform
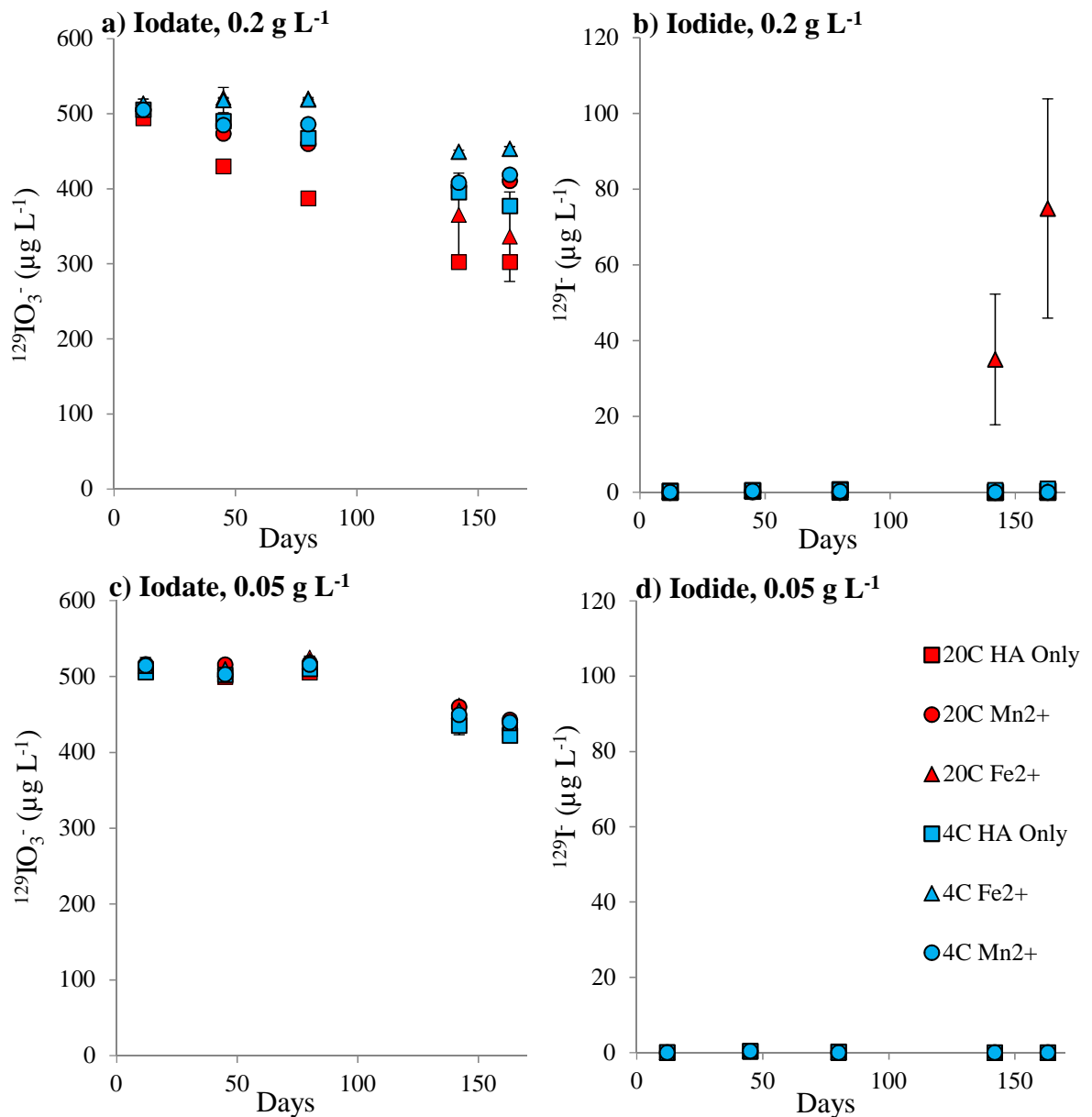
Figure 4.4. Transformations of added $^{129}IO_3^-$ (a, c) to $^{129}I^-$ (b, d) with time after an addition of 540 µg L^{-1} $^{129}IO_3^-$ to HA suspensions at pH 6 containing 0.2 g L^{-1} and 0.05 g L^{-1} with or without additions of Fe^{2+} (▲) and Mn^{2+} (●) at 4°C (blue) and 20°C (red). Error bars based on two replicates.

$^{129}IO_3^-$ was lessened. However, given the change in HA surface charge with pH, it is expected that reaction at pH 6 would be slower than that at pH 4.

Additions of Fe^{2+} and Mn^{2+} did not result in an increased rate of $^{129}IO_3^-$ reduction, the only effect observed was a slight reduction in the rate of iodate loss in the 0.2 g L^{-1} HA suspension. Systems containing Fe^{2+} did however increase the amount of $^{129}I^-$ formed at both pH 4 and pH 6.

The rate of IO_3^- reduction was increased in HA systems containing goethite (**Figure 4.5**) compared to HA only systems (**Figure 4.3**), and instantaneous sorption of IO_3^- occurred in goethite only systems at pH 4 (95% and 97% reduction at 4°C and 20°C respectively after 3 days) with no transformation to $^{129}I^-$ (**Figure 4.5**). This indicates that at pH 4, HA in combination with goethite transforms/sorbs IO_3^- more rapidly than HA alone, but not as rapidly as goethite alone. In samples at pH 6 transformation of IO_3^- is slower in comparison to HA only systems (**Figure 4.4**), and goethite alone does not result in instantaneous sorption as seen at pH 4. It is unknown whether the increased concentration of IO_3^- added (540 µg L^{-1}) to the pH 6 system is resulting in a concentration effect. Nagata & Fukushi (2010) also demonstrated increased IO_3^- adsorption onto goethite with decreasing pH. As pH decreases goethite has a greater positive surface charge (Sigg & Stumm, 1981), which aids in the adsorption of anionic IO_3^-. Humic acid adsorption onto goethite has also been demonstrated to increase with decreasing pH (Antelo *et al.*, 2007). Humic acid could therefore be in competition with IO_3^- for goethite adsorption sites hence the increased IO_3^- sorption in goethite only systems. In HA systems combined with goethite it is possible that both interaction with HA, with simultaneous adsorption on goethite, is increasing the overall rate in comparison to HA only systems.
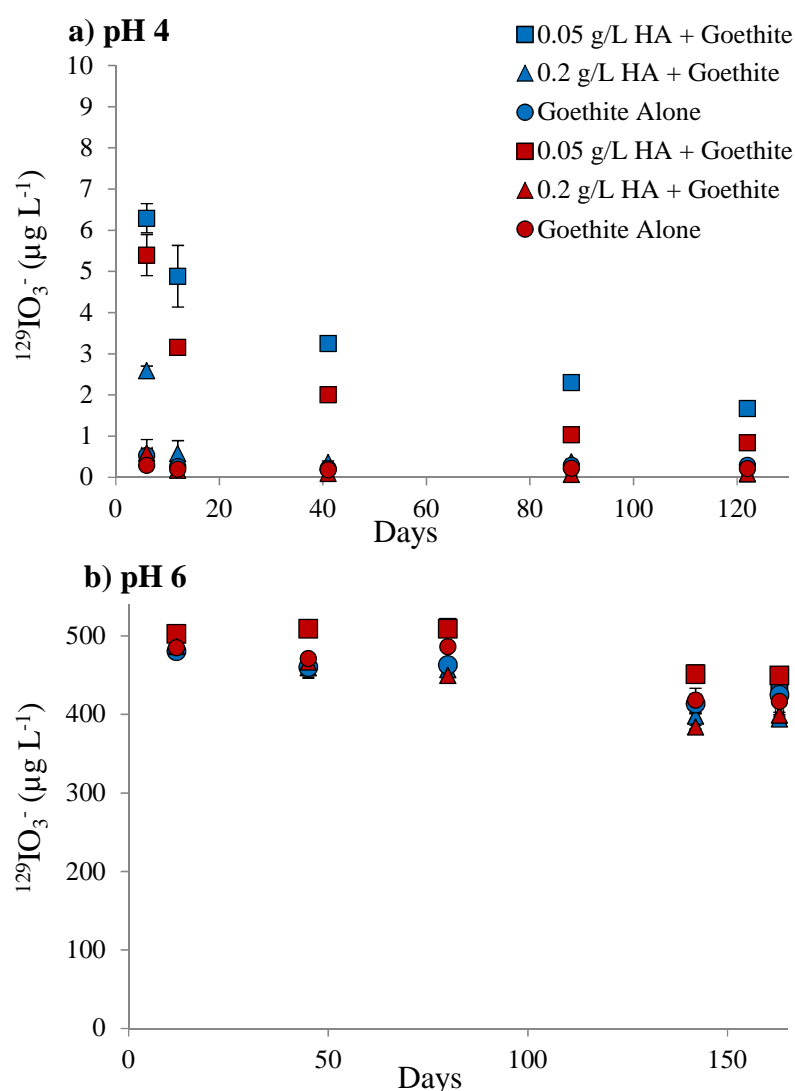
Figure 4.5. Humic acid systems (0.05 and 0.2 g L^{-1} HA) with goethite (20% by HA weight) and goethite alone, spiked at a) pH 4 with 10 µg L^{-1} $^{129}IO_3^-$ and b) pH 6 with 540 µg L^{-1} $^{129}IO_3^-$. Stored at 4°C (blue) and 20°C (red). Error bars based on two replicates.

Unlike IO_3^-, HA systems containing goethite did not result in an increased rate of I^- transformation (**Figure 4.6**) in comparison to HA only systems (**Figure 4.17**, Section 4.4.3), however goethite only systems at pH 4 did increase the rate of sorption. As previously mentioned in the case of IO_3^-, it is possible that HA is in competition with I^- for adsorption sites in the combined HA/goethite systems therefore reducing the rate of removal in comparison to goethite only systems. Compared to the instantaneous adsorption of IO_3^- to goethite at pH 4, I^- added to goethite systems demonstrated much slower adsorption at pH 4, and as with IO_3^-, no adsorption at pH 6 was observed here.

Kaplan *et al.* (2000) demonstrated no adsorption of I⁻ on goethite surfaces between pH 5.8 and 6.2. However, Nagata *et al.* (2009) demonstrated that I⁻ adsorption onto goethite could be predicted to increase with decreasing pH as observed here.
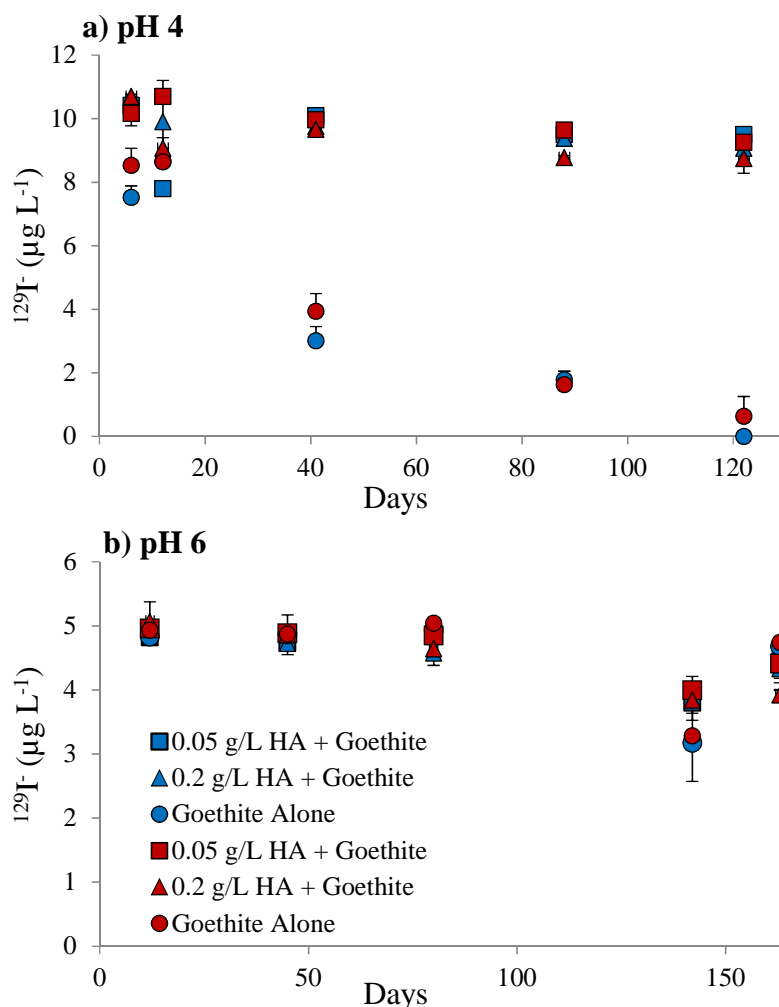
Figure 4.6. Humic acid systems (0.05 and 0.2 g L⁻¹ HA) with goethite (20% by HA weight) and goethite alone, spiked at a) pH 4 with 10 µg L⁻¹ ¹²⁹I⁻ and b) pH 6 with 5 µg L⁻¹ ¹²⁹I⁻. Stored at 4ºC (blue) and 20ºC (red). Error bars based on two replicates.

It is unlikely that the initial rapid loss of $^{129}IO_3^-$ in any of the systems was a result of volatilisation of iodine, as it has been previously demonstrated that loss in this form is minimal (Bostock *et al.*, 2003; Sheppard *et al.*, 2006). Total ^{129}I analysis of samples was undertaken to confirm this and demonstrated that there was no significant loss of iodine. Reduction is therefore more likely to be a result of transformation of $^{129}IO_3^-$ to I⁻ or

reactive intermediates such as HOI or I_2 before subsequent incorporation into aromatic structures or, in the presence of goethite, electrostatic sorption (Allard *et al*., 2009; Francois, 1987; Fuhrmann *et al.*, 1998; Reiller & Moulin, 2002; Schlegel *et al*., 2006; Steinberg *et al.*, 2008).

4.4.1.2 Effect of pH

Changes in speciation were monitored over > 3 months when HA suspensions (0.2 g L^{-1}) were spiked with 10 µg L^{-1} $^{129}IO_3^-$ at a pH range of 4-7 (0.5 pH increments). All pH systems at 4°C (**Figure 4.7**), 10°C (**Figure 4.8**) and 20°C (**Figure 4.9**) demonstrated loss of $^{129}IO_3^-$ from solution, with concomitant increases in both $^{129}I^-$ and Org-^{129}I. As previously observed; an apparently instantaneous 'loss' of $^{129}IO_3^-$ from solution was followed by slower time-dependent sorption. After just 3 days at pH 4 >50% of the added $^{129}IO_3^-$ had been reduced and transformed; by 30 days all had been transformed to $^{129}I^-$ or bound as Org-^{129}I at all three temperatures. In contrast at pH 7 ~16% was removed over the first 3 days and 51.9% on average after 30 days, suggesting a significantly slower reaction at higher pHs. As pH decreased and temperature increased there was a clear increase in the rate of $^{129}IO_3^-$ transformations.

Increased pH was demonstrated to increase the negative surface charge on the HA (Chapter 3) and therefore to increase the electrostatic repulsion of anionic species. This would explain the reduced rates of IO_3^- reduction at pH 6. It is also likely that competition between hydroxyl and iodine ions for binding sites would be greater and would contribute to this effect (Ashworth *et al.*, 2003). This interaction between negatively charged OM and IO_3^- at low pH has also been demonstrated by Steinberg *et al*. (2008) where the rate of reaction of $^{129}IO_3^-$ with *Sphagnum* peat was shown to increase as pH decreased. This

was attributed to electrostatic repulsion between the peat matrix and IO_3^- ions at high pH. The naturally high OM content of the *Sphagnum* peat would likely behave in a similar manner to the pure OM systems investigated here.
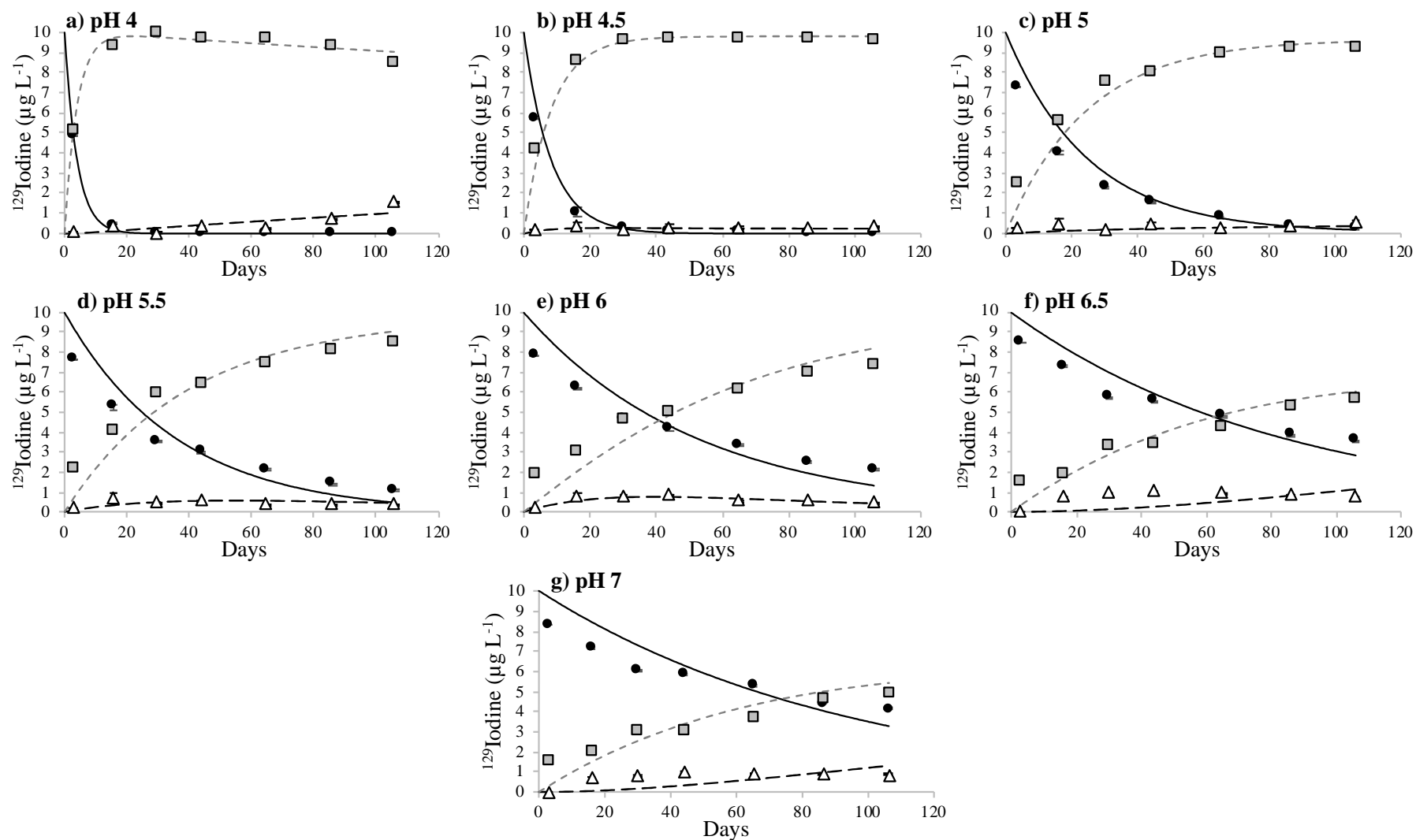
Figure 4.7. HA systems (0.2 g L^{-1}) spiked with 10 µg L^{-1} ^{129}IO$_3^-$ and incubated for 106 days at 4°C at a range of pH levels; a) pH 4.0, b) pH 4.5, c) pH 5.0, d) pH 5.5, e) pH 6.0, f) pH 6.5 and g) pH 7.0. Removal of iodate (black circles) is shown alongside an increase in iodide (white triangles) and Org-I (grey squares). Lines indicate model fits (discussed in Section 4.4.6). Error bars based on two replicates.
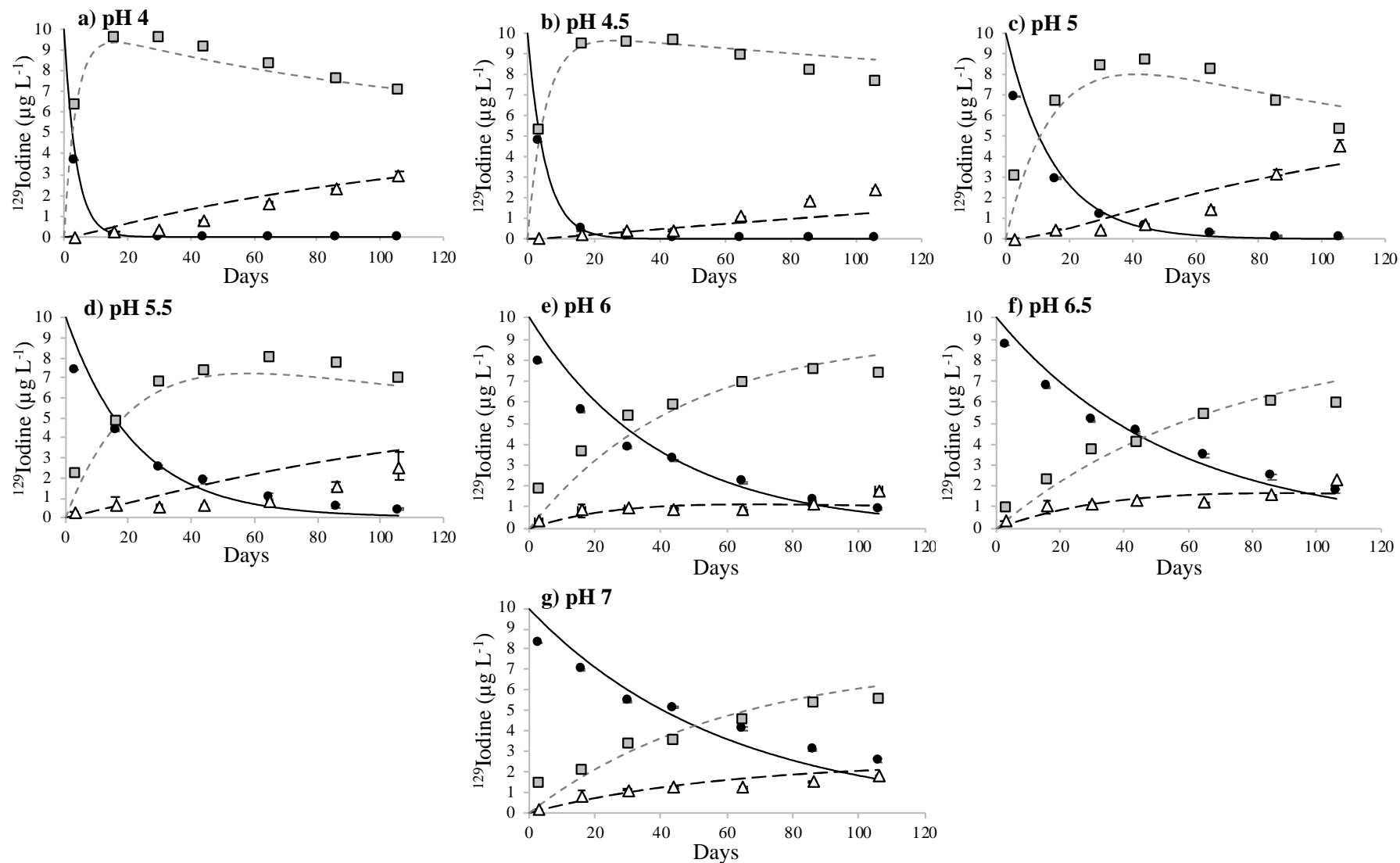
Figure 4.8. HA systems (0.2 g L^{-1}) spiked with 10 µg L^{-1} ^{129}IO$_3^-$ and incubated for 106 days at 10°C at a range of pH levels; a) pH 4.0, b) pH 4.5, c) pH 5.0, d) pH 5.5, e) pH 6.0, f) pH 6.5 and g) pH 7.0. Removal of iodate (black circles) is shown alongside an increase in iodide (white triangles) and Org-I (grey squares). Lines indicate model fits (discussed in Section 4.4.6). Error bars based on two replicates.
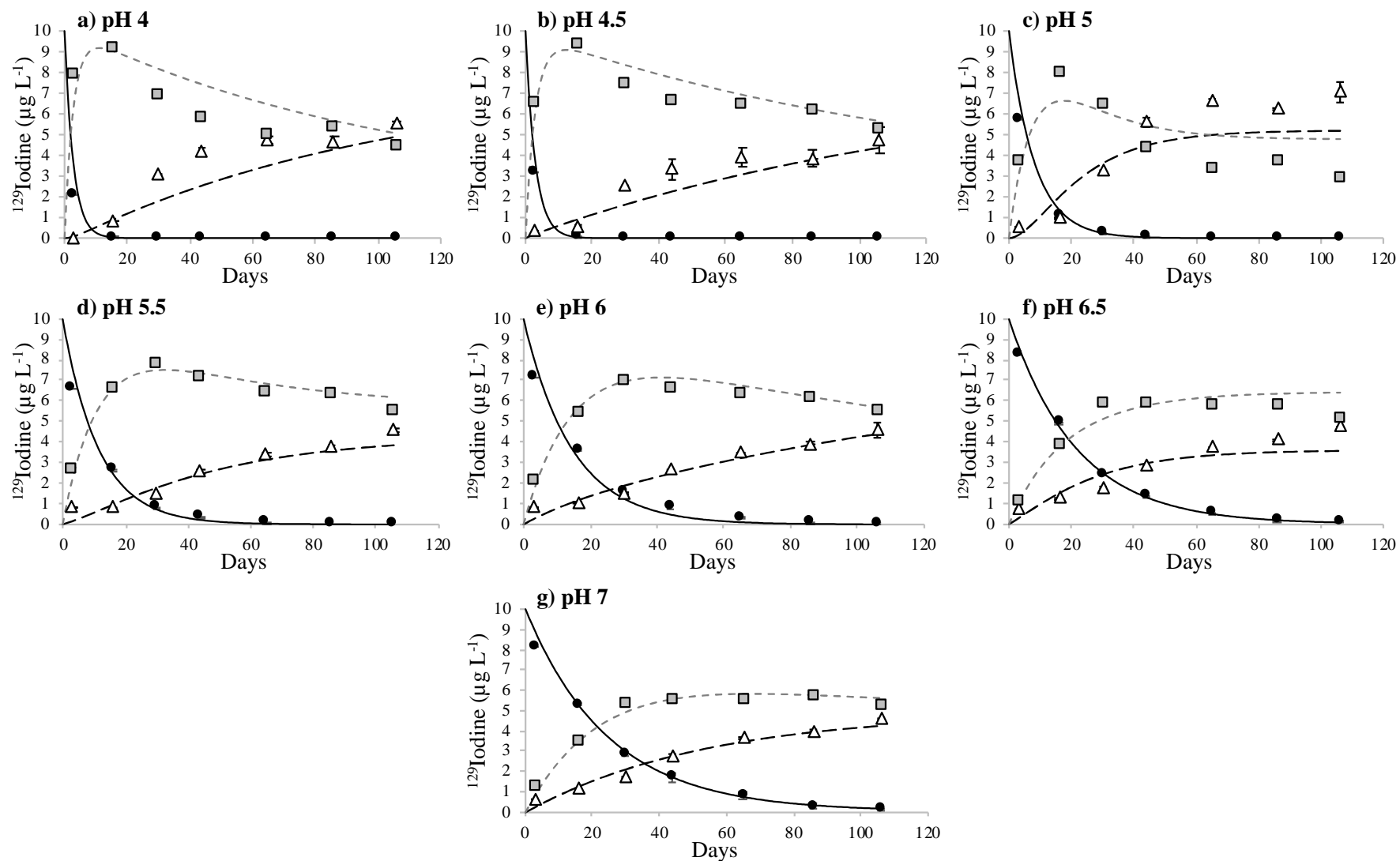
Figure 4.9. HA systems (0.2 g L^{-1}) spiked with 10 µg L^{-1} ^{129}IO$_3^-$ and incubated for 106 days at 20°C at a range of pH levels; a) pH 4.0, b) pH 4.5, c) pH 5.0, d) pH 5.5, e) pH 6.0, f) pH 6.5 and g) pH 7.0. Removal of iodate (black circles) is shown alongside an increase in iodide (white triangles) and Org-I (grey squares). Lines indicate model fits (discussed in Section 4.4.6). Error bars based on two replicates.

When $^{129}IO_3^-$ interacts with HA both $^{129}I^-$ and Org-^{129}I are formed to different degrees depending on the conditions of the system. The relationship between $^{129}I^-$ formation and pH is not as clear as that for $^{129}IO_3^-$ reduction. The general trend observed is the formation of more $^{129}I^-$ at lower pH, however temperature was also important since increased temperature resulted in greater $^{129}I^-$ formation. When samples were incubated at 20°C an average of ~57.7% (at pH 4-5) and ~46.1% (at pH 5.5-7) of the initial $^{129}IO_3^-$ spike was converted to $^{129}I^-$ after 106 days, whereas only ~32.8% and ~21.2%, and ~8.1% and ~6.5% was converted for the respective pH groups at 10°C and 4°C. Humic acid has the ability to both reduce IO_3^- and oxidise I^- in soils, therefore the $^{129}I^-$ formed can be oxidised (Yamaguchi *et al.*, 2010). However, the oxidation of I^- by OM is expected to be minimal due to the reduced reactivity of I^- towards OM (Schlegel *et al.*, 2006).

4.4.1.3 Effect of HA concentration

The effect of HA concentration on the transformations of $^{129}IO_3^-$ was investigated in suspensions containing 1, 0.5, 0.1, 0.05 and 0.01 g L^{-1} HA all spiked with 10 µg L^{-1} $^{129}IO_3^-$ at 4°C (**Figure 4.10**), 10°C (**Figure 4.11**) and 20°C (**Figure 4.12**). The rate of both $^{129}IO_3^-$ reduction and the formation of $^{129}I^-$ and Org-^{129}I increased with increasing HA concentration and temperature. Humic acid behaves as an electron acceptor, reducing IO_3^- to reactive intermediates and allowing reaction with HA carboxyl and phenolic groups. Therefore, the more HA the greater the electron supply and the more carboxyl and phenolic groups available for reaction, thus an increased rate of IO_3^- reduction and transformation to Org-I. No previous studies of iodine interaction with HA have directly altered the HA concentrations as undertaken here, there are however a number of studies that have adjusted the I:HA ratio by adding different concentrations of iodine to HA/OM systems. Both Xu *et al.* (2012) and Schwehr *et al.* (2009) varied the amount of ^{129}I added

to HA and high OM sediments, and demonstrated an increasing k_d in favour of Org-I formation when I concentration decreased. This confirmed that the transformation of I species to reactive intermediates and its association with OM is influenced by the amount of OM/HA. The effect of OM content has also been demonstrated in whole soil systems, for example Yamaguchi *et al.* (2010) demonstrated that a soil with a higher OM content retained more I in a non-exchangeable form, than a soil with a lower OM content. Conversely, Bowley *et al.* (2016) added varying concentrations of IO_3^- to HA suspensions to achieve differing I:HA ratios, and demonstrated no significant effect of I:HA ratio on the rate of IO_3^- transformation. However the HA concentration used by Bowley *et al.* (2016) was 7.18 g L^{-1}, which is c.7 times higher than the highest concentration used in this study. The IO_3^- concentrations were 22.1, 44.1 and 88.2 µg L^{-1}, again significantly higher than those used here. It is possible that the maximum rate of reaction was observed in these experiments and therefore increasing the ratio didn't increase the rate of reduction despite the I:HA ratios being similar to those investigated here. It is apparent that HA content, and consequently SOM content, has a significant effect on the rate of IO_3^- removal from solution and its transformation, however further investigation is encouraged to fully understand these mechanisms.
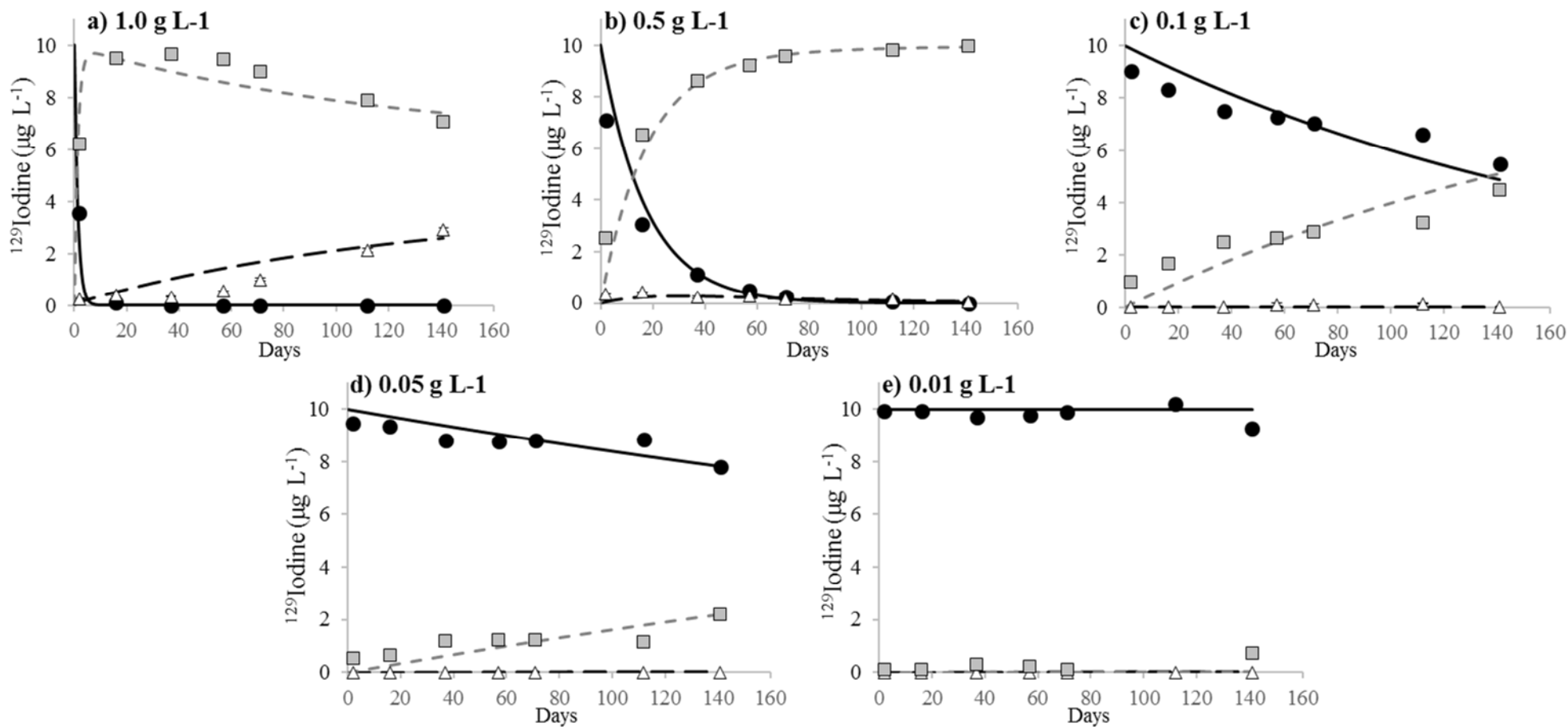
Figure 4.10. HA systems spiked with 10 µg L^{-1} ^{129}IO$_3^-$ and incubated for 141 days at 4°C at a range of HA concentrations; a) 1 g L^{-1}, b) 0.5 g L^{-1}, c) 0.1 g L^{-1}, d) 0.05 g L^{-1}, and e) 0.01 g L^{-1}. Removal of iodate (black circles) is shown alongside an increase in iodide (white triangles) and Org-I (grey squares). Lines indicate model fits. Error bars are based on two replicates.
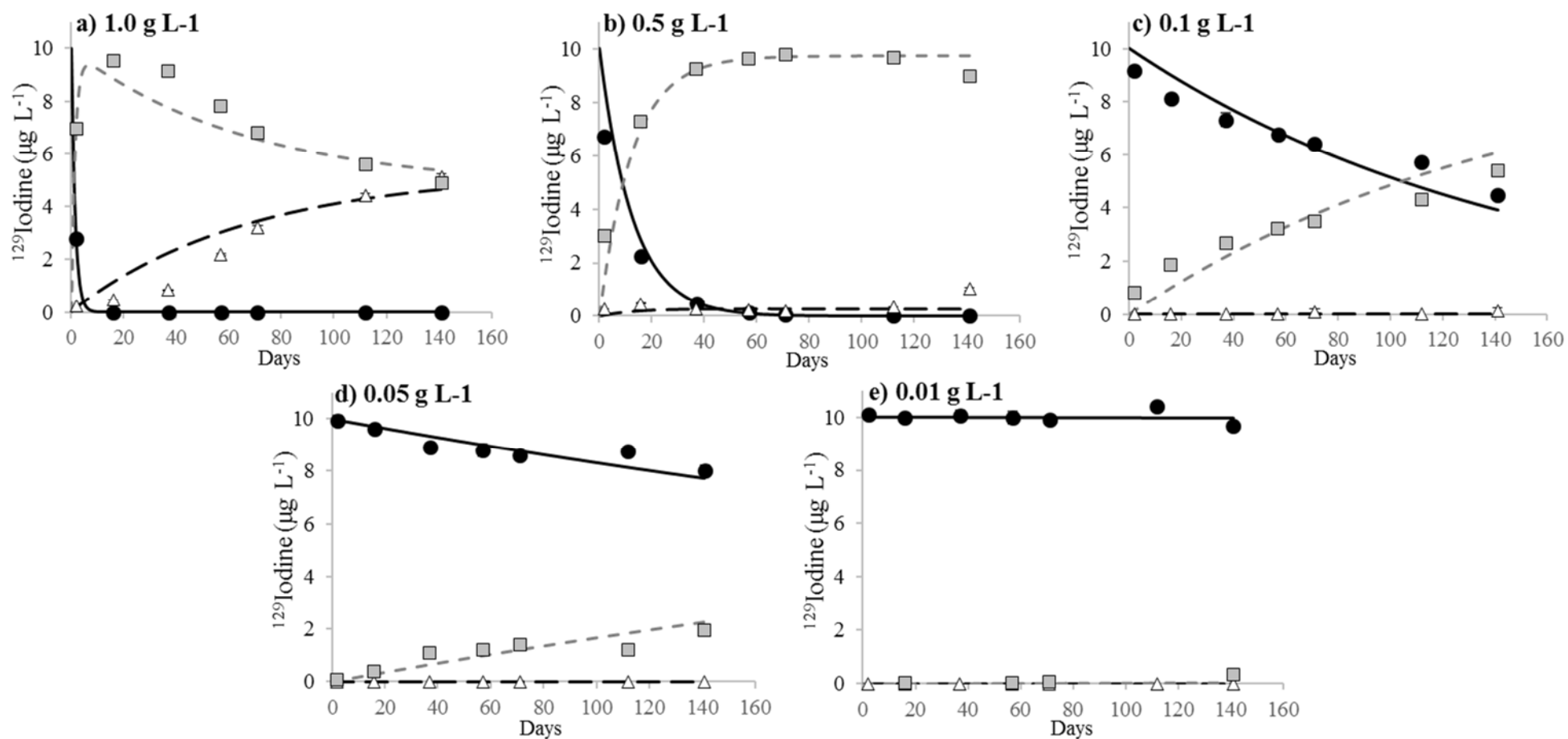
Figure 4.11. HA systems spiked with 10 µg L^{-1} ^{129}IO$_3^-$ and incubated for 141 days at 10°C at a range of HA concentrations; a) 1 g L^{-1}, b) 0.5 g L^{-1}, c) 0.1 g L^{-1}, d) 0.05 g L^{-1}, and e) 0.01 g L^{-1}. Removal of iodate (black circles) is shown alongside an increase in iodide (white triangles) and Org-I (grey squares). Lines indicate model fits. Error bars are based on two replicates.
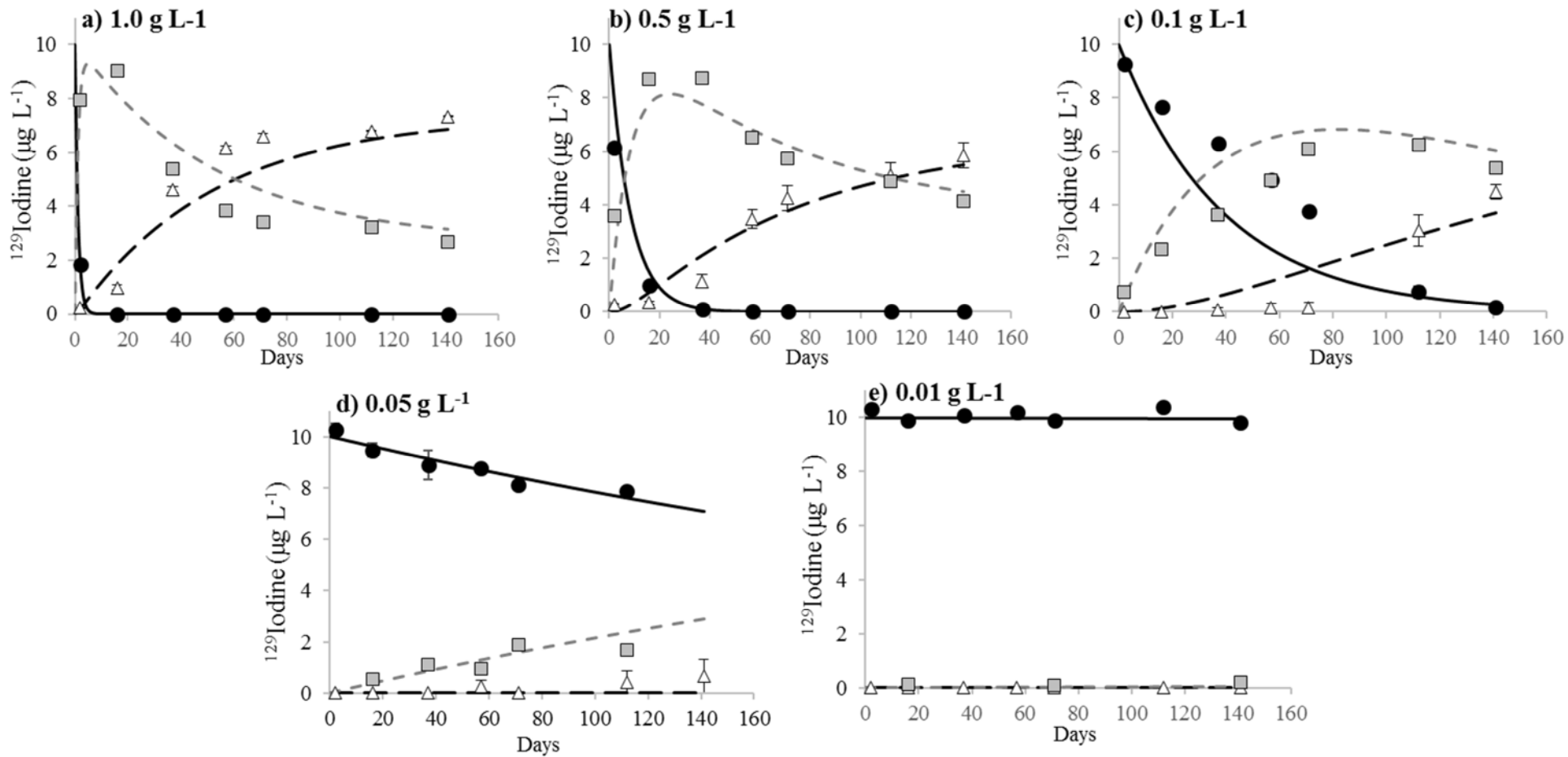
Figure 4.12. HA systems spiked with 10 µg L^{-1} ^{129}IO$_3$$^-$ and incubated for 141 days at 20°C at a range of HA concentrations; a) 1 g L^{-1}, b) 0.5 g L^{-1}, c) 0.1 g L^{-1}, d) 0.05 g L^{-1}, and e) 0.01 g L^{-1}. Removal of iodate (black circles) is shown alongside an increase in iodide (white triangles) and Org-I (grey squares). Lines indicate model fits. Error bar are based on two replicates.

4.4.1.4 Formation of organic-I species

The formation of Org-^{129}I species here has been calculated as the difference between $^{129}IO_3^-$ added and $^{129}I^-$ formed, as shown in **Figures 4.7, 4.8** and **4.9** across the 4-7 pH range and **Figures 4.10, 4.11** and **4.12** at a range of HA concentrations. Due to the ongoing formation of $^{129}I^-$ with time in most systems and the consistent reduction of $^{129}IO_3^-$, a pattern of Org-^{129}I formation and then loss was observed in some systems. For example, **Figure 4.9** demonstrates rapid formation of Org-^{129}I species followed by a slow reduction in Org-^{129}I as apparent conversion to I^- occurs. The reduction in the concentration of Org-^{129}I appeared to be more rapid at lower pHs (e.g. **Figure 4.9**) and high temperatures (e.g. **Figures 4.7-4.9**), and has not been reported before. All previous HA studies in the literature investigate the interaction of I with HA at neutral pH, where this mechanism is less obvious unless experiments are conducted over extended time periods. For example, Bowley *et al*. (2016) investigated the dynamics of IO_3^- with HA at pH 7 over 2000 hours and Org-I and I^- concentrations increased gradually before apparently reaching a plateau, a decrease in Org-I was not observed.

Size exclusion chromatograms collected alongside inorganic speciation (HPLC-ICP-MS) information demonstrated a similar trend of initial incorporation into the organic phase, followed by remobilisation back into solution with an increase in the I^- peak over time (**Figure 4.13**). A comparison of inorganic speciation data with SEC data suggested that there was accurate recovery of inorganic iodine species by SEC but Org-I was less than the total I added by an average of 3.33 µg L^{-1} (**Figure 4.14**).

Figure 4.13. Size exclusion chromatograms of ^{129}I in a HA suspension spiked with $^{129}IO_3^-$ and incubated for 106 days at 20°C. Chromatograms are offset by 2 x 10^3 counts per second to allow clear comparison.

Figure 4.14. HPLC speciation data compared to SEC data for inorganic a) iodate and b) iodide, and c) organic iodine species. Org-I species are derived from a mass balance calculation. The three-day time points for iodate (circled) are unreliable as the peak is partly hidden by the organic peak.

Total I analysis by ICP-MS confirmed that all the ^{129}I added to the samples was present, and that volatilisation had not occurred. This suggests that either SEC data is only indicative of the presence of Org-I species and cannot be used quantitatively, or the presence of an intermediate species has not been isolated by either technique. Consequently the calculated increase in Org-I concentration could include intermediate species that are formed but are not observed in the chromatograms and the increase in Org-I concentration could be more gradual. However, the increase in I^- concentration suggests that if HA is mediating the conversion of IO_3^- to I^- then the Org-I concentration must be reducing over time. Steinberg *et al.* (2008) demonstrated an initial increase in Org-^{129}I concentration when IO_3^- was added to *Sphagnum* peat followed by a decrease as I^- was formed, but this aspect of the data was not acknowledged or discussed. Steinberg *et al.* (2008) also calculated Org-I on a mass balance basis. *Sphagnum* peat soils have a very high OM content, the similarity between the results of Steinberg *et al*. (2008) and this study suggests that this mechanism should be further investigated.

Both Xu *et al.* (2012) and Schlegel *et al*. (2006) suggest that iodinated HSs are quite stable, and the covalent C-I bond can only be broken, and the I replaced, by nucleophiles or electrophiles stronger than itself. This suggests that I^- release from HSs is limited in contrast to the pattern observed here. Farrenkopf *et al*. (1997) investigated the reduction of IO_3^- in seawater in the presence of the bacteria *Shewanella putrefaciens*, and found that IO_3^- was initially reduced to HOI and I_2 which reacted rapidly with organic substrates forming C-I or N-I bonds, and following this, was re-released as I^-. These reactions were attributed to the presence of the bacteria and took place at pH 8.2; the HA systems here are much more acidic. Microbial activity is typically greater at neutral pH and is therefore

less likely to be important in these HA systems. Remobilisation of Org-I as I⁻ has implications for the bioavailability of I in systems with high OM contents.

4.4.2 Iodate interactions with FA

The reaction between IO_3^- and FA appears to occur at a similar rate to the equivalent reaction with HA (**Figure 4.15**). In reaction with HA at pH 4 (20°C) ~77% $^{129}IO_3^-$ was reduced after 4 days (based on modelled data, **Figure 4.9a**), compared to FA systems under the same conditions where after 4 days ~95% reduction was observed. However,

Figure 4.15. Comparison between FA and HA systems (both 0.2 g L⁻¹) at pH 4 and pH 6 spiked with 10 μg L⁻¹ $^{129}IO_3^-$. Samples stored at a) 4°C and b) 20°C.

significantly more $^{129}I^-$ was formed (**Figure 4.16**). The total acidity of the FA and HA were 8.225 mol kg^{-1} and 6.523 mol kg^{-1} respectively (Section 3.4.1.3). This relates to an increased proportion of carboxyl (COOH) groups in the FA. A greater proportion of reactive groups would encourage IO_3^- interaction. However, this would also result in a greater negative surface charge on the FA, increasing the electrostatic repulsion with IO_3^- at a given pH (Section 3.4.2). The increased COOH content of FA might also result in a greater proportion of I^- release from Org-I as demonstrated for HA systems (Section 4.4.1.4).

Figure 4.16. Comparison of $^{129}I^-$ formation in FA and HA systems (both 0.2 g L^{-1}) at pH 4 and pH 6 when spiked with 10 μg L^{-1} $^{129}IO_3^-$. Samples stored at a) 4°C and b) 20°C.

4.4.3 Iodide interactions with humic acid

When HA suspensions were spiked with $^{129}I^-$, its removal from solution was much slower than observed for $^{129}IO_3^-$. Removal of $^{129}I^-$ from solution in 0.05 and 0.2 g L^{-1} HA at pH 4 and pH 6, demonstrated gradual formation as Org-^{129}I, with no observed $^{129}IO_3^-$ (**Figure 4.17**). After 163 days, ~35% of the added $^{129}I^-$ had on average been transformed to Org-^{129}I in the 0.2 g L^{-1} HA samples at pH 6 (20°C), and 17% in the 0.05 g L^{-1} HA samples

under the same conditions. Although this reaction was slower than that of IO_3^-, it demonstrates an effect of increased HA concentration on the rate of reaction. Unlike $^{129}IO_3^-$, reaction was greater at pH 6 than at pH 4. The slow reaction of I^- with HA is in contrast to the rapid removal seen in whole soil systems by Shetaya *et al*. (2012). In order for $^{129}I^-$ to interact with OM it must first be oxidised to intermediate species, e.g. I_2 or HOI. Evidence suggests that the most significant oxidising agents in soils are metal oxides and enzymes, in addition to OM itself (Allard *et al.*, 2009; Gallard *et al.*, 2009; Seki *et al.*, 2013; Yamaguchi *et al.*, 2010). Bowley (2013) suggested that IO_3^- can react more readily with HA than, I^-, by polarising its negative charge towards the oxygen atoms and creating a slight positive charge around the I atom ($I^{\delta+}$) allowing it to approach the negatively charged surface of the HA. Iodide is unable to do this which would explain the greater reaction rate of $^{129}IO_3^-$ with HA compare to $^{129}I^-$. Another possible explanation is suggested by the work of Bors & Martens (1992) who investigated the contribution of microbial biomass to the adsorption of radioiodine in soils, and found that when the microbial community was reduced by as little as 10%, a detrimental effect on $^{125}I^-$ soil adsorption was observed. Seki *et al.* (2013) investigated the effect of autoclaving, heat treatment, γ-irradiation and addition of reducing agents on soil laccase activity and found that reduced laccase activity significantly reduced I^- oxidation and consequent incorporation into OM. Rapid removal of I^- from soil solution, in contrast to the slow reaction seen in HA-only systems, indicates that I^- interaction with SOM may therefore be microbially, or enzymatically, mediated. The slow reaction observed in these pure HA systems could be attributed to a lack of microbial activity and therefore enzyme activity.

Figure 4.17. Transformations of added $^{129}I^-$ over time after an addition of 10 µg L^{-1} $^{129}I^-$ to HA suspensions at pH 4 and pH 6 containing 0.05 g L^{-1} and 0.2 g L^{-1} with or without additions of Fe^{2+} (▲) and Mn^{2+} (●) at 4°C (blue) and 20°C (red). Error bars based on standard deviation of two replicates.

4.4.3.1 Redox coupling

Changes in speciation were monitored in HA systems (0.2 g L^{-1}) at pH 6 that received a mixed iodine spike containing $^{129}IO_3^-$ and $^{127}I^-$ together, compared to HA systems with $^{129}I^-$ (**Figure 4.18**) or $^{129}IO_3^-$ (**Figure 4.19**) as separate spikes. When IO_3^- was added together with I^- to HA suspensions, the rate of $^{129}IO_3^-$ reduction was not significantly increased. However, the rate of I^- oxidation was significantly increased when added as a mixed spiked compared to when added as a single spike (**Figure 4.18**). The only other experiment containing a single I^- spike for comparison was spiked with 5 µg L^{-1}, whereas the mixed spiked experiment was spiked with 10 µg L^{-1}. If there was a concentration effect, the higher concentration of I^- would effectively have a lower rate of reduction as

Figure 4.18. Single spiked system was spiked with 5 µg L^{-1} $^{129}I^-$ alone (closed markers), whereas mixed spiked system received 10 µg L^{-1} $^{127}I^-$ alongside 10 µg L^{-1} $^{129}IO_3^-$ (open markers). Both in the presence of HA (0.2 g L^{-1}) at pH 6. Error bars based on two replicates.

Figure 4.19. Reduction of $^{129}IO_3^-$ when spiked at 10 µg L^{-1} either alone (closed markers) or as a mixed spiked (open markers) alongside $^{127}I^-$ in the presence of HA (0.2 g L^{-1}) at pH 6.

the I:HA ratio would be greater, therefore it is suspected that the concentration has little effect. When I$^-$ was added alone the rate of transformation was very slow, with 32.6% reduction in concentration after 142 days. However, when spiked with IO$_3^-$ the rate of transformation significantly increased, with 92.8% reduction in I$^-$ concentration after 31 days. Similar results were observed by Bowley *et al.* (2016) where the rate of I$^-$ transformation when added together with IO$_3^-$ in HA systems was enhanced by suspected redox coupling. However the systems investigated by Bowley *et al.* (2016) also demonstrated an increased rate of IO$_3^-$ reduction and formation of Org-I in mixed systems; only a suggestion of this appears in the 20°C systems investigated here. Redox coupling of IO$_3^-$ and I$^-$ is expected according to Equation 4.7:

$$IO_3^- + 5I^- + 6H^+ \rightarrow 3I_2 + 3H_2O \tag{4.7}$$

This reaction suggests the rate of I$^-$ oxidation is 5 times faster when in combination with IO$_3^-$, with only a minor increase in IO$_3^-$ reduction depending upon the IO$_3^-$:I$^-$ ratio. This

interaction is difficult to characterize as when IO_3^- alone is added I^- is formed and redox coupling can occur. This makes determining the mechanism complex since both species are present as the same isotope (^{129}I).

4.4.4 Effect of microbes on I interactions with HA

Microbial activity is a possible confounding factor in systems prepared in non-sterile environments. Sterilisation by filtration was used to investigate any effect this could have on I interactions in HA systems. Results demonstrated that there was no effect on the rate of IO_3^- reduction in HA systems compared to unfiltered systems (**Figure 4.20 a** and **d**). However, there was a significant reduction in the amount of I^- formed (**Figure 4.20 b** and **e**) in filtered systems and consequently higher concentrations of Org-I concentrations (**Figure 4.20c** and **e**). The effect was greater at 20°C than 4°C (**Figure 4.20**). This suggests that the initial reduction of IO_3^- is an abiotic interaction, but that the subsequent formation of I^- has a biotic component. Yamaguchi *et al.* (2008) demonstrated that soils with reduced microbial activity, due to γ-irradiation, showed no retardation of IO_3^- transformation to Org-I species, providing further evidence that IO_3^- reduction to reactive intermediates is abiotic. The reduction in laccase activity observed by Seki *et al.* (2013) with significantly reduced I^- oxidation and consequent incorporation in OM, also suggests that microbial activity is important in mediating I^- reactions in soil systems.

Figure 4.20. Measured transformations of added $^{129}IO_3^-$ into $^{129}I^-$ and Org-^{129}I over time after an addition of 10 µg L^{-1} $^{129}IO_3^-$ to HA suspensions (0.2 g L^{-1}) at pH 6. Samples were either left untreated (●) or filter sterilised (□) and stored at 4°C (a, b, c) and 20°C (d, e, f). Error bars based on standard deviation of two replicates.

115

To investigate further filtered and non-filtered HA systems received additions of a filtered soil inoculum (no microbes added) or a non-filtered soil inoculum, and glucose as a food source to fuel microbial growth. Systems were also γ-irradiated but this resulted in speciation changes (identified by the inclusion of a control isotope solution) and therefore nothing useful could be ascertained.

Figure 4.21. Transformations of added $^{129}IO_3^-$ (10 µg L^{-1}) in HA systems (0.2 g L^{-1}) systems sterilized by filtering (a, b, c) or unfiltered (not sterile) (d, e, f). Systems were set up alone and in combination with a range of treatments; glucose (F), filtered soil inoculum (NM), un-filtered soil inoculum (M), NM + F and M + F. Iodate (a, c) and iodide (b, d) were measured. Error bars are based on two replicates.

In non-irradiated systems, the reduction of $^{129}IO_3^-$ was not affected by the presence of microbial activity and is therefore an entirely abiotic process (**Figure 4.21**). Again there were differing amounts of $^{129}I^-$ formed depending on the presence/absence of microbes (**Figure 4.21b** and **d**). Most $^{129}I^-$ was formed in systems containing soil inoculum (microbes) without glucose, regardless of whether the initial HA suspensions were filtered or not. In the previous experiment, filtering HA suspensions reduced the formation of I^- from IO_3^- and this effect was attributed to the lack of microbial activity. However, if this transformation was solely biotic then it would be anticipated that a system containing added microbes and glucose would have the most I^- formed, which was not the case. Studies have shown the abiotic reduction of iodate to iodide to be significant (Hu *et al*., 2004; Steinberg *et al*., 2008). A number of studies have also identified specific microorganisms in soils and waters, particularly sulfate-reducing bacteria and bacteria closely related to denitrifying bacteria, that are capable of reducing IO_3^- to I^- either directly or enzymatically (Amachi *et al.*, 2007; Councell & Lovley, 1997; Farrenkopf *et al*., 1997). It is therefore likely that IO_3^- can be reduced to I^- both biotically and abiotically making the elucidation of these mechanisms extremely complicated.

4.4.5 Effect of Fe^{2+} and Fe^{3+} on I interactions with HA

4.4.5.1 Effect of Fe on IO_3^- interactions with HA

The range finding experiment demonstrated that additions of Fe^{2+} and Mn^{2+} did not result in an increased rate of $^{129}IO_3^-$ removal from solution when compared to the HA only samples. However, it was observed that at pH 4, the addition of Fe^{2+} significantly increased the amount of $^{129}IO_3^-$ transformed to $^{129}I^-$, and consequently the amount of Org-^{129}I formed was reduced.

Both Fe^{2+} and Fe^{3+} can interact with carboxylic and phenolic groups on HA (Rose & Waite, 2003; Tipping, 1998; Weber *et al.*, 2006; Yamamoto *et al.*, 2010). It was hypothesised that HA in combination with Fe ions would increase I association with HA by creating localised positive charges, and decreasing the overall negative charge of the HA (Eqn. 4.8 and 4.9) (Weber *et al.*, 2006; Yamaguchi *et al.*, 2010):

$$RCOO^- + Fe^{3+} = [RCOO - Fe^{III}]^{2+} \tag{4.8}$$

$$RCOO^- + Fe^{2+} = [RCOO - Fe^{II}]^+ \tag{4.9}$$

Similar to reactions observed in HA systems without Fe, transformation of $^{129}IO_3^-$ and a concomitant increase in both $^{129}I^-$ and Org-^{129}I was observed in HA systems containing Fe (**Figure 4.22**, **Figure 4.23** and **Figure 4.24**). When compared to systems without, additions of Fe appear to both reduce the rate of IO_3^- reduction and increase the amount of $^{129}I^-$ formed. The behaviour of Fe^{2+} and Fe^{3+} in these systems was very similar. Given the nature of HA as both an electron donor and acceptor it is possible that HA has converted $Fe^{2+/3+}$ to the same form. Weber *et al.* (2006) found that Fe^{3+} could be reduced to Fe^{2+} in the presence of HA at low concentrations, however Tipping & Hurley (1992) hypothesised that conversion of Fe^{2+} to Fe^{3+} can occur. Both are plausible given the nature of HA and its ability to both donate and accept electrons, however no measurement of Fe oxidation state was made. The presence of Fe in these systems appears to accelerate $^{129}IO_3^-$ reduction straight to $^{129}I^-$ bypassing complexation with HA and resulting in less Org-^{129}I formation in comparison to HA only systems. This is an unexpected result suggesting that the reactive groups on the HA that are usually responsible for interacting with I are occupied by $Fe^{2+/3+}$, consequently the $Fe^{2+/3+}$ is being oxidised by $^{129}IO_3^-$, resulting in direct production of $^{129}I^-$ rather than Org-^{129}I (Eqn. 4.10 for Fe^{2+}). Anschutz

et al., (2000) demonstrated the ability of IO_3^- to oxidise Mn^{2+} to $MnOOH$, consequently reducing IO_3^- to I^- and increasing the concentration of I^- in solution. This has not been demonstrated directly for Fe^{2+} in combination with HA, however thermodynamically it may be possible. Humic acid samples containing $Fe^{2+/3+}$ were slightly darker/cloudier than samples without, however no obvious precipitation was visible:

$$Fe^{2+} + \frac{1}{6}IO_3^- + \frac{2}{3}H_2O \leftrightarrow FeOOH + \frac{1}{6}I^- + 2H^+ \qquad (4.10)$$

4.4.5.2 Effect of Fe concentration on IO_3^-

The amount of Fe^{2+}/Fe^{3+} in the system also appears to have an effect on the rate of $^{129}IO_3^-$ transformation; increased Fe^{2+}/Fe^{3+} resulted in a reduced rate of initial transformation. The greater the concentration of Fe^{2+}/Fe^{3+} the greater the proportion of carboxyl groups associated with Fe^{2+}/Fe^{3+} and therefore the slower initial rate of $^{129}IO_3^-$ transformation (**Figure 4.25** and **Figure 4.26**). If Fe is being oxidised by IO_3^-, then the increase in the $Fe:IO_3^-$ ratio could mean that the rate of oxidation of Fe is lower, thus transformation of the IO_3^- is slower. It is worth noting that alongside the addition of $^{129}IO_3^-$, about 16% $^{127}IO_3^-$ is also added (present in the stock I standard). As an indication of the reliability of the data the rate of $^{127}IO_3^-$ reduction was measured and compared to $^{129}IO_3^-$ measurements. The ratio of $^{129}IO_3^-$ to $^{127}IO_3^-$ follows a straight line indicating very similar reduction rates of both $^{129}IO_3^-$ and $^{127}IO_3^-$, demonstrating the robustness of this measurement technique and data (**Figure 4.27**). The points are scattered around the second time point due to error and around the final time point as the $^{127}IO_3^-$ concentrations were <0.1 µg L^{-1}.

Figure 4.22. HA systems (0.2 g L^{-1}) spiked with 10 µg L^{-1} $^{129}IO_3^-$ and incubated for 106 days at 4°C. Systems also contained additions of Fe^{3+} and Fe^{2+} to occupy 30% of the HA carboxyl groups, and were adjusted to pH 4 and pH 6. Removal of iodate (black circles) is shown alongside an increase in iodide (white triangles) and Org-I (grey squares). Lines indicate model fitting results; $^{129}IO_3^-$ model (solid black line), $^{129}I^-$ model (dashed black line) and Org-^{129}I model (dashed grey line). Error bar based on two replicates.

Figure 4.23. HA systems (0.2 g L^{-1}) spiked with 10 μg L^{-1} ^{129}IO$_3^-$ and incubated for 106 days at 10°C. Systems also contained additions of Fe^{3+} and Fe^{2+} to occupy 30% of the HA carboxyl groups, and were adjusted to pH 4 and pH 6. Removal of iodate (black circles) is shown alongside an increase in iodide (white triangles) and Org-I (grey squares). Lines indicate model fitting results; ^{129}IO$_3^-$ model (solid black line), ^{129}I$^-$ model (dashed black line) and Org-^{129}I model (dashed grey line). Error bar based on two replicates.

Figure 4.24. HA systems (0.2 g L^{-1}) spiked with 10 µg L^{-1} $^{129}IO_3^-$ and incubated for 106 days at 20°C. Systems also contained additions of Fe^{3+} and Fe^{2+} to occupy 30% of the HA carboxyl groups, and were adjusted to pH 4 and pH 6. Removal of iodate (black circles) is shown alongside an increase in iodide (white triangles) and Org-I (grey squares). Lines indicate model fitting results; $^{129}IO_3^-$ model (solid black line), $^{129}I^-$ model (dashed black line) and Org-^{129}I model (dashed grey line). Error bar based on two replicates.

Figure 4.25. HA systems (0.2 g L^{-1}) spiked with 10 µg L^{-1} $^{129}IO_3^-$ and incubated for 92 days at 4°C. Systems also contained additions of Fe^{3+} and Fe^{2+} at 10%, 30% and 50% of the HA carboxyl groups, and were adjusted to pH 4. Removal of iodate (black circles) is shown alongside an increase in iodide (white triangles) and Org-I (grey squares). Lines indicate model fitting results; $^{129}IO_3^-$ model (solid black line), $^{129}I^-$ model (dashed black line) and Org-^{129}I model (dashed grey line). Error bar based on two replicates.

Figure 4.26. HA systems (0.2 g L^{-1}) spiked with 10 µg L^{-1} ^{129}IO$_3^-$ and incubated for 92 days at 20°C. Systems also contained additions of Fe^{3+} and Fe^{2+} at 10%, 30% and 50% of the HA carboxyl groups, and were adjusted to pH 4. Removal of iodate (black circles) is shown alongside an increase in iodide (white triangles) and Org-I (grey squares). Lines indicate model fitting results; ^{129}IO$_3^-$ model (solid black line), ^{129}I$^-$ model (dashed black line) and Org-^{129}I model (dashed grey line). Error bar based on two replicates.

Figure 4.27. Ratio of measured $^{127}IO_3^-$ and $^{129}IO_3^-$ changes in concentration over time when a small amount (about 1.6 µg L^{-1}) of $^{127}IO_3^-$ is introduced into the HA system with the $^{129}IO_3^-$ spike of 10 µg L^{-1}.

4.4.5.3 Effect of Fe on I⁻ interaction with HA

The addition of $^{127}I^-$ to HA systems with $Fe^{2+/3+}$ demonstrated an initial instantaneous

reaction followed by a gradual re-release from the Fe-HA complex as I^- (**Figure 4.28**).

This is in stark contrast to HA systems without Fe where slow reduction occurred with

no re-release. The SEC chromatograms for these samples indicate a high concentration

Figure 4.28. Measured changes in $^{127}I^-$ concentration with time following spiking with 10 μg L^{-1} $^{127}I^-$ to HA suspensions (0.2 g L^{-1}) at pH 6 in combination with Fe^{2+} (●) or Fe^{3+} (▲) at 4 different Fe concentrations based on the % occupancy of HA carboxyl groups; 0% (■), 10% (white) , 30% (grey) and 50% (black). Stored at a) 4°C and b) 20°C. Error bar are based on two replicates.

of Org-^{127}I after the first 3 days followed by a decline in concentration over time. Since

this is not observed in HA systems without Fe it is possible that I is associated with the

HA by a Fe cation bridge prior to being re-released as I$^-$ (**Figure 4.29**). It is hypothesised

that the ^{127}I$^-$ is combining with the RCOO-Fe^{2+}/Fe^{3+} and RO-Fe^{2+}/Fe^{3+} instantaneously,

and as iron hydrolysis occurs the ^{127}I$^-$ is released back into solution (Eqn. 4.11 and 4.12):

$$[RCOO - Fe^{III} - 2I^-] + H_2O = [RCOO - Fe^{III}(OH)^+ - I^-] + I^- + H^+ \qquad (4.11)$$

$$[RCOO - Fe^{II} - I^-] + H_2O = [RCOO - Fe^{II}(OH)] + I^- + H^+ \qquad (4.12)$$
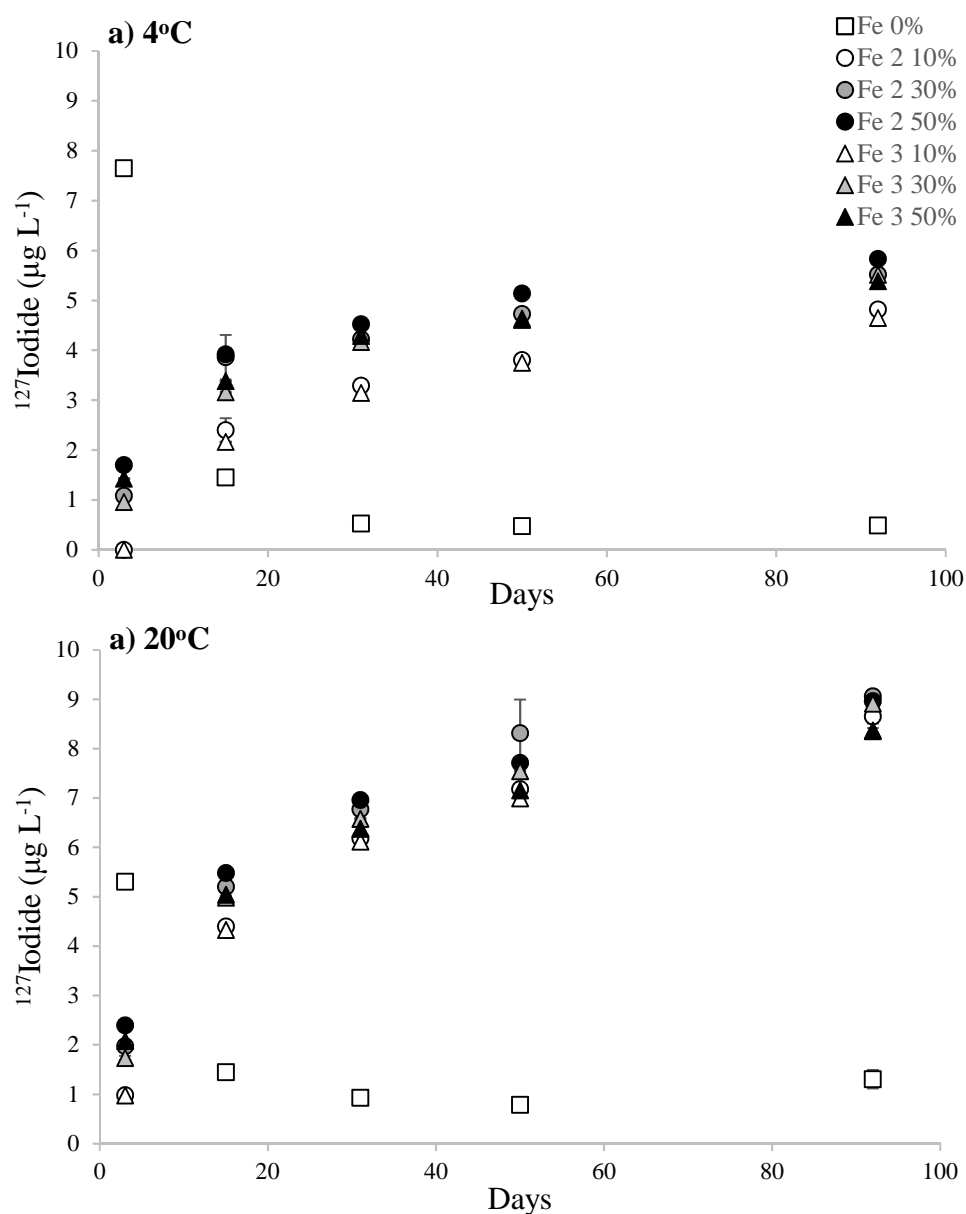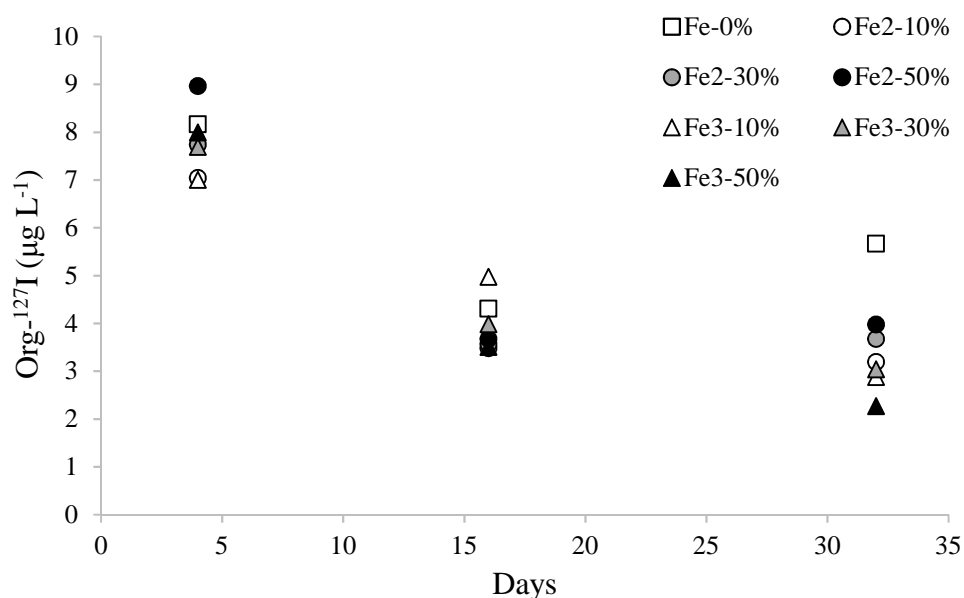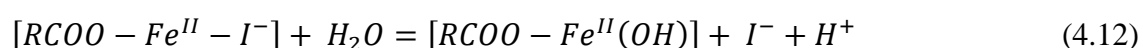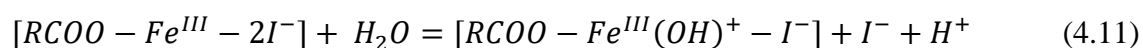
Figure 4.29. Measured changes in Org-^{127}I concentration by SEC with time
following spiking with 10 μg L^{-1} ^{127}I$^-$ to HA suspensions (0.2 g L^{-1}) at pH 6
(20°C) in combination with Fe^{2+} (●) or Fe^{3+} (▲) at 4 different Fe
concentrations based on the % occupancy of HA carboxyl groups; 0% (■),
10% (white) , 30% (grey) and 50% (black). Only a single replicate was
measured.

4.4.5.4 Effect of Fe concentration on I^-

At 4°C a higher concentration of Fe^{2+}/Fe^{3+} resulted in a marginally greater concentration of $^{127}I^-$ being re-released, most likely due to the greater degree of hydrolysis at higher Fe concentrations. However, at 20°C all systems containing Fe showed similar amounts of $^{127}I^-$ re-release regardless of the Fe concentration, which may be a consequence of the higher temperature. Throughout the duration of the experiment, systems containing Fe drifted towards a more acidic pH, whereas pH drift in systems without Fe was minimal (**Table 4.2**). This reduction in pH over time supports the idea that Fe hydrolysis could be occurring, since this reaction produces H^+ ions.

Table 4.2 pH drift in HA suspensions containing different concentrations of Fe, measured on day 1 and at completion of the experiment (Day 100).

Sample	4°C		20°C	
	Day 1	Day 100	Day 1	Day 100
Fe 0%	6.00	6.13	6.00	5.45
Fe^{2+} 10%	6.00	5.46	6.00	5.17
Fe^{2+} 30%	6.01	4.90	6.01	4.54
Fe^{2+} 50%	6.00	4.68	6.00	4.18
Fe^{3+} 10%	6.00	5.15	6.00	5.28
Fe^{3+} 30%	6.00	4.84	6.00	4.45
Fe^{3+} 50%	6.01	4.70	6.01	4.40

Sterilisation by filtration was also undertaken to observe any changes. Again the initial reduction and transformation of added $^{129}IO_3^-$ was not affected by filtration when compared to un-filtered systems at either 4°C or 20°C (**Figure 4.30**). However, I^- formation from added IO_3^- appears to be increased by filtering. This is in contrast to systems without Fe additions, where less I^- was formed in the filtered systems. This could

be due to the role iron hydrolysis is playing in the transformation of $^{129}IO_3^-$ to $^{129}I^-$ and

further investigation into these effects is necessary to fully understand the interactions.
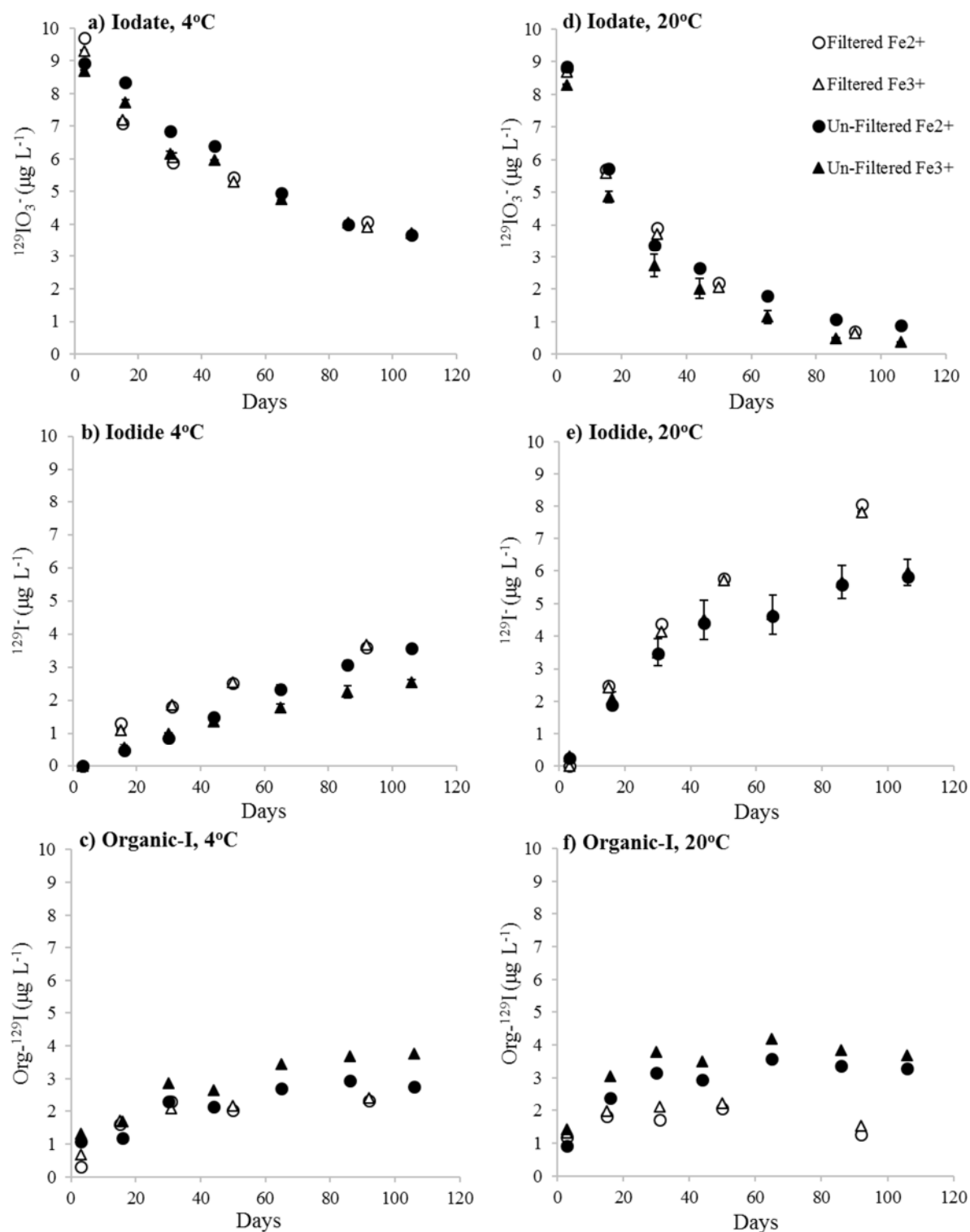
Figure 4.30. Effect of filter sterilization on measured changes in ^{129}I concentration and speciation when 10 µg L^{-1} $^{129}IO_3^-$ was added to HA suspensions (0.2 g L^{-1}) containing Fe^{2+} (∘) and Fe^{3+} (△) at pH 6 and stored at 4°C (a, b, c) and 20°C (d, e, f). Error bars based on two replicates.

4.4.6 Modelling

Fitted model predictions were compared to the observations and estimated rate coefficients were calculated. The effect of pH and HA were modelled together whilst the effect of Fe was modelled separately at a later date.

4.4.6.1 Modelling pH and HA concentration

The model fit was good (r^2 = 0.87, p < 0.001, **Figure 4.31**), supporting the model structure presented in **Figure 4.2**, however other model structures may also be supported therefore alternative model pathways were considered. For example, a pathway allowing oxidation of I^- to IO_3^- was tested. However, this was found to have no effect on the model fit, and there was no experimental evidence of IO_3^- formation. The best overall fit was achieved for IO_3^-; Org-I and I^- gave a poorer fit. The poorer fit for Org-I and I^- may be due to the large concentration increases and decreases that are observed in some systems (e.g. **Figure 4.9a**).

Iodate was rapidly converted to humic-bound forms (k_1 = 0.363-0.011) whilst IO_3^- transformation to I^- was very slow (k_2 = 0.009-0.00001). After an initial rapid increase in Org-I concentration from k_1 there was a decrease as some Org-I was remobilised to I^- (k_3 = 0.034-0.00001) simultaneously to a slow oxidation back to Org-I (k_4 = 0.060-0.0001). The estimated rate constants presented here support the suggestion (Section 4.4.1.4) that in these systems IO_3^- undergoes reduction and incorporation into the organic phase prior to remobilisation as I^-. Removal of k_2 had little or no effect on the model fit (r^2 = 0.86) demonstrating that reduction of IO_3^- directly to I^- does not appear to occur, and that in these systems reduction of IO_3^- to I^- was mediated by HA. Correlation analysis confirmed

that transformation of IO_3^- to Org-I (k_1) was significantly affected by both pH ($r = 0.82$,

Figure 4.32) and temperature ($r = 0.64$).
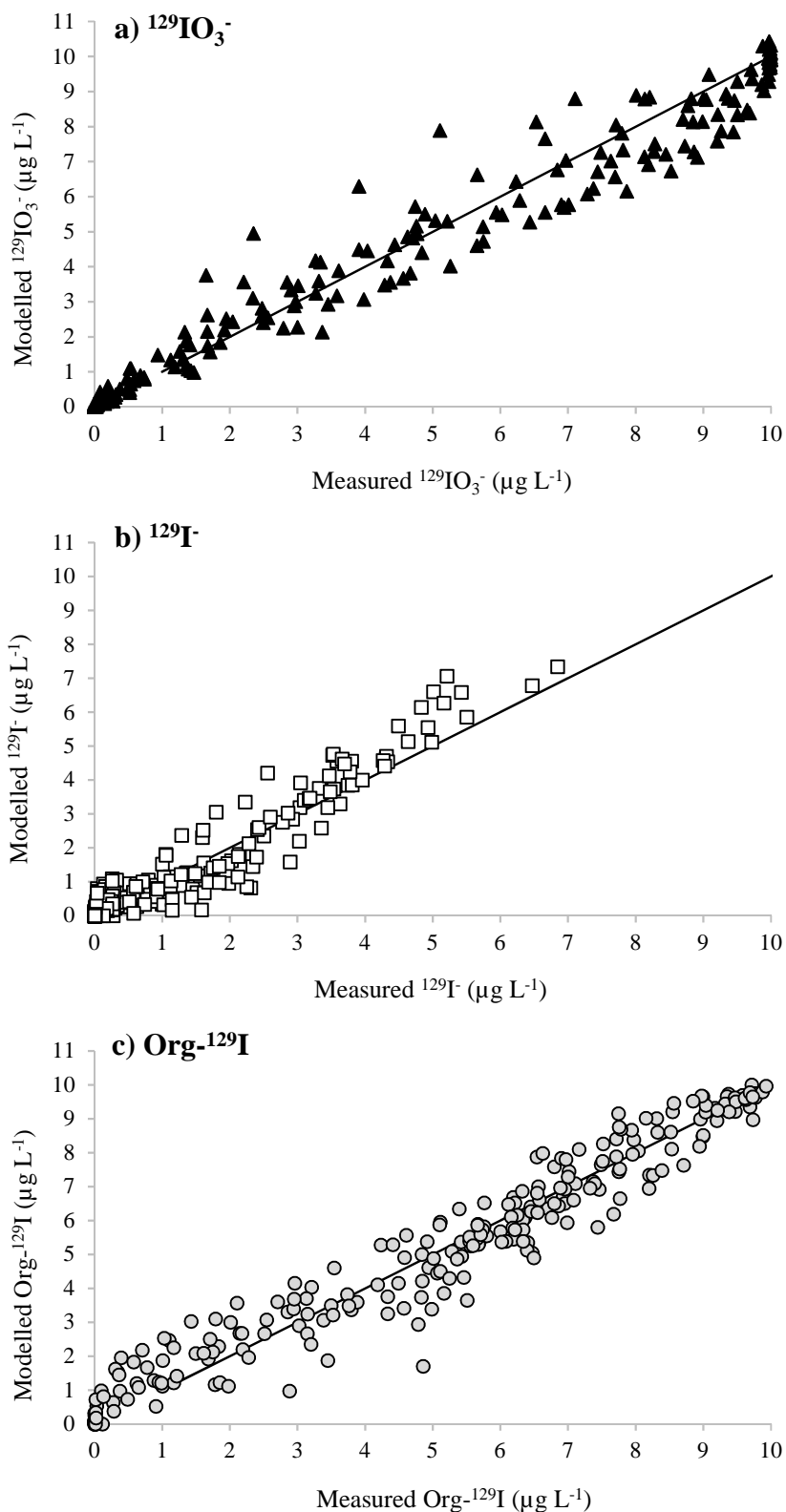
Figure 4.31. Comparison of measured and modelled concentrations of I species against a 1:1 relationship. Symbols indicate IO_3^-, I^- and Org-I species. Data includes experimentally measured values from the pH and HA experiments over 142 days.
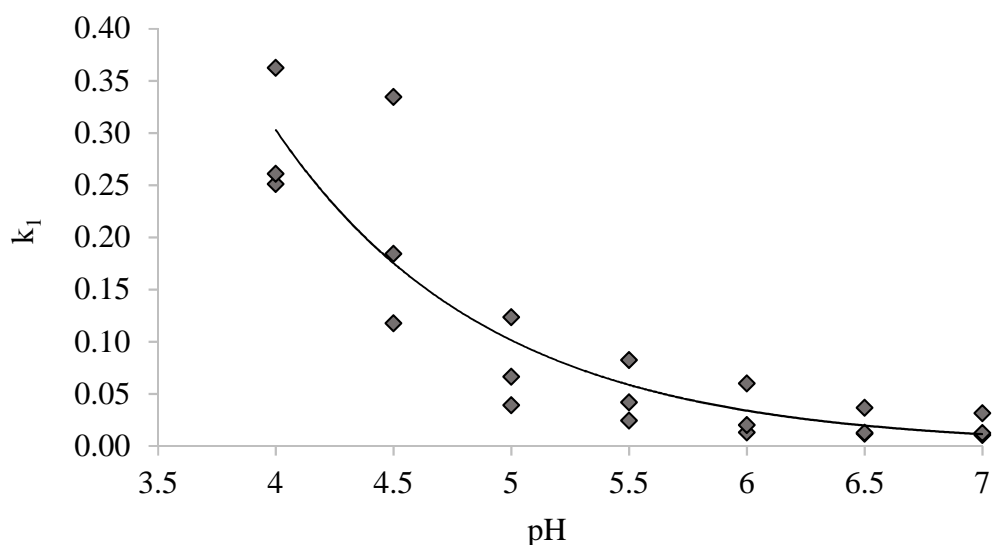
Figure 4.32. Relationship between pH and k_1 in HA systems (0.2 g L^{-1}) spiked with 10 µg L^{-1} $^{129}IO_3^-$.

There were also strong correlations between HA concentration and both the conversion of $^{129}IO_3^-$ to humic-bound species ($k_1 = 0.836$-0.00001) and the remobilisation of Org-^{129}I as ^{129}I$^-$ ($k_3 = 0.0113$-0.00001), k_1 (r = 0.92) and k_3 (r = 0.88) respectively. Multiple regression analysis demonstrated that temperature did not have a significant effect in the experiments where HA concentration was varied, however a significant non-linear relationship existed between HA concentration and k_1 (**Figure 4.33**), which can be attributed to the heterogeneity of the HA.

The HA experiment included a range of HA concentrations at pH 4, whilst the pH experiment was run at pH 4-7 with a single HA concentration of 0.2 g L^{-1} HA. This should have enabled the pH 4 data from the pH experiment, to be incorporated into the modelling of the HA concentration data at 0.2 g L^{-1} HA. However, upon attempting this it became apparent that the k_1 values obtained for 0.2 g L^{-1} in the pH experiment were significantly greater than the k_1 values for 0.5 g L^{-1} in the HA ratio experiment (**Figure**

4.33). The difference may arise from the way in which the HA stock solutions were prepared. It is unlikely that the 0.2 g L^{-1} suspensions used in the pH experiment would have a higher HA concentration than anticipated considering the way in which they were prepared (0.5 g HA dissolved in 1L). In the experiment testing the effect of a range of HA concentrations the HA (0.36 g) was dissolved in a smaller volume (250 mL) of solution and possibly resulted in incomplete dissolution of the HA and therefore a lower HA concentration than intended. Also more dilution steps were required in setting up this ratio experiment, resulting in greater potential methodological error. Despite this issue the experiment still enables comparison across a range of HA concentrations as all samples were prepared from the same stock, however the exact concentrations are suspected to be lower than those quoted.
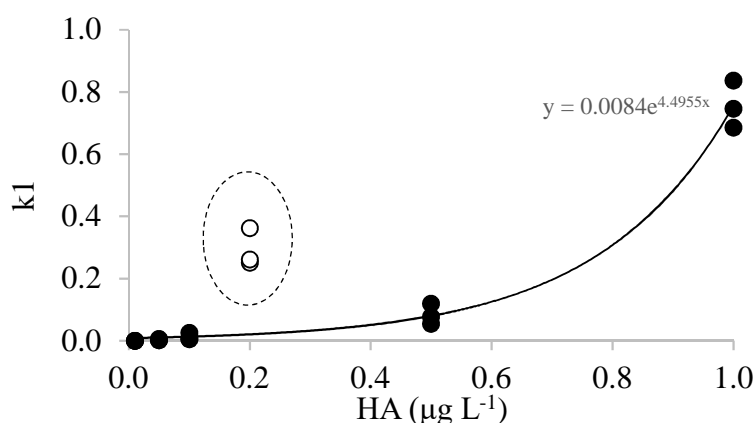
Figure 4.33. Relationship between HA concentration and k1 at pH 4. White markers are the pH 4 samples (from the pH experiment) that contained 0.2 g L^{-1} HA. These don't fit to the trend.

4.4.6.2 Modelling systems containing Fe

The same model structure (**Figure 4.2**) was used for modelling the Fe data and gave a better fit (r^2 = 0.963, **Figure 4.34**) that for the pH and HA concentration data. This is potentially because the systems containing Fe showed more gradual formation of I$^-$. The rate of IO$_3^-$ reduction was still the most rapid process (k$_1$ = 0.4064-0.0085), with minimal

conversion directly to I^- (k_2 = 0.0604 – 0.00001). When compared to systems without Fe there was greater transformation of Org-I to I^- (k_3 = 0.1279 – 0.00001) and subsequently greater oxidation of I^- to Org-I (k_4 = 0.2040 – 0.00001). Both pH and temperature had a significant effect on the rate of k_1, however since only pH 4 and 6 and 4°C and 20°C were investigated, a broader range of temperatures and pH conditions would offer a more reliable way of establishing these effects. A significant correlation (r = 0.62, p = 0.004) was observed between Fe concentration and the rate of k_3 which indicates that as the Fe concentration increases, the rate of Org-^{129}I transformation to $^{129}I^-$ increases (**Figure 4.35**). Removing the k_2 pathway resulted in a slightly poorer model fit of r^2 = 0.85 compared to r^2 = 0.97. The increased contribution of k_3 and k_2 to both the model fit and the flux of I between pools in systems containing Fe, further corroborates the discussion in Section 4.4.5. It is likely that HA groups are occupied with Fe^{2+}/Fe^{3+}, consequently Fe was oxidised by IO_3^- resulting in an increase in I^- formation both from IO_3^- directly and through association with HA first (Org-I to I^-).
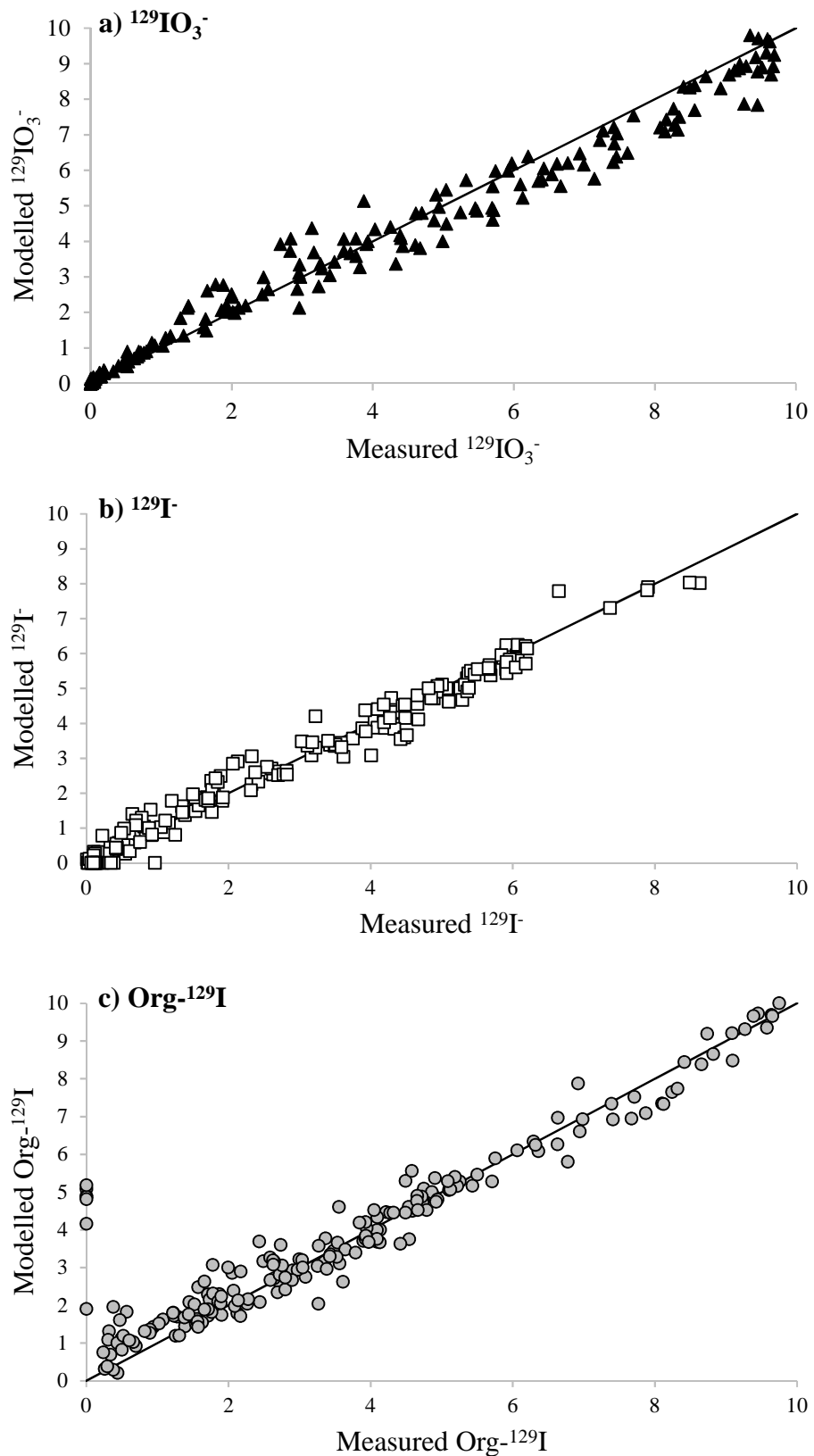
Figure 4.34. Comparison of measured and modelled concentrations of I species against a 1:1 relationship. Symbols indicate IO_3^-, I^- and Org-I species. Data includes measurements from the Fe experiments made over the course of 106 days.
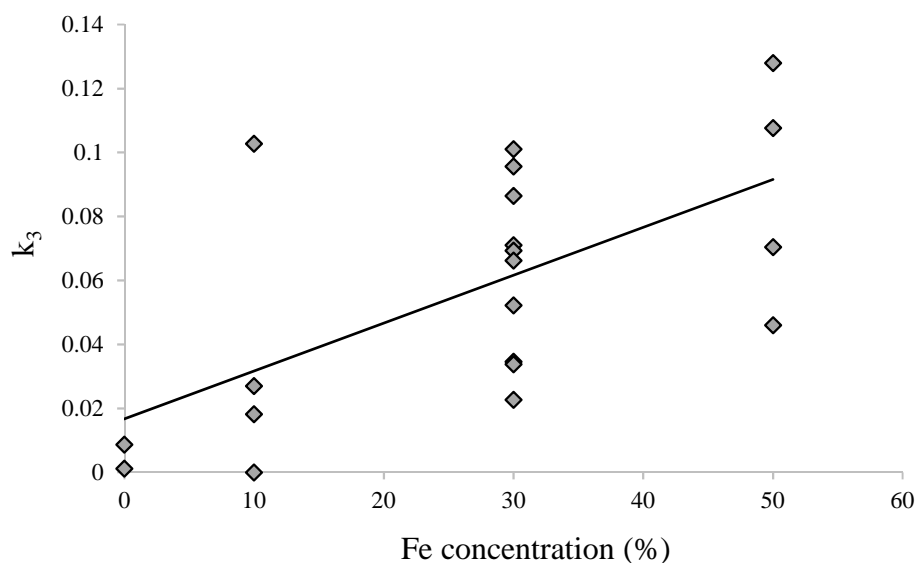
Figure 4.35. Relationship between Fe concentration (% of HA carboxyl groups) and rate constant k_3.

4.5 CONCLUSIONS

Iodine dynamics in HA and FA systems of increasing complexity have been measured and modelled over time scales up to 142 days. The change in surface charge of HA with pH affects the reduction and binding of I^- and IO_3^-. Iodate was rapidly transformed via intermediate species to both Org-I and I^-. A strong dependence on pH was observed; as pH decreased, the rate of this reduction reaction increased. Humic acid concentration was also important, with increasing concentration increasing the rate of IO_3^- reduction. Previous research has suggested that the most likely mechanism is IO_3^- reduction to I_2 which then binds with phenolic groups on OM, forming Org-I species. However, the results presented here demonstrate IO_3^- reduction and association with HA as Org-I with no evidence of initial I^- formation. Iodide is formed over time as a result of release from Org-I. Modelling confirmed this by showing minimal direct transfer of IO_3^- to I^-, indicating that HA mediates formation of I^-. This mechanism has not been suggested before.

In contrast to the rapid reduction of IO_3^- in HA systems, I^- was only slowly oxidized to reactive intermediates before forming Org-I. This is in contrast to observations in soils where rapid transformation of I^- to Org-I is measured (Shetaya *et al*., 2012). When IO_3^- and I^- were added together redox coupling was indicated, resulting in an increased rate of I^- oxidation to reactive intermediates. Further investigation of this by changing $I^-:IO_3^-$ ratios under a range of conditions in both HA/FA systems and soils is necessary in order to fully understand these interactions.

Iron in combination with HA was expected to provide a localised positive charge in order to encourage IO_3^- and I^- interactions with HA by reducing the degree of electrostatic repulsion. However, the addition of Fe slightly reduced the rate of IO_3^- reduction and significantly increased the rate of I^- formation, resulting in less Org-I formation. In systems where I^- was added, instantaneous association of I^- with HA was observed, likely via association with Fe on the HA surface, before re-release of I^-. Comparison of modelling of systems with and without Fe demonstrated increased contribution of the Org-I to I^- pathway (k_3) in the presence of Fe. Neither of these interactions have been observed before, to fully elucidate these reaction mechanisms additional batch sorption experiments and XAS experiments to investigate the nature of possible HA-Fe-I bridged species are recommended.

5. SELENIUM INTERACTION WITH SOIL GEOCOLLOIDS

5.1 INTRODUCTION

Organic matter has a significant influence on the fate of environmental $Se^{(IV)}$ and $Se^{(VI)}$ (Dhillon and Dhillon, 1999; Li *et al.*, 2017; Tolu *et al.*, 2014; Wiramanaden *et al.*, 2010a, 2010b). For example a strong correlation between extractable organic carbon and extractable Se was observed in Dutch soils with low Se concentrations (Supriatin *et al*., 2015). Sequential extraction approaches demonstrate that a significant proportion of soil Se is associated with the organic phase, (Gustafsson and Johnsson, 1994) and there has been some suggestion that microbial reductive incorporation may be an important mechanism. Humic substances (humin, HA and FA) constitute a significant portion of OM providing reactive functional groups including; carboxyl, carboxyl-phenol, phenolic and quinone groups (Traversa *et al.*, 2014), thought to be key for the association of Se with OM. Bruggeman *et al.* (2007) observed that reaction of $Se^{(IV)}$ with HSs resulted in a system dominated by colloidal Se species associated with HS after one month of contact, whilst $Se^{(VI)}$ didn't react with HSs. In addition to direct bonding of Se to HSs, ternary complex formation by cation bridging with HA has been suggested as an important mechanism for $Se^{(IV)}$ association (Martin *et al.*, 2017). No cation bridging has been observed with $Se^{(VI)}$ and detailed mechanistic understanding of the interactions of Se with HS remains very limited.

In addition to association with organic phases in soils, Se can also be incorporated into inorganic phases (Chan *et al.*, 2009; Peak, 2006; Rovira *et al.,* 2008; Scott and Morgan, 1996). Again $Se^{(IV)}$ is more reactive as it is more polar than the more oxidised $Se^{(VI)}$ ion (Wiramanaden *et al.*, 2010a). For example, the mechanism of $Se^{(IV)}$ and $Se^{(VI)}$ reaction

with goethite, is relatively well understood. Goethite rapidly bonds both $Se^{(IV)}$ and $Se^{(VI)}$, usually without reduction, however the nature of the $Se^{(VI)}$ species is not fully resolved. Both inner and outer-sphere complexation is possible, whereas $Se^{(IV)}$ forms an inner-sphere complex (Hayes *et al.*, 1987; Manceau and Charlet, 1994; Peak and Sparks, 2002). The role that inorganic phases, such as goethite, play in determining the fate of Se in soil systems may be significant since they provide a positive surface with which these oxyanions can interact.

Batch sorption experiments have been predominantly used to investigate interactions of Se with HS, with minimal investigation of the solid phase species formed. The determination of Se speciation in solids can be challenging at environmentally relevant concentrations, however determining direct Se associations with soil or soil fractions by X-ray Adsorption Spectroscopy (XAS) is well established (Kamei-Ishikawa *et al.,* 2007; Wiramanaden *et al.,* 2010b). The Se K-edge X-ray Absorption Near Edge Spectrum (XANES) is sensitive to oxidation state and chemical environment, allowing the investigation of Se speciation in complex matrices such as soils. The extended X-ray adsorption fine structure (EXAFS) spectra can be used to study the local environment of Se in these systems. In combination with aqueous-phase speciation analysis this can provide a way to undertake a comprehensive investigation of Se in combination with soil geocolloids and soils.

5.2 AIMS AND OBJECTIVES

The aim of this study was to investigate interactions of $Se^{(IV)}$ and $Se^{(VI)}$ with soil geocolloids; HA alone, HA in combination with metal ions and oxides, and FA, in order to improve understanding of Se reactions and mobility in soils.

Specific objectives included:

- Investigation of the interactions of $Se^{(IV)}$ and $Se^{(VI)}$ with HA alone and in combination with metal ions;

- Investigation of the effect of temperature, pH and metal oxides on the formation of organic-Se species;

- Investigation of the solid phase speciation of $Se^{(IV)}$ and $Se^{(VI)}$ adsorbed to soil geocolloids using X-ray absorption spectroscopy.

5.3 MATERIALS AND METHODS

5.3.1 Isotope spike solutions

Isotope spike solutions (500 µg L^{-1}) were prepared for each species ($^{77}Se^{(IV)}$, $^{77}Se^{(VI)}$ and $^{74}Se^{(VI)}$) by dilution of concentrated stocks as described in Section 2.5.2. Stocks were diluted in Milli-Q water to neutralise the pH of the concentrated stocks.

5.3.2 Humic acid batch sorption experiments

Selenium spikes were included in the experiments described in Chapter 4. A range finding experiment was first undertaken as described in Section 4.3.3. Oxidised samples were spiked with 5 µg L^{-1} $^{77}Se^{(VI)}$. Reduced samples were spiked with 5 µg L^{-1} $^{77}Se^{(IV)}$. The influence of HA concentration was determined as described in Section 4.3.5. Samples were spiked with 5 µg L^{-1} 77Se$^{(VI)}$. The effect of pH was investigated as described in Section 4.3.4. Samples were spiked with 5 µg L^{-1} 77Se$^{(VI)}$. All samples were stored and sampled as described in the relevant sections.

5.3.3 Effect of microbes on Se interactions with HA

5.3.3.1 Effect of filter sterilisation on Se interactions with HA and FA

Humic acid samples containing 0.2 g L^{-1} HA were prepared as described in Section 4.3.3 by dilution of a 1.5 g L^{-1} HA stock before adjustment to pH 4, 5, 6 and 7 using 0.1 M HNO$_3$. A spike of ^{77}Se$^{(IV)}$ and ^{74}Se$^{(VI)}$ was then added to give a final concentration of 5 µg L^{-1}. Samples were filter sterilised (0.22 µm) and stored in the dark at 4°C and 20°C. Aliquots were subsampled in a laminar flow hood using autoclaved pipette tips to maintain a sterile environment after 0, 12, 32, 51 and 93 days for ^{74}Se$^{(VI)}$ and 4, 16, 32, 51 and 93 days for ^{77}Se$^{(IV)}$.

Fulvic acid samples were prepared, filtered, stored and subsampled as described in Section 4.3.6. A mixed spiked of ^{77}Se$^{(IV)}$ and ^{74}Se$^{(VI)}$ was added to achieve a final concentration of 5 µg L^{-1}.

5.3.3.2 Effect of added microbes on Se interactions with HA

Humic acid samples were prepared, stored and subsampled according to Section 4.3.8. A spike of ^{77}Se$^{(IV)}$ and ^{74}Se$^{(VI)}$ was added to give a final concentration of 5 µg L^{-1}.

5.3.4 XAS

5.3.4.1 Sample preparation

Humic acid samples were prepared as described in Section 4.3.3 to achieve a final concentration of 0.8 g L^{-1}. Samples were converted to Ca-humate by flocculation with 1 M Ca(NO$_3$)$_2$ and centrifugation at 3000 g. The supernatant was discarded and the Ca-humate was re-suspended with 0.01 M Ca(NO$_3$)$_2$. Adjustment to pH 4 and pH 6 was

achieved with 0.1 M HNO_3. A spike of Na_2SeO_3 and Na_2SeO_4 was then added to give a final concentration of 10 and 100 mmol kg^{-1} from stock solutions (salts dissolved in Milli-Q water). Samples were stored in the dark at 20^oC for 60 days.

Humic acid samples containing Fe^{3+} were prepared as described above with an addition of $FeCl_3$ to achieve 20% occupancy of the HA COOH groups. Adjustment to pH 4 and pH 6 was achieved with 0.1 M HNO3. A spike of Na_2SeO_3 and Na_2SeO_4 was then added to give a final concentration of 100 mmol kg^{-1} from stock solutions. This was performed 1 day prior to analysis. Samples were converted to Ca-humate by flocculation with 1 M $Ca(NO_3)_2$ and centrifugation at 3000 g.

The goethite stock prepared in Section 4.3.3 was used here. Adjustment to pH 4 and pH 6 was achieved using 0.1 M HNO_3. Spikes of Na_2SeO_3 and Na_2SeO_4 were then added to give final concentrations of 10 and 100 mmol kg^{-1}. Samples were stored in the dark at 20^oC for 60 days.

Two soils were selected based on their carbon content and pH characteristics; a Derbyshire grassland soil (DY-G, pH 3.9, 11.4% Org-C), and a grassland soil from Stoke Rochford (SR-G, pH 7.04, 5.7% Org-C). Spikes of Na_2SeO_3 and Na_2SeO_4 were added to 2 g of the soil to give final Se concentrations of 1 and 10 mmol kg^{-1}. Samples were stored moist (aerobic) at 20^oC for 60 days. After this period samples were repeatedly washed with Milli-Q water (resuspension followed by centrifugation at 3000 g) to remove excess Se prior to analysis with XAS. Two selenium standards of 308 mg L^{-1} Na_2SeO_3 and Na_2SeO_4 solutions were also prepared as standards for XAS analysis.

5.3.4.2 Data collection/analysis

The concentration of Se in the supernatant after sample washing was determined by ICP-MS. The concentration of Se sorbed to the solid phase was then determined as (Eqn. 5.1):

$$Se_m = C_o \left(\frac{V_0}{1000}\right) \left(\frac{V_p}{V_o}\right) \left(\frac{V_p}{V_w}\right)^n \tag{5.1}$$

Where; Se_m is the mass of Se (µg) entrained in the solution phase of the centrifuged sample plug, C_0 is the concentration of Se (µg L^{-1}) in the supernatant solution following initial equilibration, V_0 is the initial solution volume (mL) equilibrated with the solid material (25 mL), V_p is the volume (mL) of entrained liquid following centrifugation and after discarding the supernatant, V_w is the volume (mL) of the wash solution (20 mL) and n is the number of wash steps.

All XAS data was collected in fluorescence mode at beamline I20-Scanning at the Diamond Light Source (Oxfordshire, UK) using a Si 111 monochromator. Calibration was achieved using elemental Se where the maximum in the first derivative on the edge was set at 12658 eV. The Se k-edge XAS data was measured using a 64 element solid-state Ge fluorescent detector. The k-range of the EXAFS spectra was limited to 10 Å^{-1} in the soil samples due to the presence of a Pb-L3 adsorption edge at 13043 eV, which distorted the EXAFS signal beyond this point. All samples were analysed as pastes at liquid N_2 temperature in an Al-holder with Kapton® windows. Between 4 and 12 scans were taken per sample depending on the concentration of Se present. Reduction of Se by the beam was observed when repeated scans were taken at the same point on the sample therefore the beam position on the sample was adjusted between scans. Multiple XAS scans for each sample were summed and averaged using Athena v 0.9.25. The EXAFS spectra were then fitted in k-space using Artemis v 0.9.25 (Ravel and Newville, 2005).

5.3.5 ICP-MS Analysis

Measurement of Se total concentration was undertaken using ICP-MS as described in Section 2.5.1. Chromatography to separate Se species used a Dionex ICS-3000 HPLC (Chromeleon software) coupled to ICP-MS as described in Section 2.5.2. Separation of organic Se species from inorganic species was carried out using SEC-ICP-MS as described in Section 2.5.3.

5.4 RESULTS AND DISCUSSION

5.4.1 Interactions with humic acid

5.4.1.1 Range finding results

When HA systems were spiked with $^{77}Se^{(IV)}$ and $^{77}Se^{(VI)}$ changes in speciation were observed over the course of 160 days, predominantly in systems at lower pH and higher temperature (**Figure 5.1**). Samples at pH 4 showed rapid instantaneous Se adsorption at 20°C (81% after 12 days) followed by a slower time-dependent removal. At pH 4 the rate of $Se^{(VI)}$ loss was much slower than $Se^{(IV)}$, with 70% lost from solution after 41 days (**Figure 5.2**). Selenium is most soluble and mobile as $Se^{(VI)}$ in contrast to $Se^{(IV)}$ which is usually associated with OM (Kamei-Ishikawa *et al.*, 2007; Zawislanski *et al*., 2003). Greatest initial removal of $Se^{(IV)}$ and $Se^{(VI)}$ was observed at pH 4, with minimal/no removal observed at pH 6 at either temperature. Reaction of both $Se^{(IV)}$ and $Se^{(VI)}$ was less at 4°C compared to 20°C, demonstrating a clear temperature dependency. Humic acid concentration appears to have minimal effect on the rate of $Se^{(IV)}$ removal, and no effect on $Se^{(VI)}$. Indeed systems containing 0.05 g L^{-1} HA showed more reduction of $Se^{(VI)}$ over 160 days compared to those with 0.2 g L^{-1} HA. A similar result was observed for

Se$^{(IV)}$ at pH 6 where 28% of the Se was removed at the lower HA concentration, compared to 15% at the higher concentration. If the method of Se removal in the presence of HA is through association with the HA itself then it would be expected that a increased HA concentration would result in increased removal. Pezzarossa *et al.* (1999) found that soils with a higher OM content removed more inorganic Se$^{(VI)}$ from solution, than soils with a lower OM content, as would be expected if Se complexes with the OM. The lack of an effect of HA concentration of Se removal in this study was therefore unexpected and will be considered in more detail in Section 5.4.1.3.
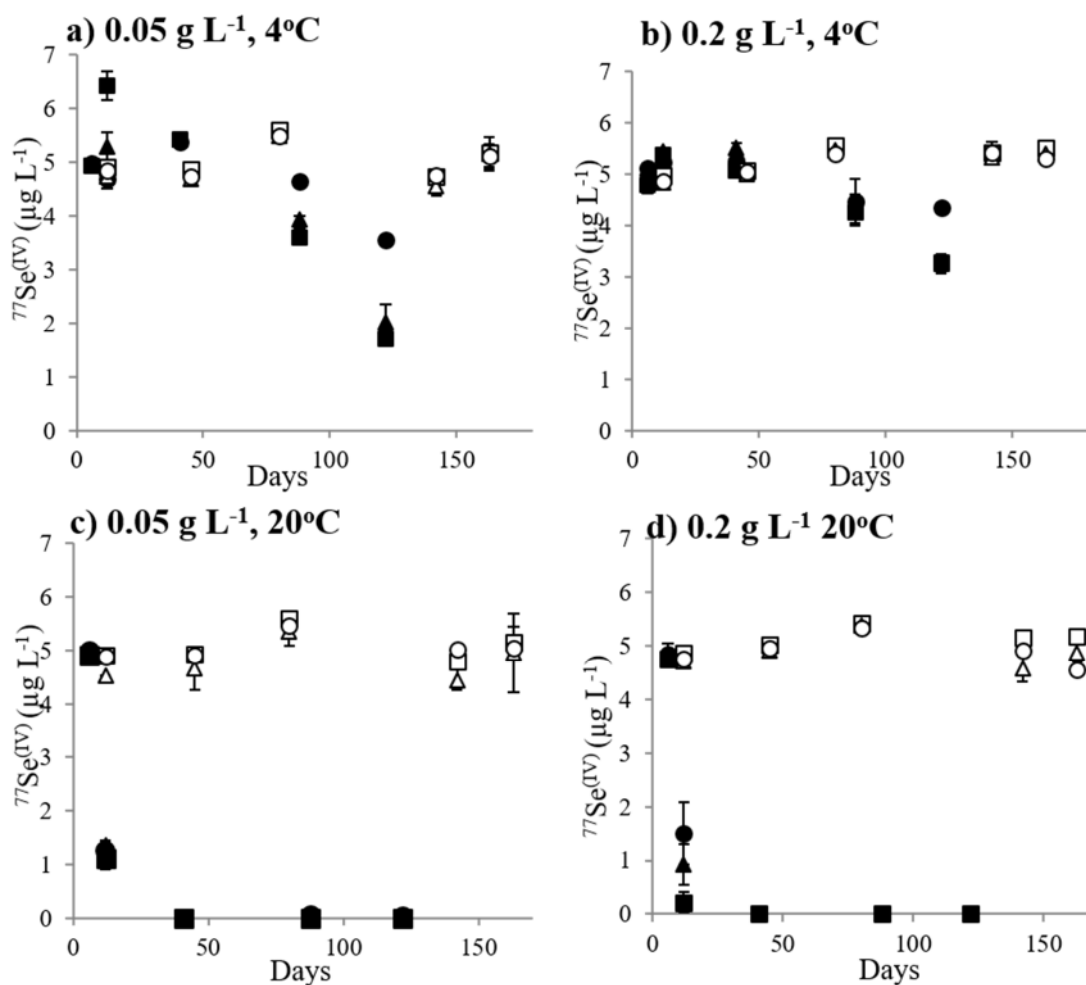
Figure 5.1. Humic acid suspensions at 0.05 g L^{-1} and 0.2 g L^{-1} alone (square markers) and in combination with Fe$^{(2+)}$ (triangles) and Mn^{2+} (circles) spiked with 5 µg L^{-1} ^{77}Se$^{(IV)}$ at pH 4 (closed symbols) and pH 6 (open symbols). Samples were stored in the dark. Error bar based on two replicates.
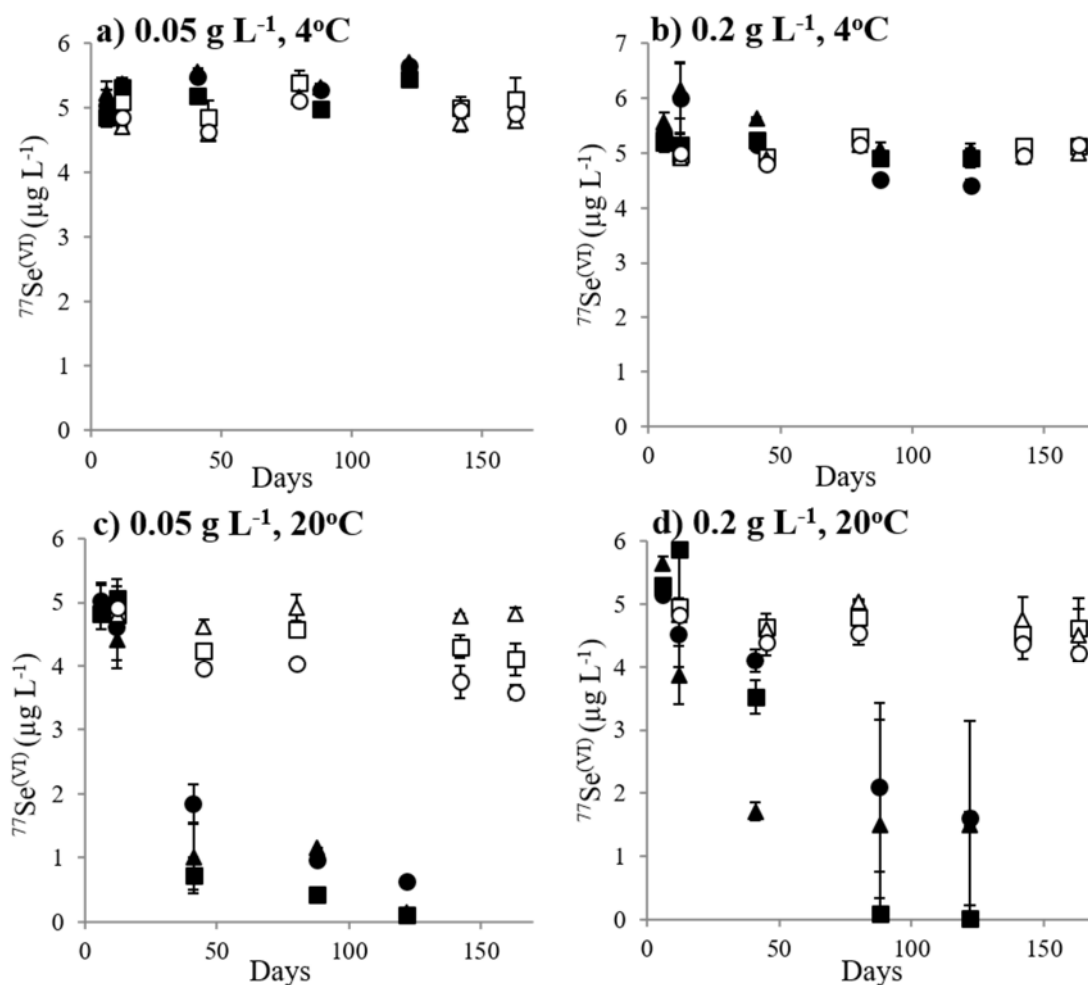
Figure 5.2. Humic acid suspensions at 0.05 g L^{-1} and 0.2 g L^{-1} (squares) and in combination with Fe$^{(2+)}$ (triangles) and Mn^{2+} (circles) spiked with 5 µg L^{-1} ^{77}Se$^{(VI)}$ at pH 4 (closed symbols) and pH 6 (open symbols). Samples were stored in the dark. Error bar based on two replicates.

5.4.1.2 Effect of iron and manganese on Se sorption

The presence of Fe^{2+} and Mn^{2+} appears to have no effect on the rate of ^{77}Se$^{(IV)}$ and ^{77}Se$^{(VI)}$ removal (**Figure 5.1** and **Figure 5.2**). Despite this a number of papers have discussed the potential for metal-humic complexes to play an important role in the sorption of Se in soils (Bruggeman *et al*., 2007; Gustafsson and Johnsson, 1994; Martin *et al.*, 2017).

5.4.2.3 Selenium interactions with Goethite

Humic acid systems that contained goethite at pH 4 demonstrated increased removal of Se$^{(IV)}$ (**Figure 5.3**) from solution when compared to HA only systems (Section 5.4.1.1), with a minor reduction in the rate of Se$^{(VI)}$ removal (**Figure 5.4**). Humic acid systems in combination with goethite and the pure goethite systems at pH 4 both demonstrated instantaneous sorption of Se$^{(IV)}$. This is likely due to absorption onto goethite directly, or through association by Se-HA-Goethite complexes (Tam *et al.*, 1995). Selenate in combination with goethite alone at pH 4 also demonstrated instantaneous sorption, however when present in HA systems containing goethite the rate of removal from solution was slower than that observed in HA only systems. Humic acid is known to adsorb onto goethite with decreasing pH (Antelo *et al.*, 2007), therefore there could be some degree of competition thus slowing Se$^{(VI)}$ absorption onto goethite in mixed systems. Interactions with goethite systems at pH 6 are significantly slower than those observed at pH 4. This is likely due to the surface charge properties of goethite, i.e. at low pH the positive surface charge is greater therefore the Se oxyanions are likely to interact more with the goethite surface (Rovira *et al.*, 2008). Combined HA/goethite systems at pH 6 resulted in increased Se$^{(IV)}$ removal from solution compared to pure HA systems at pH 6. This may also be explained by slight positive charge contribution from goethite compared to the negatively charged pure HA systems. Removal of both Se$^{(IV)}$ and Se$^{(VI)}$ was more rapid in combination with pure goethite when compared to pure HA systems, particularly for Se$^{(VI)}$. Again this is likely attributable to the surface properties of goethite and HA; goethite is positively charged and therefore more likely to interact with anionic species than the negatively charged HA.
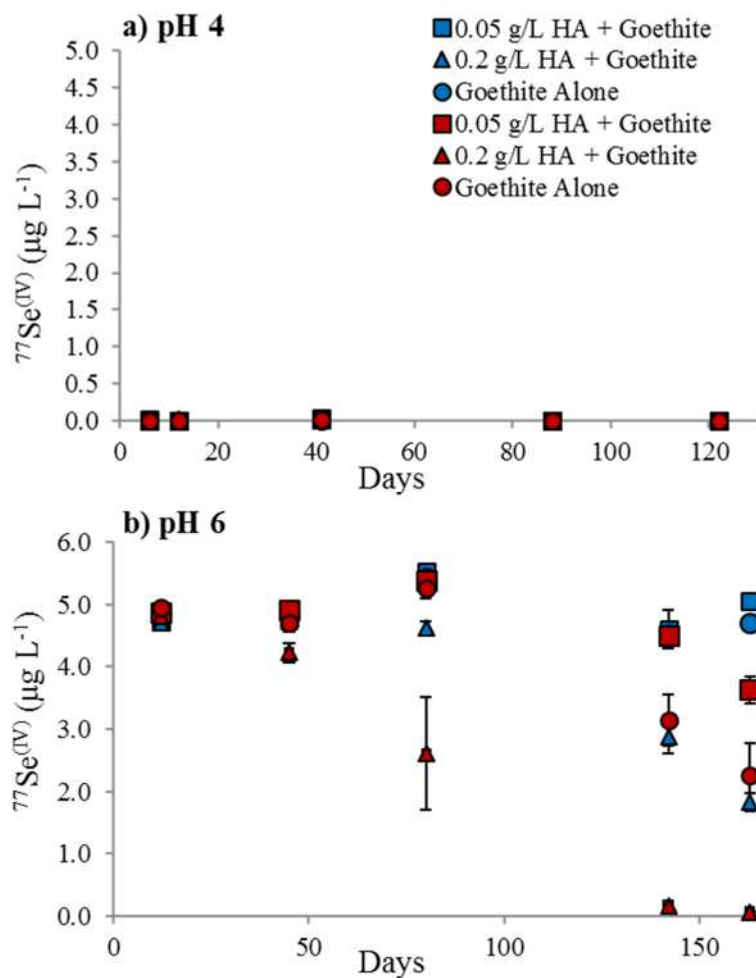
Figure 5.3. HA suspensions (0.05 and 0.2 g L^{-1} HA) with goethite (20% of HA weight) and goethite alone, spiked with 5µg L^{-1} ^{77}Se$^{(IV)}$ at a) pH 4 and b) pH 6. Stored at 4°C (blue) and 20°C (red). Error bars based on two replicates.
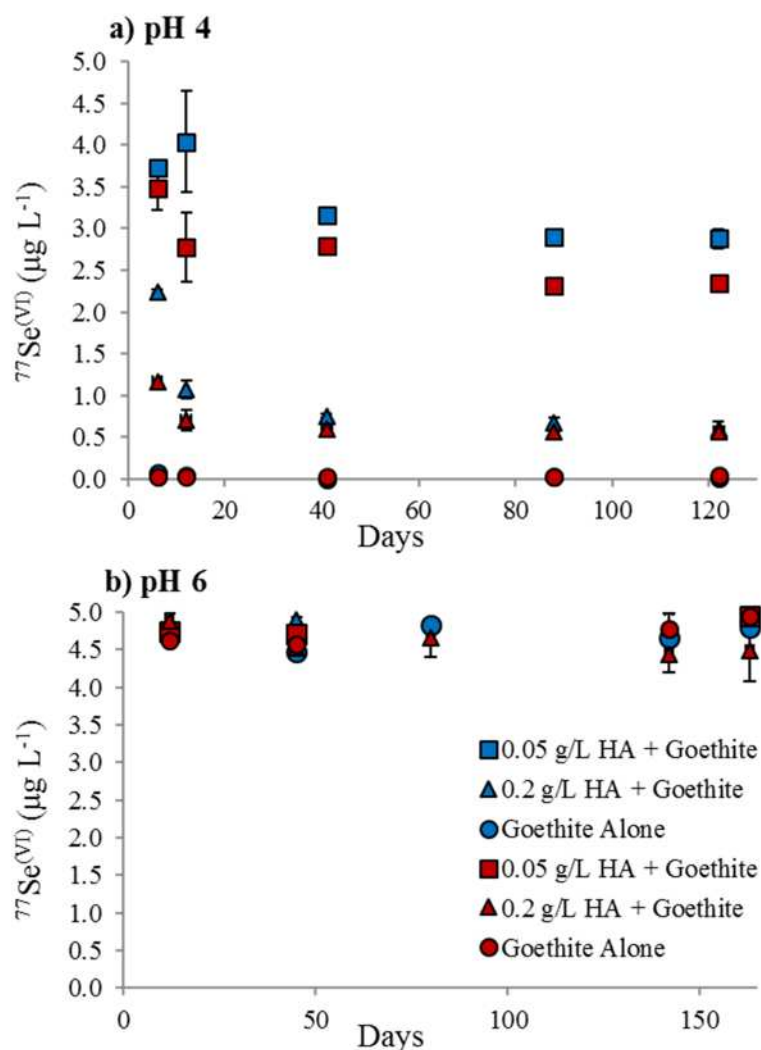
Figure 5.4. HA suspensions (0.05 and 0.2 g L^{-1} HA) with goethite (20% of HA weight) and goethite alone, spiked with 5µg L^{-1} $^{77}Se^{(VI)}$ at a) pH 4 and b) pH 6. Stored at 4°C (blue) and 20°C (red). Error bars based on two replicates.

5.4.1.4 Effect of humic acid concentration

As observed in the range finding experiment, HA concentration appears to have little influence on the rate of $Se^{(VI)}$ removal (**Figure 5.5**). Soil OM is a known sink for Se under certain conditions (i.e. low pH), where positive correlations have been demonstrated between increasing soil OM content and increased soil Se concentrations (Spadoni *et al.*, 2007; Tolu *et al.*, 2014). This usually then correlated with reduced plant Se uptake. Therefore, it is expected that a positive correlation should exist between HA

151

concentration and $Se^{(VI)}$ transformation into Org-Se species. Systems containing 1 g L^{-1} of HA had an increased rate of $Se^{(VI)}$ removal compared to systems with 0.01 g L^{-1} HA. The pattern observed as a function of HA concentration was more complex with 0.5, 0.05 and 0.1 g L^{-1} HA suspensions removing 40, 75 and 100 % of the $Se^{(VI)}$ respectively at 10°C. If the reactive sites on the HA were responsible for the reduction of $Se^{(VI)}$ forming Org-Se species then as the concentration of HA increased so would the quantity of reactive sites, consequently the rate of $Se^{(VI)}$ reduction would also increase. The lack of this relationship suggests that although the HA may be a sink for Se in soil, another soil component could be responsible for the reduction of Se prior to its incorporation in OM.

There are no previous studies for comparison that investigate the effect of HA concentration on $Se^{(VI)}$ interactions since $Se^{(VI)}$ has been described as showing no interaction with HA (Bruggeman *et al.*, 2007; Martin *et al.*, 2017). However comparisons can be made for the effect of HA concentration on $Se^{(IV)}$ interactions in Section 5.4.1.1 where similar results were observed as greater transformation in samples containing 0.05 g L^{-1} HA than 0.2 g L^{-1} (**Figure 5.1**). For example, Kamei-Ishikawa *et al.* (2007) concluded that decreasing solid/solution ratio (HA concentration) increased $Se^{(IV)}$ sorption on HA at pH 5-6. This is in agreement with the results of the range finding experiment for $Se^{(IV)}$ (**Figure 5.1**). Humic acid structure is expected to vary as a function of concentration, pH and ionic strength (Stevenson, 1982). This led Kamei-Ishikawa *et al.* (2007) to hypothesise that the trends observed were related to a more linear HA structure at low HA concentrations and therefore increased accessibility of reactive sites for Se. However, although Kamei-Ishikawa *et al*. (2007) concluded that there was a relationship between $Se^{(IV)}$ transformation and HA concentration, closer inspection of the figures presented in the study appears to show no relationship between HA concentration

and $Se^{(IV)}$ transformation. The solid/liquid ratio of 0.05 often resulted in greater $Se^{(IV)}$ transformation than 0.01, and this shouldn't be the case if a decreasing solid/liquid ratio results in increased $Se^{(IV)}$ transformation.

Measurement of sample pH at the end of the experiment demonstrated some pH drift had occurred. Most samples remained within one pH unit, however some showed more significant changes. Samples at 20°C showed the greatest drift, with 4°C systems showing negligible change. Samples containing 0.1 g L^{-1} HA at pH 4 showed the greatest change; pH 5.77 (4°C), pH 5.72 (10°C) and pH 6.30 (20°C). Significant transformation of $Se^{(VI)}$ was observed in the systems demonstrating the greatest pH drift, and since previously no transformation of $Se^{(VI)}$ was observed at pH 6 (**Figure 5.2**), it is suspected that the pH drift occurred during the experiment. These results make it difficult to determine the mechanisms occurring during reduction of $Se^{(VI)}$ in the presence of HA. It is apparent that Se interaction with HA is more complicated than a simple sorption reaction and it is likely that multiple reactions are involved.
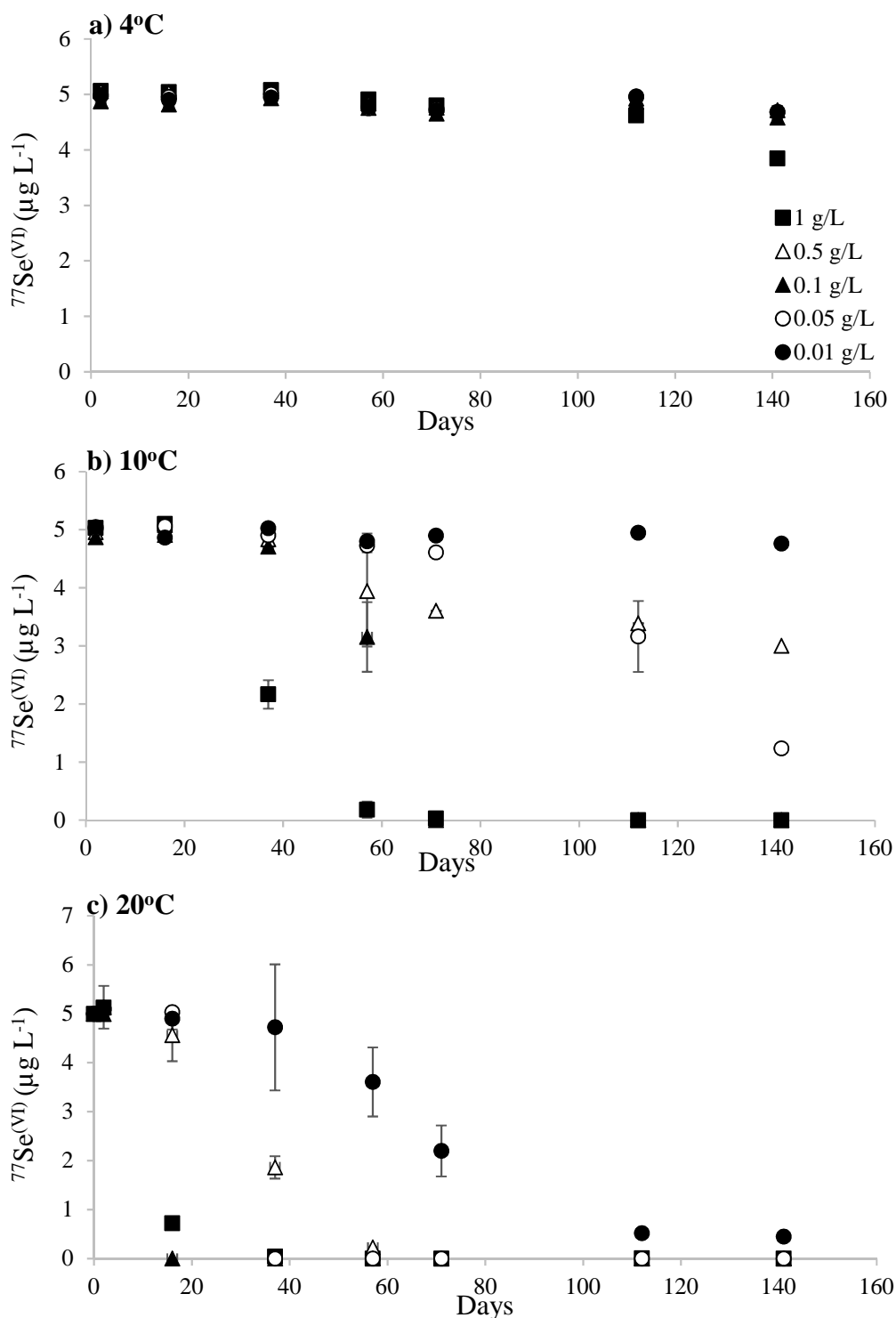
Figure 5.5. Humic acid suspensions at 1, 0.5, 0.1, 0.05 and 0.01 g L^{-1}, spiked with 5 µg L^{-1} ^{77}Se$^{(VI)}$ at pH 4 and stored in the dark at a) 4°C, b) 10°C and c) 20°C. Error bar based on two replicates.

5.4.1.5 Effect of pH

Humic acid suspensions over the pH range 4-7 demonstrated increased $Se^{(VI)}$ removal with decreasing pH (**Figure 5.6**). Removal of 98%, 100%, 35%, 17%, 0%, and 5% of $Se^{(VI)}$ was observed at pH 4.0, 4.5, 5.0, 5.5, 6.0, 6.5 and 7.0 respectively at 20°C. After 106 days of incubation there was a significant positive correlation ($r^2 = 0.81$) between pH and available $Se^{(VI)}$. However, neither the 4°C nor the 10°C show any $Se^{(VI)}$ reduction suggesting that the activation energy for this reaction has not been overcome at these temperatures. There is evidence in the literature to indicate that pH has a significant effect on Se adsorption in soils, where increasing pH results in less adsorbed Se and therefore greater Se plant uptake (De Temmerman *et al.*, 2014; Gustafsson and Johnsson, 1994). Goh and Lim (2004) concluded that $Se^{(IV)}$ and $Se^{(VI)}$ adsorption decreased with increasing pH, which also correlated with decreasing soil surface charge density as pH increased. As in the case of iodine, this indicates that adsorption could be inhibited at high pH due to the increased quantity of OH^- ions present in solution, resulting in a greater degree of electrostatic repulsion between the Se oxyanions and the hydroxylic functional groups of the HA. This would suggests that at low pH, when electrostatic repulsion is reduced, $Se^{(VI)}$ reaction with HA would be encouraged.
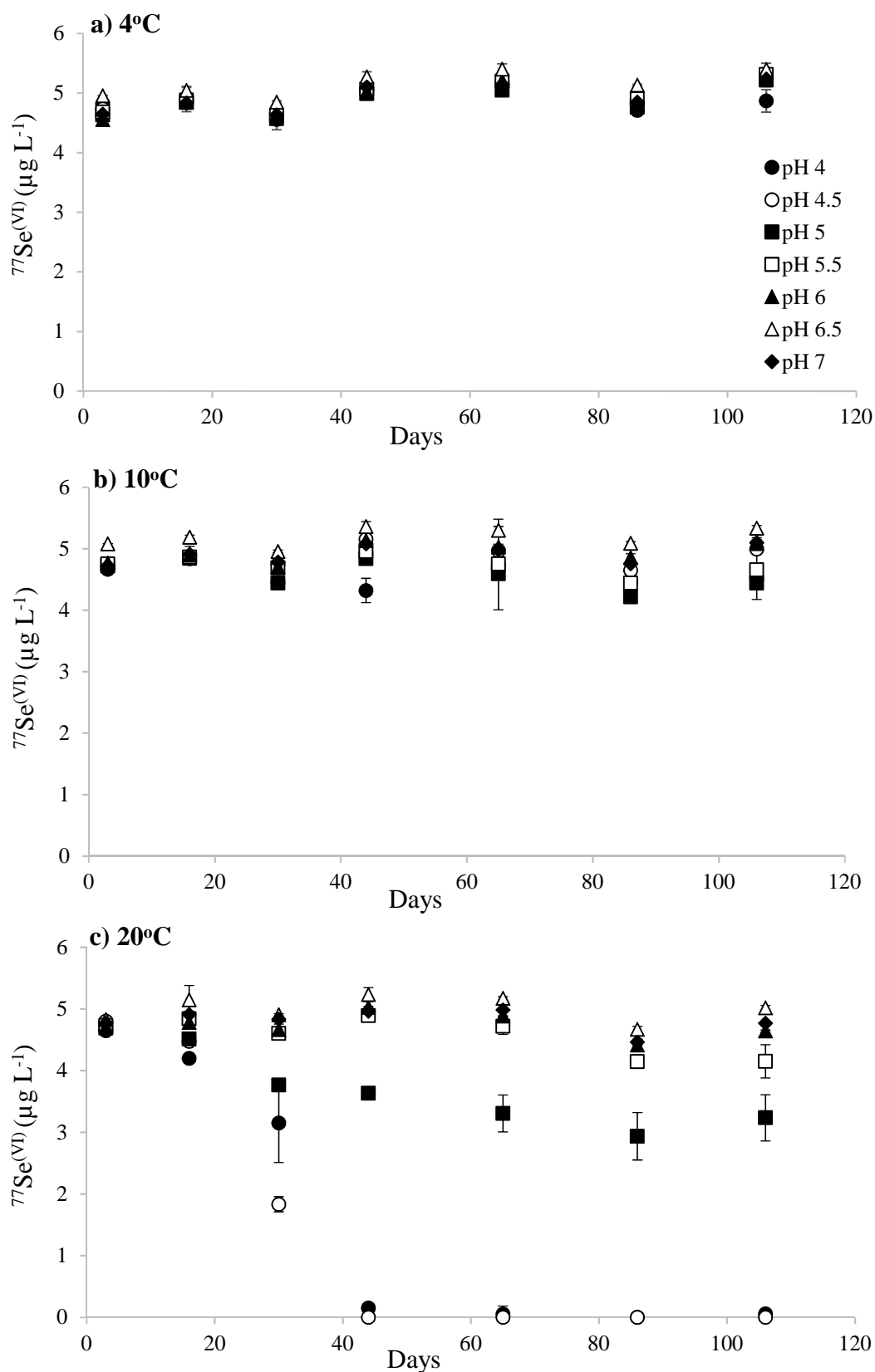
Figure 5.6. Humic acid suspensions (0.2 g L^{-1}) spiked with 5 µg L^{-1} ^{77}Se$^{(VI)}$ at pH 4.0, 4.5, 5.0, 5.5, 6.0, 6.5 and 7.0. Samples were stored in the dark at a) 4°C, b) 10°C and c) 20°C. Error bar based on two replicates.

These results also demonstrated a delay in the reaction. Little/no reduction took place in the 20°C system during the first 16 days, following this, reduction happened rapidly in the most acidic systems. This pattern is not typical of adsorption kinetics where initial rapid reaction is usually followed by slower time-dependent sorption. This initial delay could suggest that the reaction is microbially driven, whereby it takes time for a microbial community to establish before $Se^{(VI)}$ removal can occur. For example, *D. desulfuricans* has been shown to have a delay in growth when grown on media containing $Se^{(IV)}$ or $Se^{(VI)}$, with the lag period extending in the case of $Se^{(VI)}$ (Tomei *et al*., 1995). It was observed that samples grown with $Se^{(IV)}$ formed $Se^{(0)}$ more rapidly than those grown with $Se^{(VI)}$. However, this experiment investigated microbial growth on Se enriched medium, and was performed at pH 6.5 to encourage growth of *D. desulfuicans*, whereas the experiment undertaken here saw Se removal at more acidic pH. This makes comparisons difficult but raises the possibility of a mechanisms capable of explaining the discrepancies between the experiments so far observed.

5.4.2 Effect of microbes on Se interactions with HA

5.4.2.1 Effect of filter sterilisation on Se interactions with HA and FA

Filtering solution samples (0.22 µm) with a sterile filter unit has been shown to be effective for bacterial and mould sterilisation (Walsh and Denyer, 2013). The possibility of a microbial reaction resulting in the delay in $Se^{(VI)}$ removal in the range finding, pH and HA concentration experiments was investigated by filtering HA suspensions spiked with 5 µg L^{-1} $^{77}Se^{(IV)}$ and $^{74}Se^{(VI)}$. No removal of $^{77}Se^{(IV)}$ (**Figure 5.7**) or $^{74}Se^{(VI)}$ (**Figure 5.8**) over 92 days at pH 4 or pH 6 was observed. Filtering of FA samples spiked with 5

µg L^{-1} ^{77}Se$^{(IV)}$ and ^{74}Se$^{(VI)}$ also resulted in no removal of either Se species from solution (**Figure 5.9**).
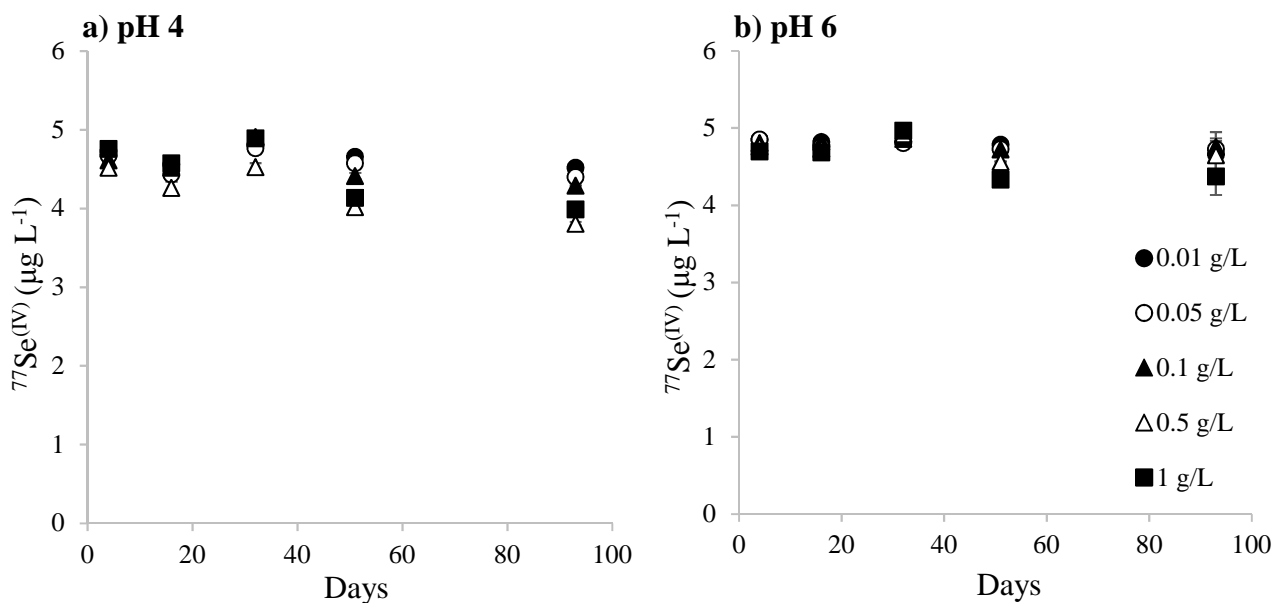
Figure 5.7. Humic acid suspensions at a range of concentrations; 1, 0.5, 0.1, 0.05 and 0.01 g L^{-1}. Spiked with 5 µg L^{-1} ^{77}Se$^{(IV)}$ at a) pH 4 and b) pH 6, stored in the dark for 92 days at 20°C. Error bars based on two replicates.
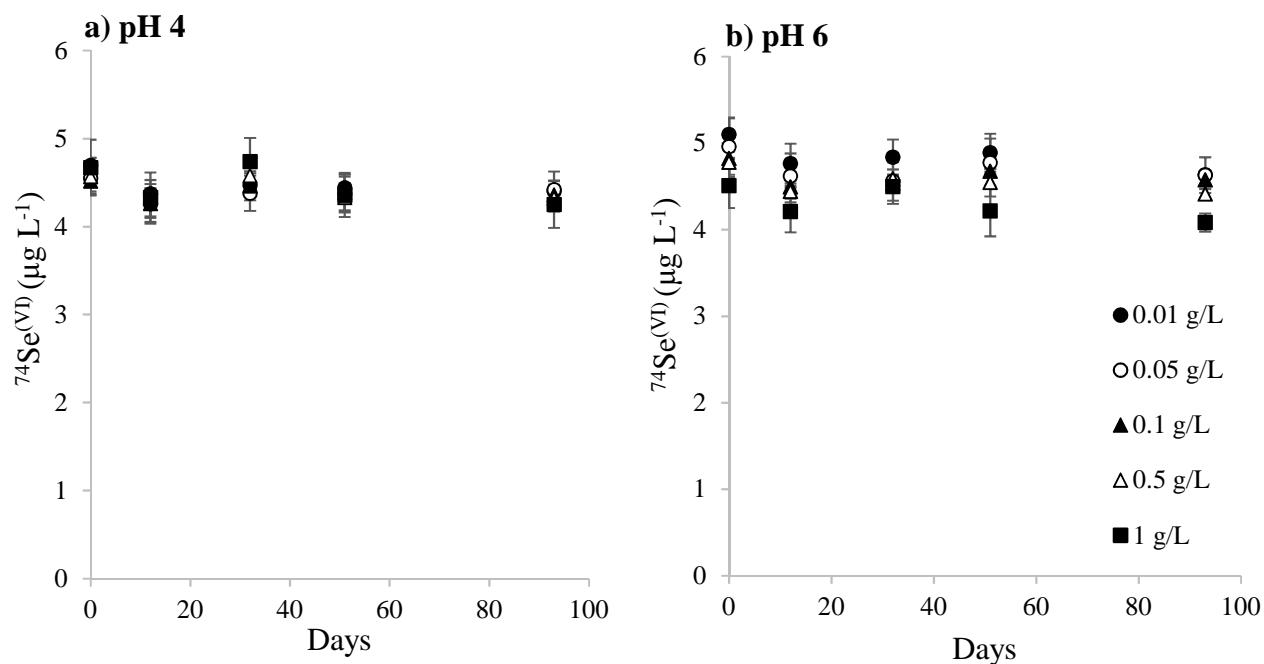
Figure 5.8. Filtered suspensions at 1, 0.5, 0.1, 0.05 and 0.01 g L^{-1} HA spiked with 5 µg L^{-1} ^{74}Se$^{(VI)}$ at a) pH 4 and b) pH 6 before storage in the dark at 20°C. Error bars are based on two replicates.
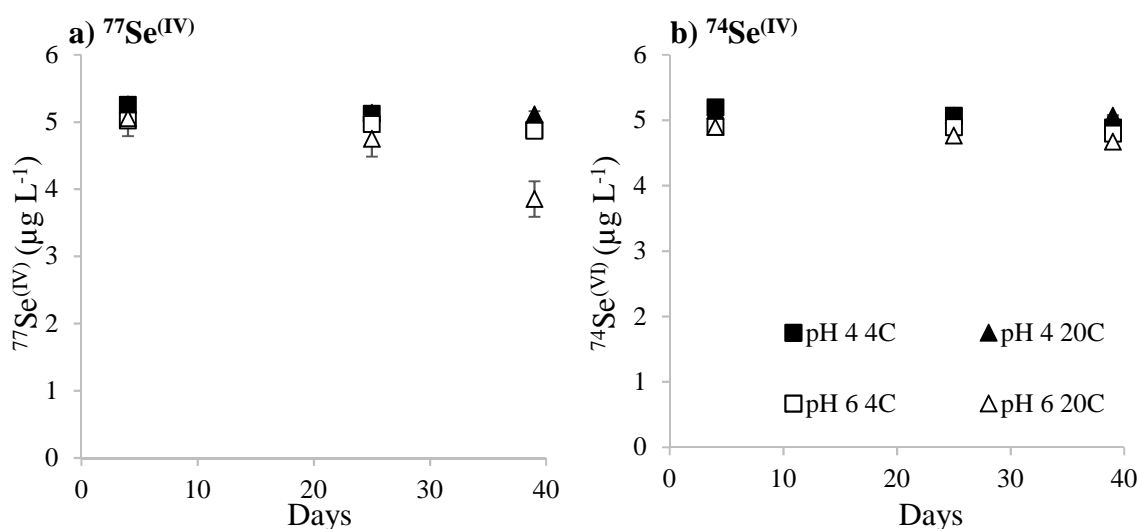
Figure 5.9. Fulvic acid suspensions (0.2 g L^{-1}) filtered (0.22 µm) at pH 4 spiked with 5 µg L^{-1} ^{77}Se$^{(IV)}$ and ^{74}Se$^{(VI)}$. Sampled over 40 days. Error bars based on two replicates.

As Se$^{(IV)}$ and Se$^{(VI)}$ were both removed from suspension in non-sterile HA systems, it is likely that a similar reaction would occur in non-sterile FA systems, since FA has a higher total acidity. For example, IO$_3^-$ showed a marginal increase in rate of removal in the presence of FA compared to HA. However as FA systems were not tested without filtration, comparisons between non-filtered and filtered systems cannot be made. It is apparent however that the reactions of Se$^{(IV)}$ and Se$^{(VI)}$ with both HA and FA is not abiotic indicating that the Se removal observed in the unfiltered systems is most likely microbially mediated, either directly or enzymatically.

5.4.2.2 Effect of added microbes on Se interactions with HA

Filtered and unfiltered, irradiated and non-irradiated suspensions of HA were supplied with additions of microbes from a soil inoculum and glucose (as a food source) in order to establish whether or not the mechanisms observed were biotic. All irradiated systems showed little/no reduction of Se$^{(IV)}$ or Se$^{(VI)}$ over time (**Figure 5.10**) with the exception of non-filtered HA systems where samples containing microbial and glucose additions

demonstrated removal of both $Se^{(IV)}$ and $Se^{(VI)}$. If this was the result of Se adsorption onto particulate matter introduced in the soil inoculum, then it would demonstrate rapid adsorption by abiotic kinetic mechanisms. This is not the case therefore it is more likely that irradiation hasn't completely sterilised these samples. Ideally samples should be γ-irradiated to achieve a dose between 10-35 kGy for complete sterilisation (Berns *et al.*, 2008; McNamara *et al.*, 2003). These samples however were only been irradiated to achieve a dose of 6.5 kGy. This dose rate was selected on the basis that the HA had been acid and alkaline treated during extraction, freeze dried and then re-dissolved in the lab and therefore any microbial community present would be minimal, certainly less than what you would find in an average soil sample.
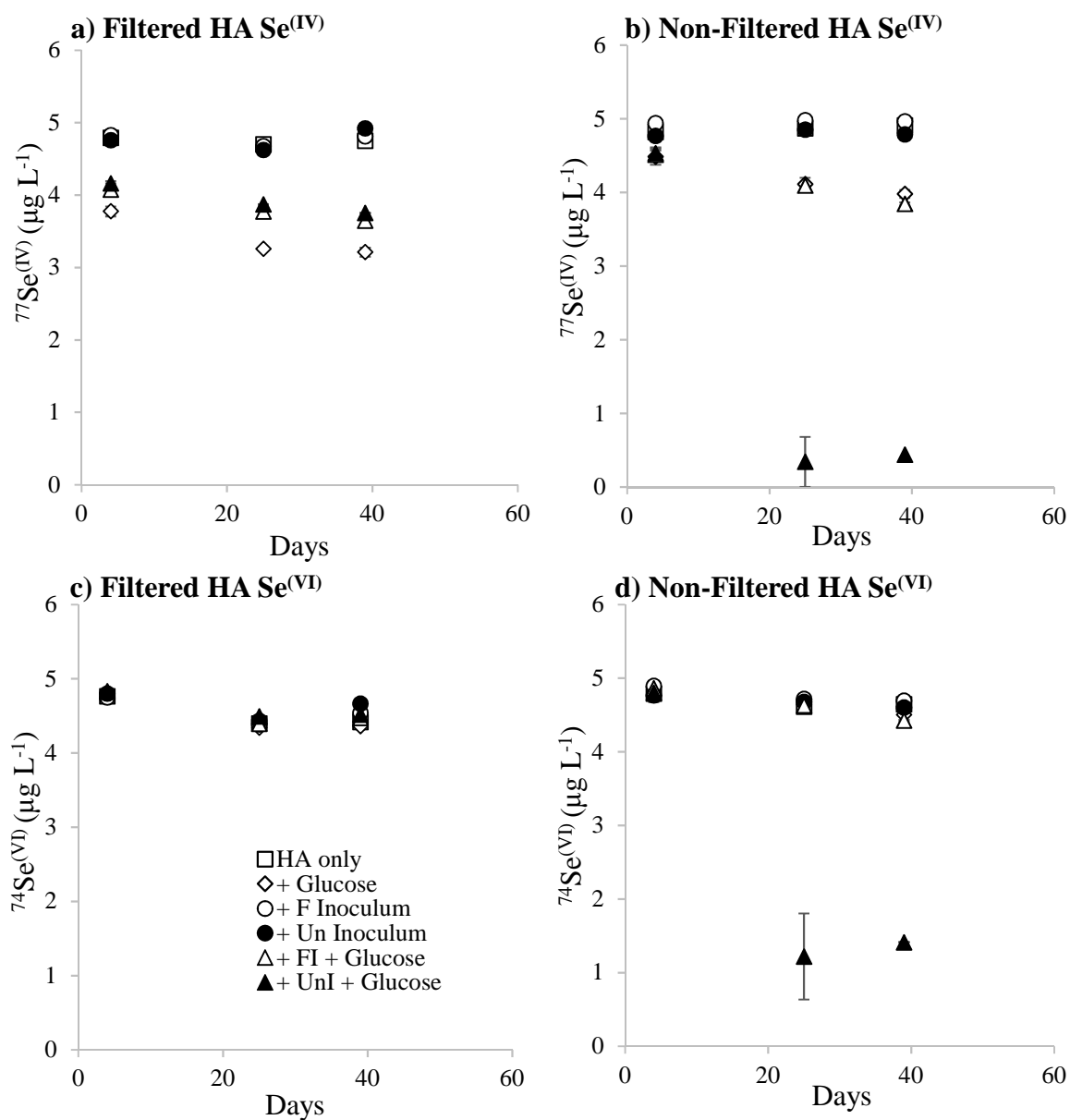
Figure 5.10. Irradiated HA systems (0.2 g L^{-1}) spiked with 5 µg L^{-1} ^{77}Se$^{(IV)}$ and ^{74}Se$^{(VI)}$. Samples were either filter sterilised (a, c) or non-filtered (not sterile) (b, d). Systems were set up alone and in combination with a range of treatments; glucose (G), filtered soil inoculum (FI), un-filtered soil inoculum (UnI), FI + G and UnI + G. Error bars based on two replicates.

161

Non-irradiated systems demonstrated the greatest removal of $Se^{(IV)}$ and $Se^{(VI)}$ where soil inoculum and glucose had been added (**Figure 5.11**), indicating that microbes are playing a significant role in the reduction of Se. **Figure 5.11d** demonstrates significant $Se^{(VI)}$ removal in *non-filtered* HA systems that received filtered inoculum alongside glucose. Filtering the inoculum would have removed any microbes present from the soil therefore this reduction must result from microbes present in the HA solution. Selenite reduction in *non-filtered* HA systems (**Figure 5.11b**) demonstrated almost complete removal in all systems regardless of added microbes or added glucose. Again this indicates that microbes already present in the HA solutions and microbes added from the soil inoculum are inducing $Se^{(IV)}$ removal. Although removal was observed in un-filtered HA systems and those with added microbes, it is unlikely that the microbes introduced from the soil inoculum are the same as those already present in the un-filtered HA systems, yet reduction is observed in both cases.

When no microbes are actively added to the *filtered* HA systems, i.e. HA only, glucose only and filtered inoculum systems, then less removal of $Se^{(IV)}$ and $Se^{(VI)}$ was observed (**Figure 5.11a** and **c**). The literature suggests that $Se^{(IV)}$ reduction and consequent incorporation tends to occur much more readily and extensively than $Se^{(VI)}$ reduction (Ike *et al.*, 2000) which agrees with the results observed here.

There is evidence to suggest that $Se^{(IV)}$ reduction occurs both biotically and abiotically (Lusa, 2015), however since the rate and relative contribution of biological reactions is likely larger (Li *et al.*, 2017), the biotic reactions are possibly hiding the abiotic. These results confirm the significant role microbes play in the reduction of $Se^{(IV)}$ and $Se^{(VI)}$ either to $Se^{(0)}$ or prior to incorporation into humic substances as Org-Se species.

Gustafsson and Johnsson (1994) used two antimicrobial agents; sodium azide and chloroacetic acid, to investigate the effects of microbes on Se incorporation into soil humic substances and found that both significantly reduced Se incorporation. Humic acid itself can act as an electron donor during microbial reduction of Se species (Lovley *et al.*, 1999), likely by microbial reduction of quinone groups (Scott *et al.*, 1998), although this has only previously been demonstrated in anaerobic systems.
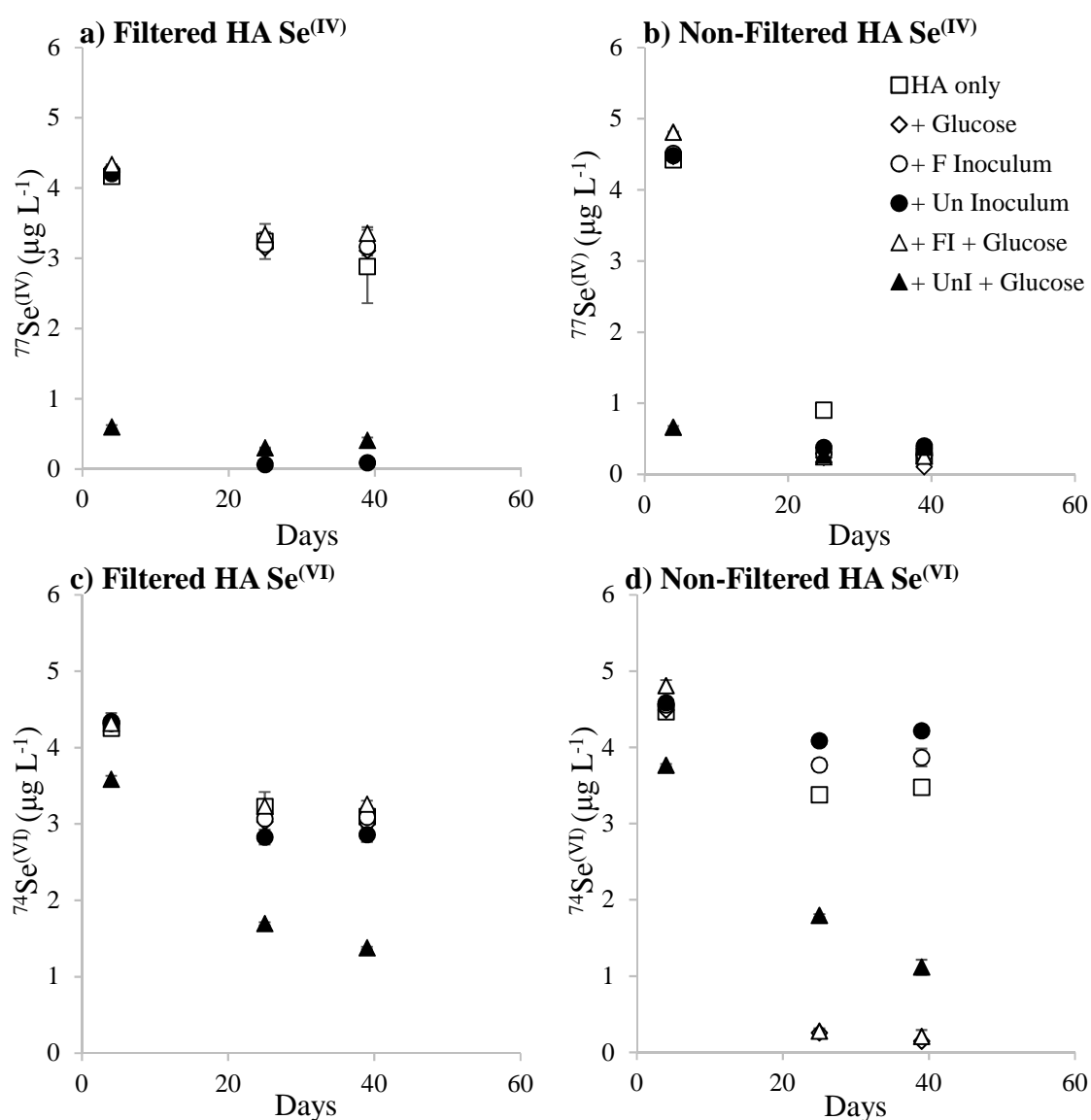
Figure 5.11. Non-irradiated HA systems (0.2 g L^{-1}) spiked with 5 µg L^{-1} ^{77}Se$^{(IV)}$ and ^{74}Se$^{(VI)}$. Samples were either filter sterilised (a, c) or non-filtered (not sterile) (b, d). Systems were set up alone and in combination with a range of treatments; glucose (G), filtered soil inoculum (FI), un-filtered soil inoculum (UnI), FI + G and UnI + G. Error bars based on two replicates.

Irradiated samples did not demonstrate any visible "growth", however a number of the non-irradiated samples showed significant growth with small brown colonies forming in the solution (**Figure 5.12**). It is suspected that the "brown colonies" are actually colonies of bacteria/fungi that have flocculated and collected the HA. This is because the HA solution appears to be lighter in samples with growth in comparison to those without growth. A record of which solutions demonstrated growth is presented in **Table 5.1** and correlates well with the systems that showed the most significant reduction of $Se^{(IV)}$ and $Se^{(VI)}$. Identification of the microbial species responsible for these reactions was not within the scope of this study but is an area that warrants further investigation.
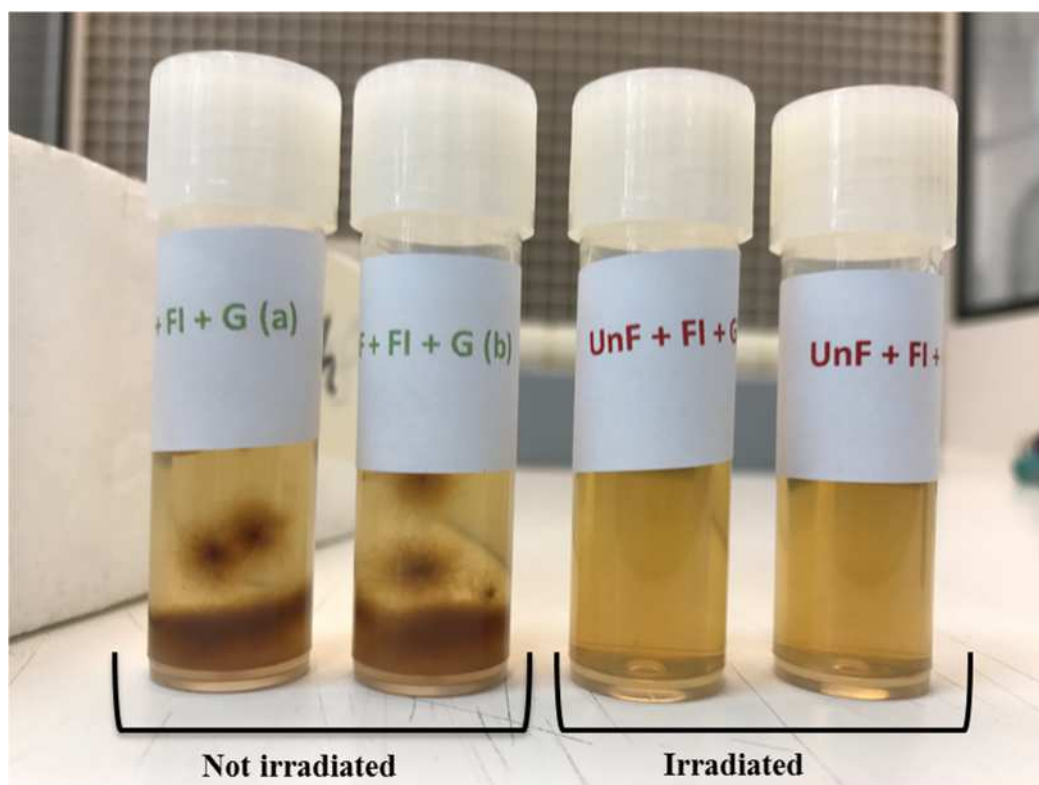
Figure 5.12. Brown colony growth in unfiltered HA samples that have received an addition of filtered inoculum and glucose. The samples showing no growth have been irradiated.

Table 5.1. Presence of colonies in *non-irradiated* samples compared to the amount of $^{77}Se^{(IV)}$ and $^{74}Se^{(VI)}$ reduction (loss as a %) after an initial spike of 5 µg L^{-1}. Average based on two replicates.

Filtered	Growth	Loss of $^{77}Se^{(IV)}$ (%)	Loss of $^{74}Se^{(VI)}$ (%)	Non-Filtered	Growth	Loss of $^{77}Se^{(IV)}$ (%)	Loss of $^{74}Se^{(VI)}$ (%)
HA only	-	42.3	38.1	HA only	-	94.9	30.5
+ G	-	37.8	40.0	+ G	✓	**97.9**	**97.1**
+ FI	-	36.7	38.3	+ FI	-	94.4	22.7
+ UnI	✓	**98.3**	**42.8**	+ UnI	✓	**92.1**	**15.7**
+ FI + G	-	32.9	34.9	+ FI + G	✓	**95.0**	**95.9**
+ UnI + G	✓	**91.8**	**72.5**	+ UnI + G	✓	**92.4**	**77.7**

In the presence of a suitable electron donor, selenium oxyanions can be utilised as the terminal electron acceptor for a range of different bacterial species. The literature describes a number of other bacterial species capable of either directly respiring Se (dissimilatory selenate reduction, DSeR) or indirectly for detoxification purposes; these include *Pseudomonas spp.*, specifically, *P. stutzeri* and *W. succinogenes* (Hockin and Gadd, 2003; Kuroda et al., 2011; Lovley et al., 1996). Stolz and Oremland (1999) describe the ability of *T. selenatis*, *S. barnesii*, *B. selenitireducens* and *B. arsenicoselenatis* in Se reduction. *D. desulfuricans,* a species of sulfate-reducing bacteria, has also demonstrated a capacity in Se bioremediation by reducing $Se^{(IV)}$ and $Se^{(VI)}$ to $Se^{(0)}$ (Tomei *et al.*, 1995). All of these species are thought to be widespread across different soil types and conditions, in particular *Pseudomonas spp.* therefore it is equally likely that any might be present in the soil inoculum used here. Lovley *et al.* (1999) demonstrated the capacity of *W. succinogenes* in using a HS analogue

anthrahydroquinone-2,6,-disulphonate (AHQDS) as an electron shuttle in $Se^{(VI)}$ reduction. If this species were present it could reduce the HA, consequently the HA could then transfer an electron to $Se^{(IV)}$ or $Se^{(VI)}$ causing reduction, leaving the HA oxidised and capable of accepting electrons from *W.succinogenes*.

One key problem with the results presented here however is that bacteria tend to work most effectively in neutral to high pH (pH 6-9) systems (Hageman *et al.*, 2013), with *B. selenitireducens* and *B. arsenicoselenatis* even being alkaliphilic (pH 9.8). It is therefore unusual that the microbial species that seem to be present in the HA systems appear to work most effectively at low pH. All experiments that were not sterilised show most significant Se reduction at pH 4 compared to pH 6; if microbes are driving this it would be expected that reduction would be greatest at higher pH. The soil used to prepare the inoculum was collected from an acidic woodland soil (pH 3.87), consequently the microbes collected are likely capable of working at low pH levels. Samples with inoculum added and non-sterile HA suspensions show the same pattern of microbial growth. However, only ~1% of bacterial species present in environmental samples are culturable (Ultee *et al.*, 2004), meaning that although the occurrence of colonies correlates with samples demonstrating the greatest Se reduction, it's not necessarily a causal relationship. Also given the process required to extract and purify HA, it would seem unlikely that a bacterial species would survive and, if it had, then the probability of that species being capable of reducing Se is slim. It is also possible that rather than being bacterially mediated, the reactions observed may be fungal. It is possible that introduction of bacteria/fungi could occur from the lab, but again the likelihood of introducing a Se reducing species seems small. All of these contradictory factors make the results difficult

to interpret in terms identifying a direct mechanism, however it does appear that microbes have an important role to play.

5.4.4 Formation of Org-Se species

Throughout these experiments it has been assumed that inorganic Se has been reduced to form Org-Se. This suggests rapid formation of Org-Se species in systems at low pH and high temperature. However, SEC of pH 4 ($20^{o}C$) samples demonstrated only a very minor increase in the organic part of the chromatogram (**Figure 5.13**), indicating that although inorganic $Se^{(VI)}$ was reduced, only a small fraction was organically bound. Analysis of total Se in both the pH and HA concentration experiments also demonstrated a missing fraction of Se (**Figure 5.14**). In the systems that show significant reduction of $Se^{(VI)}$ concentration, there is a lower overall Se concentration.
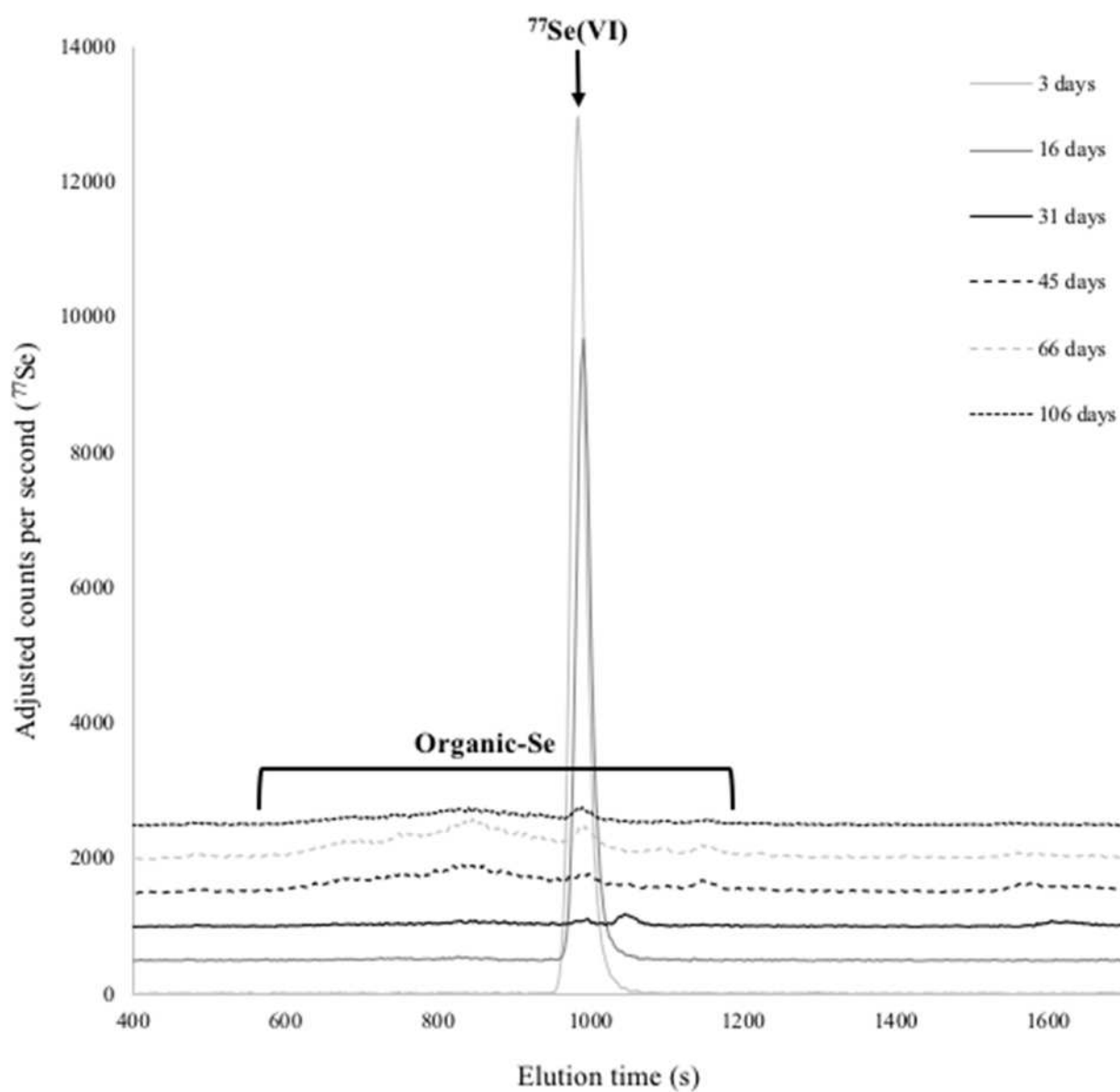
Figure 5.13. Size exclusion chromatogram showing the incorporation of 5 µg L^{-1} ^{77}Se$^{(VI)}$ into HA (0.2 g L^{-1}) at pH 4 and 20°C over 106 days.
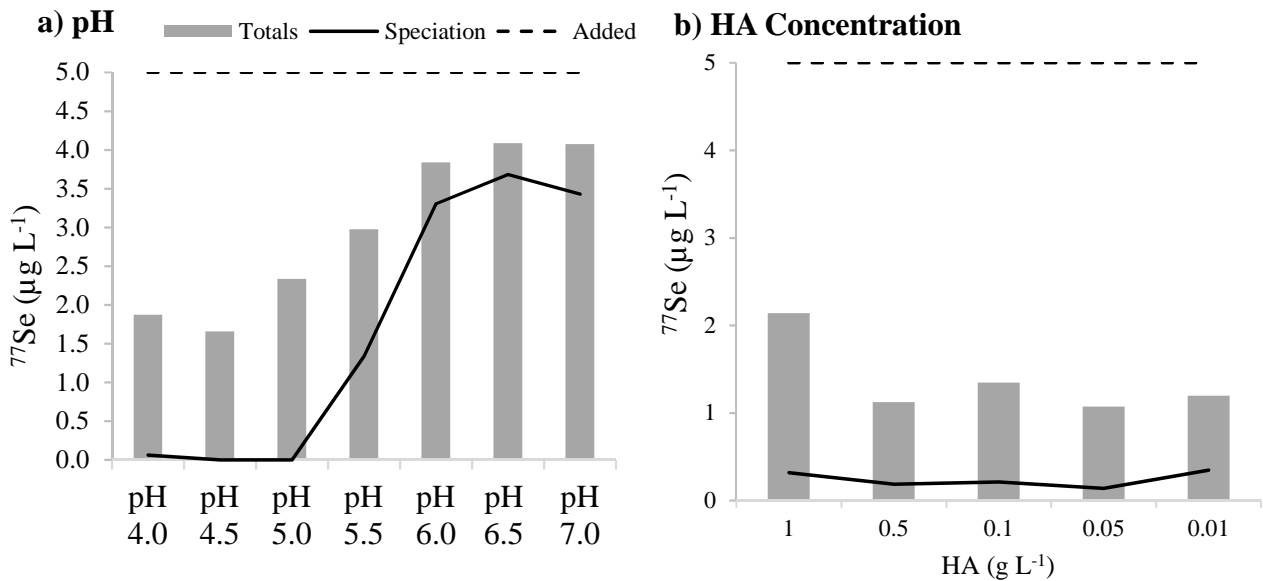
Figure 5.14. Selenium totals (µg L^{-1}) (bars) compared to the summed species calculated using speciation (µg L^{-1}) (solid line) after the end of the a) pH experiment and b) HA concentration experiment. Dashed line indicates initial Se addition (5 µg L^{-1}).

Any Se associated with the HA would be accounted for during analysis of total Se, which implies the missing Se is not organically bound. On average 3 µg L^{-1} Se has been lost from systems that have shown significant Se reduction (low pH). It's possible that this fraction has been lost through volatilisation as a number of experimental studies have identified micro-organisms capable of volatilising inorganic and organic Se forms (Azaizeh *et al.*, 1996; Zieve and Peterson, 1984). Darcheville *et al*. (2008) investigated Se partitioning in an oxic sandy soil and found that Se volatilisation did not occur in sterilised samples, however in non-sterile samples volatilisation resulted in the loss of some Se from the system (0.0014-0.0087%). Therefore, it is possible that Se in these samples could have been lost through volatilisation, yet in some systems there was as much as 60% loss of Se and it is unlikely that this could all be accounted for by volatilisation. Another possible explanation is that Se$^{(VI)}$ has been reduced to elemental Se$^{(0)}$ and precipitated. Bruggeman *et al*. (2007) hypothesised that the reduction in total Se concentration observed over time, when Se$^{(IV)}$ was in combination with HS, could be

attributed to the reduction and precipitation of $Se^{(IV)}$ to $Se^{(0)}$ since it is possible for HS to aid reduction of Se species. Shaking of the sample tubes with 1% TMAH was able to account for as much as an extra 1 µg L^{-1} ^{77}Se, in some samples, on top of that accounted for in the solution sample totals, suggesting that some Se was potentially retained on the tube walls. However this still indicates a missing fraction of 2 µg L^{-1} on average. This warrants further investigation into the formation of Org-Se species in HA systems, the volatilisation of Se in microbial HA systems, and the potential interaction of Se with polypropylene tubes.

5.4.5 Formation of 'Se unknown'

In many chromatograms an 'Se unknown' species was observed; in the range finding experiment it was observed in samples spiked with ^{77}Se$^{(VI)}$ at 20°C at pH 4 and pH 6, with more at pH 6. The unknown species appeared on the chromatogram before the retention time of the ^{77}Se$^{(IV)}$ peak (40-50 seconds). The unidentified species was integrated separately where it appeared. Results collected from the range finding experiment demonstrated a steady increase in this peak over 163 days at pH 6, whereas at pH 4 it appeared to increase and then decrease to zero over 125 days (**Figure 5.15**). At pH 6 it was observed in all 20°C samples, and at both 0.05 g L^{-1} and 0.2 g L^{-1} HA concentrations. At pH 4 it was only observed in 0.05 g L^{-1} samples at 20°C. The concentration of this unknown species was very low (<1 µg L^{-1}) in all cases. It is suspected that it is an intermediate, transient, species formed during the reduction of Se$^{(VI)}$ prior to binding, or a soluble organic species. At pH 4 where the reduction of Se was greatest, the unidentified species increased then decreased rapidly. It was formed more gradually and remained in solution longer at pH 6, which could be due to slower reactions at higher pH. Bruggeman *et al.* (2007) also discovered an unknown Se species present in HS samples spiked with Se$^{(IV)}$, but to a greater degree than observed here, and observed no formation when spiked with Se$^{(VI)}$. Given that it was only observed here in systems spiked with Se$^{(VI)}$ it could be a

different unknown species to that observed in Bruggeman *et al.* (2007), although it is difficult to conclude since no identification was possible in either case. They suggested it was an organically bound Se species that indicated an abiotic route for the association of $Se^{(IV)}$ with OM, with further spectroscopic evidence required.
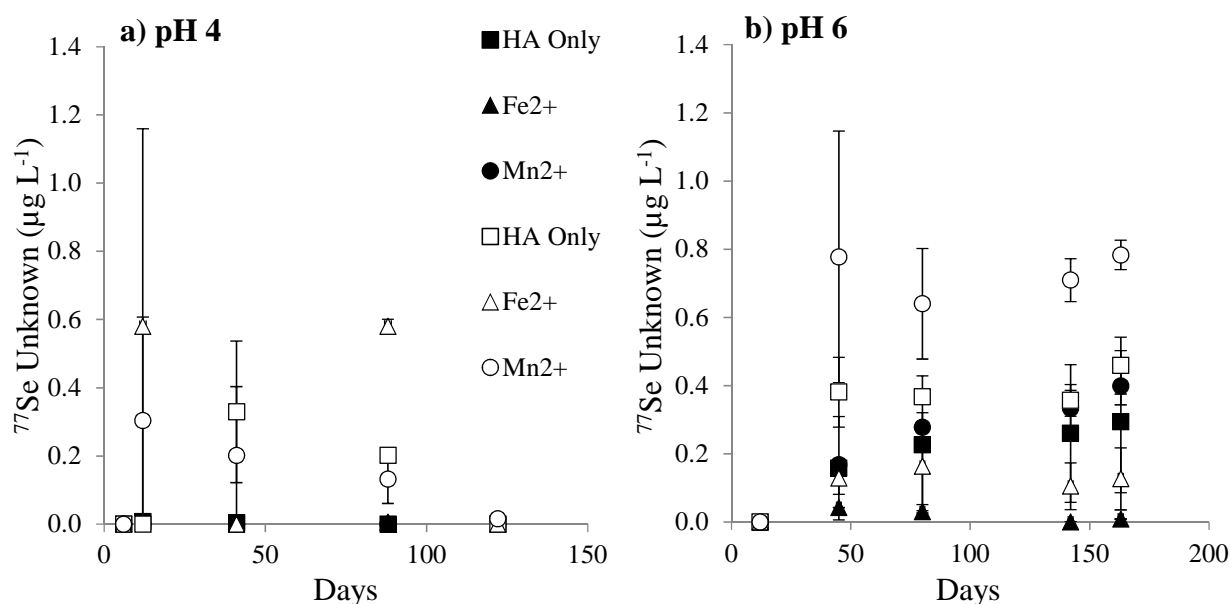
Figure 5.15. Formation of Se Unknown species in HA systems containing 0.05 g L^{-1} HA (open symbols) and 0.2 g L^{-1} HA (closed symbols) at pH 4 and pH 6, spiked with $^{77}Se^{(VI)}$. Systems containing HA only (squares), and additions of Fe^{2+} (triangles) or Mn^{2+} (circles).

5.4.6 X-ray absorption spectroscopy

Entrained Se present in the each paste sample was measured in order to demonstrate that the XAS data collected was for Se in the solid phase. A sample of Ca-humate with 100 mmol kg^{-1} $Se^{(IV)}$, was weighed after each wash step and the amount of entrained Se calculated from Equation 1. Assuming a minimum of 15% of added Se was associated with HA, there was ~231 ppb Se in the solid phase and ~8.99 ppb in the entrained solution after 3 washes with Milli-Q water. Given that the detection limit of Se by XAS is ~200 ppb Se, all results presented must relate to Se bonded to the solid phase.

X-ray absorption near-edge structure (XANES) and EXAFS spectra were obtained for all Ca-humate and Ca-humate combined with $Fe^{(III)}$ samples at pH 4 and spiked soil samples (with the except of the DY-G soil spiked with Na_2SeO_4). All Ca-humate plus goethite samples prepared at pH 6 failed to show a Se edge at any Se concentration, a result that was anticipated from the batch sorption experiments, where no transformation of inorganic $Se^{(IV)}$ or $Se^{(VI)}$ was observed at pH 6 in the presence of HA or goethite.

5.4.5.1 XANES

The XANES spectra show Se was present at a range of oxidation states depending on the initial spike and the type of sample (**Figure 5.16**). Selenium was reduced to some extent in the majority of samples, either from $Se^{(VI)}$ to $Se^{(IV)}$, or $Se^{(IV)}$ to $Se^{(0)}$, and in one case from $Se^{(VI)}$ to $Se^{(0)}$. Data collected from goethite samples demonstrated no change in Se oxidation state when spiked with $Se^{(IV)}$, and a small degree of reduction when spiked with $Se^{(VI)}$. Goethite has previously been shown to preserve $Se^{(VI)}$ and $Se^{(IV)}$ oxidation states during association (Das *et al.*, 2013; Hayes *et al.*, 1987; Manceau and Charlet, 1994) so this was unexpected. A small degree of Se reduction was observed in the beam during the experiment and this was minimised by moving the sample position before each scan, but it cannot be ruled out that this small degree of $Se^{(VI)}$ reduction is the result of photo-reduction.
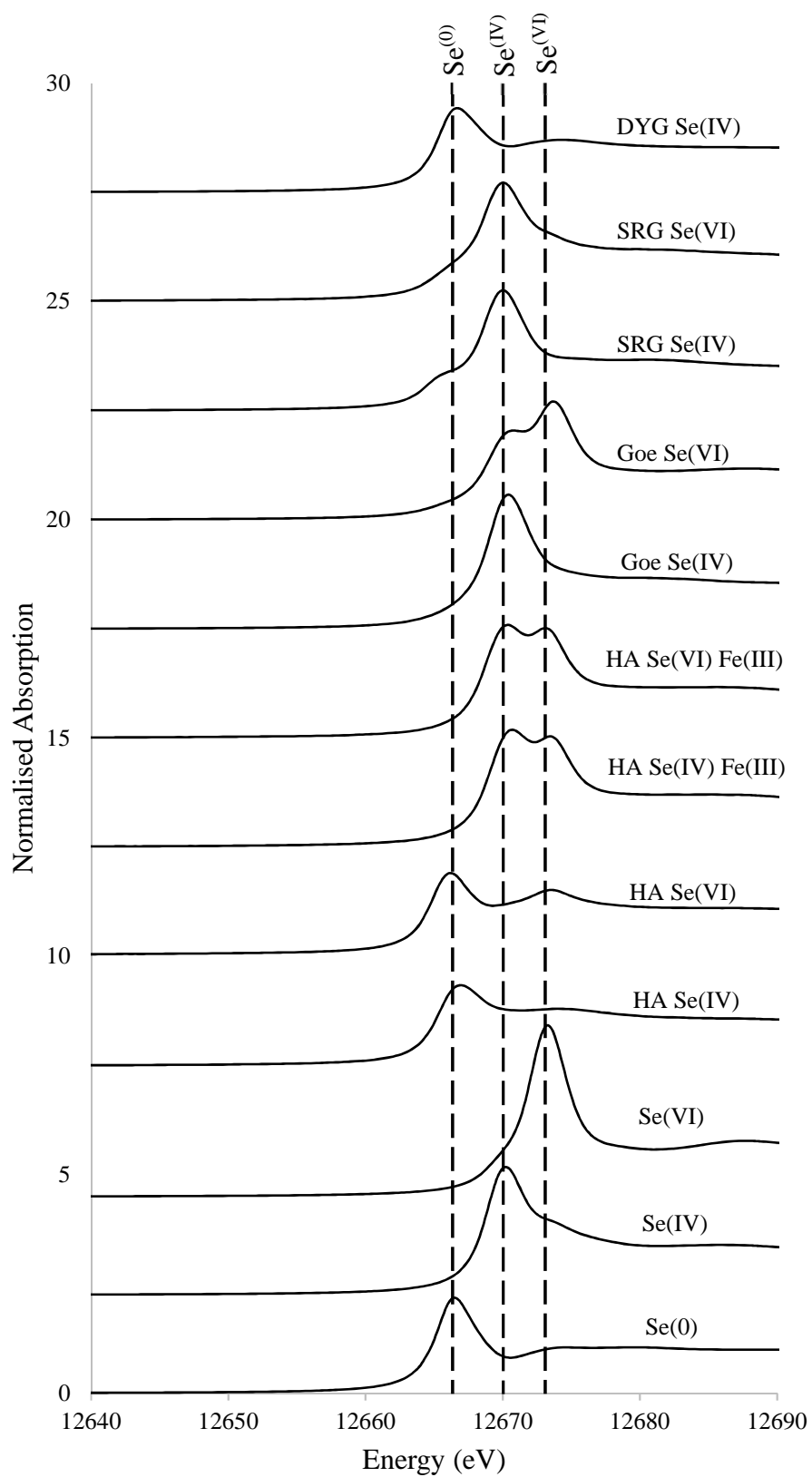
Figure 5.16. Se k-edge XANES spectra of samples and standards, where standards are $Se^{(VI)}$ as Na_2SeO_4, $Se^{(IV)}$ as Na_2SeO_3 and $Se^{(0)}$.

Elemental Se dominates the XANES spectra of the Ca-humate samples, demonstrating the strong ability of Ca-humate to reduce both $Se^{(IV)}$ and $Se^{(VI)}$ to $Se^{(0)}$. When Ca-humate was in combination with $Fe^{(III)}$ ions there was incomplete reduction to $Se^{(0)}$, with some reduction from $Se^{(VI)}$ to $Se^{(IV)}$. Given that Fe is both capable of reducing Se species and has been shown to form ternary complexes between $Se^{(IV)}$ and HA this is in-keeping with the literature (Martin *et al*., 2017; Struyk and Sposito, 2001). The SR-G soils showed a capacity to reduce $Se^{(VI)}$ to $Se^{(IV)}$, and incorporate both $Se^{(IV)}$ and $Se^{(0)}$ into the solid phase, whilst the DY-G soil spiked with $Se^{(IV)}$ showed the most significant reduction to $Se^{(0)}$. Given that DY-G has a higher OM content and lower pH when compared to SR-G, this may be why more complete reduction to $Se^{(0)}$ was observed.

5.4.5.2 Linear Combination Fitting (LCF)

Linear combination fitting can be used to investigate the relative contribution of each standard, in the fitting of a sample (**Table 5.2**). In the SR-G soil samples, spiked with $Se^{(IV)}$ and $Se^{(VI)}$, it was apparent that Goethite-$Se^{(IV)}$ interactions made up a large proportion (66 %) of the associations. Oxides analysis of the soil indicate that the SR-G soil has a much higher Fe-oxide (50.8 mg kg^{-1}) content than the DY-G soil (6.9 g kg^{-1}), and alongside a higher pH this could explain why Goethite-$Se^{(IV)}$ interactions contribute more in the case of SR-G but not DY-G. In soil DY-G the fit was predominantly explained by the presence of Se(0) in the sample (42 %), and by HA-$Se^{(IV)}$ and HA-$Se^{(VI)}$ interactions (both 28 %) which are expected due to its higher OM content and lower pH.

Table 5.2. Relative contribution of each standard and sample to the LCF fitting for each XANES sample.

Sample	$Se^{(0)}$	$Se^{(IV)}$	$Se^{(VI)}$	HA $Se^{(IV)}$	HA $Se^{(VI)}$	Goethite $Se^{(IV)}$	Goethite $Se^{(VI)}$	HA $Se^{(IV)}$ $Fe^{(III)}$
HA $Se^{(IV)}$	74.1	23.0	2.9	0.0	0.0	0.0	0.0	0.0
HA $Se^{(VI)}$	77.1	11.7	11.2	0.0	0.0	0.0	0.0	0.0
Goethite $Se^{(IV)}$	3.1	96.9	0.0	0.0	0.0	0.0	0.0	0.0
Goethite $Se^{(VI)}$	4.4	50.5	45.2	0.0	0.0	0.0	0.0	0.0
HA $Se^{(IV)}$ $Fe^{(III)}$	0.0	25.9	7.8	0.0	0.0	28.3	38.0	0.0
HA $Se^{(VI)}$ $Fe^{(III)}$	0.0	45.0	14.2	0.0	0.0	5.4	35.4	0.0
SRG $Se^{(IV)}$	15.4	18.3	0.0	0.0	0.0	66.3	0.0	0.0
SRG $Se^{(VI)}$	0.0	0.0	5.8	0.0	11.9	65.9	0.0	16.4
DYG $Se^{(IV)}$	42.1	0.0	0.0	28.2	28.2	0.0	1.6	0.0

Samples containing Ca-humate plus $Fe^{(III)}$ demonstrate the importance of Fe for Se association with HA. In sample HA-$Se^{(IV)}$-$Fe^{(III)}$, Goethite-$Se^{(IV)}$ contributes 28% and Goethite-$Se^{(VI)}$ 38% of the fit. The increased contribution of Goethite-$Se^{(VI)}$ was unexpected and unexplained as this sample was spiked with $Se^{(IV)}$, suggesting some degree of oxidation. The HA-$Se^{(VI)}$-$Fe^{(III)}$ sample demonstrates a contribution of 35% from Goethite-$Se^{(VI)}$, no contribution from Goethite-$Se^{(IV)}$, and significant reduction to $Se^{(IV)}$ (45%), which is likely as OM in combination with Fe has been demonstrated to result in significant reduction in previous studies (Bruggeman *et al.*, 2007). However in isolation linear combination fitting only provides limited information on the nature of the Se species present.

5.4.5.3 EXAFS

Spectra of raw and fitted k^3 weighted EXAFS data are shown in **Figure 5.17**. Fourier transformed data for $Se^{(IV)}$ and $Se^{(VI)}$ are presented in **Figure 5.18**. All path distances and fits are tabulated in **Table 5.3**. Analysis of the EXAFS k^3 weighted data demonstrates the amount of noise present; SRG-$Se^{(VI)}$, HA-$Se^{(VI)}$-$Fe^{(III)}$ and HA-$Se^{(IV)}$-$Fe^{(III)}$ samples have the most noise and this will negatively impact model fitting results (**Figure 5.17**). The Fourier transform magnitude was dominated by a strong peak at ~1.3Å, which arises from backscattering of the oxygen atoms in the coordination sphere (**Figure 5.18**) (Hayes *et al.*, 1987). This peak can be fitted with Se-O paths depending on the presence of $Se^{(IV)}$ or $Se^{(VI)}$ in the samples (1.65-1.71Å). In all cases however the spectra cannot be completely described by fitting just oxygen atoms, suggesting the formation of inner-sphere surface complexes.
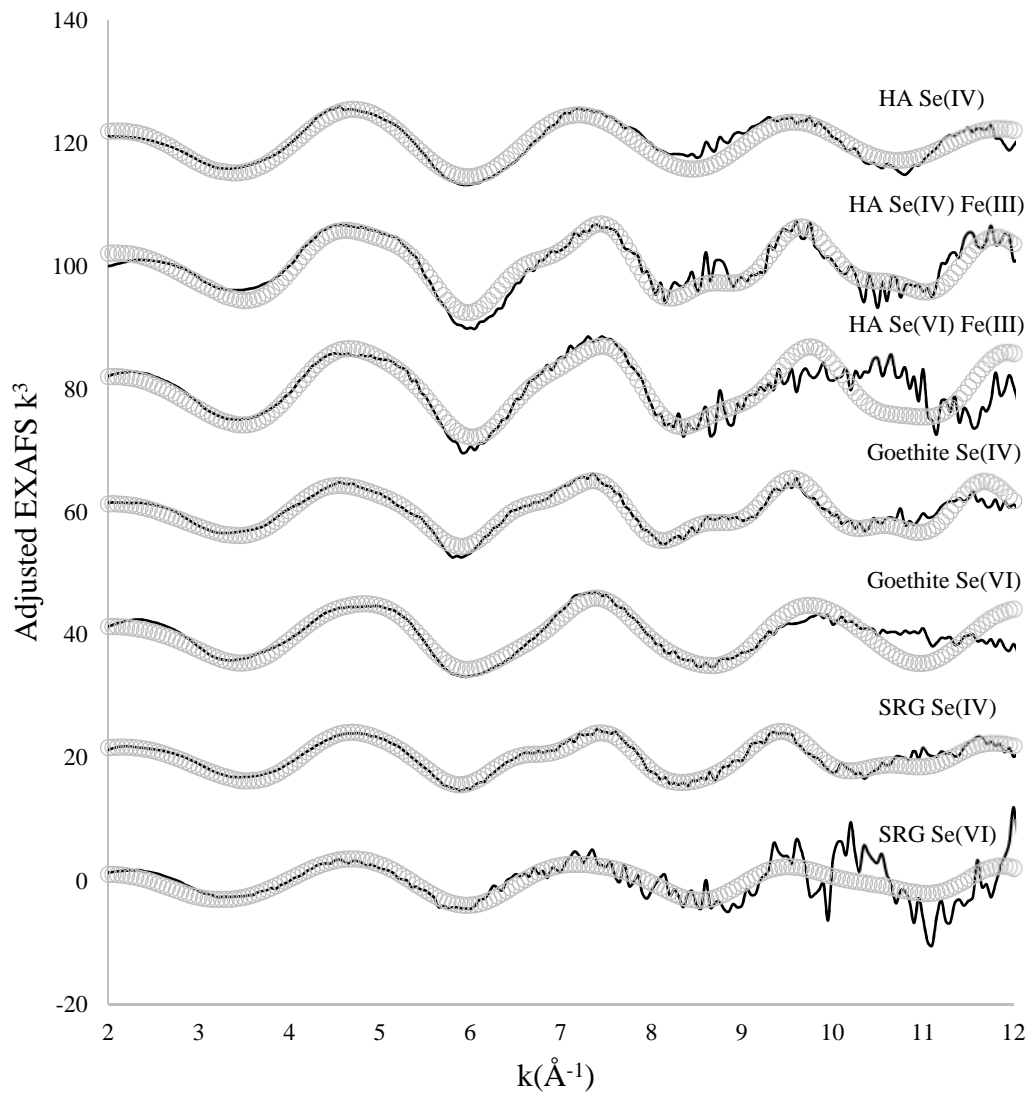
Figure 5.17. The k^3 weighted EXAFS spectra for the raw data (solid lines) and model fit (circles).
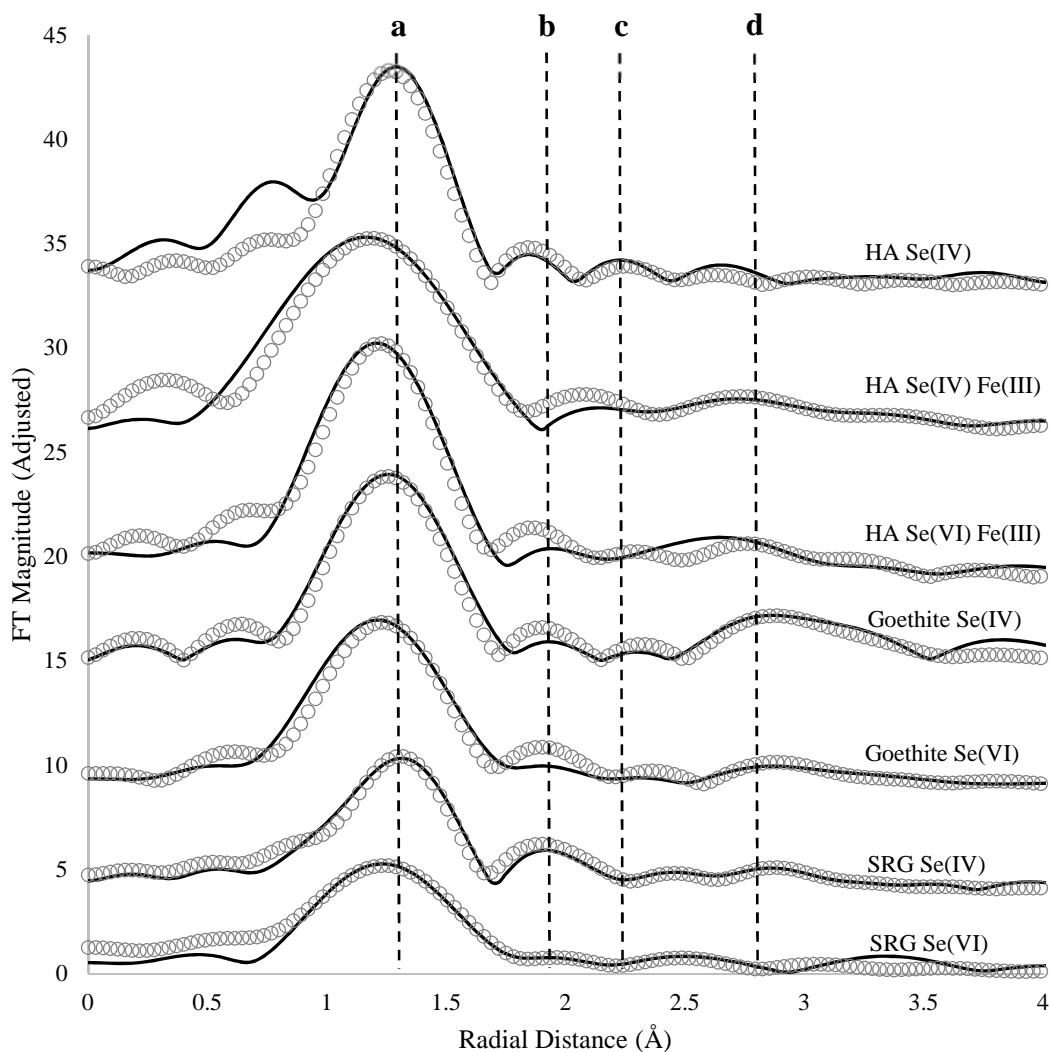
Figure 5.18. Fourier transform magnitude ($k^2X(k)$) of the EXAFS spectra for $Se^{(IV)}$ and $Se^{(VI)}$ incorporated into samples of Ca-humate, goethite and soil SRG. Solid lines correspond to raw data and symbols to model fits. The magnitude has been adjusted to show all samples on one plot. Lines indicate key paths/interatomic distances in the spectra; a) Se-O, b) Se-Se, c) Se-C and d) Se-Fe.

Table 5.3. EXAFS fitting results.

Sample	Path	N	SO²	R(Å)	σ²(Å²)	e0	Reduced Chi²	R-Factor
			Coordination Shell					
HA Se$^{(IV)}$ (pH 4)	Se-O	3.0	1.0	1.68	0.004	6.81	356	0.014
	Se-C	1.0	1.0	2.74	0.008	6.81		
HA Se$^{(IV)}$ Fe$^{(III)}$ (pH 4)	Se-O	2.8	1.0	1.67	0.001	7.51	165	0.021
	Se-Fe	1.8	1.0	3.30	0.006	7.51		
HA Se$^{(VI)}$ Fe$^{(III)}$ (pH 4)	Se-O	3.0	1.0	1.66	0.001	7.83	128	0.025
	Se-Fe	1.0	1.0	3.28	0.003	7.83		
Goethite Se$^{(IV)}$ (pH 4)	Se-O	2.5	0.9	1.69	0.002	7.91	509	0.014
	Se-Fe	1.5	0.9	3.34	0.005	7.91		
Goethite Se$^{(VI)}$ (pH 4)	Se-O	2.7	0.9	1.65	0.001	4.24	734	0.021
	Se-Fe	2.0	0.9	3.33	0.014	4.24		
SR-G Se$^{(IV)}$	Se-O	2.0	0.9	1.71	0.002	9.99	324	0.017
	Se-Se	0.6	0.9	2.39	0.006	9.99		
	Se-Fe	1.0	0.9	3.36	0.006	9.99		
SR-G Se$^{(VI)}$	Se-O	2.0	1.0	1.67	0.004	4.72	46	0.030
	Se-C	1.0	1.0	2.87	0.002	4.72		

Ca-humate

Ca-humate samples spiked with Se$^{(IV)}$ were completely described by a two-shell fit including a C atom at 2.75Å in addition to O (**Figure 5.18**). Considering that Se-C direct bonds tend to have a bond distance of ~1.97 Å (Weast, 1982), it's likely that this path represents a Se-O-C chain (**Figure 5.19**). The presence of this Se-O-C interaction is evidence of an association with carboxyl or phenolic groups on the HA surface, demonstrating direct association with Ca-humate. There is little previous evidence of the association of Se with Ca-humate/HA using XAS; typically the association of Se with HA/HS is demonstrated using sorption studies. For example, Gustafsson and Johnsson (1994) described the association of Se with low molecular weight humic substances using sequential extraction and chromatographic techniques, however direct Se-O-C association could not be documented. This is the first study using spectroscopic techniques to demonstrate this link between Se$^{(IV)}$ and the carboxyl/phenolic groups of humic substances, without the need for ternary complex formation.
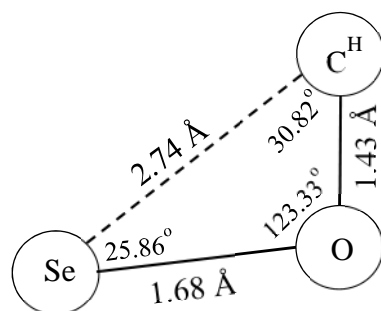
Figure 5.19. Schematic demonstrating the bond lengths (Å) and angles (°) formed during Se(IV) association with Ca-humate (C^H) carboxyl or hydroxyl groups.

Although the association of Se with OM has been demonstrated without ternary complex formation, it is believed that such complexes contribute significantly to Se interactions (Fernández-Martínez and Charlet, 2009). Adding Fe$^{(III)}$ ions to Ca-humate was

undertaken to allow the possibility of the formation of such complexes. It has previously been demonstrated that when $Fe^{(III)}$ is combined with HS the principal binding form was as $FeOH^{2+}$ at all pH values in the range 4-9 (Tipping and Rey-Castro, 2002) thus reducing the net negative surface charge of the HS whilst providing cations for interaction with the Se oxyanions. This Se-Fe-HA interaction, via a chain containing O atoms, has been demonstrated in the case of $Se^{(IV)}$ but not for $Se^{(VI)}$ (Martin *et al*., 2017). It is clear from the EXAFS results presented here that in the case of both $Se^{(IV)}$ and $Se^{(VI)}$ added to Ca-humate in combination with $Fe^{(III)}$, Fe atoms at 3.28-3.31Å (alongside O atoms at 1.66Å) are required for a good fit to be achieved (**Figure 5.18**). These Fe interatomic distances are consistent with those observed in the literature (Das *et al.*, 2013; Manceau & Charlet, 1994) and although these papers tend to be studies of iron oxy-hydroxides, it still provides strong evidence that both $Se^{(IV)}$ and $Se^{(VI)}$ can form ternary complexes with Ca-humate in the presence of $Fe^{(III)}$ ions. Martin *et al.* (2017) using ICP-MS and UV absorbance provide evidence that $Fe^{(III)}$ is capable of forming a cation bridge between $^{78}Se^{(IV)}$ and HA, however there is currently no literature proposing the formation of $Se^{(VI)}$-Fe-HA complexes observed here. The pH of the samples in the Martin *et al* (2017) study were not reported, and reaction time was short (overnight) which, if in combination with high pH, could explain the absence of a ternary $Se^{(VI)}$ species.

Selenium has a clear association with HA in the absence of Fe, and when Fe was present cation bridging dominated. The sorption experiments presented earlier (Section 5.4.1.1) demonstrated that Fe^{2+} did not increase the rate of Se reduction or incorporation as Org-Se species, therefore it is suggested that Se-Fe-HA cation bridging is more thermodynamically favourable and dominates when Fe is present, but in the absence of Fe, Se remains capable of forming a direct bond with HA. However Fe concentrations

used in this XAS investigation differ from those in the sorption study and further work is necessary to enable direct comparison.

Goethite

The presence of iron in the fits indicates that both $Se^{(IV)}$ and $Se^{(VI)}$ bonding with goethite are through the formation of inner-sphere complexes. Model fits for $Se^{(IV)}$ combined with goethite required 2.5 O atoms at 1.69 Å and 1.5 Fe atoms at 3.34 Å. For $Se^{(VI)}$ 2.7 O atoms at 1.65 Å and 2 Fe atoms at 3.33 Å were required (**Figure 5.18**). Again, these interatomic Fe distances suggest that both $Se^{(IV)}$ and $Se^{(VI)}$ are forming inner-sphere complexes with goethite. Using a Fe-O bond length of ~1.95 Å (Hayes *et al.*, 1987) it was possible to create schematic diagrams of two of the possible inner-sphere complex structures formed (**Figure 5.20**). Some debate exists in the literature as to whether $Se^{(VI)}$ forms outer- or inner-sphere complexes with goethite. Hayes *et al.* (1987) provided evidence of weak outer-sphere association of $Se^{(VI)}$ with goethite, whereas Manceau and Charlet (1994) demonstrated inner-sphere complexation. Peak & Sparks (2002) concluded that $Se^{(VI)}$ was capable of forming a mixture of both depending on conditions such as pH and ionic strength. As the EXAFS spectra collected here were for samples at pH 4 it is likely that at a higher pH level neither species would show inner-sphere complexation.
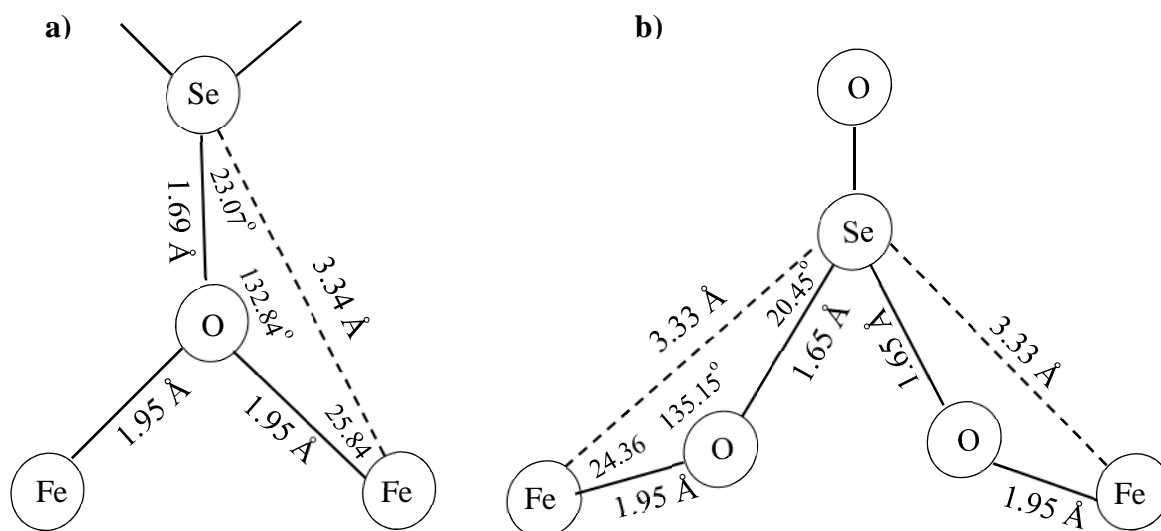
Figure 5.20. Two possible structures for inner-sphere complex formation on the oxide surface for selenite (a) and selenate (b) adsorbed to goethite based on the bond distances fitted here.

Soils

The SRG soil proved much more complex to fit than other simpler systems. The SRG-Se$^{(IV)}$ EXAFS spectra required a large O contribution, with smaller Se and Fe contributions, the Se$^{(VI)}$ fit was described by the inclusion of O and Fe paths (**Figure 5.18**). The SRG soil spiked with Se$^{(IV)}$ showed a small Se-path contribution to the model fitting, compared to when spiked with Se$^{(VI)}$ where no Se contribution was observed. This could be explained by the greater reduction of Se$^{(IV)}$ to Se$^{(0)}$ in the soil. Significant formation of Se$^{(0)}$ was also observed in the DYG soil and confirmed by both XANES and LCF analysis. It was anticipated that the higher OM content and lower pH of the DYG soil, would result in overall more complexation of Se than observed in the SRG soil, however this does not appear to be the case. The oxide content of the two soils varies greatly, indicating that the Fe-oxide content of the soils has a greater effect on Se complexation within whole soil systems than OM content for these soils, indicated by the significant Fe contribution in the SRG soil, and lack thereof in the DYG soil.

However, considering the interactions between Fe-oxides and OM (Fernández-Martínez and Charlet, 2009), it is likely that this is again evidence for the ability of Fe to assist in complexation with OM via ternary complexes. The retention of Se oxyanions within soil systems is likely dependent on multiple factors including Fe-oxide content, OM content and pH.

5.4.7 Conclusions

The mechanisms of Se associations with soil geocolloids are highly dependent on Se speciation, pH, the presence of microbial communities and iron. Humic acid can bind Se, but the lack of an effect of HA concentration suggests that the OM content of a soil doesn't solely drive these reactions. Reduction of both $Se^{(IV)}$ and $Se^{(VI)}$ was significantly influenced by pH, with decreasing pH resulting in an increased rate of reduction. Specifically in the case of $Se^{(VI)}$ which was investigated in the range pH 4-7, a correlation exists between decreasing pH and increased $Se^{(VI)}$ reduction (r=0.81). In sterilised systems $Se^{(IV)}$ and $Se^{(VI)}$ reduction did not occur, indicating a biotic component. When soil inoculum was added to HA at pH 4 increased $Se^{(IV)}$ and $Se^{(VI)}$ reduction was observed but it is difficult to understand the mechanism responsible as bacterial reactions are typically most effective at neutral/high pH. Further investigation of the role of microbial reduction in the reaction of Se with HSs is suggested.

In the batch sorption experiments neither Fe^{2+} nor Mn^{2+} increased the rate of $Se^{(IV)}$ or $Se^{(VI)}$ reduction and incorporation into HA. However, XAS results indicated that cation bridging could occur. Analysis of Se spiked Ca-humate, Ca-humate plus Fe^{3+}, goethite and soils provided insights into the mechanisms involved in Se associations with soil geocolloids and soils as a whole. Reduction of both $Se^{(IV)}$ and $Se^{(VI)}$ to $Se^{(0)}$ was observed

in the presence of Ca-humate and the DY-G soil, with varying degrees of reduction observed in other systems. Goethite demonstrated a significant capacity to bind $Se^{(IV)}$ and $Se^{(VI)}$ (whilst preserving Se oxidation state) via inner-surface complexation at pH 4. Selenite showed some capacity to associate with Ca-humate directly via carboxyl or phenolic groups, and also via cation bridging with Fe. Although no spectra were collected showing $Se^{(VI)}$ binding to Ca-humate directly, cation bridging with Fe was demonstrated at pH 4. This is the first study to demonstrate ternary complex formation in a $Se^{(VI)}$ - Ca-humate system. The SR-G soil demonstrated the complexity of Se incorporation into the solid phase with Se-Se, Se-C and Se-Fe bonds being required to fit the EXAFS spectra.

Together this data demonstrates the complexity of Se reactions in soils. It is apparent that no one abiotic factor drives incorporation rather that biological mechanisms such as microbial reduction alongside pH, temperature, Fe-oxide and OM content significantly influence the interaction. Consequently, modelling the interactions of Se within soils is challenging and further work is necessary in order to successfully model these interactions.

6. TECHNETIUM INTERACTION WITH SOIL GEOCOLLOIDS

6.1 INTRODUCTION

Upon release into the environment, ^{99}Tc entering the biologically active zone of soil undergoes time-dependent transformation to relatively stable organic forms within humus or is occluded within other phases (Abdelouas *et al.,* 2005). These interactions are likely to be very complex and affected by factors such as pH, temperature, Eh, metal oxide content and OM content. Direct interaction between humic substances (HS) and Tc has been demonstrated (Geraedts *et al.*, 2002; Maes *et al*., 2004). However, these investigations have predominantly been under anoxic conditions because, to interact with soil phases, Tc$^{(VII)}$ must undergo reduction from a higher to a lower oxidation state before association, predominantly as hydrous Tc$^{(IV)}$ phases (Boggs *et al.*, 2011; Wildung *et al.*, 2004).

Reduction of Tc$^{(VII)}$ to Tc$^{(IV)}$ in soils can be significant under certain conditions, and many studies have investigated the effects that metal oxides, metal ions, OM and microbial communities have on this reaction (Section 1.5.2). There is significant evidence for the incorporation of Tc into the organic phases of aerobic soils over time, for example Abdelouas *et al.* (2005) demonstrated slow but significant reduction of Tc$^{(VII)}$ in an aerobic soil with a high OM content, alongside minimal/no reduction in an aerobic soil with a low OM content. However, the processes, and rate-determining factors, that control the 'transfer-to-sink' of Tc under these conditions is poorly understood. Here Tc$^{(VII)}$ will be combined with HA and FA systems under aerobic conditions, alongside additions of Fe^{2+}, Mn^{2+}, and Fe(oxy)hydroxides and inclusion or exclusion of microbial influence in order to try and elucidate the ongoing mechanism.

6.2 AIMS

The aim of this work was to investigate the interactions of technetium with soil geocolloids, including HA and FA alone, and HA in combination with metal ions and oxides, to increase our understanding of Tc mobility within the soil environment.

Specific objectives included:

- Investigation of the dynamics of pertechnetate (^{99}Tc$^{(VII)}$), when combined with HA alone and in combination with metal ions;

- Investigation of the dynamics and fate of Tc$^{(VII)}$ when added to a range of different soil types;

- Determine the effect of temperature, pH and metal oxides on the formation of organic technetium species;

6.3 MATERIALS AND METHODS

Most of the iodine and selenium mixed spike experiments described in Chapters 4 and 5 also contained 1 µg L^{-1} ^{99}Tc$^{(VII)}$, therefore the sections where the methods have been described will be referenced.

6.3.1 Humic acid stock solution

The humic acid stock solution used throughout these experiments was prepared as described in Section 4.3.1.

6.3.2 Interactions of Tc with HA

The range-finding experiment was as described in Section 4.3.3 and included a spike of 1 µg L^{-1} ^{99}Tc$^{(VII)}$.

6.3.3 Interactions of Tc with FA

The fulvic acid experiment was designed according to Section 4.3.6 and included a spike of 1 µg L^{-1} ^{99}Tc$^{(VII)}$.

6.3.4 Effect of microbes on Tc interactions with HA

Humic acid samples were prepared as described in Section 4.3.8 with an added spike of 1 µg L^{-1} ^{99}Tc$^{(VII)}$.

6.3.5 Speciation analysis

Chromatography to separate technetium species used an HPLC (Dionex ICS-3000) coupled to ICP-MS and using 50 mM NaClO$_4$ as eluent as described in Chapter 2 (Section 2.5.2). Each chromatographic run usually required 5 min per sample. Data processing was carried out with Plasmalab software for all species, as described in Chapter 2 (Section 2.5.2).

6.3.6 XAS experiment

6.3.6.1 Sample Spiking

The TREE soils selected were: BC-M, BY-M, DY-G, DY-M, F1-T, F2-T, IH-W, PE-W, SB-G, TK-G and WK-W; the characteristics of each soil are provided in **Table 6.1**. Soils were stored in the dark at 10°C. An aerobic environment was maintained with regular agitation to try and prevent anaerobic microsites developing. Subsamples of each soil were weighed in quadruplet, duplicate for soil samples and duplicate for HA extraction, into centrifuge tubes to achieve ~5 g weight. A stock of 3.7 MBq in 5 ml solution (1172 mg L^{-1}) was diluted to achieve 293 mg L^{-1} Tc. The diluted stock was used to spike

samples to achieve 11.73 mg kg^{-1} ^{99}Tc. It was assumed that HA may constitute 5% of the soil so that if the HA adsorbed all of the added ^{99}Tc then it would contain approximately 234 mg kg^{-1} ^{99}Tc. Samples were stored in the dark at room temperature for ~5 months prior to preparation for analysis.

Table 6.1. Soil properties.

Sample	Major elements (mg kg^{-1})					Incubation moisture content (% wt)
	Org-C (%)	pH	Al	Mn	Fe	
F1-T	0.7	3.32	2211	19	421	11
F2-T	42.6	3.42	7261	34	8427	41
BC-M	5.5	4.18	21124	77	16124	15
BY-W	10.6	3.41	30226	141	22966	21
DY-G	11.4	3.90	15841	43	6925	31
DY-M	38.6	3.46	10439	43	5759	36
IH-W	9.5	3.88	27554	185	18013	20
PE-W	7.1	3.82	18022	91	7655	12
SB-G	5.0	6.02	22103	460	13775	15
TK-G	6.3	5.32	40942	303	25256	20
WK-W	24.4	3.87	11025	233	13202	37

6.3.6.2 Preparation of soil and HA for XAS analysis

Soil samples spiked with Tc were washed thrice with Milli-Q water (resuspension followed by centrifugation at c. 3000 g) to remove any excess Tc$^{(VII)}$ in solution prior to analysis. To determine the concentration of Tc in the supernatant the washes were acidified using 50% HNO$_3$ ready for ICP-MS analysis. After washing the soil samples; the duplicate samples to be kept as soils were ground into a homogenous paste (whilst moist) using a pestle and mortar under a fume hood. The HA was extracted from the second set of duplicate samples by titration to pH 10 using 0.1 M NaOH to extract the HA from the soil, then centrifuged at c. 3000 g for 10 min. The soil plug was discarded and the supernatant solution titrated to pH 2.0 using concentrated HCl before

centrifugation once again at c. 3000 g for 15 min to recover the flocculated HA. All samples were transferred into PCR tubes which were then placed inside a 2 ml capacity Nalgene tube. The Nalgene tube was the correct size to fit directly into the XAS sample holder with a drop of wax in the bottom to lift the sample so that it was positioned half way up the tube and would intercept the X-ray beam. All samples were stored at 4°C prior to transportation to the Diamond Light Facility and XAS analysis.

6.3.6.3 XAS Analysis

Technetium K-edge data was collected at the Diamond Light Source, UK, on Beamline B18 (16-18th January 2017) using a double crystal (Si(111) and Si(311)) monochromator. Calibration was achieved using TcO_4^- solution. Samples were analysed in fluorescence mode using a 9 element Ge detector, and were measured at liquid N_2 temperatures (c. 77 K).

6.3.6.4 Chemical analysis of XAS samples

The concentration of Tc in the soils solid phase was determined by hot plate acid digestion. This was not undertaken on HA extracts, only intact soil pastes. Since this is a destructive method this was performed following XAS analysis. Soil samples were dried and 0.2 g was weighed into digestion tubes. Both nitric acid reflux digestion and hydrofluoric acid (HF) evaporative digestion were used to dissolve the soil samples for determination of the Tc concentration. Nitric acid reflux involved adding 10 ml concentrated HNO_3 to each Digitube, with watches on top, and heated at 95°C for 2 hours. After allowing the samples to cool, each sample was made up to 50 mL volume with Milli-Q water before a 1-in-10 dilution (with Milli-Q) for ICP-MS analysis. The HF digestion involved adding 2 ml HNO_3 alongside 1 ml $HClO_4$, and heating at 80°C for 8

hr and then 100°C for 2 hr. Following this 2.5 ml HF was added and then heated at 120°C for 1 hr, 140°C for 3 hr and then 160°C for 4 hr. Once finished the temperature was reduced to 50°C, 2.5 ml HNO_3 and 2.5 ml Milli-Q water was added and the sample heated for 1 hr. Following cooling the volume was made up to 50 mL and diluted (both in Milli-Q water) for analysis by ICP-MS. Alongside each of the samples, 3 soils were added with a known spike of ^{99}Tc (5 µg L^{-1}) in order to check that all Tc was recovered by both methods.

6.4 RESULTS AND DISCUSSION

6.4.1 Interactions of $Tc^{(VII)}$ with HA

Pertechnetate ($^{99}Tc^{(VII)}O_4^-$) was added to the same HA systems as $^{129}IO_3^-$ and $^{77}Se^{(VI)}$ (Section 4.3.3). Pertechnetate in combination with HA showed no change in speciation, in almost all cases, over the course of 581 days (pH 4) or 622 days (pH 6) at either HA concentration, pH level or temperature (**Figure 6.1**). However, in the HA-only samples
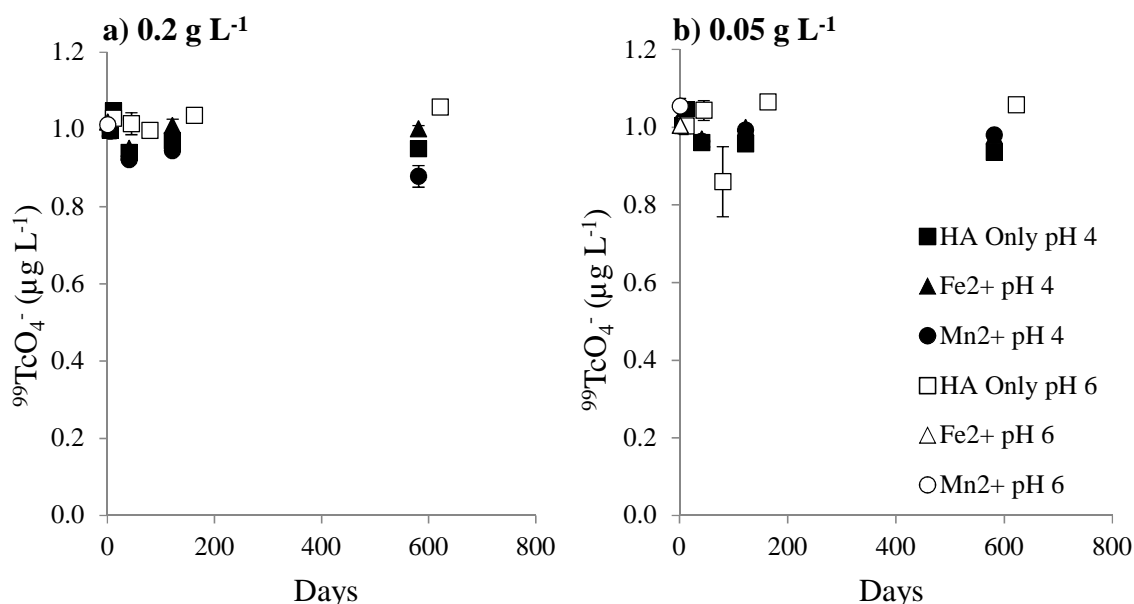
Figure 6.1. Humic acid suspensions at 0.2 g L^{-1} (a) and 0.05 g L^{-1} (b). HA was spiked with 1 µg L^{-1} $^{99}TcO_4^-$ with additions of Fe^{2+} (triangle) and Mn^{2+} (circle) at pH 4 (black) and pH 6 (white). Samples were stored at 20°C for 581 days (pH 4) and 622 days (pH 6). Error bars are the standard error of two replicates.

(0.05 g L^{-1}), and samples containing Mn^{2+}, at pH 4 and 20°C a small concentration (<0.005 ppb) of Tc was eluted as an unidentified peak near the start of the chromatogram (30 seconds) (**Figure 6.2**). The peak first appeared at around 125 d of incubation but the species of ^{99}Tc that this represents is not known.
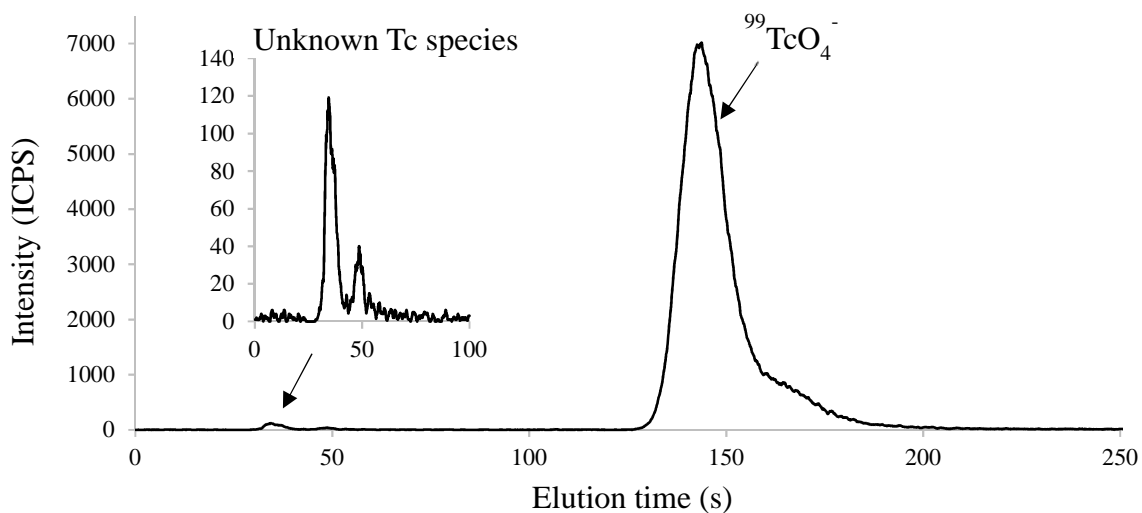
Figure 6.2. HPLC-ICP-MS chromatogram showing an unknown species around 30 s in a sample containing 0.2 g L^{-1} HA and Mn^{2+} at pH 4 and 20°C.

Sequential extractions of soils have shown significant removal of Tc from solution, and incorporation into the organic phase (Abdelouas *et al.*, 2005; Keith-Roach *et al.*, 2003; Sheppard *et al.*, 1990; Stalmans *et al.*, 1986; Uchida *et al.*, 1999). Therefore, it was expected that abiotic reduction and interaction of Tc might occur in the presence of HA, either alone or in combination with potential reducing agent Fe^{2+} or Mn^{2+}. A few studies have been able to demonstrate an interaction of Tc with humic substances directly (Boggs *et al.*, 2011; Geraedts *et al.*, 2002; Maes *et al.*, 2004), however always in the presence of a strong reducing agent. For example, Sekine *et al.* (1993) added Tc$^{(VII)}$ to HA suspensions containing Sn^{2+} and demonstrated co-precipitation of Tc-HA complexes, likely as Tc$^{(IV)}$, at pH 4 alongside a corresponding reduction in Tc$^{(VII)}$ concentration in solution. In the absence of Sn^{2+} no interaction was observed. Boggs *et al.* (2011)

demonstrated significant association of $Tc^{(IV)}$ with HS as TcO(OH)-HA at the same pH range as investigated here. However, since $Tc^{(VII)}$ was added reduction must occur prior to this interaction. It was also expected that HA samples containing additions of Fe^{2+} and Mn^{2+} might encourage the reduction of $Tc^{(VII)}$ to $Tc^{(IV)}$. However, no reduction was observed here either.

No reduction or association of $Tc^{(VII)}$ with goethite in HA suspensions was observed (**Figure 6.3**). Iron (hydro)oxides under reducing conditions have demonstrated a significant capacity in associating $Tc^{(IV)}$ on surfaces thus reducing Tc mobility (Druteikiene *et al.*, 2014; Li and Kaplan, 2012). A study performed by Um *et al.* (2011) showed that Fe^{2+} in combination with a goethite suspension significantly reduced $Tc^{(VII)}$ mobility. It was considered that Fe^{2+} incorporation into goethite was capable of catalyzing the reduction of $Tc^{(VII)}$ to $Tc^{(IV)}$ prior to incorporation into the goethite structure. The systems investigated here likely didn't demonstrate any reduction since the goethite suspensions lacked a strong electron donor to encourage reduction. Humic
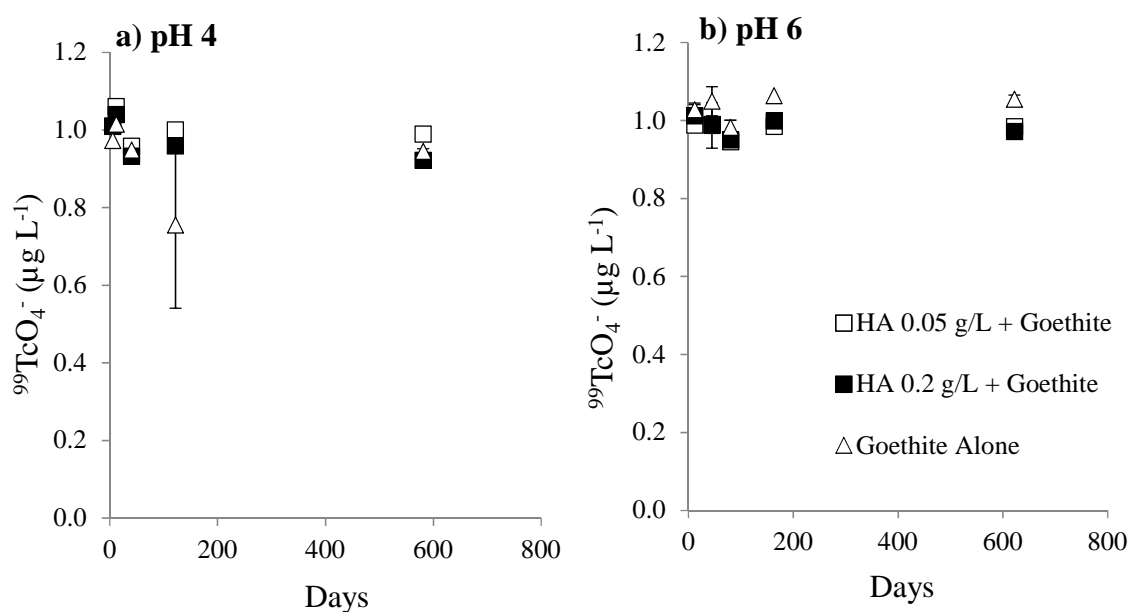
Figure 6.3. Humic acid suspensions (0.2 g L^{-1} and 0.05 g L^{-1}) spiked with 1 µg L^{-1} $^{99}TcO_4^-$ with additions goethite (20%), and goethite alone at a) pH 4 and b) pH 6. Stored at 20°C for 581 days at pH 4 and 622 days at pH 6. Error bars based on two replicates.

acid has been shown to behave as an electron donor under certain conditions, however it was not observed here. No associations of $Tc^{(VII)}$ with HA alone or in combination with metal ions or oxides was observed in this study.

6.4.2 Interactions of TcO_4^- with FA

Fulvic acid suspensions (0.2 g L^{-1}) containing 1 µg L^{-1} $Tc^{(VII)}$ also showed no change in Tc speciation. It was important to investigate FA as well as HA, as it constitutes the more soluble fraction of HS thus has greater implications for Tc transportation. The interaction between Tc and FA might also be expected to be affected by the greater degree of oxy-acid substitution in FA and the lower level of condensed aromatic structures when compared to HA (Gondar *et al.*, 2005). This could potentially result in an increased reactivity of FA towards Tc when compared to HA. However once again no interaction was observed, likely due to the absence of a strong electron donor and reducing conditions capable of inducing reduction from $Tc^{(VII)}$ to $Tc^{(IV)}$.

6.4.3 Effect of microbes on Tc interactions with HA

Pertechnetate was added to systems that were filter-sterilized, and not filter-sterilized, irradiated and not irradiated, and with additions of soil inoculum (filtered and un-filtered) alongside glucose additions to encourage microbial growth (Section 6.3.4; Chapter 4 Section 4.3.8). No reduction and consequent change in speciation was observed in any of the described systems (**Figure 6.4**). Both iron-reducing and sulfate-reducing microbes have previously demonstrated an ability to reduce $Tc^{(VII)}$ (Lloyd *et al.*, 2000, 1999) immobilizing the mobile radionuclide usually as insoluble $Tc^{(IV)}$. *Escherichia coli*, *Desulfovibrio desulfuricans*, *Geobacter sulfurreducens*, *Geobacter metallireducens* and *Shewanella putrefaciens* have all been shown to reduce TcO_4^- to insoluble species (Lloyd

et al., 2000, 1999; Wildung *et al.*, 2000). Burke *et al.* (2010) demonstrated 99% removal of TcO_4^- from solution in microcosms containing sediments undergoing active microbial $Fe^{(III)}$-reduction, with the end product being hydrous $Tc^{(VI)}O_2^-$ like phases. It was found that 70% of the Tc ended up in the SOM fraction, with 28-30% of that being associated with humic substances. Fredrickson *et al.* (2004) also demonstrated the same interaction in the case of *S. putrefaciens* added to sediments, resulting in >99% reduction of TcO_4^- in <2 days when the system was bio-reduced for just 17 days. No effort was made to identify the species found in the HA systems investigated here or the soil inoculum, therefore no conclusions about the species present was possible. The inoculated systems demonstrated visible growth of microbial species, and alongside this significant reduction of selenium oxyanions, but clearly no reduction of TcO_4^- or incorporation into HA by the species present was seen.
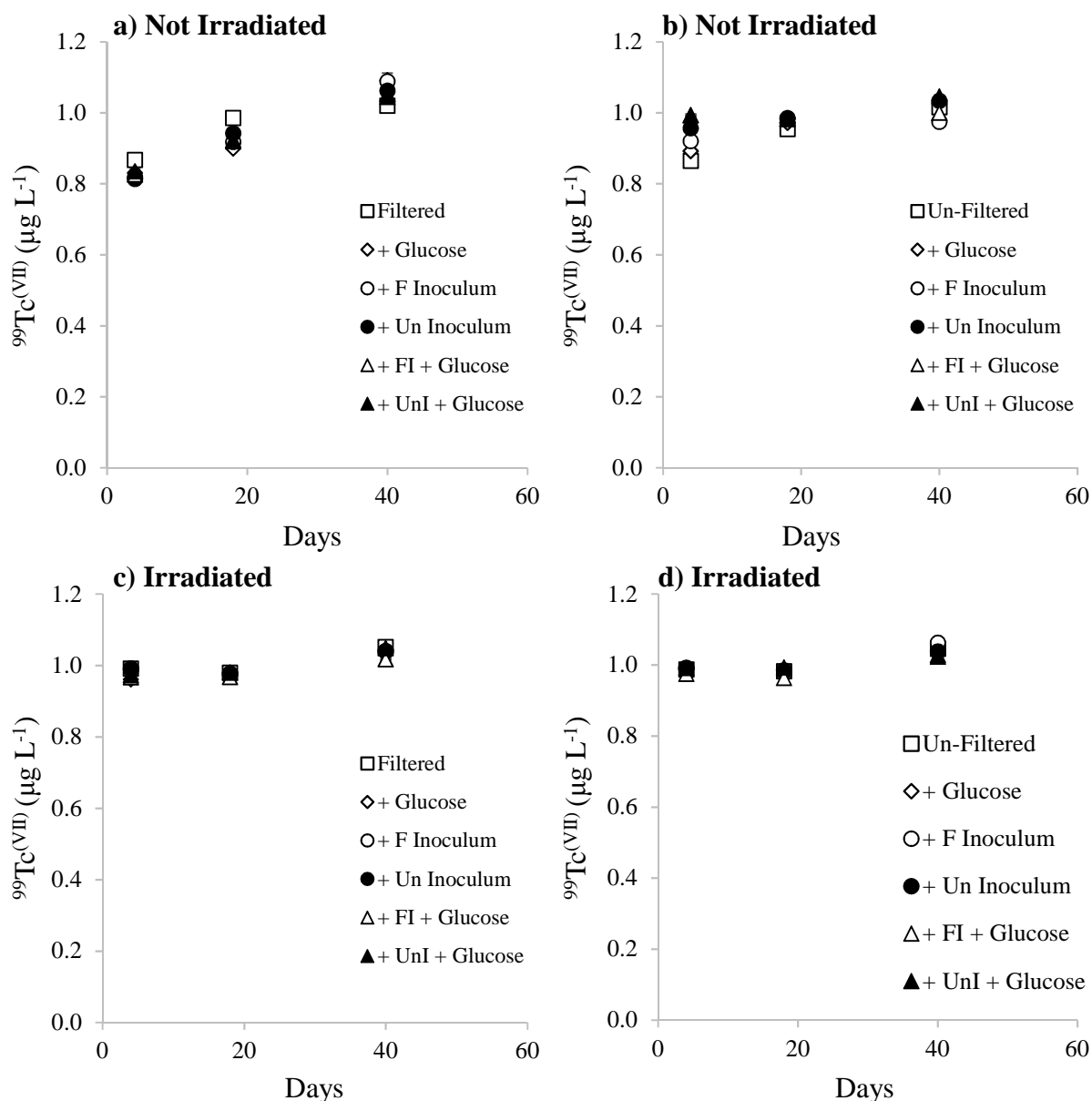
Figure 6.4. Non-irradiated (a, b) and irradiated (c, d) HA systems (0.2 g L^{-1}) spiked with 1 µg L^{-1} ^{99}TcO$_4^-$. Samples were either filter sterilised (a, c) or non-filtered (not sterile) (b, d). Systems were set up alone and in combination with a range of treatments: glucose (G), filtered soil inoculum (no microbes), un-filtered soil inoculum (microbes present), filtered inoculum with glucose and un-filtered inoculum with glucose. Error bars are ±standard error of two replicates.

6.4.4 XAS results

Spectra were collected for a Tc$^{(VII)}$ aqueous standard, however all other samples failed to provide any spectra. Upon further investigation it became evident that the ^{99}Tc stock solution used to spike the samples had been labelled incorrectly and the samples had been

196

spiked at a lower activity than planned. The intention was to produce a final concentration of 11.7 mg kg^{-1} Tc in 5 g of soil. When concentrated into the HA and flocculated could result in as much as 240 mg kg^{-1} Tc in the soils with high HA concentrations for analysis. However, measurement of the actual concentration of the stock solution suggested that the actual spike concentration was ~0.629 mg kg^{-1} Tc in 5 g of soil. Even if all of this was concentrated into the HA and flocculated for analysis the highest possible concentration would be ~12.58 mg kg^{-1} for analysis.

The soils were spiked 5 months prior to the diamond experiment which was deemed long enough for >70% of the ^{99}Tc to be incorporated into the organic phase, based on results from the long-term soils incubation experiment (to be published). However, given that the spiked activity was much less than expected, this time frame was not sufficient for enough Tc to be incorporated to a high enough concentration for reliable measurement by XAS. The samples were washed multiple times, prior to analysis, with Milli-Q water in order to remove any remaining Tc from solution to enable measurement of organically-bound Tc without interference from entrained Tc$^{(VII)}$ in solution. From the analysis of both the sample washes and the acid digests of the soil samples by ICP-MS it transpired that the stock used was in fact 0.0397 MBq ml^{-1} given that the soils had 0.91-0.60 mg kg^{-1} ^{99}Tc in total. The data from this analysis also indicates that 29-72% of the added Tc was not associated with the soils, depending on the soil type, and so a large proportion of the added Tc was washed out prior to XAS analysis, indicating that a longer contact time was necessary (**Table 6.2**). Acid digestion of the soils indicated that a few i.e. BY-M, DY-G and DY-M, had retained a significant proportion of the Tc added (67.8-72.9%). However given the low concentration of ^{99}Tc and the high detection limit of XAS, this was insufficient to achieve any successful scans. Based on the data collected here and

given the detection limits of the instrument, the interaction of Tc with soil or HA would need to be encouraged by using a strong reducing agent in order to get any usable data. However, the aim of this experiment was to investigate the interactions of Tc with soils under realistic aerobic soil conditions. There has already been considerable work examining changes in redox speciation of Tc in anaerobic systems, often involving added reducing agents.

Table 6.2. Technetium concentration in XAS sample washes and in soils after acid digestion.

Soil	Tc in washes mg kg^{-1}	Tc in solid mg kg^{-1}	Total Tc mg kg^{-1}	Tc in washes %	Tc in solids %
BC-M a	0.29	0.32	0.60	47.4	52.6
BC-M b	0.27	0.33	0.60	45.1	54.9
BY-M a	0.20	0.45	0.65	31.1	68.9
BY-M b	0.23	0.45	0.68	33.2	66.8
DY-M a	0.19	0.55	0.74	26.0	74.0
DY-M b	0.20	0.52	0.72	28.1	71.9
DY-G a	0.17	0.54	0.71	24.2	75.8
DY-G b	0.30	0.61	0.91	32.7	67.3
F1-T a	0.37	0.30	0.67	55.1	44.9
F1-T b	0.34	0.31	0.65	52.7	47.3
F2-T a	0.40	0.35	0.76	53.3	46.7
F2-T b	0.39	0.36	0.75	51.5	48.5
IH-W a	0.34	0.37	0.71	48.3	51.7
IH-W b	0.32	0.37	0.69	46.0	54.0
PE-W a	0.27	0.38	0.65	41.5	58.5
PE-W b	0.25	0.35	0.59	41.5	58.5
SB-G a	0.57	0.20	0.77	74.2	25.8
SB-G b	0.47	0.20	0.67	69.6	30.4
TK-G a	0.40	0.29	0.70	57.8	42.2
TK-G b	0.37	0.35	0.72	51.5	48.5
WK-W a	0.36	0.40	0.77	47.4	52.6
WK-W b	0.39	0.39	0.78	49.8	50.2

6.5 CONCLUSIONS

There is significant evidence of Tc interaction with the organic phase of soils, and even with HA and FA directly under reducing conditions. However, in the HA and FA systems investigated here, no $Tc^{(VII)}$ reduction and association with HA/FA was observed. The aerobic suspensions of isolated geocolloids showed little or no interaction of Tc with HA ($\pm$ Fe^{2+} or Mn^{2+}) and goethite or soil inoculum did not encourage reduction and interaction of Tc with the absorbent phases studied. Although the XAS soil samples did not provide any usable XAS data, it was clear that there was significant incorporation into the solid phase in samples with relatively high humus contents and low pH values. Consequently, it is apparent that Tc reduction and incorporation into the organic-phase can occur to a significant degree in soils which are aerobic in terms of bulk redox characteristics. However, since no interaction with isolated HA or FA was seen under aerobic conditions there is a missing (soil) factor necessary to drive the reduction of $Tc^{(VII)}$. It is possible that these interactions are biotic or abiotic but the experiments described in this chapter were unable to elucidate the mechanisms involved.

7. SUMMARY, CONCLUSIONS AND FUTURE WORK

7.1 IODINE

7.1.1 Summary and conclusions

Iodine added to HA systems reacts rapidly with the rate of reaction being dependent on speciation, pH, Fe content and OM content. Speciation largely determines the rate of transformation from inorganic species to organically-bound species. Iodate is rapidly transformed to Org-I species with some reduction to I^- with HA and FA. The similarities observed between the HA and FA systems suggest a similar reaction mechanism. The rate of IO_3^- reduction was quicker at low pH, higher temperature and greater HA concentrations. Modelling of IO_3^- reduction in the presence of HA demonstrated a significant negative relationship between pH and the rate of IO_3^- reduction, and a positive (non-linear) relationship with HA concentration.

In addition to IO_3^- reduction and formation of Org-I, re-release of I^- from Org-I species was observed, complicating prediction of Org-I formation. The rapid formation of Org-I at low pH followed by a decrease in its concentration as I^- was released was successfully modelled. It has been previously thought that Org-I species are relatively stable (Schlegel *et al.,* 2006; Xu *et al.*, 2012), however the results presented here indicate that Org-I species undergo some reduction to I^- in almost all of the systems investigated. The conditions that determine the release of I^- from Org-I are not well understood and appear highly variable and complex.

When I^- was added to HA systems the rate of oxidation to reactive intermediates, and subsequent formation of Org-I was slow compared to the IO_3^- spiked systems. The

oxidation reactions that transform I^- to I_2 or HOI before formation of Org-I are microbially driven and therefore more complex than the IO_3^- reduction reaction.

When Fe was present in combination with HA there was a slight reduction in the rate of IO_3^- reduction compared to systems without Fe, with significantly more I^- formed. Modelling of this interaction demonstrated that the pathway transforming Org-I to I^- was increased when Fe was present in the systems, i.e. a positive relationship exists between Fe concentration and the rate of Org-I transformation to I^-. When I^- was added in the presence of Fe instantaneous association of I^- with the HA occurred, possibly by cation bridging with Fe, followed by gradual re-release as I^- over time. This re-release is likely to be a consequence of ongoing Fe hydrolysis in the system. This is probably not a process occurring in soil systems, as the Fe is likely to have been associated with the HA for extended periods of time, and therefore less likely to be undergoing hydrolysis.

Iodate and I^- removal from soil solution differs from that observed in HA systems and is highly dependent on the soil type. Kodama *et al.* (2006) who investigated the reaction of IO_3^- and I^- with soil phases, observed increased sorption of IO_3^-, due to its higher affinity for solid phases. However only one soil type was investigated here, a light clay soil from a paddy field (pH 5.7; Org-C 1.86%) and therefore only provides a snapshot of I interactions in soils. Shetaya *et al.* (2010) investigated the changes in iodine speciation and solubility across a wide range of soils with differing OM contents, Fe/Mn oxide contents, and pH properties. They demonstrated that the rate of conversion of $^{129}I^-$ to Org-^{129}I species was more rapid than that of $^{129}IO_3^-$, the opposite of what is observed in HA systems. The removal of $^{129}I^-$ from solution was most significant in soils with high pH and OM contents, where complete transformation to Org-^{129}I species could occur within

8 hours. This indicates that the oxidation of I^- to Org-I species requires a further component and is likely biotic rather than abiotic (Seki *et al.* 2013). Although I^- behaviour in HA systems differs from that in soils, IO_3^- interactions with soils correlate well with the observed interactions with HA alone. Steinberg *et al.* (2008) investigated IO_3^- interactions with a peat soil (high OM content), and the reactions observed (accounting for the systems being run at a significantly higher temperature) agree with the results observed here for pure HA systems. The modelled data for IO_3^- interactions with HA will likely be able to predict a large amount of the interactions determining IO_3^- reduction and association within organic soils, since this interaction appears to be entirely abiotic. However elucidating the mechanisms associated with I^- incorporation within soil OM appears to be much more complex.

7.1.2 Implications

The investigations of I with HA and FA, alone and in combination with metal ions, has furthered our understanding of the interactions of I within the natural environment. The data generated here will inform assemblage models accounting for the complex interactions within soils, developing our knowledge of I geochemistry. This data has implications for radioactive waste disposal of [129]I, accidental aerial releases of [129]I into the environment, and interactions of [127]I as an agricultural fertiliser. Reliably modelling the mechanisms of I within soil systems is vital in terms of understanding and predicting its environmental transfer. The final pathway that determines the breakthrough of [129]I species into the biosphere from a GDF is transfer from groundwater to soils. Therefore, understanding how I interacts with different soil conditions is vital in order to build a reliable post-closure safety assessment for GDF's. For example, in the event of radionuclide release from a GDF located under a predominantly organic soil

environment, ^{129}I is likely to be immobilised rapidly and thus limit soil-plant transfer to a significant degree. In terms of iodine biofortification; different fertiliser application techniques must be considered in order to determine the most efficient and cost-effective method of increased iodine intake (Cakmak *et al.*, 2017). Speciation determines the bioavailability of I added as either a soil-application or foliar-application, therefore the mechanisms described within this thesis could be vital in determining the most effective fertilisation method.

The mechanistic information gained here in combination with the data collected during the TREE soil incubation study will dramatically improve the understanding of I mobility in soils. The short-term modelling of the soils (2.5 years) alongside the mechanistic modelling demonstrated here will enable the development of long-term models to predict biosphere transfers of I depending on the soil properties and conditions.

7.1.3 Future work

This study has made significant progress in understanding the fate of I in soils, specific through interactions with SOM, however further investigations are necessary given the complexity of soil systems. Further investigation of the remobilization of Org-I as I^- is necessary to fully understand the interactions between I and Fe^{2+}/Fe^{3+} and HA. There is also a lack of information on redox coupling of IO_3^- and I^- in HA and FA systems. Increasing the complexity of HS systems through the addition of microbes, metal oxides/ions and other soil constituents, with analysis by HPLC-ICP-MS, SEC-ICP-MS and XAS, would enable a more mechanistic understanding of I behavior to be elucidated.

7.2 SELENIUM

7.2.1 Summary and conclusions

Speciation has a significant effect on the rate and extent of Se reduction in the presence of HA. Selenite is more rapidly reduced than $Se^{(VI)}$. This confirms our current understanding of Se interactions within the terrestrial environment; where $Se^{(VI)}$ is considered the most mobile and therefore bioavailable species (Zawislanski *et al.*, 2003). Both $Se^{(IV)}$ and $Se^{(VI)}$ reacted with HA, with faster reaction at low pH and higher temperature. Unlike IO_3^-, $Se^{(IV)}$ and $Se^{(VI)}$ were not influenced by HA concentration suggesting that the availability of binding sites on the HA is not rate limiting. Low pH increased the rate of both $Se^{(IV)}$ and $Se^{(VI)}$ reduction in HA systems at 20^oC. This agrees with literature demonstrating that an increase in pH results in less Se sorption within soils, resulting in increased Se plant uptake (Goh and Lim, 2004). Interaction of $Se^{(VI)}$ with HA has not previously been observed but has been demonstrated in this work. This is likely to be a consequence of the time scale and pH range over which these reactions have been investigated; other studies have only investigated reactions over very short time-scales at neutral pH. Selenate reduction in the presence of HA has a lag time of up to 10 days, thought to be due to the involvement of microbial activity, hence studies performed over hours/days would not observe reaction between $Se^{(VI)}$ and HA.

Filtration of HA systems prevented reduction of $Se^{(IV)}$ or $Se^{(VI)}$, whereas both species were reduced in unfiltered systems. This indicates microbial activity within the HA which was confirmed by experiments including soil inoculum and glucose additions with and without γ-sterilization. Selenate especially became more reduced in systems with added microbes suggesting that the interaction is biotic. A confounding factor however,

is that most reduction was observed at pH 4 and bacterial activity tends to be more predominant at neutral-high pH.

Varying degrees of reduction were observed by XAS in HA samples spiked with $Se^{(IV)}$ and $Se^{(VI)}$. In HA and in soil reduction of $Se^{(IV)}$ and $Se^{(VI)}$ to $Se^{(0)}$ was observed, whereas goethite bonded Se without reduction. Selenite association with HA was via a Se-O-C chain, with a Se-C interatomic distance of 2.75Å. When Fe^{3+} was present cation bridging to Fe atoms at 3.28-3.31Å was observed which has not previously been demonstrated. During sorption experiments Fe additions did not increase the rate of $Se^{(IV)}$ or $Se^{(VI)}$ reduction suggesting that although it is involved in bonding it is not acting as reductant. Inner-sphere complexation of $Se^{(IV)}$ and $Se^{(VI)}$ on goethite agreed well with existing literature.

It is difficult to compare Se behaviour in HA systems with behaviour in soils. Se reduction was greatest in acidic HA systems and this has also been demonstrated in soils where a higher pH results in lower soil Se adsorption (Goh and Lim, 2004). Soil OM his an important sink for Se in the environment (Di Tullo *et al*., 2016; Li *et al.*, 2017; Tolu *et al.*, 2014), however no link between HA concentration and Se reduction was observed. This suggests that HA/OM can be a sink for Se but that it doesn't necessarily drive the reduction. Microbial reductive incorporation of Se into organic phases has been suggested as the method of Se association (Lusa *et al.*, 2015), and this is suspected to have played a role here. The work in this thesis complements the information available for Se within whole soil systems, but continues to highlight the complexity surrounding modelling its environmental behavior.

7.2.2 Implications

Selenium is not only an essential element for humans and animals, but also an anthropogenic contaminant from coal combustion, oil refinery discharge and radioactive waste (Section 1.4.2). Understanding Se mobility and bioavailability is vital for environmental risk assessments and in managing, for example, Se biofortification. The interactions of $Se^{(IV)}$ and $Se^{(VI)}$ with HA, alone and in combination with metal ions, furthers our understanding of Se in whole soil systems and will contribute to the development of models predicting Se behavior in the terrestrial environment. A similar discussion applies here as given for iodine in Section 7.1.2; Selenium-79 has a long half-life and could contribute significant dose rates to human and wildlife populations if released. It is therefore of high importance with regards to GDF safety assessments. Both speciation and microbial activity have a significant influence on the mobility and bioavailability of Se within the terrestrial environment. Therefore, understanding how these mechanisms are interlinked within whole soils systems, and modelling these under different conditions is especially important in order to understand movement into the biosphere and soil-plant transfer. Although no modelling was performed here this data will complement and advise on the interpretation of TREE soil incubation modelling, with the goal of developing complex and reliable biosphere models able to predict Se behavior over long-time scales.

7.2.3 Future work

Although this work has improved understanding of Se reaction with OM, and consequently whole soil, the interactions and mechanisms remain incompletely understood. Further work is required to build a comprehensive understanding of the mechanisms controlling the fate of Se especially the role of microorganisms. Further

investigation of the role of bridged cations in binding Se in soils is also recommended, over a range of pH and Fe and Mn additions.

7.3 TECHNETIUM

7.3.1 Summary and conclusions

Pertechnetate added to HA and FA systems demonstrated no reduction or incorporation into HA or FA alone or in combination with Fe^{2+}, Mn^{2+} or goethite. This is likely due to the lack of a reducing environment or reductant capable of catalysing $Tc^{(VII)}$ reduction to $Tc^{(IV)}$ prior to incorporation. Gu *et al.* (2011) demonstrated that HA could in fact increase the oxidation and oxidative dissolution of reduced $Tc^{(IV)}$ solids under oxidizing conditions. This is in contrast to reactions observed in some soil and sediment systems where rapid reduction of Tc has been observed followed by incorporation into the organic phase (Abdelouas *et al.*, 2005; Keith-Roach *et al.*, 2003; Stalmans *et al.*, 1986). Soils can't truly be considered as aerobic systems, since anaerobic 'pockets' will likely exist in areas where oxygen is depleted by microbial activity (Stalmans *et al.,* 1986), therefore although $Tc^{(VII)}$ reduction is observed in "aerobic" soils it's most likely occurring in areas where Eh is lower and conditions more reducing. Abdelouas *et al.* (2004) discussed the role of microbes in the reduction of $Tc^{(VII)}$ into the organic phases of soils and demonstrated that the growth of Fe-reducing bacteria, as indicated by an increase in Fe^{3+} reduction to Fe^{2+}, corresponded with a drop in Eh and consequently an increase in $Tc^{(VII)}$ reduction to $Tc^{(IV)}$. Reduction of Tc in the presence of HA was not observed here as the systems are aerobic and although not sterile, they likely don't contain the "right" microbial community under the best conditions to encourage Tc reduction. Reduction and incorporation into HA is possible and has been demonstrated under many different conditions (Boggs *et al.*, 2015, 2011; Geraedts *et al.*, 2002; Maes *et al.*, 2004), however

this study is no closer to elucidating the mechanisms involved in surface soils. Given that soils systems are significantly more complex than the HA systems here, there is likely a missing factor that determines significant incorporation into HA in soils.

7.3.2 Implications

Although unable to identify Tc reduction in the presence of HA alone and in combination with metal ions, this work has developed our understanding of the mechanisms within whole soil systems. It is reasonable to conclude that incorporation of Tc into humus is not driven by reduction from HA, and that a factor, or multiple factors, are missing from pure HA systems responsible for this reaction. The information gained here will inform discussions of Tc reduction and bioavailability within soils since it eliminates the abiotic reduction of Tc by HA as a mechanism.

7.3.3 Future work

It is apparent from this work that Tc does not interact with aerobic HA or FA systems, regardless of Fe additions, therefore more studies investigating Tc interactions in whole soil systems are recommended.

REFERENCES

Abdelouas, A., Grambow, B., Fattahi, M., Andrès, Y., Leclerc-Cessac, E., 2005. Microbial reduction of ^{99}Tc in organic matter-rich soils. Sci. Total Environ. 336, 255–268.

Adani, F., Genevini, P., Tambone, F., Montoneri, E., 2006. Compost effect on soil humic acid: A NMR Study. Chemosphere 65, 1414–1418.

Allard, S., Gunten, U. Von, Sahli, E., Nicolau, R., Gallard, H., 2009a. Oxidation of iodide and iodine on birnessite (d -MnO₂) in the pH range 4 – 8 Δ log K. Water Res. 43, 3417–3426.

Amachi, S., 2008. Microbial contribution to global iodine cycling: volatilisation, accumulation, reduction, oxidation, and sorption of iodine. Microbes Environ. 23, 269–276.

Amachi, S., Kawaguchi, N., Muramatsu, Y., Tsuchiya, S., Watanabe, Y., Shinoyama, H., Fujii, T., 2007. Dissimilatory iodate reduction by marine *Pseudomonas sp.* strain SCT. Appl. Environ. Microbiol. 73, 5725–5730.

Anschutz, P., Sundby, B., Lefrançois, L., Luther, G.W., Mucci, A., 2000. Interactions between metal oxides and species of nitrogen and iodine in bioturbated marine sediments. Geochim. Cosmochim. Acta 64, 2751–2763.

Antelo, J., Arce, F., Avena, M., Fiol, S., Lopez, R., Macias, F., 2007. Adsorption of a soil humic acid at the surface of goethite and its competitive interaction with phosphate. Geoderma 138, 12–19.

Ashworth, D.J., Shaw, G., Butler, A.P., Ciciani, L., 2003. Soil transport and plant uptake of radio-iodine from near-surface groundwater. J. Environ. Radioact. 70, 99–114.

Avena, M.J., Koopal, L.K., van Riemsdijk, W.H., 1999. Proton binding to humic acids: Electrostatic and intrinsic interactions. J. Colloid Interface Sci. 217, 37–48.

Azaizeh, H.A., Gowthaman, S., Terry, N., 1996. Microbial selenium volatilization in rhizosphere and bulk soils from a constructed wetland. J. Environ. Qual. 26, 666–672.

Baidoo, E., Ephraim, J.H., Darko, G., Akoto, O., 2014. Potentiometric studies of the acid–base properties of tropical humic acids. Geoderma 217–218, 18–25.

Begg, J.D.C., Burke, I.T., Morris, K., 2007. The behaviour of technetium during microbial reduction in amended soils from Dounreay, U.K. Sci. Total Environ. 373, 297–304.

Bell, J.N.B., Shaw, G., 2005. Ecological lessons from the Chernobyl accident. Environ. Int. 31, 771–777.

Benedetti, M.F., van Riemsdijk, W.H., Koopal, L.K., Kinniburgh, D.G., Gooddy, D.C., Milne, C.J., 1996. Metal ion binding by natural organic matter: from the model to the field. Geochim. Cosmochim. Acta 60, 2503–2513.

Bennett, R., Willey, N., 2003. Soil availability, plant uptake and soil to plant transfer of [99]Tc—A review. J. Environ. Radioact. 65, 215–231.

Berns, A.E., Philipp, H., Narres, H.D., Burauel, P., Vereecken, H., Tappe, W., 2008. Effect of gamma-sterilization and autoclaving on soil organic matter structure as studied by solid state NMR, UV and fluorescence spectroscopy. Eur. J. Soil Sci. 59, 540–550.

Bienvenu, P., Cassette, P., Andreoletti, G., Bé, M.-M., Comte, J., Lépy, M.-C., 2007. A new determination of [79]Se half-life. Appl. Radiat. Isot. 65, 355–64.

Boggs, M. a, Minton, T., Dong, W., Lomasney, S., Islam, M.R., Gu, B., Wall, N. a, 2011. Interactions of Tc[(IV)] with humic substances. Environ. Sci. Technol. 45, 2718–24.

Bors, J., Martens, R., 1992. The contribution of microbial biomass to the adsorption of radioiodide in soils. J. Environ. Radioact. 15, 35–49.

Bostock, A.C., Shaw, G., Bell, J.N.B., 2003. The volatilisation and sorption of [129]I in coniferous forest, grassland and frozen soils. J. Environ. Radioact. 70, 29–42.

Bowles, E., Antweiler, R.., MacCarthy, P., 1994. Acid-base titration and hydrolysis of fulvic acid from the Suwannee River. In: Humic substances in the Suwannee River, Georgia: Interaction, properties and proposed structures. U.S. Geological Survey. pp. 87-557.

Bowley, H.E., 2013. Iodine dynamics in the terrestrial environment. University of Nottingham.

Bowley, H.E., Young, S.D., Ander, E.L., Crout, N.M.J., Watts, M.J., Bailey, E.H., 2016. Iodine binding to humic acid. Chemosphere 157, 208–214.

Brown, C.F., Geiszler, K.N., Lindberg, M.J., 2007. Analysis of [129]I in groundwater samples: Direct and quantitative results below the drinking water standard. Appl. Geochemistry 22, 648–655.

Bruggeman, C., Maes, a., Vancluysen, J., 2007. The interaction of dissolved Boom Clay and Gorleben humic substances with selenium oxyanions (selenite and selenate). Appl. Geochemistry 22, 1371–1379.

Burke, I.T., Livens, F.R., Lloyd, J.R., Brown, A.P., Law, G.T.W., McBeth, J.M., Ellis,

B.L., Lawson, R.S., Morris, K., 2010. The fate of technetium in reduced estuarine sediments: Combining direct and indirect analyses. Appl. Geochemistry 25, 233–241.

Cakmak, I., Prom-u-thai, C., Guilherme, L.R.G., Rashid, A., Hora, K.H., Yazici, A., Savasli, E., Kalayci, M., Tutus, Y., Phuphong, P., Rizwan, M., Martins, F.A.D., Dinali, G.S., Ozturk, L., 2017. Iodine biofortification of wheat, rice and maize through fertilizer strategy. Plant Soil. 418, 319–335.

Catrouillet, C., Davranche, M., Dia, A., Bouhnik-Le Coz, M., Marsac, R., Pourret, O., Gruau, G., 2014. Geochemical modeling of Fe$^{(II)}$ binding to humic and fulvic acids. Chem. Geol. 372, 109–118.

Chan, Y.T., Kuan, W.H., Chen, T.Y., Wang, M.K., 2009. Adsorption mechanism of selenate and selenite on the binary oxide systems. Water Res. 43, 4412–4420.

Collins, R.N., Tran, N.D., Bakkaus, E., Avoscan, L., Gouget, B., 2006. Assessment of isotope exchange methodology to determine the sorption coefficient and isotopically exchangeable concentration of selenium in soils and sediments. Environ. Sci. Technol. 40, 7778–7783.

Cook, R.L., Langford, C.H., 1998. Structural Characterization of a Fulvic Acid and a Humic Acid Using Nuclear Magnetic Resonance. Environ. Sci. Technoiogy 32, 719–725.

Cooke, T.D., Bruland, K.W., 1987. Aquatic Chemistry of Selenium: Evidence of Biomethylation. Environ. Sci. Technol. 21, 1214–1219.

Coppin, F., Chabroullet, C., Martin-Garin, A., 2009. Selenite interactions with some particulate organic and mineral fractions isolated from a natural grassland soil. Eur. J. Soil Sci. 60, 369–376.

Councell, T.B., Landa, E.R., Lovley, D.R., 1997. Microbial reduction of iodate. Water Air Soil Pollut. 100, 99–106.

Couture, R.A., Seitz, M.G., 1983. Sorption of anions of iodine by iron oxides and kaolinite. Nucl. Chem. Waste Manag. 4, 301–306.

Dai, J.L., Zhang, M., Hu, Q.H., Huang, Y.Z., Wang, R.Q., Zhu, Y.G., 2009. Adsorption and desorption of iodine by various Chinese soils: II. Iodide and iodate. Geoderma 153, 130–135.

Darab, J.G., Smith, P.A., 1996. Chemistry of technetium and rhenium species during low-level radioactive waste vitrification. Chem. Mater. 8, 1004–1021.

Darcheville, O., Février, L., Haichar, F.Z., Berge, O., Martin-Garin, A., Renault, P.,

2008. Aqueous, solid and gaseous partitioning of selenium in an oxic sandy soil under different microbiological states. J. Environ. Radioact. 99, 981–992.

Das, S., Jim Hendry, M., Essilfie-Dughan, J., 2013. Adsorption of selenate onto ferrihydrite, goethite, and lepidocrocite under neutral pH conditions. Appl. Geochemistry 28, 185–193.

De Luca, G., De Philip, P., Dermoun, Z., Rousset, M., Vermeglio, A., 2001. Reduction of Technetium$^{(VII)}$ by *Desulfovibrio fructosovorans* is mediated by the nickel-iron hydrogenase. Appl. Environ. Microbiol. 67, 4583–4587.

De Temmerman, L., Waegeneers, N., Thiry, C., Du Laing, G., Tack, F., Ruttens, A., 2014. Selenium content of Belgium cultivated soils and its uptake by field crops and vegetables. Sci. Total Environ. 468–469, 77–82.

Defra, BERR, 2008. Managing Radioactive Waste Safely: A Framework for Implementing Geological Disposal.

Dhillon, K., Dhillon, S., 1999. Adsorption–desorption reactions of selenium in some soils of India. Geoderma 93, 19–31.

Doran, J.W., Alexander, M., 1977. Microbial transformations of selenium. Appl. Environ. Microbiol. 33, 31–37.

Doskocil, L., Burdikova-Szewieczkova, J., Enev, V., Kalina, L., Wasserbauer, J., 2018. Spectral characterization and comparison of humic acids isolated from some european lignites. Fuel 123–132.

Druteikiene, R., Lukšiené, B., Peĉiulyté, D., Mažeika, K., Gudelis, A., Baltrunas, D., 2014. Behaviour of ^{99}Tc in aqueous solutions in the presence of iron oxides and microorganisms. Appl. Radiat. Isot. 89, 85–94.

Fabryka-Martin, J., Bentley, H., Elmore, D., Airey, P.L., 1985. Natural iodine-129 as an environmental tracer. Geochim. Cosmochim. Acta 49, 337–347.

Farrenkopf, A.M., Dollhopf, M.E., Chadhain, S.N., Luther III, G.W., Nealson, K.H., 1997. Reduction of iodate in seawater during Arabian Sea shipboard incubations and in laboratory cultures of the marine bacterium Shewanella putrefaciens strain MR-4. Mar. Chem. 57, 347–354.

Fernández-Martínez, A., Charlet, L., 2009. Selenium environmental cycling and bioavailability: A structural chemist point of view. Rev. Environ. Sci. Biotechnol. 8, 81–110.

Fordyce, F.M., 2013. Selenium deficiency and toxicity in the environment. Essentials Med. Geol. Revis. Ed. 375–416.

Francois, R., 1987. The influence of humic substances on the geochemistry of iodine in nearshore and hemipelagic marine sediments. Geochim. Cosmochim. Acta 51, 2417–2427.

Fredrickson, J.K., Zachara, J.M., Kennedy, D.W., Kukkadapu, R.K., McKinley, J.P., Heald, S.M., Liu, C., Plymale, A.E., 2004. Reduction of TcO_4^- by sediment-associated biogenic $Fe^{(II)}$. Geochim. Cosmochim. Acta 68, 3171–3187.

Fuge, R., 1996. Geochemistry of iodine in relation to iodine deficiency diseases. In: Appleton, J.D., Fuge, R., McCall, G.J.H. (Eds.), Environmental Geochemistry and Health. The Geological Society, London, pp. 201–213.

Fuge, R., 2005. Soils and Iodine Deficiency. In: Selinus, O., Alloway, B.., Centeno, J.., Finkelman, R.., Fuge, R., Lindh, U., Smedley, P. (Eds.), Essentials of Medical Geology: Impacts of the Natural Environment on Public Health. Elsevier Inc., pp. 417–432.

Fuge, R., Johnson, C.C., 1986. The geochemistry of iodine - a review. Environ. Geochem. Health 8, 31–54.

Fuge, R., Johnson, C.C., 2015. Iodine and human health, the role of environmental geochemistry and diet, a review. Appl. Geochemistry 63, 282–302.

Fuhrmann, M., Bajt, S., Schoonen, M. a a, 1998. Sorption of iodine on minerals investigated by X-ray absorption near edge structure (XANES) and ^{125}I tracer sorption experiments. Appl. Geochemistry 13, 127–141.

Fukushima, M., Tanaka, S., Hasebe, K., Taga, M., Nakamura, H., 1995. Interpretation of the acid-base equilibrium of humic acid by a continuous pK distribution and electrostatic model. Analyt. Chimi. Acta. 302, 365-373.

Gallard, H., Allard, S., Nicolau, R., Von Gunten, U., Croué, J.P., 2009. Formation of iodinated organic compounds by oxidation of iodide-containing waters with manganese dioxide. Environ. Sci. Technol. 43, 7003–7009.

Gamble, D.S., 1972. Potentiometric Titration of Fulvic Acid: Equivalence Point Calculations and Acidic Functional Groups. Can. J. Chem. 50, 2680–2690.

Garcia-León, M., 2005. [99]Tc in the Environment : Sources , Distribution and Methods. J. Nucl. Sci. Technol. 6, 253–259.

Geraedts, K., Bruggeman, C., Maes, A., Van Loon, L., Rossberg, A., Reich, T., 2002. Evidence for the existence of $Tc^{(IV)}$ - humic substance species by X-ray absorption near-edge spectroscopy. Radiochim. Acta 90, 879–884.

Goh, K.H., Lim, T.T., 2004. Geochemistry of inorganic arsenic and selenium in a tropical

soil: Effect of reaction time, pH, and competitive anions on arsenic and selenium adsorption. Chemosphere 55, 849–859.

Gómez-Guzmán, J.M., Holm, E., Enamorado-Báez, S.M., Abril, J.A., Pinto-Gómez, A.R., López-Gutiérrez, J.M., García-León, M., 2013. Pre- and post-Chernobyl accident levels of ^{129}I and ^{137}Cs in the Southern Baltic Sea by brown seaweed Fucus vesiculosus. J. Environ. Radioact. 115, 134–142.

Gómez-Guzmán, J.M., Holm, E., Niagolova, N., López-Gutiérrez, J.M., Pinto-Gómez, a. R., Abril, J. a., García-León, M., 2014. Influence of releases of ^{129}I and ^{137}Cs from European reprocessing facilities in Fucus vesiculosus and seawater from the Kattegat and Skagerrak areas. Chemosphere 108, 76–84.

Gondar, D., Lopez, R., Fiol, S., Antelo, J.M., Arce, F., 2005. Characterization and acid-base properties of fulvic and humic acids isolated from two horizons of an ombrotrophic peat bog. Geoderma 126, 367–374.

González Pérez, M., Martin-Neto, L., Saab, S.C., Novotny, E.H., Milori, D.M.B.P., Bagnato, V.S., Colnago, L.A., Melo, W.J., Knicker, H., 2004. Characterization of humic acids from a Brazilian Oxisol under different tillage systems by EPR,^{13}C NMR, FTIR and fluorescence spectroscopy. Geoderma 118, 181–190.

Goure-Doubi, H., Martias, C., Lecomte-Nana, G.L., Nait-Ali, B., Smith, A., Thune, E., Villandier, N., Gloaguen, V., Soubrand, M., Konan, L.K., 2014. Interfacial reactions between humic-like substances and lateritic clay: application to the preparation of "geomimetic" materials. J. Colloid Interface Sci. 434, 208–17.

Grambow, B., 2008. Mobile fission and activation products in nuclear waste disposal. J. Contam. Hydrol. 102, 180–6.

Gu, B., Dong, W., Liang, L., Wall, N. a, 2011. Dissolution of technetium$^{(IV)}$ oxide by natural and synthetic organic ligands under both reducing and oxidizing conditions. Environ. Sci. Technol. 45, 4771–7.

Güngör, E.B.Ö., Bekbölet, M., 2010. Zinc release by humic and fulvic acid as influenced by pH, complexation and DOC sorption. Geoderma 159, 131–138.

Gustafsson, J.P., Johnsson, L., 1994. The Association between Selenium and Humic Substances in Forested Ecosystems-Laboratory Evidence. Appl. Organomet. Chem. 8, 141–147.

Hageman, S.P.W., Van der Weijden, R.D., Weijma, J., Buisman, C.J.N., 2013. Microbiological selenate to selenite conversion for selenium removal. Water Res. 47, 2118–2128.

Hansen, D., Duda, P.J., Zayed, A., Terry, N., 1998. Selenium removal by constructed wetlands: Role of biological volatilization. Environ. Sci. Technol. 32, 591–597.

Hansen, V., Roos, P., Aldahan, A., Hou, X., Possnert, G., 2011. Partition of iodine ([129]I and [127]I) isotopes in soils and marine sediments. J. Environ. Radioact. 102, 1096–1104.

Hatcher, P.G., 1980. ^{1}H and ^{13}C NMR of marine humic acids. Org. Geochem. 2, 77–85.

Hayes, K.F., Roe, a L., Brown, G.E., Hodgson, K.O., Leckie, J.O., Parks, G. a, 1987. In Situ X-ray Absorption Study of Surface Complexes: Selenium Oxyanions on α-FeOOH. Science 238, 783–6.

Hinojosa Reyes, L., Marchante Gayòn, J.M., Garcîa Alonso, J.I., Sanz-Medel, A., 2003. Determination of selenium in biological materials by isotope dilution analysis with an octapole reaction system ICP-MS. J. Anal. At. Spectrom. 18, 11–16.

Hockin, S.L., Gadd, G.M., 2003. Linked Redox Precipitation of Sulfur and Selenium under Anaerobic Conditions by Sulfate-Reducing Bacterial Biofilms Linked Redox Precipitation of Sulfur and Selenium under Anaerobic Conditions by Sulfate-Reducing Bacterial Biofilms. Appl. Enivironmental Microbiol. 69, 7063–7072.

Hou, X., Hansen, V., Aldahan, A., Possnert, G., Lind, O.C., Lujaniene, G., 2009. A review on speciation of iodine-129 in the environmental and biological samples. Anal. Chim. Acta 632, 181–196.

Hu, Q., Moran, J.E., Blackwood, V., 2009. Geochemical Cycling of Iodine Species in Soils. Compr. Handb. Iodine 93–105.

Hu, Q., Zhao, P., Moran, J.E., Seaman, J.C., 2004. Sorption and Transport of Iodine Species in Sediments from the Savannah River and Hanford Sites. J. Cont. Hydrol. 78 (3), 185-205.

Hu, Q.H., Moran, J.E., Gan, J.Y., 2012. Sorption, degradation, and transport of methyl iodide and other iodine species in geologic media. Appl. Geochemistry 27, 774–781.

Ike, M., Takahashi, K., Fujita, T., Kashiwa, M., Fujita, M., 2000. Selenate reduction by bacteria isolated from aquatic environment free from selenium contamination. Water Res. 34, 3019–3025.

Istok, J.D., Senko, J.M., Krumholz, L.R., Watson, D., Bogle, M.A., Peacock, A., Chang, Y.J., White, D.C., 2004. In Situ Bioreduction of Technetium and Uranium in a Nitrate-Contaminated Aquifer. Environ. Sci. Technol. 38, 468–475.

Izmer, A. V., Boulyga, S.F., Zoriy, M. V., Becker, J.S., 2004. Improvement of the

detection limit for determination of [129]I in sediments by quadrupole inductively coupled plasma mass spectrometer with collision cell. J. Anal. At. Spectrom. 19, 1278.

Jaisi, D., Plymale, A., 2009. Reduction and long-term immobilization of technetium by Fe[(II)] associated with clay mineral nontronite.

Johnson, C.C., 2003. The geochemistry of iodine and its application to environmental strategies for reducing the risks from iodine deficiency disorders (IDD). Br. Geol. Surv. Comm. Rep. 1–54.

Johnson, C.C., 2003. Database of the iodine content of soils populated with data from published literature. Br. Geol. Surv. Comm. Rep. 40.

Jones, G.D., Droz, B., Greve, P., Gottschalk, P., Poffet, D., Mcgrath, S.P., Seneviratne, S.I., 2017. Selenium deficiency risk predicted to increase under future climate change. PNAS, 1–6.

Kamei-Ishikawa, N., Nakamaru, Y., Tagami, K., Uchida, S., 2008. Sorption behavior of selenium on humic acid under increasing selenium concentration or increasing solid/liquid ratio. J. Environ. Radioact. 99, 993–1002.

Kamei-Ishikawa, N., Tagami, K., Uchida, S., 2007. Sorption kinetics of selenium on humic acid. J. Radioanal. Nucl. Chem. 274, 555–561.

Kang, Y., Yamada, H., Kyuma, K., Hattori, T., Kigasawa, S., 1991. Selenium in soil humic acid. Soil Sci. Plant Nutr. 37, 241–248.

Kaplan, D.I., Serne, R.J., Parker, K.E., Kutnyakov, I. V., 2000. Iodide sorption to subsurface sediments and illitic minerals. Environ. Sci. Technol. 34, 399–405.

Keith-Roach, M.J., Morris, K., Dahlgaard, H., 2003. An investigation into technetium binding in sediments. Mar. Chem. 81, 149–162.

Keith-Roach, M.J., Stürup, S., Oughton, D.H., Dahlgaard, H., 2002. Comparison of two ICP-MS set-ups for measuring ^{99}Tc in large volume water samples. Analyst 127, 70–75.

Kerndorff, H., Schnitzer, M., 1980. Sorption of metals on humic acid. Geochim. Cosmochim. Acta 44, 1701–1708.

Kodama, S., Takahashi, Y., Okumura, K., Uruga, T., 2006. Speciation of iodine in solid environmental samples by iodine K-edge XANES: Application to soils and ferromanganese oxides. Sci. Total Environ. 363, 275–284.

Kuroda, M., Notaguchi, E., Sato, A., Yoshioka, M., Hasegawa, A., Kagami, T., Narita, T., Yamashita, M., Sei, K., Soda, S., Ike, M., 2011. Characterization of

Pseudomonas stutzeri NT-I capable of removing soluble selenium from the aqueous phase under aerobic conditions. J. Biosci. Bioeng. 112, 259–264.

Leblanc, C., Colin, C., Cosse, A., Delage, L., La Barre, S., Morin, P., Fiévet, B., Voiseux, C., Ambroise, Y., Verhaeghe, E., Amouroux, D., Donard, O., Tessier, E., Potin, P., 2006. Iodine transfers in the coastal marine environment: the key role of brown algae and of their vanadium-dependent haloperoxidases. Biochimie 88, 1773–1785.

Li, D., Kaplan, D.I., 2012. Sorption coefficients and molecular mechanisms of Pu, U, Np, Am and Tc to Fe (hydr)oxides: a review. J. Hazard. Mater. 243, 1–18.

Li, Z., Liang, D., Peng, Q., Cui, Z., Huang, J., Lin, Z., 2017. Interaction between selenium and soil organic matter and its impact on soil selenium bioavailability: A review. Geoderma 295, 69–79.

Liu, Y., Von Gunten, H.R., 1988. Paul Scherrer Institut. Migration Chemistry and Behaviour of Iodine Relevant to Geological Disposal of Radioactive Wastes - A Literature Review with a Compilation of Sorption Date.

Lloyd, J.R., Ridley, J., Khizniak, T., Lyalikova, N.N., Macaskie, L.E., 1999. Reduction of technetium by *Desulfovibrio desulfuricans*: Biocatalyst characterization and use in a flowthrough bioreactor. Appl. Environ. Microbiol. 65, 2691–2696.

Lloyd, J.R., Sole, V.A., Van Praagh, C.V.G., 2000. Direct and Fe[(II)] -Mediated Reduction of Technetium by Fe[(III)] -Reducing Bacteria. Society 66, 3743–3749.

López-Gutiérrez, J.M., García-León, M., Schnabel, C., Suter, M., Synal, H. a., Szidat, S., García-Tenorio, R., 2004. Relative influence of [129]I sources in a sediment core from the Kattegat area. Sci. Total Environ. 323, 195–210.

Lovley, D.R., Coates, J.D., BluntHarris, E.L., Phillips, E.J.P., Woodward, J.C., 1996. Humic substances as electron acceptors for microbial respiration. Nature. 382 ,445-448.

Lovley, D.R., Fraga, J.L., Coates, J.D., Blunt-Harris, E.L., 1999. Humics as an electron donor for anaerobic respiration. Environ. Microbiol. 1, 89–98.

Lusa, M., Bomberg, M., Aromaa, H., Knuutinen, J., Lehto, J., 2015. The microbial impact on the sorption behaviour of selenite in an acidic, nutrient-poor boreal bog. J. Environ. Radioact. 147, 85–96.

Lusa, M.J., 2015. Sorption behaviour of I[-] , SeO_3^{2-} and Cs^+ in an ombrotrophic boreal bog A study on microbial effects.

Lützenkirchen, J., 1999. The Constant Capacitance Model and Variable Ionic Strength: An Evaluation of Possible Applications and Applicability. J. Colloid Interface Sci.

217, 8–18.

Luykx, F., 1986. Technetium discharges into the environment. In: Desmet, G., Myttenaere, C. (Eds.), Technetium in the Environment. Springer, Dordrecht, pp. 21–27.

Maes, a., Geraedts, K., Bruggeman, C., Vancluysen, J., Rossberg, a., Hennig, C., 2004. Evidence for the Interaction of Technetium Colloids with Humic Substances by X-ray Absorption Spectroscopy. Environ. Sci. Technol. 38, 2044–2051.

Malcom, R.L., 1976. Method and importance of obtaining humic and fulvic acids of high purity. J. Res. U.S. Geol. Surv. 4, 37–40.

Manceau, A., Charlet, L., 1994. The Mechanism of Selenate Adsorption on Goethite and Hydrous Ferric Oxide. J. Colloid Interface Sci. 168, 87–93.

Manzak, A., Kursun, C., Yildiz, Y., 2017. Characterization of humic acid extracted from aqueous solutions with polymer inclusion membranes. J. Taiwan Inst. Chem. Eng. 81, 14–20.

Marivoet, J., Weetjens, E., 2012. An Assessment of the Impact of Advanced Nuclear Fuel Cycles on Geological Disposal. In: Rahman, R.A. (Ed.), Radioactive Waste. InTech, Shanghai, pp. 487–500.

Marshall, M.J., Plymale, A.E., Kennedy, D.W., Shi, L., Wang, Z., Reed, S.B., Dohnalkova, A.C., Simonson, C.J., Liu, C., Saffarini, D. a, Romine, M.F., Zachara, J.M., Beliaev, A.S., Fredrickson, J.K., 2008. Hydrogenase- and outer membrane c -type cytochrome-facilitated reduction of technetium[VII] by Shewanella oneidensis MR-1 10, 125–136.

Marshall, S.J., Young, S.D., Gregson, K., 1995. Humic acid-proton equilibria: A comparison of two models and assessment of titration error. Eur. J. Soil Sci. 46, 471–480.

Martin, D.P., Seiter, J.M., Lafferty, B.J., Bednar, A.J., 2017. Exploring the ability of cations to facilitate binding between inorganic oxyanions and humic acid. Chemosphere 166, 192–196.

Más, J.L., Garcia-León, M., Bolívar, J.P., 2002. [99]Tc atom counting by quadrupole ICP-MS. Optimisation of the instrumental response. Nucl. instruments methods Phys. Res. A 484, 660–667.

McNamara, N.P., Black, H.I.J., Beresford, N.A., Parekh, N.R., 2003. Effects of acute gamma irradiation on chemical, physical and biological properties of soils. Appl. Soil Ecol. 24, 117–132.

Milne, C.J., Kinniburgh, D.G., Tipping, E., 2001. Generic NICA-Donnan model parameters for proton binding by humic substances. Environ. Sci. Technol. 35, 2049–2059.

Muramatsu, Y., Yoshida, S., Fehn, U., Amachi, S., Ohmomo, Y., 2004. Studies with natural and anthropogenic iodine isotopes: Iodine distribution and cycling in the global environment. J. Environ. Radioact. 74, 221–232.

Nagata, T., Fukushi, K., 2010. Prediction of iodate adsorption and surface speciation on oxides by surface complexation modeling. Geochim. Cosmochim. Acta 74, 6000–6013.

Nagata, T., Fukushi, K., Takahashi, Y., 2009. Prediction of iodide adsorption on oxides by surface complexation modeling with spectroscopic confirmation. J. Colloid Interface Sci. 332, 309–316.

Nederlof, M.M., Dewit, J.C.M., Vanriemsdijk, W.H., Koopal, L.K., 1993. Determination of Proton Affinity Distributions for Humic Substances. Environ. Sci. Technol. 27, 846–856.

Newsome, L., Cleary, A., Morris, K., Lloyd, J.R., 2017. Long-Term Immobilization of Technetium via Bioremediation with Slow-Release Substrates. Environ. Sci. Technol. 51, 1595–1604.

Ohno, T., Muramatsu, Y., Shikamori, Y., Toyama, C., Okabe, N., Matsuzaki, H., 2013. Determination of ultratrace ^{129}I in soil samples by Triple Quadrupole ICP-MS and its application to Fukushima soil samples. J. Anal. At. Spectrom. 28, 1283.

Oremland, R.S., Hollibaugh, J.T., Maest, a S., Presser, T.S., Miller, L.G., Culbertson, C.W., 1989. Selenate reduction to elemental selenium by anaerobic bacteria in sediments and culture: biogeochemical significance of a novel, sulfate-independent respiration. Appl. Environ. Microbiol. 55, 2333–2343.

Paul, M., 2016. Analysis of Selenium in Diffi cult Samples. Dreieich, Germany.

Peak, D., 2006. Adsorption mechanisms of selenium oxyanions at the aluminum oxide/water interface. J. Colloid Interface Sci. 303, 337–345.

Peak, D., Sparks, D.L., 2002. Mechanisms of Selenate Adsorption on Iron Oxides and Hydroxides. Environ. Sci. Technol. 36, 1460–1466.

Peng, H., Zhang, N., He, M., Chen, B., Hu, B., 2015. Simultaneous speciation analysis of inorganic arsenic, chromium and selenium in environmental waters by 3-(2-aminoethylamino) propyltrimethoxysilane modified multi-wall carbon nanotubes packed microcolumn solid phase extraction and ICP-MS. Talanta 131, 266–272.

Peretyazhko, T., Zachara, J.M., Heald, S.M., Kukkadapu, R.K., Liu, C., Plymale, a. E., Resch, C.T., 2008. Reduction of Tc$^{(VII)}$ by Fe$^{(II)}$ Sorbed on Al (hydr)oxides. Environ. Sci. Technol. 42, 5499–5506.

Perminova, I. V, Frimmel, F.H., Kudryavtsev, a, Kulikova, N. a, Abbt-Braun, G., Hesse, S., Petrosyan, V.S., 2003. Molecular weight characleristics of humic substances from different environments as determined by size exclusion chromatography and their statistical evaluation. Environ. Sci. Technol. 37, 2477–2485.

Pezzarossa, B., Piccotino, D., Petruzzelli, G., 1999. Sorption and desorption of selenium in different soils of the mediterranean area. Commun. Soil Sci. Plant Anal. 30, 2669–2679.

Piccolo, A., 2002. The supramolecular structure of humic substances: A novel understanding of humus chemistry and implications in soil science. Adv. Agron. 75, 57–134.

Press, W.H., Teukolsky, S.A., Bethe, H.A., Vetterling, W.T., Flannery, B.P., 2007. Numerical Recipes: The Art of Scientific Computing, 3rd ed. Cambridge University Press, Cambridge.

Rameback, H., Albinsson, Y., Skalberg, M., Eklund, U.B., 1998. Determination of ^{99}Tc in bentonite clay samples using inductively coupled plasma mass spectrometry. Fresenius. J. Anal. Chem. 362, 391–394.

Rao, U., Fehn, U., 1999. Sources and reservoirs of anthropogenic Iodine-129 in Western New York. Geochim. Cosmochim. Acta 63, 1927–1938.

Ravel, B., Newville, M., 2005. ATHENA, ARTEMIS, HEPHAESTUS: data analysis for X-ray absorption spectroscopy using IFEFFIT. J. Synchrotron Radiat. 12, 537–541.

Rayman, M.P., 2000. The importance of selenium to human health. Lancet 356, 233–241.

Reid, H.J., Bashammakh, A.A., Goodall, P.S., Landon, M.R., O'Connor, C., Sharp, B.L., 2008. Determination of iodine and molybdenum in milk by quadrupole ICP-MS. Talanta 75, 189–197.

Reiller, B.P., Gimenez, N., Barr, N., 2006. Iodination of humic acid samples from different origins. Radiochim. Acta 745, 739–745.

Reiller, P., Moulin, V., 2002. Influence of organic matter in the prediction of iodine migration in natural environment. MRS Proc. 757.

Ritchie, J.D., Michael Perdue, E., 2003. Proton-binding study of standard and reference fulvic acids, humic acids, and natural organic matter. Geochim. Cosmochim. Acta

67, 85–93.

Rose, A.L., Waite, T.D., 2003. Kinetics of iron complexation by dissolved natural organic matter in coastal waters. Mar. Chem. 84, 85–103.

Rosenfield, I., Beath, O.A., 1964. Selenium: Geobotany, Biochemistry, Toxicity and Nutrition. Academic Press inc., New York.

Rovira, M., Giménez, J., Martínez, M., Martínez-Lladó, X., de Pablo, J., Martí, V., Duro, L., 2008. Sorption of selenium$^{(IV)}$ and selenium$^{(VI)}$ onto natural iron oxides: Goethite and hematite. J. Hazard. Mater. 150, 279–284.

Santos, E.B.., Esteves, V.., Rodrigues, J.P.., Duarte, A.., 1999. Humic substances' proton-binding equilibria: assessment of errors and limitation of potentiometric data. Anal. Chim. Acta 392, 333–341.

Schlegel, M.L., Reiller, P., Mercier-Bion, F., Barré, N., Moulin, V., 2006. Molecular environment of iodine in naturally iodinated humic substances: Insight from X-ray absorption spectroscopy. Geochim. Cosmochim. Acta 70, 5536–5551.

Schlesinger, W.H., 1990. Evidence from chronosequence studies for a low carbon-storage potential of soils. Nature 348, 232–234.

Schnitzer, M., Khan, S.U., 1972. Humic Substances in the Environment, Illustrate. ed. M. Dekker, Minnesota.

Schwehr, K.A., Santschi, P.H., Kaplan, D.I., Yeager, C.M., Brinkmeyer, R., 2009. Organo-iodine formation in soils and aquifer sediments at ambient concentrations. Environ. Sci. Technol. 43, 7258–7264.

Scott, D.T., Mcknight, D.M., Blunt-Harris, E.L., Kolesar, S.E., Lovley, D.R., 1998. Quinone moieties act as electron acceptors in the reduction of humic substances by humics-reducing microorganisms. Environ. Sci. Technol. 32, 2984–2989.

Scott, M.J., Morgan, J.J., 1996. Reactions at oxide surfaces. 2. Oxidation of Se$^{(IV)}$ by synthetic birnessite. Environ. Sci. Technol. 30, 1990–1996.

Seki, M., Oikawa, J.I., Taguchi, T., Ohnuki, T., Muramatsu, Y., Sakamoto, K., Amachi, S., 2013. Laccase-catalyzed oxidation of iodide and formation of organically bound iodine in soils. Environ. Sci. Technol. 47, 390–397.

Sekine, T., Watanabe, A., Yoshihara, K., Kim, J.I., 1993. Complexation of Technetium with Humic Acid. Radiochim. Acta 63, 87–90.

Shaw, G., Ashworth, D., 2011. Selenium: Radionuclides. Encycl. Inorg. Bioinorg. Chem.

Sheppard, M.I., Hawkins, J.L., 1995. Iodine and microbial interactions in an organic soil. J. Environ. Radioact. 29, 91–109.

Sheppard, S.C., Sheppard, M.I., Evenden, W.G., 1990. A novel method used to examine variation in Tc sorption among 34 soils, aerated and anoxic. J. Environ. Radioact. 11, 215–233.

Sheppard, S.C., Sheppard, M.I., Tait, J.C., Sanipelli, B.L., 2006. Revision and meta-analysis of selected biosphere parameter values for chlorine, iodine, neptunium, radium, radon and uranium. J. Environ. Radioact. 89, 115–37.

Shetaya, W.H., Young, S.D., Watts, M.J., Ander, E.L., Bailey, E.H., 2012. Iodine dynamics in soils. Geochim. Cosmochim. Acta 77, 457–473.

Sigg, L., Stumm, W., 1981. The interaction of anions and weak acid with the hydrous goethite (a-FeOOH) surface. Colloids and Surfaces 2, 101–117.

Slavin, G., 2005. Derbyshire neck and iodine deficiency. Mercian Geol. 16, 79–88.

Spadoni, M., Voltaggio, M., Carcea, M., Coni, E., Raggi, A., Cubadda, F., 2007. Bioaccessible selenium in Italian agricultural soils: Comparison of the biogeochemical approach with a regression model based on geochemical and pedoclimatic variables. Sci. Total Environ. 376, 160–77.

Sposito, G., 2008. Chemistry of Soils. Oxford University Press, New York.

Stalmans, M., Maes, A., Cremers, A., 1986. Role of Organic Matter as a Geochemical Sink for Technetium in Soils and Sediments. In: Desmet, G., Myttenaere, C. (Eds.), Technetium in the Environment: Seminar on the Behaviour of Technetium in the Environment. Elsevier Applied Science, London, pp. 91–113.

Steinberg, S.M., Kimble, G.M., Schmett, G.T., Emerson, D.W., Turner, M.F., Rudin, M., 2008. Abiotic reaction of iodate with *Sphagnum* peat and other natural organic matter. J. Radioanal. Nucl. Chem. 277, 185–191.

Stevenson, F.J., 1982. Humus chemistry: Genesis, composition, reactions. John Wiley & Sons ltd., New York.

Stolz, J.F., Oremland, R.S., 1999. Bacterial respiration of arsenic and selenium. FEMS Microbiol. Rev. 23, 615–627.

Struyk, Z., Sposito, G., 2001. Redox properties of humic acids. Geoderma 102, 329–346.

Supriatin, S., Weng, L., Comans, R.N.J., 2015. Selenium speciation and extractability in Dutch agricultural soils. Sci. Total Environ. 532, 368–382.

Szecsody, J.E., Jansik, D.P., McKinley, J.P., Hess, N.J., 2014. Influence of alkaline co-contaminants on technetium mobility in vadose zone sediments. J. Environ. Radioact. 135, 147–60.

Tagami, K., Uchida, S., 1996. Microbial role in the immobilization of technetium in soil

under waterlogged conditions. Chemosphere 33, 217–225.

Tam, S., Chow, A., Hadley, D., 1995. Effects of organic component on the immobilization of selenium on iron oxyhydroxide. Sci. Total Environ. 164, 1–7.

Tarsitano, D., Young, S.D., Crout, N.M.J., 2011. Evaluating and reducing a model of radiocaesium soil-plant uptake. J. Environ. Radioact. 102, 262–269.

Thorpe, C.L., Boothman, C., Lloyd, J.R., Law, G.T.W., Bryan, N.D., Atherton, N., Livens, F.R., Morris, K., 2014. The interactions of strontium and technetium with $Fe^{(II)}$ bearing biominerals: Implications for bioremediation of radioactively contaminated land. Appl. Geochemistry 40, 135–143.

Thurman, E.M., Malcolm, R.L., 1981. Preparative isolation of aquatic humic substances. Environ. Sci. Technol. 15, 463–6.

Tipping, E., 1994. WHAMC—A chemical equilibrium model and computer code for waters, sediments, and soils incorporating a discrete site/electrostatic model of ion-binding by humic substances. Comput. Geosci. 20, 973–1023.

Tipping, E., 1998. Humic ion-binding model VI: An improved description of the interactions of protons and metal ions with humic substances. Aquat. Geochemistry 4, 3–48.

Tipping, E., 2002. Cation binding by humic substances. Cambridge University Press.

Tipping, E., Hurley, M.., 1992. A unifying model of cation binding by humic substances. Geochim. Cosmochim. Acta 56, 3627–3641.

Tipping, E., Rey-Castro, C., 2002. $Al^{(III)}$ and $Fe^{(III)}$ binding by humic substances in freshwaters, and implications for trace metal speciation. Geochim. Cosmochim. Acta 66, 3211–3224.

Tolu, J., Thiry, Y., Bueno, M., Jolivet, C., Potin-Gautier, M., Le Hécho, I., 2014. Distribution and speciation of ambient selenium in contrasted soils, from mineral to organic rich. Sci. Total Environ. 479–480, 93–101.

Tomei, F.A., Barton, L.L., Lemanski, C.L., Zocco, T.G., Fink, N.H., Sillerud, L.O., 1995. Transformation of selenate and selenite to elemental selenium by *Desulfovibrio desulfuricans*. J. Ind. Microbiol. 14, 329–336.

Traversa, A., D'Orazio, V., Mezzapesa, G.N., Bonifacio, E., Farrag, K., Senesi, N., Brunetti, G., 2014. Chemical and spectroscopic characteristics of humic acids and dissolved organic matter along two Alfisol profiles. Chemosphere 111, 184–94.

Turner, R.J., Weiner, J.H., Taylor, D.E., 1998. Selenium metabolism in *Escherichia coli.* Biometals 11, 223–227.

Uchida, S., Tagami, K., Ruhm, W., Wirth, E., 1999. Determination of ^{99}Tc deposition on the ground within the 30-km zone around the Chernobyl reactor and estimation of ^{99}Tc released into atmosphere by the accident. Chemosphere 39, 2757–2766.

Ultee, A., Souvatzi, N., Maniadi, K., König, H., 2004. Identification of the culturable and nonculturable bacterial population in ground water of a municipal water supply in Germany. J. Appl. Microbiol. 96, 560–568.

Um, W., Chang, H., Icenhower, J.P., Lukens, W.W., Je, R., Qafoku, N.P., Westsik, J.H., Buck, E.C., Smith, S.C., 2011. Immobilization of 99-Technetium$^{(VII)}$ by Fe$^{(II)}$ - Goethite and Limited Reoxidation. Environ. Sci. Technol. 45, 4904–4913.

Van Oijen, M., Rougier, J., Smith, R., 2005. Bayesian calibration of process-based forest models: bridging the gap between models and data. Tree Physiol. 25, 915–927.

Vinceti, M., Mandrioli, J., Borella, P., Michalke, B., Tsatsakis, A., Yoram, F., 2014. Selenium neurotoxicity in humans: Bridging laboratory and epidemiologic studies. Toxicol. Lett. 105, 75–77.

Walsh, S.E., Denyer, S.P., 2013. Filter Sterilization. In: Fraise, A.P., Maillard, J.-Y., Sattar, S.A. (Eds.), Russell, Hugo & Ayliffe's: Principles and Practice of Disinfection, Preservation and Sterilization. Wiley-Blackwell, Oxford, UK., pp. 343–370.

Wang, Z., Gao, Y., 2001. Biogeochemical cycling of selenium in Chinese environments. Appl. Geochemistry 16, 1345–1351.

Weast, R.C., 1982. Handbook of Chemistry and Physics, 63rd ed. CRC Press, Boca Raton, FL.

Weber, J., Wilson, S., 1975. The isolation and characterization of fulvic acid and humic acid from river water. Water Res. 9, 1079–1084.

Weber, T., Allard, T., Tipping, E., Benedetti, M.F., 2006. Modeling iron binding to organic matter. Environ. Sci. Technol. 40, 7488–7493.

Whitehead, D.C., 1973. The sorption of iodide by soils as influenced by equilibrium conditions and soil properties. J. Sci. Food Agric. 24, 547–556.

Whitehead, D.C., 1984. The distribution and transformations of iodine in the environment. Environ. Int. 10, 321–339.

Wildung, R.E., Gorby, Y.A., Krupka, K.M., Hess, N.J., Li, S.W., Plymale, A.E., McKinley, J.P., Fredrickson, J.K., 2000. Effect of electron donor and solution chemistry on products of dissimilatory reduction of technetion by *Shewanella putrefaciens.* Appl. Environ. Microbiol. 66, 2451–2460.

Wildung, R.E., Li, S.W., Murray, C.J., Krupka, K.M., Xie, Y., Hess, N.J., Roden, E.E., 2004. Technetium reduction in sediments of a shallow aquifer exhibiting dissimilatory iron reduction potential. FEMS Microbiol. Ecol. 49, 151–162.

Wiramanaden, C.I.E., Forster, E.K., Liber, K., 2010a. Selenium distribution in a lake system receiving effluent from a metal mining and milling operation in Northern Saskatchewan, Canada. Environ. Toxicol. Chem. 29, 606–616.

Wiramanaden, C.I.E., Liber, K., Pickering, I.J., 2010b. Selenium speciation in whole sediment using x-ray absorption spectroscopy and micro x-ray fluorescence imaging. Environ. Sci. Technol. 44, 5389–5394.

Xiong, J., Koopal, L.K., Tan, W., Fang, L., Wang, M., Zhao, W., Liu, F., Zhang, J., Weng, L., 2013. Lead binding to soil fulvic and humic acids: NICA-Donnan modeling and XAFS spectroscopy. Environ. Sci. Technol. 47, 11634–42.

Xu, C., Chen, H., Sugiyama, Y., Zhang, S., Li, H.-P., Ho, Y.-F., Chuang, C., Schwehr, K. a, Kaplan, D.I., Yeager, C., Roberts, K. a, Hatcher, P.G., Santschi, P.H., 2013. Novel molecular-level evidence of iodine binding to natural organic matter from Fourier transform ion cyclotron resonance mass spectrometry. Sci. Total Environ. 449, 244–252.

Xu, C., Miller, E.J., Zhang, S., Li, H., Ho, Y., Schwehr, K. a, Kaplan, D.I., Otosaka, S., Roberts, K. a, Brinkmeyer, R., Yeager, C.M., Santschi, P.H., 2011. Sequestration and Remobilization of Radioiodine (^{129}I) by Soil Organic Matter and Possible Consequences of the Remedial Action at Savannah River Site. Environ. Sci. Technol. 45, 9975–9983.

Xu, C., Zhong, J., Hatcher, P.G., Zhang, S., Li, H.P., Ho, Y.F., Schwehr, K. a., Kaplan, D.I., Roberts, K. a., Brinkmeyer, R., Yeager, C.M., Santschi, P.H., 2012. Molecular environment of stable iodine and radioiodine (^{129}I) in natural organic matter: Evidence inferred from NMR and binding experiments at environmentally relevant concentrations. Geochim. Cosmochim. Acta 97, 166–182.

Yamada, H., Hisamori, I., Yonebayashi, K., 2002. Identification of organically bound iodine in soil humic substances by size exclusion chromatography/inductively coupled plasma mass spectrometry (SEC/ICP-MS). Soil Sci. Plant Nutr. 48, 379–385.

Yamada, H., Kiriyama, T., Onagawa, Y., Hisamori, I., Miyazaki, C., Yonebayashi, K., 1999. Speciation of iodine in soils. Soil Sci. Plant Nutr. 45, 563–568.

Yamaguchi, N., Nakano, M., Takamatsu, R., Tanida, H., 2010. Inorganic iodine

incorporation into soil organic matter: Evidence from iodine K-edge X-ray absorption near-edge structure. J. Environ. Radioact. 101, 451–457.

Yamamoto, M., Nishida, A., Otsuka, K., Komai, T., Fukushima, M., 2010. Evaluation of the binding of iron$^{(II)}$ to humic substances derived from a compost sample by a colorimetric method using ferrozine. Bioresour. Technol. 101, 4456–4460.

Zachara, J.M., Heald, S.M., Jeon, B.-H., Kukkadapu, R.K., Liu, C., 2007. Reduction of pertechnetate [Tc$^{(VII)}$] by aqueous Fe$^{(II)}$ and the nature of solid phase redox products. Geochim. Cosmochim. Acta 71, 2137–2157.

Zawislanski, P.T., Benson, S.M., Terberg, R., Borglin, S.E., 2003. Selenium speciation, solubility, and mobility in land-disposed dredged sediments. Environ. Sci. Technol. 37, 2415–2420.

Zech, W., Senesi, N., Guggenberger, G., Kaiser, K., Lehmann, J., Miano, T.M., Miltner, A., Schroth, G., 1997. Factors controlling humification and mineralization of soil organic matter in the tropics. Geoderma 79, 117–161.

Zieve, R., Peterson, P.J., 1984. Volatilization of selenium from plants and soils. Sci. Total Environ. 32, 197–202.